frontiers | Research Topics

Bispecific antibodies and their conjugates in solid tumors and hematological malignancies

Edited by
Miroslawa Puskulluoglu and Renata Pacholczak-Madej

Published in
Frontiers in Immunology
Frontiers in Oncology

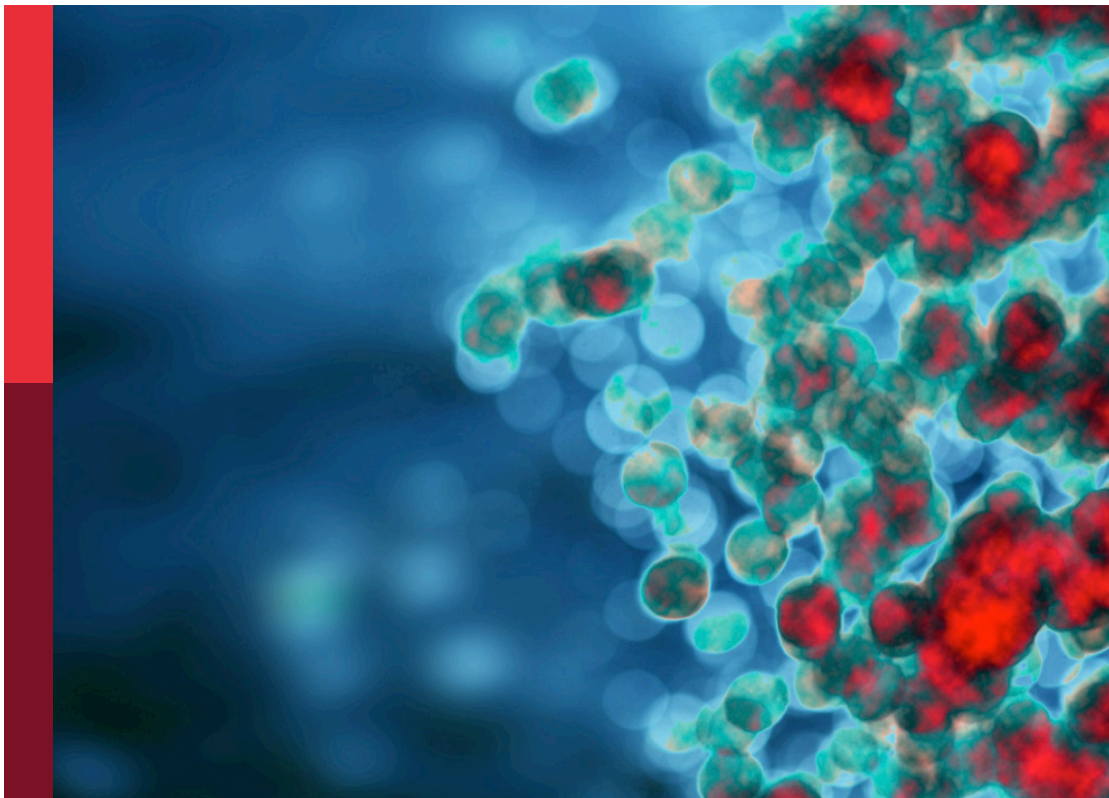

ISSN 1664-8714
ISBN 978-2-8325-7297-9
DOI 10.3389/978-2-8325-7297-9

Generative AI statement
Any alternative text (Alt text) provided alongside figures in the articles in this ebook has been generated by Frontiers with the support of artificial intelligence and reasonable efforts have been made to ensure accuracy, including review by the authors wherever possible. If you identify any issues, please contact us.

About Frontiers

Frontiers is more than just an open access publisher of scholarly articles: it is a pioneering approach to the world of academia, radically improving the way scholarly research is managed. The grand vision of Frontiers is a world where all people have an equal opportunity to seek, share and generate knowledge. Frontiers provides immediate and permanent online open access to all its publications, but this alone is not enough to realize our grand goals.

Frontiers journal series

The Frontiers journal series is a multi-tier and interdisciplinary set of open-access, online journals, promising a paradigm shift from the current review, selection and dissemination processes in academic publishing. All Frontiers journals are driven by researchers for researchers; therefore, they constitute a service to the scholarly community. At the same time, the *Frontiers journal series* operates on a revolutionary invention, the tiered publishing system, initially addressing specific communities of scholars, and gradually climbing up to broader public understanding, thus serving the interests of the lay society, too.

Dedication to quality

Each Frontiers article is a landmark of the highest quality, thanks to genuinely collaborative interactions between authors and review editors, who include some of the world's best academicians. Research must be certified by peers before entering a stream of knowledge that may eventually reach the public - and shape society; therefore, Frontiers only applies the most rigorous and unbiased reviews. Frontiers revolutionizes research publishing by freely delivering the most outstanding research, evaluated with no bias from both the academic and social point of view. By applying the most advanced information technologies, Frontiers is catapulting scholarly publishing into a new generation.

What are Frontiers Research Topics?

Frontiers Research Topics are very popular trademarks of the *Frontiers journals series*: they are collections of at least ten articles, all centered on a particular subject. With their unique mix of varied contributions from Original Research to Review Articles, Frontiers Research Topics unify the most influential researchers, the latest key findings and historical advances in a hot research area.

Find out more on how to host your own Frontiers Research Topic or contribute to one as an author by contacting the Frontiers editorial office: frontiersin.org/about/contact

Bispecific antibodies and their conjugates in solid tumors and hematological malignancies

Topic editors

Miroslawa Puskulluoglu — Maria Sklodowska-Curie National Research Institute of Oncology, Poland

Renata Pacholczak-Madej — Maria Skłodowska-Curie National Institute of Oncology, Poland

Citation

Puskulluoglu, M., Pacholczak-Madej, R., eds. (2026). *Bispecific antibodies and their conjugates in solid tumors and hematological malignancies*. Lausanne: Frontiers Media SA. doi: 10.3389/978-2-8325-7297-9

Table of contents

frontiers | Frontiers in Immunology

TYPE Editorial
PUBLISHED 09 December 2025
DOI 10.3389/fimmu.2025.1752360

OPEN ACCESS

EDITED AND REVIEWED BY
Peter Brossart,
University of Bonn, Germany

*CORRESPONDENCE
Mirosława Püsküllüoğlu
miroslawa.puskulluoglu@krakow.nio.gov.pl
Renata Pacholczak-Madej
renata.pacholczak@uj.edu.pl

RECEIVED 23 November 2025
ACCEPTED 03 December 2025
PUBLISHED 09 December 2025

CITATION
Püsküllüoğlu M and Pacholczak-Madej R (2025) Editorial: Bispecific antibodies and their conjugates in solid tumors and hematological malignancies.
Front. Immunol. 16:1752360.
doi: 10.3389/fimmu.2025.1752360

Editorial: Bispecific antibodies and their conjugates in solid tumors and hematological malignancies

Mirosława Püsküllüoğlu[1]* and Renata Pacholczak-Madej[2,3]*

[1]Department of Clinical Oncology, Maria Skłodowska-Curie National Research Institute of Oncology, Kraków, Poland, [2]Department of Gynecological Oncology, Maria Skłodowska-Curie National Research Institute of Oncology, Kraków, Poland, [3]Department of Anatomy, Jagiellonian University Medical College, Kraków, Poland

KEYWORDS

bispecific antibodies, antibody-drug conjugates, hematological malignancies, solid tumors, emerging antibody technologies

Editorial on the Research Topic
Bispecific antibodies and their conjugates in solid tumors and hematological malignancies

Bispecific antibodies and related multispecific formats have evolved remarkably quickly from conceptual immuno-oncology tools to routine components of therapeutic algorithms in hematology and, increasingly, in solid tumors (1–3). This Research Topic was conceived to capture that transition across the full translational continuum: from antibody engineering and mechanistic studies in complex preclinical models, through early and late-phase clinical data, to systematic syntheses and critical evaluation of real-world and trial-based evidence. The articles collected here illustrate how rapidly the field is evolving, but also how heterogeneous the underlying biology, clinical development strategies and toxicity profiles remain.

Several contributions focus on acute leukemia, where bispecific T cell engagers were first clinically established. Cao et al. summarize the most recent bispecific antibody data presented at the 66th American Society of Hematology meeting, encompassing both acute lymphoblastic leukemia (ALL) and acute myeloid leukemia, as well as combinations with chemotherapy and other targeted agents. Their conference-based overview highlights not only consistently high measurable residual disease (MRD) negativity rates in relapsed/refractory B-ALL but also the diversification of targets and platforms entering clinical testing, as well as the operational challenges of delivering these agents outside highly specialized centers.

Blinatumomab, as the prototypical Cluster of differentiation (CD)19×CD3 T cell engager, is examined in depth in two complementary articles focused on pediatric B-ALL. Cheng and Liu provide a structured review of clinical trials of blinatumomab in children, emphasizing how disease burden, endogenous T cell competence, CD19 antigen modulation and lineage switch influence efficacy and relapse patterns, and how cytokine release syndrome and neurotoxicity can be anticipated and managed in this age group. In parallel, Zhang et al. report a multicenter pediatric cohort in which blinatumomab was used both as preemptive therapy in MRD-positive or chemotherapy-delayed patients and as

reinduction in relapsed/refractory disease. They document high MRD-eradication rates in chemotherapy-delayed and MRD-positive cohorts, response rates in frank relapse comparable to those seen in registrational trials, and identify adverse cytogenetics, CD19 loss and Breakpoint cluster region–Abelson 1 fusion positivity as predictors of inferior response. Together, these two articles illustrate how a single bispecific antibody can be integrated at different decision points along the paediatric ALL treatment trajectory, and how careful characterization of response determinants can guide patient selection and sequencing with transplantation or Chimeric antigen receptor T cell therapy.

In multiple myeloma, Li et al. present a systematic review and meta-analysis of teclistamab, a B cell maturation antigen×CD3 bispecific antibody, across clinical trials and real-world cohorts. Their synthesis confirms a survival advantage over existing regimens in relapsed/refractory disease, with robust response rates and deep remissions, while also demonstrating that patients treated outside of trials tend to have somewhat lower survival outcomes, likely reflecting shorter follow-up and higher baseline risk. Subgroup analyses suggest that combination regimens can further enhance response depth, at the cost of added toxicity. At the opposite end of the evidence spectrum, Chu et al. describe the successful use of the CD20×CD3 bispecific antibody glofitamab as salvage therapy in a patient with primary refractory diffuse large B cell lymphoma/high-grade B cell lymphoma-MYC proto-oncogene/B cell lymphoma 2 transformed from follicular lymphoma and resistant to modern chemoimmunotherapy. This carefully documented case illustrates how bispecific antibodies can provide meaningful disease control even in highly adverse biological subsets and argues for their timely consideration in transformed and double-hit lymphomas.

Beyond hematologic malignancies, several articles address dual-target and multispecific strategies in lung cancer and other solid tumors. Zhang et al. conducted a systematic review and meta-analysis of phase III randomized trials of dual-target immunotherapies in advanced non-small cell lung cancer, including bispecific antibodies and other dual-pathways. Their analysis shows improvements in progression-free survival and objective response compared with conventional regimens, but no clear overall survival benefit to date, and a consistent increase in treatment-related toxicity, particularly with Epidermal growth factor receptor/MET proto-oncogene-directed strategies. These findings underscore the need for better biomarker-driven patient selection and rational toxicity mitigation when multiple signaling or immune pathways are targeted simultaneously. Complementing this, Chen et al. provide a focused review of bispecific antibodies in lung cancer, describing the structural diversity of these agents, the range of antigen combinations under clinical investigation, and the mechanistic rationale for engaging immune effector cells or co-targeting oncogenic drivers. The accompanying correction, in which the authors amend the global lung cancer incidence figure, serves as a reminder that the rapid pace of progress must be matched by equal rigor in epidemiological and contextual reporting.

Three contributions illustrate how antibody engineering is being used to refine the balance between potency, selectivity and developability of next-generation molecules. Lin et al. characterize JS207, a bispecific antibody targeting Programmed cell death protein 1 and Vascular endothelial growth factor A, designed to deliver localized dual checkpoint and anti-angiogenic blockade. They show preserved binding to both targets, effective T cell activation, favorable internalization properties and encouraging antitumor activity in preclinical models, together with enhanced thermal stability relevant for manufacturing and shelf life. Ma et al. develop B7 homolog 6–targeted bispecific antibodies combined with Interleukin-15 receptor alpha chain sushi fusion to co-engage T and Natural killer cells against solid tumors resistant to chemotherapy. In xenograft models, they demonstrate dose-dependent tumor suppression and synergistic effects of combining two B7-H6–directed formats, supporting the concept that simultaneous recruitment of distinct effector compartments may overcome resistance in heavily pretreated disease. Löffler et al. introduce an engineered Fab–Fab-engineered immunoglobulin (eFab-eIg) trispecific platform that incorporates one classical Fab and two eFab moieties to achieve co-targeting of the human epidermal growth factor receptor 2 (HER2)/human epidermal growth factor receptor 3 (HER3) with CD3 engagement. Using two-dimensional and three-dimensional cancer models, they show that this modular architecture enables potent T cell retargeting against HER2/HER3-expressing tumor cells, while illustrating how stoichiometry and spatial arrangement can be exploited to tune activity and potentially reduce off-tumor effects.

This Research Topic shows bispecific and other multispecific antibodies that move from hematologic malignancies into lung and other solid tumors, including heavily pretreated, high-risk patients. They enable MRD-focused strategies, options for such disease and precision use guided by immunophenotype and genetics, but at the price of immune toxicities, serious infections and infusions that require close monitoring (4, 5). Translational work on cytokine-fusion, trispecific and other advanced formats shows how they remodel the tumor microenvironment, mobilize effector cells and counter immune escape and other resistance. Meta-analyses, real-world cohorts and smaller clinical series define priorities: biomarker-based target selection, integration with cellular therapies and radiation therapy, and long-term safety, sequencing, and survivorship study. Built to bridge diseases and disciplines, this 2024–2025 snapshot spans diverse cancers and study stages and aims to inform the next generation of bispecific and multispecific therapies.

Author contributions

MP: Writing – original draft. RP-M: Writing – review & editing.

Acknowledgments

We thank all contributing authors, reviewers, and the patients and families whose participation made this Research Topic possible.

Conflict of interest

The author(s) declared that this work was conducted in the absence of any commercial or financial relationships that could be construed as a potential conflict of interest.

Generative AI statement

The author(s) declared that generative AI was used in the creation of this manuscript. During preparation of this editorial, the authors used a generative artificial intelligence–based assistant (ChatGPT) to support language editing. All content was reviewed and approved by the authors, who take full responsibility for the final text.

Any alternative text (alt text) provided alongside figures in this article has been generated by Frontiers with the support of artificial intelligence and reasonable efforts have been made to ensure accuracy, including review by the authors wherever possible. If you identify any issues, please contact us.

Publisher's note

References

1. Yuan Z, Yang X, Jin H, Cui S, Li JB. Strategies for the generation of bispecific antibodies. *Chembiochem*. (2025) 2:e202500575. doi: 10.1002/CBIC.202500575

2. Lopatnikova JA, Sennikov SV. Bispecific immunotherapy based on antibodies, T-cell receptors, and aptamers: mechanisms of action, adverse effects, and future perspectives. *Front Immunol*. (2025) 16:1679092. doi: 10.3389/FIMMU.2025.1679092

3. Borrelli R, Brussino L, Negrini S, Felice Brizzi M. From molecular engineering to clinical applications: The expanding role of bispecific antibodies in onco-immunology. *Pharmacol Res*. (2025) 221:108000. doi: 10.1016/j.phrs.2025.108000

4. Pan D, Richter J. Management of toxicities associated with BCMA, GPRC5D, and fcRH5-targeting bispecific antibodies in multiple myeloma. *Curr Hematol Malig Rep*. (2024) 19:237–45. doi: 10.1007/S11899-024-00740-Z

5. Doig C, Yannakou CK. Toxicities associated with lymphoma-targeting bispecific antibodies-a review. *Front Med (Lausanne)*. (2025) 12:1582975. doi: 10.3389/FMED.2025.1582975

frontiers | Frontiers in Immunology

TYPE Case Report
PUBLISHED 31 March 2025
DOI 10.3389/fimmu.2025.1566035

OPEN ACCESS

EDITED BY
Renata Pacholczak-Madej,
Maria Skłodowska-Curie National Institute of Oncology, Poland

REVIEWED BY
Stefano Poletto,
IRCCS Candiolo Cancer Institute, Italy
Sandra Martinez Martin,
Peptomyc S. L., Spain

*CORRESPONDENCE
Jun Qian
qianjun@ujs.edu.cn
Jing-dong Zhou
zhoujingdong@ujs.edu.cn

†These authors have contributed equally to this work

RECEIVED 24 January 2025
ACCEPTED 13 March 2025
PUBLISHED 31 March 2025

CITATION
Chu M-q, Zhang T-j, Feng Y, Shao X, Ji Y-h, Qian J and Zhou J-d (2025) Successful treatment of primary refractory DLBCL/HGBL - MYC/BCL2 transformed from FL using glofitamab: a case report.
Front. Immunol. 16:1566035.
doi: 10.3389/fimmu.2025.1566035

Successful treatment of primary refractory DLBCL/HGBL - MYC/BCL2 transformed from FL using glofitamab: a case report

Ming-qiang Chu[1,2,3,4†], Ting-juan Zhang[1,2,3,4,5†], Yuan Feng[1,2,3,4†], Xun Shao[6], Yong-hui Ji[1,2,3,4], Jun Qian[1,2,3,4*] and Jing-dong Zhou[1,2,3,4*]

[1]Department of Hematology, The Affiliated People's Hospital of Jiangsu University, Zhenjiang, Jiangsu, China, [2]Institute of Hematology, Jiangsu University, Zhenjiang, Jiangsu, China, [3]Zhenjiang Clinical Research Center of Hematology, Zhenjiang, Jiangsu, China, [4]The Key Lab of Precision Diagnosis and Treatment of Zhenjiang City, Zhenjiang, Jiangsu, China, [5]Department of Oncology, The Affiliated People's Hospital of Jiangsu University, Zhenjiang, Jiangsu, China, [6]Department of Nuclear Medicine, The Affiliated People's Hospital of Jiangsu University, Zhenjiang, Jiangsu, China

Diffuse large B-cell lymphoma/high-grade B-cell lymphoma with *MYC* and *BCL2* rearrangements (DLBCL/HGBL-*MYC*/*BCL2*) represents a distinct entity of mature aggressive B-cell lymphoma, constituting a substantial gap in the clinical management of DLBCL. Conventional R-CHOP-like chemoimmunotherapy regimens have demonstrated limited efficacy in DLBCL/HGBL-*MYC*/*BCL2*, and the clinical outcome remains poor, with a median overall survival of less than 2 years, and even shorter in cases transformed from indolent lymphoma. We reported a 66-year-old female was firstly diagnosed with follicular lymphoma, but presented with disease progression to DLBCL/HGBL-*MYC*/*BCL2* during the treatment with BR regimen. Moreover, the patient was also primary refractory to Pola-R-CHP. The patient achieved partial response following treatment with the CD20×CD3 bispecific antibody glofitamab and maintained long-term remission. Although only one successful case is presented, glofitamab could be considered as salvage therapy for transformed relapsed/refractory DLBCL/HGBL-*MYC*/*BCL2*.

KEYWORDS

DLBCL/HGBL-MYC/BCL2, transformed, primary refractory, glofitamab, case report

Introduction

Diffuse large B-cell lymphoma/high-grade B-cell lymphoma with *MYC* and *BCL2* rearrangements (DLBCL/HGBL-*MYC*/*BCL2*) represents a distinct entity of mature aggressive B-cell lymphoma, which is either *de novo* DLBCL or transformed from indolent lymphoma (1, 2). The efficacy of R-CHOP-like chemoimmunotherapy regimens in these patients has been demonstrated to be limited (3–5). The median overall survival (OS) of these patients is less than 2 years, shorter than in patients with single or no *MYC*

rearrangements (6, 7). In the patients who have transformed from follicular lymphoma (FL), the median OS is only 7.9 months (8). The inferior clinical outcomes of these patients are attributed to distinctive cytomolecular genetics (9), with *MYC* and *BCL2* rearrangements having been revealed as pivotal contributors to the evolution of resistance (10). The median OS of the primary refractory patients was only 7.1 months (11). To address this dilemma, a range of treatment strategies are currently being investigated, including the dose-adjusted chemotherapy regimens, the incorporation of targeted agents, bispecific antibodies and chimeric antigen receptor T-cell (CAR-T). Few prospective trials have been reported for treating DLBCL/HGBL-*MYC*/*BCL2* patients. Although, in the ZUMA-12 trial, outcomes for patients with double-hit lymphoma were analyzed as a prespecified subgroup, showing high efficacy following axi-cel treatment, larger validation in ongoing phase 3 trials is critical given the limited subgroup size in this single-arm study (12, 13). Herein, we reported a case of DLBCL/HGBL-*MYC*/*BCL2* transformed from FL during the treatment with BR (bendamustine and rituximab) regimen, was primary refractory to Pola-R-CHP (polatuzumab vedotin, rituximab, cyclophosphamide, doxorubicin, and prednisone), and ultimately responded to the CD20×CD3 bispecific antibody glofitamab with a long-term partial response.

Case report

A 66-year-old Chinese woman was presented to our hospital on November 28, 2023, with a three-day history of abdominal pain. The patient had no significant medical history. No personal or family history of malignancies was documented. Psychosocial assessment revealed a retired factory worker living with spouse, with no history of smoking, alcohol use, or psychotropic medication. Physical examination showed that the bilateral supraclavicular lymph nodes were enlarged. Abdominal computed tomography (CT) scan showed multiple enlarged lymph nodes with partially fused, located around the abdominal cavity, along the retroperitoneal abdominal aorta, and adjacent to bilateral iliac arteries. Laboratory data showed that lactate dehydrogenase was elevated (760 U/L). Epstein-Barr virus-DNA test was positive (11200 copies/mL). Positron-emission tomography-computed tomography (PET-CT) showed high uptake of ^{18}F-fluorodeoxyglucose in multiple lymphadenopathies distributed across the abdominal, retroperitoneum, left upper mediastinum, left cervical III and V regions, left peri-clavicular and bilateral diaphragmatic feet posterior regions (Figure 1A). Then, the abdomen lymph node biopsy was performed. Histopathological examination confirmed low-grade FL in the lymph nodes. The immunohistochemical (IHC) results were as follows: CD20 (+), Ki67 (30%+), CD10 (+), Bcl2 (+), CD3 (-), CK (-), CD56 (-), Cyclin D1 (-), CD5 (-), PAX5 (-), c-Myc (-), Bcl6 (-) and MUM-1 (-). The bone marrow (BM) examination did not reveal any lymphoma cells infiltration. The patient was diagnosed with FL (stage III, group A), classified as high risk by the FL International Prognostic Index [FLIPI (score 3)] and low risk by FLIPI-2 (score 1). Subsequently, the patient was treated with BR (rituximab 600mg day 0 and bendamustine 125 mg day 1-2) and continued this protocol for 3 cycles. No adverse events were observed in this treatment.

The patient was assessed in progressive disease (PD) after 3 cycles of BR therapy by PET-CT with a substantial increase in the size of the formed enlarged lymph nodes (Figure 1B). Consequently, a second abdominal lymph node biopsy was conducted. The lymph nodes pathology was high-grade B-cell lymphoma with a tendency toward DLBCL originating within germinal center B-cell-like (GCB). The IHC results were as follows: CD20 (diffuse +), CD3 (scatter +), Ki67 (60%+), CD10 (+), Bcl2 (+), Bcl6 (+), CD30 (-), CD5 (-), MUM-1 (-), Cyclin D1 (-) and c-Myc (-), and. BM examination revealed no lymphoma cells infiltration. The patient was diagnosed with DLBCL/tFL (GCB, stage III, group A), classified as high intermediate risk by the National Cancer Institute-International Prognostic Index (score 4), and low intermediate risk by Central Nervous System-International Prognostic Index (score 3). The patient was subsequently treated with Pola-R-CHP (rituximab 600mg day 0, polatuzumab vedotin 90mg day 1, cyclophosphamide 1000mg day 1, epirubicin 90mg day 1 and prednisone 85 mg day 1-5). On day 10 following the first cycle of Pola-R-CHP therapy, the patient developed grade 4 neutropenia (Common Terminology Criteria for Adverse Events v5.0), which resolved promptly with granulocyte colony-stimulating factor support.

Unfortunately, the patient was assessed in PD after 2 cycles of Pola-R-CHP by PET-CT (Figure 1C). Subsequent cell-free DNA detection revealed that the molecular subtype was LymphGen-EZB/MYC$^+$ with *EZH2*, *TNFRSF14*, *ETV6*, *SOCS1*, *BCL2* and *MYC* mutations. The fluorescence *in situ* hybridization revealed *MYC* and *BCL2* rearrangements without *BCL6* translocation, thus leading to the diagnosis of DLBCL/HGBL-*MYC*/*BCL2*. Given the primary refractory status of this patient to first-line therapy and the double-hit (DHIT) of *MYC* and *BCL2* rearrangements, the prognosis was considered adverse, and salvage treatment was only possible if a new treatment scheme was adopted. After a thorough deliberation, the CD20×CD3 bispecific antibody glofitamab was administered in a step-up dosage regimen, with 2.5 mg on day 8 and 10 mg on day 15 (cycle 1) followed by a 30 mg flat dose on day 1 (cycle 2-12) with each cycle spanning 21 days. The patient developed only grade 1 cytokine release syndrome (CRS) during cycle 1, which resolved with symptomatic management. No other significant adverse events (e.g., neurotoxicity, prolonged cytopenia) or unanticipated complications were observed. A partial response (PR) was observed on PET-CT evaluation after 3 and 6 cycles of glofitamab treatment (Figure 1D, E). In order to enhance the effect of glofitamab, the immunomodulatory agent lenalidomide was

Abbreviations: DLBCL/HGBL-*MYC*/*BCL2*, diffuse large B-cell lymphoma/high-grade B-cell lymphoma with *MYC* and *BCL2* rearrangements; FL, follicular lymphoma; DHIT, double-hit; GCB, germinal center B-cell-like; CAR-T, chimeric antigen receptor T-cell; FLIPI, FL International Prognostic Index; SD, stable disease; PR, partial response; PD, progressive disease; OS, overall survival; R/R, relapsed/refractory; CT, computed tomography; PET-CT, positron-emission tomography-computed tomography; IHC, immunohistochemical; BM, bone marrow; IQR, Interquartile Range.

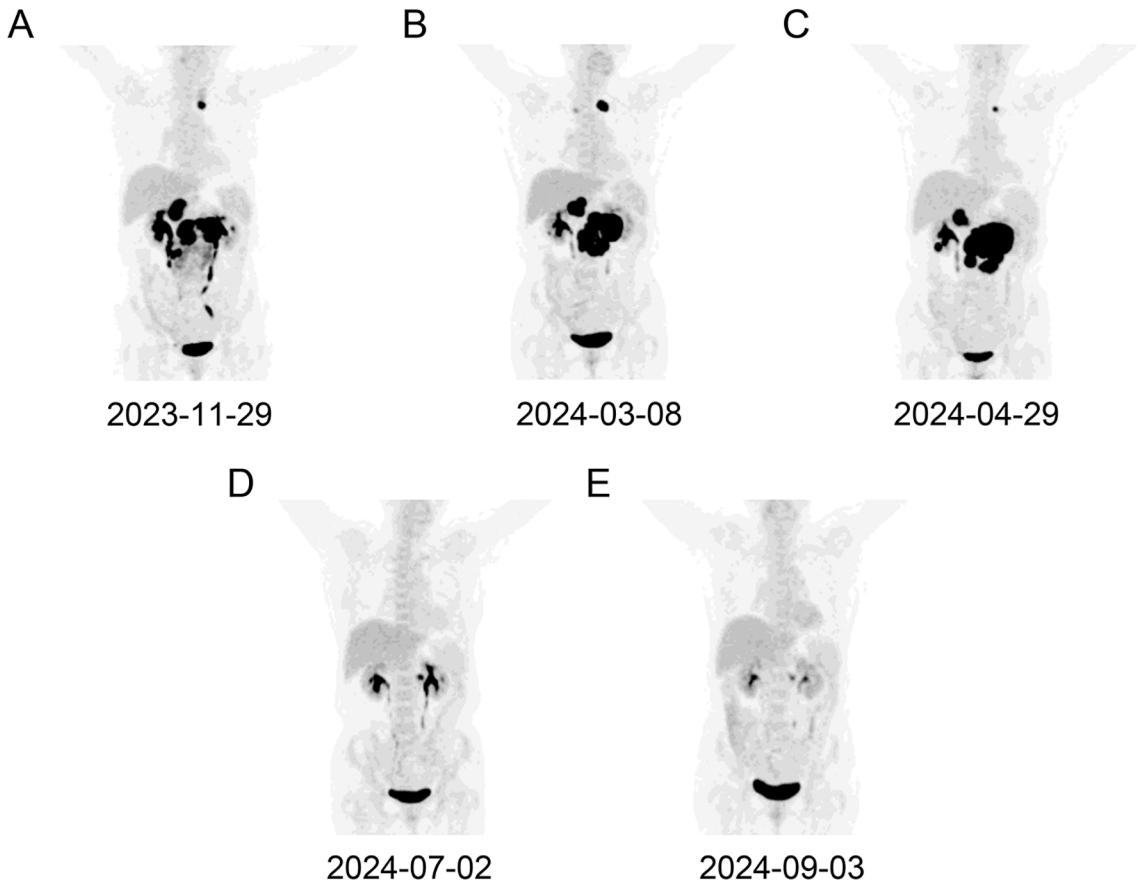

FIGURE 1
A dynamic evaluation of enlarged lymph nodes with PET-CT. The enlargement and reduction of lymph nodes at initial diagnosis **(A)**, PD following BR treatment **(B)**, PD following Pola-R-CHP treatment **(C)**, PR following glofitamab treatment **(D, E)**, respectively.

included in the treatment. Subsequently, the patient received glofitamab in combination with lenalidomide maintenance therapy until December 6th, 2024. The most recent CT scan revealed that the enlarged lymph nodes had ongoing shrunk after eight cycles of glofitamab therapy. Following glofitamab therapy, the median Functional Assessment of Cancer Therapy-Lymphoma (FACT-Lym) total score significantly increased from 93 [Interquartile Range (IQR): 86-110] to 140 (IQR: 131-155) at 6-month follow-up. The timeline of therapy is shown in Figure 2.

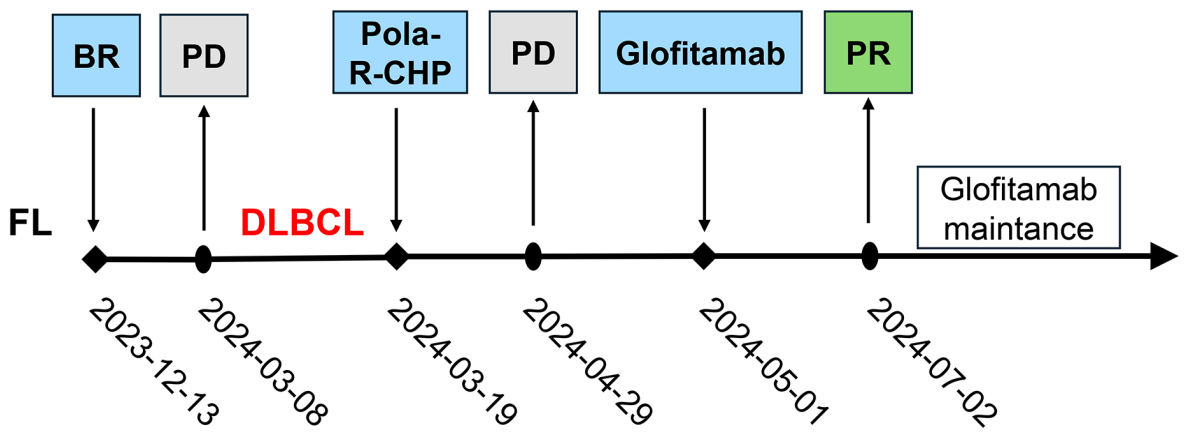

FIGURE 2
The timeline of treatment process in this case. FL, Follicular lymphoma; BR, bendamustine and rituximab; PD, progressive disease; DLBCL, Diffuse large B-cell lymphoma; Pola-R-CHP, polatuzumab vedotin, rituximab, cyclophosphamide, doxorubicin, and prednisone; PD, progressive disease; PR, partial response.

Discussion

The available treatment options for relapse/refractory (R/R) DLBCL include second-line immunochemotherapy without cross-resistance, targeted therapy, immunotherapy, autologous hematopoietic stem cell transplantation and CAR-T (9, 11). However, the clinical outcome of R/R DLBCL remains unsatisfactory, particularly for those who are refractory to frontline treatment with an objective response rate of merely 20% and 1-year survival rate of only 29% (14). Herein, we present an elderly DLBCL patient who experienced transformation from FL, accompanied by DHIT, *MYC* and *BCL2* mutations, and LymphGen-EZB/MYC^{+} subtype. Transformed FL (tFL) has been observed to exhibit worse clinical outcomes, particularly in cases of histological transformation following frontline treatments (15–17). However, there is an absence of a consensus regarding therapeutic regimens for primary refractory DLBCL/HGBL-*MYC*/*BCL2* (18).

A paucity of prospective trials has been reported for the treatment of DHIT patients, of which extant reports on such patients are predominantly constituted by retrospective analyses or empirical treatments. Currently, precision and targeted therapy is a promising strategy to delay and overcome treatment resistance. For R/R DLBCL, current developments are focused on the utilization of CAR-T cell treatment and bispecific antibodies (19). CAR-T cell treatment has been demonstrated to be efficacious in R/R DLBCL with durable remission in 30%-40% (19). However, hindrance of CAR-T broader application is its intricate manufacturing process with a minimum of 3-4 weeks of production time and a high cost. Actually, these R/R patients exhibit rapid clinical progression and necessitate more expeditious treatment. Bispecific antibodies offer a distinct advantage in this regard, as they are readily available. To date, two bispecific antibodies, epcoritamab and glofitamab, have been granted approval by the Food and Drug Administration for use in DLBCL patients who have received ≥3 prior lines of therapy (20, 21).

A recent phase III controlled clinical trial confirmed a superior efficacy of the combination with glofitamab in R/R DLBCL (22). However, it should be noted that the tFL and DHIT patients were excluded from this clinical trial. Several retrospective clinical analyses have revealed that glofitamab improves the prognosis of R/R DLBCL, including tFL and DHIT patients (23–26). However, these analyses were conducted on small clinical cohorts, with even fewer cases of tFL and DHIT. We hereby present a complex case with multiple adverse events in addition to DHIT, as well as primary resistance to front-line intensive chemoimmunotherapy. In the present report, we applied glofitamab to an elderly patient with refractory DLBCL/HGBL-*MYC*/*BCL2*. The patient exhibited PR following 3 cycles of glofitamab treatment and was subsequently treated with glofitamab for a period exceeding 7 months. Currently, the patient is assessed as maintain the PR and continues to benefit from glofitamab therapy. The incorporation of lenalidomide into the Glofitamab formulation may have facilitated disease management through its immunomodulatory properties, encompassing heightened T-cell activation and a synergistic effect with bispecific antibodies. The present case demonstrates the efficacy of glofitamab in DLBCL/HGBL-*MYC*/*BCL2*, thereby establishing a foundation for subsequent studies in this field. Nevertheless, further clinical trials with larger sample sizes are required to ascertain the efficacy of these bispecific antibodies in these specific subtypes of DLBCL/HGBL patients. Such trials should address the diagnostic challenges inherent to this entity, which require integration of histopathology with molecular techniques (e.g., Fluorescence *in situ* hybridization for *MYC*/*BCL2* rearrangements or next-generation sequencing) to avoid misclassification. To ensure meaningful results, study designs should prioritize multicenter collaboration to overcome recruitment barriers and incorporate adaptive trial frameworks with biomarker-driven stratification. Potential feasibility challenges include centralized molecular profiling to confirm eligibility, management of bispecific antibodies related CRS in high-risk populations, and long-term follow-up to assess delayed neurotoxicity. Addressing these considerations will be essential to translate targeted immunotherapies into clinically actionable strategies for this molecularly defined subgroup.

In this case report, a patient with primary refractory DLBCL/HGBL-MYC/BCL2 achieved PFS of over 7 months (ongoing) with glofitamab, exceeding the median OS of 6.3 months reported in the international SCHOLAR-1 study (11). Notably, this response aligns with the subset of patients in Hsu et al. (60% 1-year PFS in responders) and Shumilov et al. (19% with sustained complete remission at 6 months) (24, 25), demonstrating durable benefits in aggressive, heavily pretreated disease. The outcome highlights the potential of glofitamab to induce prolonged disease control even after multiple prior therapies, including CAR-T and bendamustine-based regimens.

Conclusion

In conclusion, we successfully treated a patient with transformed primary refractory DLBCL/HGBL-*MYC*/*BCL2* using the CD20×CD3 bispecific antibody glofitamab. Although only one successful case is presented, glofitamab could be considered as salvage therapy for transformed R/R DLBCL/HGBL-*MYC*/*BCL2*.

Data availability statement

The original contributions presented in the study are included in the article/Supplementary Material. Further inquiries can be directed to the corresponding author.

Ethics statement

The studies involving humans were approved by Ethics Committee of the Affiliated People's Hospital of Jiangsu University, Zhenjiang, China. The studies were conducted in accordance with the local legislation and institutional requirements. Written informed consent for participation was not required from the participants or the participants' legal guardians/

next of kin in accordance with the national legislation and institutional requirements. Written informed consent was obtained from the individual(s) for the publication of any potentially identifiable images or data included in this article.

Author contributions

MC: Data curation, Formal Analysis, Funding acquisition, Investigation, Writing – original draft. TZ: Funding acquisition, Investigation, Methodology, Writing – original draft. YF: Formal Analysis, Resources, Writing – original draft. XS: Data curation, Formal Analysis, Writing – original draft. YJ: Data curation, Resources, Writing – original draft. JQ: Conceptualization, Funding acquisition, Writing – review & editing. JZ: Conceptualization, Funding acquisition, Methodology, Validation, Writing – review & editing.

Funding

The author(s) declare that financial support was received for the research and/or publication of this article. The work was supported by National Natural Science Foundation of China (82300164, 82270179), Natural Science Foundation of Jiangsu Province (BK20221287, BK20230296), Research Project of Jiangsu Commission of Health (M2022123), Social Development Foundation of Zhenjiang (SH2022027, SH2023009), Graduate Research and Innovation Projects of Jiangsu Province (KYCX22_3718).

Conflict of interest

The authors declare that the research was conducted in the absence of any commercial or financial relationships that could be construed as a potential conflict of interest.

Generative AI statement

The author(s) declare that no Generative AI was used in the creation of this manuscript.

Publisher's note

References

1. Alaggio R, Amador C, Anagnostopoulos I, Attygalle AD, Araujo IBO, Berti E, et al. The 5th edition of the world health organization classification of haematolymphoid tumours: lymphoid neoplasms. *Leukemia*. (2022) 36:1720–48. doi: 10.1038/s41375-022-01620-2

2. Davies AJ. The high-grade B-cell lymphomas: double hit and more. *Blood*. (2024) 144:2583–92. doi: 10.1182/blood.2023020780

3. Johnson NA, Savage KJ, Ludkovski O, Ben-Neriah S, Woods R, Steidl C, et al. Lymphomas with concurrent BCL2 and MYC translocations: the critical factors associated with survival. *Blood*. (2009) 114:2273–9. doi: 10.1182/blood-2009-03-212191

4. Petrich AM, Gandhi M, Jovanovic B, Castillo JJ, Rajguru S, Yang DT, et al. Impact of induction regimen and stem cell transplantation on outcomes in double-hit lymphoma: a multicenter retrospective analysis. *Blood*. (2014) 124:2354–61. doi: 10.1182/blood-2014-05-578963

5. Oki Y, Noorani M, Lin P, Davis RE, Neelapu SS, Ma L, et al. Double hit lymphoma: the MD Anderson Cancer Center clinical experience. *Br J Haematol*. (2014) 166:891–901. doi: 10.1111/bjh.2014.166.issue-6

6. Rosenwald A, Bens S, Advani R, Barrans S, Copie-Bergman C, Elsensohn MH, et al. Prognostic significance of MYC rearrangement and translocation partner in diffuse large B-cell lymphoma: A study by the lunenburg lymphoma biomarker consortium. *J Clin Oncol*. (2019) 37:3359–68. doi: 10.1200/JCO.19.00743

7. El-Sharkawi D, Sud A, Prodger C, Khwaja J, Shotton R, Hanley B, et al. A retrospective study of MYC rearranged diffuse large B-cell lymphoma in the context of the new WHO and ICC classifications. *Blood Cancer J*. (2023) 13:54. doi: 10.1038/s41408-023-00827-5

8. Li S, Lin P, Fayad LE, Lennon PA, Miranda RN, Yin CC, et al. B-cell lymphomas with MYC/8q24 rearrangements and IGH@BCL2/t(14;18)(q32;q21): an aggressive disease with heterogeneous histology, germinal center B-cell immunophenotype and poor outcome. *Mod Pathol*. (2012) 25:145–56. doi: 10.1038/modpathol.2011.147

9. He MY, Kridel R. Treatment resistance in diffuse large B-cell lymphoma. *Leukemia*. (2021) 35:2151–65. doi: 10.1038/s41375-021-01285-3

10. Ennishi D, Mottok A, Ben-Neriah S, Shulha HP, Farinha P, Chan FC, et al. Genetic profiling of MYC and BCL2 in diffuse large B-cell lymphoma determines cell-of-origin-specific clinical impact. *Blood*. (2017) 129:2760–70. doi: 10.1182/blood-2016-11-747022

11. Crump M, Neelapu SS, Farooq U, Van Den Neste E, Kuruvilla J, Westin J, et al. Outcomes in refractory diffuse large B-cell lymphoma: results from the international SCHOLAR-1 study. *Blood*. (2017) 130:1800–8. doi: 10.1182/blood-2017-03-769620

12. Neelapu SS, Dickinson M, Munoz J, Ulrickson ML, Thieblemont C, Oluwole OO, et al. Axicabtagene ciloleucel as first-line therapy in high-risk large B-cell lymphoma: the phase 2 ZUMA-12 trial. *Nat Med*. (2022) 28:735–42. doi: 10.1038/s41591-022-01731-4

13. Chavez JC, Dickinson M, Munoz J, Ulrickson ML, Thieblemont C, Oluwole OO, et al. Three-year follow-up analysis of first-line axicabtagene ciloleucel in high-risk large B-cell lymphoma (ZUMA-12). *Blood*. (2025). doi: 10.1182/blood.2024027347

14. Sehn LH, Salles G. Diffuse large B-cell lymphoma. *N Engl J Med*. (2021) 384:842–58. doi: 10.1056/NEJMra2027612

15. Casulo C, Burack WR, Friedberg JW. Transformed follicular non-Hodgkin lymphoma. *Blood*. (2015) 125:40–7. doi: 10.1182/blood-2014-04-516815

16. Rusconi C, Anastasia A, Chiarenza A, Marcheselli L, Cavallo F, Rattotti S, et al. Outcome of transformed follicular lymphoma worsens according to the timing of transformation and to the number of previous therapies. A retrospective multicenter study on behalf of Fondazione Italiana Linfomi (FIL). *Br J Haematol*. (2019) 185:713–7. doi: 10.1111/bjh.2019.185.issue-4

17. Zha J, Fan L, Yi S, Yu H, Zheng Z, Xu W, et al. Clinical features and outcomes of 1845 patients with follicular lymphoma: a real-world multicenter experience in China. *J Hematol Oncol*. (2021) 14:131. doi: 10.1186/s13045-021-01139-6

18. Nowakowski GS, Blum KA, Kahl BS, Friedberg JW, Baizer L, Little RF, et al. Beyond RCHOP: A blueprint for diffuse large B cell lymphoma research. *J Natl Cancer Inst*. (2016) 108:djw257. doi: 10.1093/jnci/djw257

19. Trabolsi A, Arumov A, Schatz JH. Bispecific antibodies and CAR-T cells: dueling immunotherapies for large B-cell lymphomas. *Blood Cancer J*. (2024) 14:27. doi: 10.1038/s41408-024-00997-w

20. Dickinson MJ, Carlo-Stella C, Morschhauser F, Bachy E, Corradini P, Iacoboni G, et al. Glofitamab for relapsed or refractory diffuse large B-cell lymphoma. *N Engl J Med*. (2022) 387:2220–31. doi: 10.1056/NEJMoa2206913

21. Thieblemont C, Phillips T, Ghesquieres H, Cheah CY, Clausen MR, Cunningham D, et al. Epcoritamab, a novel, subcutaneous CD3xCD20 bispecific T-cell-engaging antibody, in relapsed or refractory large B-cell lymphoma: dose

expansion in a phase I/II trial. *J Clin Oncol*. (2023) 41:2238–47. doi: 10.1200/JCO.22.01725

22. Abramson JS, Ku M, Hertzberg M, Huang HQ, Fox CP, Zhang H, et al. Glofitamab plus gemcitabine and oxaliplatin (GemOx) versus rituximab-GemOx for relapsed or refractory diffuse large B-cell lymphoma (STARGLO): a global phase 3, randomised, open-label trial. *Lancet*. (2024) 404:1940–54. doi: 10.1016/S0140-6736(24)01774-4

23. Birtas Atesoglu E, Gulbas Z, Uzay A, Ozcan M, Ozkalemkas F, Dal MS, et al. Glofitamab in relapsed/refractory diffuse large B-cell lymphoma: Real-world data. *Hematol Oncol*. (2023) 41:663–73. doi: 10.1002/hon.v41.4

24. Hsu YT, Wu SJ, Kao HW, Hsiao SY, Liao CK, Chen TY, et al. Glofitamab as a salvage treatment for B-cell lymphomas in the real world: A multicenter study in Taiwan. *Cancer*. (2024) 130:1972–81. doi: 10.1002/cncr.v130.11

25. Shumilov E, Wurm-Kuczera R, Kerkhoff A, Wang M, Melchardt T, Holtick U, et al. Safety and efficacy of glofitamab for relapsed/refractory large B-cell lymphoma in a multinational real-world study. *Blood Adv*. (2024). doi: 10.1182/bloodadvances.2024014903

26. Song YQ, Zhang HL, Huang HQ, Zhang QY, Jing HM, Wang C, et al. Glofitamab monotherapy induces high complete response rates and manageable safety in Chinese patients with heavily pretreated relapsed or refractory diffuse large B-cell lymphoma. *Haematologica*. (2024) 109:1269–73. doi: 10.1111/bjh.15816

frontiers | Frontiers in Oncology

TYPE Mini Review
PUBLISHED 09 April 2025
DOI 10.3389/fonc.2025.1566202

OPEN ACCESS

EDITED BY
Renata Pacholczak-Madej,
Maria Skłodowska-Curie National Institute of Oncology, Poland

REVIEWED BY
Nai-Kong Cheung,
Memorial Sloan Kettering Cancer Center, United States
Mohamad Khawandanah,
Oklahoma State University Oklahoma City, United States

*CORRESPONDENCE
Jifeng Yu
Yujifengzzu@163.com
Xuejun Guo
pygxj@163.com

†These authors have contributed equally to this work

RECEIVED 24 January 2025
ACCEPTED 20 March 2025
PUBLISHED 09 April 2025

CITATION
Cao W, Ma S, Han L, Xing H, Li Y, Jiang Z, Guo X and Yu J (2025) Bispecific antibodies in immunotherapy for acute leukemia: latest updates from the 66th annual meeting of the American society of hematology, 2024. *Front. Oncol.* 15:1566202. doi: 10.3389/fonc.2025.1566202

Bispecific antibodies in immunotherapy for acute leukemia: latest updates from the 66th annual meeting of the American society of hematology, 2024

Weijie Cao[1†], Shuhan Ma[2†], Lijie Han[1†], Hanzhou Xing[1], Yingmei Li[1], Zhongxing Jiang[1], Xuejun Guo[2*] and Jifeng Yu[1*]

[1]Department of Hematology, The First Affiliated Hospital of Zhengzhou University, Zhengzhou, Henan, China, [2]Department of Hematology/Oncology, Puyang Oilfield General Hospital Affiliated with Xinxiang Medical College, Puyang, China

Bispecific antibodies (BsAbs) are cutting-edge immunotherapy agents that can bind two distinct antigens or epitopes simultaneously. They hold significant potential in targeting leukemic cell markers and activating immune cells like T cells or NK cells to eliminate malignant cells. BsAb treatments showed encouraging outcomes for both acute myeloid leukemia (AML) and acute lymphoblastic leukemia (ALL). In relapsed/refractory (R/R) ALL, BsAbs improved overall survival (OS) and achieved measurable residual disease (MRD) negativity in most patients. Blinatumomab plus standard chemotherapy or in combination with other treatments, such as Mini-Hyper-CVD and Inotuzumab Ozogamicin, improved disease-free survival (DFS) in B-ALL. In AML and related conditions, novel BsAbs like AFM28 (CD123xCD16A) and Vibecotamab (CD123xCD3) showed promising efficacy in heavily pretreated R/R AML and in MDS/CMML following the failure of treatment with hypomethylating agents (HMA). The meeting underscored the transformative potential of BsAbs, especially in ALL-focused trials, with ongoing research aiming to evaluate their safety and efficacy in broader patient populations and combination regimens. This summary highlights the latest progress in BsAb-based immunotherapy presented at the ASH 2024 meeting, held from December 7–10 in San Diego, California.

KEYWORDS

bispecific antibodies, acute lymphoblastic leukemia, acute myeloid leukemia, myelodysplastic syndrome (MDS), immunotherapy

Introduction

Bispecific antibodies (BsAbs) offer a novel and promising approach in cancer immunotherapy. With two distinct binding domains, these antibodies can simultaneously target either two different antigens or two epitopes of a single antigen. Recently, various BsAbs, such as CD19xCD3, CD123xCD16A, and CD123xCD3, have been developed to target specific B-cell markers or myeloid-cell markers on malignant leukemic cells with the goal of eradicating leukemic cells by engaging T cells or NK cells. These BsAbs have previously shown encouraging outcomes in heavily pretreated patients with relapsed/refractory (R/R) acute lymphoblastic leukemia (ALL) and acute myeloid leukemia (AML) (1, 2). This summary highlights the latest advancements in BsAb-based immunotherapy for acute leukemia, as presented at the 66th American Society of Hematology (ASH) 2024 annual meeting, held from December 7–10 in San Diego, California. Using the words "antibody" and "acute leukemia", "Bispecific" and "acute leukemia" combination search, we found 161 and 78 abstracts, respectively. We have selected 9 representative abstracts from these abstracts to summarize the novel bispecific antibodies and bispecific T-cell engagers (BITEs) that have entered clinical trials for the treatment of acute leukemia.

BsAb immunotherapy in ALL

Blinatumomab, a bispecific antibody (BsAb), helps CD3-positive T cells recognize and eliminate CD19-positive ALL. It has been approved for use in patients with R/R ALL. Research has shown that blinatumomab treatment significantly improves overall survival (OS) compared to chemotherapy in R/R B-ALL patients. Additionally, it has proven to be both safe and effective as a first-line therapy for children and young adults with B-ALL who are either resistant or intolerant to chemotherapy (1, 2). Numerous clinical trials are also underway to assess its use in R/R B-ALL, particularly in Philadelphia chromosome-positive (Ph+) ALL (Table 1).

A phase 1b trial with long-term follow-up found that subcutaneous (SC) blinatumomab treatment in heavily pretreated patients with R/R B-ALL resulted in high response rates and sustained remissions. Among the 27 patients, 24 (89%) achieved complete remission (CR) or CR with partial/incomplete hematological recovery (CRh/CRi) within two treatment cycles. In the 250μg/500μg dose group, 86% reached remission, while 92% in the 500μg/1000μg group did the same. In terms of measurable residual disease (MRD), 83% and 100% of responders in the two respective groups were MRD-negative (MRD $<10^{-4}$). After a median follow-up of 5.0 months (range 0.49–10.9), 88% of patients remained relapse-free, with a median overall survival (OS) of 9.8 months (range 6.5–14.3 months) (3).

A phase II trial investigating the combination of Mini-Hyper-CVD, Inotuzumab Ozogamicin (INO), and blinatumomab in R/R B-ALL patients showed promising results. The overall response rate (ORR) was 86%, with 65% achieving CR, among the 132 evaluable patients. Assessed by flow cytometry, MRD negativity was observed in 53% of patients following the first treatment cycle and in 85% overall. Following a median follow-up of 40 months (range 3–136), the 3-year OS and relapse-free survival (RFS) rates were 45% and 44%, respectively. The "dose-dense" (D-D) regimen, which involved administering Mini-Hyper-CVD and INO along with blinatumomab from day 4 to day 21 in a 28-day cycle for up to 6 cycles, yielded significantly improved outcomes. The 1-year OS rate for the D-D regimen was 94%, compared to 51% in Cohort 1 (Mini-Hyper-CVD and INO) and 66% in Cohort 2 (Mini-Hyper-CVD, INO, and blinatumomab for 4 cycles). The combination of blinatumomab and fractionated INO improved both safety and efficacy. The D-D approach showed high rates of early and deep MRD responses, suggesting it could be more effective than sequential treatment with these agents (4). A phase II trial combining Mini-Hyper-CVD, rituximab, INO, and blinatumomab in pediatric R/R B-ALL is also ongoing, with results pending (5).

A phase II study of Hyper-CVAD, with or without INO, and sequential blinatumomab in newly diagnosed B-ALL patients demonstrated that adding INO to the Hyper-CVAD + blinatumomab regimen improved overall OS in 75 patients with Ph-negative B-ALL. With a median follow-up of 38 months (range, 5–91 months), the 30-month RFS rates were 91% in the INO group versus 74% in the non-INO group (P=0.05), and OS rates were 100% versus 82% (P=0.008). In high-risk patients, the 30-month RFS was 92% in the INO group compared to 67% in the non-INO group (P=0.07), with OS rates of 100% versus 76% (P=0.05) (6).

A study evaluating the combination of Olverembatinib, Blinatumomab, and Chidamide (ABC regimen) in older patients with newly diagnosed Ph+ ALL demonstrated strong efficacy and safety. Among 9 patients, the regimen achieved an 88.8% complete molecular response (CMR) rate at 3 months. Additionally, the 1.5-year OS and event-free survival (EFS) rates were both 100%, with no relapses or deaths observed. These promising results suggest that the ABC regimen may significantly improve long-term survival in this patient population (7).

A phase III trial demonstrated that adding blinatumomab to chemotherapy improves DFS in newly diagnosed pediatric B-ALL with standard-risk. With a median follow-up of 2.5 years (IQR = 1.6-3.2) and 1440 evaluable patients, the 3-year DFS was 96.0 ± 1.2% for those in the blinatumomab group, compared to 87.9 ± 2.1% in the control group. This addition represents a significant breakthrough, establishing a new standard of care with important implications for treating children with newly diagnosed B-ALL (8).

Another phase III trial evaluating frontline ponatinib plus blinatumomab in adult Ph+ ALL patients showed promising results. Among 95 evaluable patients, 93 (98%) achieved complete hematologic remission (CHR), and 73% had a MRD response, including CMR and positive non-quantifiable results. After a median follow-up of 6.4 months (range 0.1–32.3), the estimated 18-month OS rate was 91.6%. These findings highlight the feasibility and efficacy of a chemo-free induction and consolidation regimen with ponatinib and blinatumomab in adults with Ph+ ALL, regardless of age. The combination was

TABLE 1 Clinical trials investigating bispecific antibodies for patients with acute leukemia.

ASH Abstract# (Reference #)	Leukemia types	Clinical trial phase	Regimen	Setting	Enroll number	Median number of prior LOT (range)	Median age (range) years	mFU (range) month	CR% or mCR %	ORR %	mDOR, month (range)	mPFS,or OS month	CRS total incidence % (grade >3, %)
1440 (#3)	ALL	Ib	SC blinatumomab as monotherapy	R/R B-ALL	27	2 (1-5)	52 (19-78)	5.0 (0.49-10.9)	89%	89%	5.2 (0.66-10.9)	3.8 (1.8-8.4)	N/A
2811 (#4)		II	Mini-Hyper-CVD with Inotuzumab Ozogamicin and Blinatumomab	R/R B-ALL	133	NA	37 (17-87)	40 (3-136)	65.00%	86.00%	N/A	3 yrs OS 45%, RFS 44%	N/A
1431.1 (#5)		II	Hyper-CVAD, with or without Inotuzumab Ozogamicin, and Sequential Blinatumomab	Newly diagnosed B-ALL	75	N/A	33 (18-59)	38 (5-91)	100.00%	100.00%	N/A	3 yrs OS 90%	N/A
1439 (#6)		II	Combination of 3rd Generation TKI Olverembatinib, Blinatumomab and Chidamide	Older newly diagnosed Ph+ ALL	9	N/A	61 (50-73)	14	100%	100%	N/A	1.5 yrs OS and EFS 100%	11% (0%)
1 (#8)		III	Blinatumomab Added to Chemotherapy	Newly diagnosed standard risk children B-ALL	1440	N/A	4.3 (2.8-6.4)	2.5 yrs (1.6-3.2 yrs)	N/A	N/A	N/A	3 yrs DFS 96.0% in treatment group vs 87.9% in control group; 3 yrs DFS 97.5% in treatment group vs 84.8% in control group.	N/A (0.3%)
835 (#9)		III	Frontline Ponatinib Plus Blinatumomab	Adult Ph+ ALL Patients of All Ages	133	N/A	57 (20-87)	6.4 (0.1-32.3)	98%	98%	N/A	Estimated 18-months OS 91.6%	N/A (1.5%)
738 (#10)	AML	I	bispecific CD123/ CD16A ICE	R/R AML	24	2 (1-3)	72 (28-82)	N/A	33% CR in 250mg group; 50% CR in 300mg group	N/A	N/A	N/A	8.3% (4.2%)

(Continued)

10.3389/fonc.2025.1566202

10.3389/fonc.2025.1566202

TABLE 1 Continued

ASH Abstract# (Reference #)	Leukemia types	Clinical trial phase	Regimen	Setting	Enroll number	Median number of prior LOT (range)	Median age (range) years	mFU (range) month	CR% or mCR %	ORR %	mDOR, month (range)	mPFS,or OS month	CRS total incidence % (grade >3, %)
1007 (#11)		II	Vibecotamab, a CD123xCD3 Bispecific T-Cell Engaging Antibody	MDS or CMML after								Hypomethylating Failure and in MRD-Positive AML	37
N/A	N/A	N/A	19 MDS, respond rate 68%,mCR 63%; 18 AML, 28% MRD-	N/A	N/A	N/A	68% (5%)						

BsAbs, bispecific antibodies; R/R B-ALL, relapsed/refractory B-cell acute lymphoblastic leukemia; T-ALL, T-cell acute lymphoblastic leukemia; R/R AML, relapsed/refractory acute myeloid leukemia; NR, not reached; NA, not available; CR, complete response; mCR, marrow complete remission; CRS, cytokine release syndrome; LOT, lines of therapy; mDOR, median duration of response; mPFS, median progression free survival; OS, overall survival; mFU, median follow-up; CMR, complete molecular response; ORR, overall response rate; mORR, median overall response rate; CI, confidence interval; CRi, CR with incomplete hematologic recovery; MDS, myelodysplastic syndrome; CMML, chronic myelomonocytic leukemia; MRD, minimal residual disease.

generally well tolerated, with few treatment discontinuations, even in elderly patients. This suggests that adjusting ponatinib dosing based on age may help reduce severe toxicities (9).

Overall, subcutaneous blinatumomab demonstrated similar or better efficacy than IV blinatumomab with a more convenient administration route. Mini-Hyper-CVD with inotuzumab and blinatumomab improved outcomes, with 1-year OS of 94% vs 51% in control group. Hyper-CVAD with blinatumomab and inotuzumab showed high MRD-negative rates and superior OS, with a 30-month OS of 100% vs 76% in control group. Blinatumomab significantly improved DFS in pediatric ALL, with a 3-year DFS of 96% vs 87.9% in control group, prompting early termination of randomization. Ponatinib + blinatumomab achieved excellent CR and OS rates in Ph+ ALL, outperforming prior ponatinib-based regimens.

BsAbs immunotherapy in acute myeloid leukemia

AFM28, a bispecific tetravalent innate cell engager (ICE) targeting CD123 and CD16A, was evaluated in a first-in-human phase 1 study among 24 R/R AML patients. AFM28 monotherapy demonstrated early clinical efficacy and a manageable safety profile at doses up to 300 mg per week. In the two highest dose cohorts, 4 out of 12 patients (33.3%) achieved either CR or CRi. At the highest dose (300 mg), 3 out of 6 patients achieved CR or CRi. These findings suggest that AFM28 may hold potential as a treatment for R/R AML (10).

Results from a phase II study of Vibecotamab, a CD123xCD3 bispecific T-cell engager (TCE) antibody, were reported in 37 patients with myelodysplastic syndrome (MDS), chronic myelomonocytic leukemia (CMML) following hypomethylating agent (HMA) treatment failure, and MRD-positive AML. Among the 19 MDS/CMML patients, 13 (68%) responded, with 12 (63%) achieving marrow complete remission (mCR) and 1 (5%) showing hematologic improvement (HI). Of the 16 MDS patients, 9 (56%) achieved mCR, 4 of whom (31%) also showed HI, and 1 (6%) had HI alone. For responders, the median duration of response was 5.2 months, and the overall survival (OS) was 10.3 months. In the 18 AML MRD-positive patients, 5 (28%) achieved MRD negativity, all after just 1 cycle. At the last follow-up, 2 responders relapsed after completing protocol therapy (1.2- and 5.6-months post-treatment), while 3 remained in MRD-negative remission, with durations of 4.1, 24.6, and 25.6 months. This study showed that Vibecotamab was safe and effective for treating low-blast, high-risk myeloid diseases, achieving a 68% response rate in MDS/CMML following HMA treatment failure and a 27% response rate in MRD-positive AML. Notably, 8 of the 10 relapses happened following the protocol therapy completion. As a result, the protocol was amended to allow indefinite treatment with Vibecotamab for responders. The clinical activity of Vibecotamab, particularly in high-risk patients and its lack of significant myelosuppression, suggests it may be a promising candidate for combination therapy in AML, MDS, and CMML (11).

Both studies highlight the potential of targeting CD123 in hematological malignancies, with encouraging results in patient subsets that are typically hard to treat. The therapies could be promising options in relapsed or refractory settings and warrant further investigation, especially in combination strategies.

In summary, the 66th ASH annual meeting showcased encouraging outcomes for various BsAbs in treating R/R ALL and R/R AML, with particularly notable success in R/R ALL trials. These therapies demonstrated significant potential, especially in heavily pretreated patients. Ongoing large-scale studies aim to further assess the efficacy, safety, and toxicity of BsAbs across different treatment settings and in combination with other therapeutic agents. Blinatumomab have received FDA approval for treating relapsed/refractory B-ALL (BLINCYTO® injection for the treatment of adults and children with CD19+B-cell precursor ALLin first or second CR with MRD ≥0.1%, or RR CD19+B-cell precursor ALL). Integrating BsAbs/BITEs into standard treatment regimens has demonstrated improved efficacy, the ability to overcome resistance, and synergy with other immunotherapies. These therapies may also serve as a bridge to CAR-T or hematopoietic stem cell transplantation in relapsed patients. Although challenges such as toxicity—particularly cytokine release syndrome (CRS)—and logistical issues persist, advancements in engineering longer-lasting molecules and combination approaches could help establish them as a cornerstone of cancer treatment.

Author contributions

WC: Writing – original draft, Data curation, Investigation. SM: Writing – original draft, Data curation, Investigation. LH: Writing – original draft, Data curation, Investigation. HX: Writing – review & editing, Investigation. YL: Writing – review & editing, Investigation. ZJ: Resources, Writing – review & editing. XG: Resources, Writing – review & editing. JY: Supervision, Writing – review & editing, Conceptualization.

Funding

The author(s) declare that financial support was received for the research and/or publication of this article. This paper was funded by the Science and Technology Department of Henan Province (CN) SBGJ202402041, granted to Dr. Jifeng Yu.

Acknowledgments

The authors would like to thank all the patients and their families for participating in clinical trials testing the drugs mentioned in this review.

Conflict of interest

The authors declare that the research was conducted in the absence of any commercial or financial relationships that could be construed as a potential conflict of interest.

Generative AI statement

The author(s) declare that no Generative AI was used in the creation of this manuscript.

Publisher's note

References

1. Hodder A, Mishra AK, Enshaei A, Baird S, Elbeshlawi I, Bonney D, et al. Blinatumomab for first-line treatment of children and young persons with B-ALL. *J Clin Oncol*. (2024) 42:907–14. doi: 10.1200/JCO.23.01392

2. Han L, Xing H, Cao W, Song Y, Jiang Z, Yu J. Bispecific antibodies in immunotherapy for adult acute leukemia: latest updates from the 65th American Society of Hematology 2023 Annual Meeting. *Expert Opin Biol Ther*. (2024) 24:221–3. doi: 10.1080/14712598.2024.2333793

3. Jabbour E, Zugmaier G, Sanchez PM, Rifon JJ, Agrawal V, Cassaday RD, et al. Single-agent subcutaneous blinatumomab for advanced B-cell acute lymphoblastic leukemia: long-term follow-up from a phase 1b dose expansion cohort. *Blood*. (2024) 144:1440. doi: 10.1182/blood-2024-205662

4. Habib D, Kantarjian HM, Haddad FG, Short NJ, Jain N, Senapati J, et al. Updated results of the combination of mini-hyper-CVD with inotuzumab ozogamicin and blinatumomab in patients with relapsed/refractory B-cell ALL. *Blood*. (2024) 144:2811. doi: 10.1182/blood-2024-210501

5. McCall D, Gibson A, Garcia MB, Nunez C, Roth ME, Cuglievan B. Phase II study of pedi-crib: mini-hyper-CVD with condensed rituximab, inotuzumab ozogamicin and blinatumomab (cRIB) for relapsed therapy for pediatric patients with B-cell lineage acute lymphocytic leukemia. *Blood*. (2024) 144:1431.1. doi: 10.1182/blood-2024-212144

6. Nguyen D, Kantarjian H, Short NJ, Jain N, Haddad FG, Yilmaz M, et al. Updated results from a phase II study hyper-CVAD, with or without inotuzumab ozogamicin, and sequential blinatumomab in patients with newly diagnosed B-cell acute lymphoblastic leukemia. *Blood*. (2024) 144:1439. doi: 10.1182/blood-2024-208854

7. Chen J, Zhou H, Liu Q. ABC regimen: combination of 3rd generation TKI olverembatinib, blinatumomab and chidamide for older new diagnosed ph-positive ALL patients. *Blood*. (2024) 144:5881. doi: 10.1182/blood-2024-200685

8. Rau RE, Gupta S, Kairalla JA, Rabin KR, Angiolillo A, Wang C, et al. Blinatumomab added to chemotherapy improves disease-free survival in newly diagnosed NCI standard risk pediatric B-acute lymphoblastic leukemia: results from the randomized children's oncology group study AALL1731. *Blood*. (2024) 144:1. doi: 10.1182/blood-2024-207450

9. Chiaretti S, Leoncin M, Elia L, Soddu S, Piciocchi A, Matarazzo M, et al. Efficacy and toxicity of frontline ponatinib plus blinatumomab for adult ph+ ALL patients of all ages. Intermediate analysis of the gimema ALL2820. *Blood*. (2024) 144:835. doi: 10.1182/blood-2024-207892

10. Montesinos P, Arnan M, Botton SD, Calbacho M, Veiga RR, Bories P, et al. Engaging innate immunity by AFM28, an innate cell engager (ICE®) targeting CD123-positive leukemic cells in patients with relapsed/refractory acute myeloid leukemia: safety and efficacy results of a first-in-human phase 1 study. *Blood*. (2024) 144:738. doi: 10.1182/blood-2024-194356

11. Nguyen D, Ravandi F, Wang SA, Jorgensen JL, Wang W, Loghavi S, et al. Updated results from a phase II study of vibecotamab, a CD3-CD123 bispecific T-cell engaging antibody, for MDS or CMML after hypomethylating failure and in MRD-positive AML. *Blood*. (2024) 144:1007. doi: 10.1182/blood-2024-208684

Glossary

ALL	acute lymphoblastic leukemia
AML	acute lymphoblastic leukemia
ASH	American Society of Hematology
BsAbs	bispecific antibodies
CHR	complete hematologic remission
CMML	chronic myelomonocytic leukemia
CMR	complete molecular response
CR	complete response
CRh	complete remission with partial hematological recovery
CRi	complete remission with incomplete hematological recovery
D-D	dose-dense
HI	hematologic improvement
HMA	hypomethylating agents
ICE	innate cell engager
INO	Inotuzumab Ozogamicin
mCR	marrow complete remission
MDS	myelodysplastic syndrome
MRD	minimal residual disease
OS	overall survival
RFS	relapse-free survival
R/R	relapsed or refractory

frontiers | Frontiers in Immunology

TYPE Systematic Review
PUBLISHED 25 April 2025
DOI 10.3389/fimmu.2025.1565407

OPEN ACCESS

EDITED BY
Renata Pacholczak-Madej,
Maria Skłodowska-Curie National Institute of Oncology, Poland

REVIEWED BY
Minh Diem Vu,
Independent Researcher, Zurich, Switzerland
Xiaoyang Li,
Shanghai Jiao Tong University, China

*CORRESPONDENCE
Xiaojing Yan
yanxiaojing_pp@hotmail.com

†These authors have contributed equally to this work and share first authorship

RECEIVED 23 January 2025
ACCEPTED 28 March 2025
PUBLISHED 25 April 2025

CITATION
Li W, Zhao D, Jiao Y, Dong W, Wang Z and Yan X (2025) Effectiveness and safety of teclistamab for relapsed or refractory multiple myeloma: a systematic review and meta-analysis.
Front. Immunol. 16:1565407.
doi: 10.3389/fimmu.2025.1565407

Effectiveness and safety of teclistamab for relapsed or refractory multiple myeloma: a systematic review and meta-analysis

Wenze Li[1†], Defeng Zhao[2†], Yu Jiao[1], Weilin Dong[1], Ziyi Wang[1] and Xiaojing Yan[1*]

[1]Department of Hematology, The First Affiliated Hospital of China Medical University, Shenyang, China, [2]Department of Thoracic Surgery, The First Affiliated Hospital of China Medical University, Shenyang, China

Background: Multiple myeloma (MM) is a hematological malignancy with limited treatment options for patients with relapsed/refractory MM (RRMM). Teclistamab, a B-cell maturation antigen (BCMA) × CD3 bispecific antibody, has shown promising results in clinical trials and real-world studies.

Methods: PubMed/MEDLINE, Web of Science, EMBASE, Cochrane Library, ClinicalTrials.gov, and meeting libraries were searched from inception to 14 November 2024. The assessed outcomes included overall survival (OS), progression-free survival, time to next treatment, duration of response, overall response rate (ORR), ≥complete response (≥CR), ≥very good partial response (≥VGPR), VGPR, partial response, and adverse events.

Results: In total, 34 studies involving 4,064 patients were included. In pairwise meta-analysis, teclistamab demonstrated superior OS [hazard ratio (HR) = 0.69, 95% confidence interval (CI): 0.54–0.89; p = 0.037] compared to existing RRMM treatments. Real-world studies showed comparable ORR (62%, 95% CI: 58%–66%) but slightly lower survival outcomes, possibly because of shorter follow-up times and higher-risk populations. Subgroup analyses revealed enhanced efficacy with combination therapies (ORR: 85% vs 62%, p < 0.0001) and notable clinical benefits in the China cohort (≥VGPR: 77%, ≥CR: 58%). Safety profiles indicated manageable cytokine release syndrome and immune effector cell-associated neurotoxicity syndrome, though infection risks required vigilant management.

Conclusions: Teclistamab continues to be a promising and effective treatment option for RRMM patients, including those previously exposed to BCMA-targeted therapies, and offers new hope for overcoming resistance and achieving better early disease control. Further research is needed to optimize its application in diverse populations, particularly in Asian cohorts.

Systematic Review Registration: https://www.crd.york.ac.uk/prospero/#myprospero, identifier CRD42025633838.

KEYWORDS

teclistamab, relapsed or refractory multiple myeloma, meta-analysis, bispecific antibodies, systematic review

1 Introduction

Multiple myeloma (MM) is a plasma cell malignancy characterized by uncontrolled overproduction of monoclonal immunoglobulin protein (M protein) and accounts for nearly 12% of hematological cancers (1, 2). Standard treatments for MM include proteasome inhibitors (PIs), immunomodulatory imide drugs (IMiDs), and anti-CD38 monoclonal antibodies. However, despite significant advancements in treatment options, MM remains an incurable disease. Available therapies for patients who are refractory to at least three drug classes (PIs, IMiDs, and anti-CD38 monoclonal antibodies) are limited, and their outcomes are generally poor (2–5). With a deepening understanding of disease biology, innovative therapeutic approaches continue to emerge.

In recent years, B-cell maturation antigen (BCMA)-directed therapies, including antibody-drug conjugates, chimeric antigen receptor (CAR) T-cells, and bispecific antibodies (BsAbs), have offered a new era of hope to patients with relapsed or refractory MM (RRMM). Teclistamab (JNJ-64007957, Janssen) is a bispecific antibody that targets the CD3 receptor complex on T cells and BCMA on MM cells (6). Preclinical studies have demonstrated the potent activity of teclistamab in MM cell lines, patient samples, and *in vivo* xenograft models (7). Teclistamab monotherapy was first demonstrated by the European Medicines Agency (EMA) on 23 August 2022 for the treatment of patients with RRMM who had received at least three prior lines of therapies including a PI, an IMiD, and an anti-CD38 antibody (8). Based on the positive response rates observed in the phase I/II MajesTEC-1 trial, the U.S. Food and Drug Administration (FDA) subsequently granted accelerated approval for teclistamab in patients with RRMM who had received at least four prior lines of therapy (9). Since the approval of teclistamab, many real-world studies have been conducted across various regions, including populations that did not meet the eligibility criteria of the MajesTEC-1 trial. Additionally, MajesTEC-1 also targeted another cohort of patients previously treated with BCMA-targeted therapies and reported promising efficacy (10).

With the increasing use of teclistamab in real-world settings, the number of related publications has also been steadily rising. Therefore, we conducted a comprehensive systematic review and meta-analysis aiming to compile and summarize the key data from all compared studies, clinical trials, and newly published real-world studies to deepen our clinical understanding of these therapies and provide significant insights into real-world physicians' decision-making.

2 Materials and methods

This systematic review and meta-analysis adhered to the PRISMA guidelines. The analysis was registered in PROSPERO (CRD42025633838).

2.1 Data source and search strategy

Eligible studies were identified by searching databases including PubMed/MEDLINE, Web of Science, EMBASE, Cochrane Library, and ClinicalTrial.gov. The main international hematology meetings, including the American Society of Clinical Oncology (ASCO), the American Society of Hematology (ASH), and the European Hematology Association (EHA), were also searched to identify additional newly published relevant studies. The search only included articles published before 14 November 2024. Search terms included ("Multiple Myeloma" OR "Kahler Disease" OR "Plasma Cell Myeloma" OR "Myelomatose") AND ("Teclistamab" OR "JNJ-64007957" OR "Bispecific antibody"). The specific search terms and strategies are listed in Supplementary Table S1.

2.2 Study selection

Potential trials were screened according to the following criteria: (1) patients diagnosed with RRMM; (2) randomized controlled trials (RCTs) and cohort studies; (3) teclistamab monotherapy or combined therapy was under investigation, with no restrictions on drug dosage; (4) clinical outcomes including any one or more of the following: overall survival (OS), progression-free survival (PFS), time to next treatment (TTNT), duration of response (DOR), overall response rate (ORR), ≥complete response (≥CR), ≥very good partial response (≥VGPR), VGPR, partial response (PR), and adverse events (AEs); (5) studies published in English language only.

The exclusion criteria were: (1) patients diagnosed with MM but not RRMM; (2) animal studies, comments, letters, reviews, and case reports; (3) the control arm was another CD3 × BCMA drug; (4) unpublished clinical trials; and (5) studies in which outcome data could not be extracted from texts, tables, or figures. Given the relatively short time since the approval of teclistamab, many clinical trials and real-world studies have presented their findings in the form of conference abstracts which were not excluded from the study.

2.3 Data extraction and quality assessment

Two authors (Li and Zhao) independently screened the literature and extracted the data, with any disagreements resolved by a third author (Jiao). The following extracted data were sorted into designed spreadsheets. (1) General study information including first author, publication years, article type, trial phase, National Clinical Trial (NCT) number, drug usage, and country. (2) Basic patients' information included age, sex, refractory status, time to onset years, Eastern Cooperative Oncology Group (ECOG) scores, cytogenic risk status, International Staging System (ISS) stage, lines of previous therapies, and anti-BCMA exposure rate. (3) The main outcomes assessed were OS, PFS, TTNT, and DOR [hazard ratio (HR) and 95% confidence interval (CI)]; ORR, ≥CR, ≥VGPR, VGPR, and PR [relative risk (RR) or odds ratio (OR)]; and any-grade or grade ≥3 AEs, i.e., infection, neutropenia, anemia, cytokine release syndrome (CRS). and immune effector cell-associated neurotoxicity syndrome (ICANS). For articles that did not report OR or RR, the results were calculated using the MedCalc

website (11). The extracted raw data can be found in Supplementary Tables S2 and S3. To avoid duplicate data, only the most recent records were included and the long-term follow-up and subgroup analysis of the MajesTEC-1 trial were not included in the subsequent analysis. Most of the included studies were derived from conference abstracts, therefore, it was challenging and inaccurate to conduct a quality assessment.

2.4 Statistical analysis

Statistical analysis was performed using R 4.3.2 software. Because of the expected heterogeneity across the included studies, we chose a random-effects model over a fixed-effects model (12). HRs for survival outcomes (OS, PFS, TTNT, and DOR) and RRs and ORs for binary outcomes (ORR, ≥CR, ≥VGPR, VGPR, PR, and any-grade and severe-grade AEs) were calculated, along with their 95% CIs. The single-arm meta-analysis was conducted to calculate the overall rates of objective response and AEs of each treatment strategy from all eligible studies. Statistical heterogeneity among the studies was evaluated using the I^2 statistic (13). Subgroup analyses were performed based on common characteristics across the included trials, such as region, study design, anti-BCMA exposure, and mono- or combined therapy. To address potential publication bias, weight functions were incorporated into the models to adjust the overall effect size estimates, and sensitivity analyses were conducted to assess their impact. Publication bias was corrected using a trim-and-fill method, which accounted for funnel plot asymmetry (14).

3 Results

3.1 Study selection and characteristics

A total of 2,674 studies describing teclistamab for RRMM were found, with 581 studies from PubMed, 822 from Web of Science, 1,134 from EMBASE, 58 from Cochrane Library, and 79 from ClinicalTrials.gov. Furthermore, 12 additional records were identified through hand-searching conference abstracts. After removing 721 duplicate records, we reviewed the titles and abstracts of 1,065 articles, identifying 91 articles as potentially relevant for further analysis. After the application of the eligibility criteria to full-text review, 34 studies were included, with 9 studies that compared the efficacy and safety of teclistamab with currently and commonly used treatments for RRMM (15–23); 11 studies that were single-arm teclistamab clinical trials (9, 10, 24–32); and 14 studies that focused on real-world applications of teclistamab monotherapy (33–46). The complete screening process is listed in Figure 1, and the titles of excluded articles and the reasons for their omission are listed in Supplementary Table S4. There was a total of 4,064 patients in the included studies, with an average age of ~66 years. The baseline characteristics are summarized in Table 1.

3.2 Efficacy and safety of teclistamab in compared studies

To compare the efficacy between teclistamab and currently used treatments for RRMM, we synthesized data on OS, PFS, TTNT, and DOR. The treatment measurements for the control group included selinexor plus dexamethasone (15), daratumumab (DARA) trials (18), belantamab mafodotin (19), pomalidomide plus dexamethasone (22), CAR-T (21, 23), and real-world clinical practice (16, 17, 20). Eight studies reported OS, six studies described PFS, four studies reported TTNT, and three studies reported DORs. In terms of survival outcomes, teclistamab demonstrated superior therapeutic advantages (Figure 2). The HR values for pooled OS, PFS, TTNT, and DOR were 0.69 [(95%CI: 0.54–0.89), p = 0.037], 0.49 [(95%CI: 0.42–0.57), p < 0.0001], 0.38 [(95%CI: 0.30–0.48), p < 0.0001], and 0.19 [(95%CI: 0.06–0.59), p = 0.0044], respectively. Considering the differences in variability in the data sources and the lack of baseline characteristic balancing in some studies, we conducted subgroup analyses of OS (Supplementary Figure S1). Four studies reported ORs (15, 18, 19, 21) and three studies describe RRs (16, 20, 21), respectively. As for the ORs, no significant differences were observed for ORR [effect size (ES) = 1.69, 95%CI: 0.51–5.58] and ≥CR (ES = 2.67, 95%CI: 0.31–24.25). As for RR, there was no statistically significant difference in ORR (ES = 1.51, 95%CI: 0.64–3.53) and ≥CR (ES = 7.39, 95%CI: 0.03–1810.94) as well (Figures 3A, B). However, after excluding the study that did not balance the baseline characteristics (21), regardless of whether OR or RR was reported, both ORR and ≥CR showed statistically significant differences (Supplementary Figure S2), suggesting that teclistamab achieved a higher response rate compared with existing treatment options. Compared to current treatments, teclistamab demonstrated superior outcomes in ≥VGPR (ES for RR = 5.94, 95% CI: 4.39–8.03; ES for OR = 6.55, 95% CI: 1.87–22.96) (Figure 3C). In the safety analysis, no significant differences were observed for any-grade ICANs (ES = 0.81, 95% CI: 0.53–1.25). However, compared to CAR-T, teclistamab was associated with lower incidences of any-grade CRS (ES = 0.77, 95% CI: 0.64–0.93) (Figure 3D).

3.3 Efficacy and safety of teclistamab in real-world events

In the real-world events meta-analysis, 11 studies reported ORRs (33–41), 7 studies reported ≥VGPRs (33, 36, 38, 40, 44–46), 6 studies reported ≥CRs (33, 37–39, 44, 45) and 7 studies reported PRs (33, 36, 38, 40, 44–46). Across all the teclistamab studies, regardless of region and ethnicities, the pooled ORR was 62% (95%CI: 58%–66%), ≥VGPR was 43% (95% CI: 36%–50%) (Figures 4A, B), ≥CR was 22% (95%CI: 16%–28%), and PR was 10% (95% CI: 7%–13%) (Supplementary Figure S3). The pooled incidence of any-grade CRS was 57% (95%CI: 53%–61%) and any-grade ICANs was 9% (95%CI: 7%–13%) (Figures 4C, D). Other AEs were all pooled and are shown in Supplementary Figure S4.

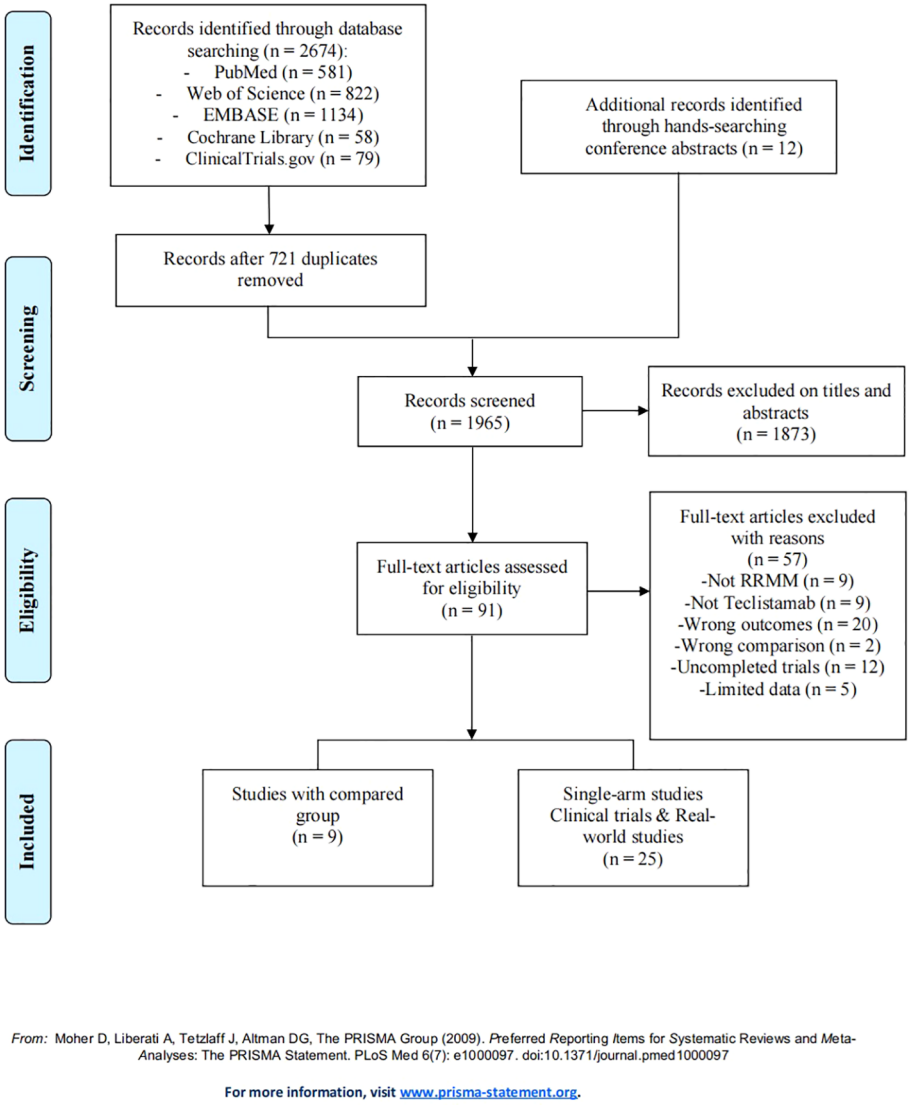

FIGURE 1
PRISMA flow diagram.

3.4 Subgroup analysis of single-arm studies

First, to explore whether there were differences in efficacy and safety between teclistamab monotherapy and combination therapy, we conducted a subgroup analysis. Three clinical trials reported a combination therapy with teclistamab (24, 25, 28). The combination therapy group displayed a higher ORR (85% vs 62%, $p < 0.0001$) and a higher ≥VGPR (68% vs 48%, $p = 0.0247$) than monotherapy while showing a similar ≥CR with monotherapy (29% vs 28%, $p = 0.8481$) (Supplementary Figure S5). For AEs, no statistically significant differences were observed for any-grade anemia, CRS, infection, and neutropenia, and grade ≥3 anemia, CRS, ICANS, infection, and neutropenia (Supplementary Figure S6).

Second, there were no significant differences in efficacy between clinical trials and real-world studies, except for ≥VGPR (60% vs 48%, $p = 0.0247$) and ≥CR (41% vs 22%, $p = 0.0052$). The pooled ORR, VGPR, and PR were 63% versus 62% ($p = 0.7992$), 19% versus 25% ($p = 0.4222$), and 13% versus 10% ($p = 0.8171$), respectively. The forest plot can be found in Supplementary Figure S7. For hematological AEs, compared to clinical trials, real-world studies exhibited a lower risk of neutropenia (any-grade: 79% vs 45%, $p = 0.0017$; grade ≥3: 66% vs 33%, $p = 0.0001$). No significant differences were observed in the risk of anemia (any-grade: 63% vs 66%, $p = 0.8549$; grade ≥3: 39% vs 23%, $p = 0.1003$). For non-hematological AEs, real-world studies had a lower risk of any-grade CRS (79% vs 58%, $p = 0.0301$), a lower risk of infection (any-grade: 81% vs 47%, $p = 0.0002$; grade ≥3: 50% vs 24%, $p = 0.0003$), and a higher risk of ICANS (any-grade: 3% vs 10%, $p = 0.0297$) (Supplementary Figure S8).

Third, compared with a Western population, the China cohort demonstrated superior ≥VGPR (77% vs 45%, $p = 0.0021$) and ≥CR (58% vs 25%, $p = 0.0020$). There were no statistically significant differences in ORR (77% vs 62%, $p = 0.1098$). As for AEs, the China

TABLE 1 Characteristics of the included studies.

A)												
Comparative studies												
Author	Year	Article type	Drug name	Patient (n)	Age (years)	Sex (F/M, n)	Refractory status (5/4,3/other, n)	Time to onset (years)	ECOG scores (0/1, n)	Cytogenic risk status (high/standard/unknown, n)	ISS stage (I/II/III, n)	Lines of previous therapy
Bahlis, N. J (15).	2022	Conference abstract	Tec	37	NR	NR	NR	NR	NR	NR	NR	≥3 prior LOT
			Sel+ Dex	122								
Delforge, M (16).	2023	Conference abstract	Tec	165	NR	NR	NR	NR	NR	NR	NR	≥3 prior LOT
			RWPC	112								
Krishnan, A (17).	2023	Article	Tec	165	≥65: 47.9%	69/96	50/78/37	≥6: 50.9%	55/110	38/110/17	87/58/20	> 4 prior LOT: 52.7%
			RWPC	326	≥65: 48.1%	152/174	107/151/68	≥6: 52.3%	112/214	74/217/35	172/116/38	> 4 prior LOT: 56%
Mateos, M.V (18)	2023	Article	Tec	165	≥65: 47.9%	69/96	50/78/37	≥6: 50.9%	55/110	38/110/17	87/58/20	> 4 prior LOT: 52.7%
			Dara trials	264	≥65: 46.9%	133/131	75/120/69	≥6: 47.5%	119/145	58/179/27	142/94/28	> 4 prior LOT: 52.5%
Moreau, P (19).	2023	Conference abstract	Tec	165	NR	NR	NR	NR	NR	NR	NR	≥3 prior LOT
			BM	97								
Moreau, P (20).	2023	Article	Tec	165	≥65: 47.9%	69/96	50/78/37	≥6: 50.9%	55/110	NR	87/58/20	> 4 prior LOT: 52.7%
			RWPC	302	≥65: 44.1%	132/170	108/129/64	≥6: 54.3%	93/209	NR	163/104/35	> 4 prior LOT: 55.9%
Rakesh Popat (22)	2024	Conference abstract	Tec	165	NR	NR	NR	NR	NR	NR	NR	≥3 prior LOT
			Pom+Dex	645								
Dima, D (21).	2024	Conference abstract	Tec	45	Median: 68	19/26	Penta:26	NR	≥2:16	High:25	III:16	Median 6 prior LOT
			CAR-T	65	Median: 62	28/37	Penta:26	NR	≥2:9	High:19	III:17	Median 6 prior LOT
Song, J (23).	2024	Conference abstract	Tec	458	Median: 66	391/458	NR	NR	NR	NR	NR	≥4 prior LOT
			CAR-T	391								

10.3389/fimmu.2025.1565407

B)

Single-arm clinical trials

Author	Year	Trial #	Study Design	Drug name	Usage	Patient (n)	Median age in years (range)	Median follow-up in months (range)	Sex (F/M, n)	Refractory status (5/4,3/other, n)	Time to onset (years)	ECOG scores (0/1, n)	Cytogenic risk status (n)	ISS stage (I/II/III, n)	Lines of previous therapy	Anti-BCMA exposed (%)
Moreau, P (9).	2022	MajesTEC-1: NCT03145181 NCT04557098	Open label, single-arm, phase 1-2 study	Tec	SC 1.5mg/kg	165	64.0 (33.0-84.0)	14.1 (0.3-24.4)	69/96	50/78/37	6 (0.8-22.7)	55/110	High: 38	85/57/20	Median 5 prior LOT	Not allowed
Rodríguez-Otero, P (24).	2022	NCT04108195	Phase 1b multicohort TRIMM-2 study	Tec + Dara	Dara: SC 1800 mg/schedule Tec: SC 1.5–3 mg/kg	46	67 (50–79)	7.2 (0.1-16.6)	24/22	NR	NR	NR	NR	NR	Median 6 prior LOT	15%
Cohen,Y. C (25).	2023	NCT04586426	Phase 1b RedirecTT-1 trial	Tec + Tal	NR	63	67 (39–81)	14.4 (0.5-21.9)	NR	Triple-class refractory: 49	NR	NR	High: 15	NR	Median 5 prior LOT	NR
Donk, N.1 (26)	2023	MajesTEC-1	Subgroup analysis	Tec	SC 1.5mg/kg	165	64.0 (33.0-84.0)	23	69/96	50/78/37	6 (0.8-22.7)	55/110	High: 38	85/57/20	Median 5 prior LOT	Not allowed
Donk, N.2 (26)	2023	MajesTEC-1	MajesTEC-1 Update	Tec	SC 1.5mg/kg	165	64.0 (33.0-84.0)	22	69/96	50/78/37	6 (0.8-22.7)	55/110	High: 38	85/57/20	Median 5 prior LOT	Not allowed
Searle, E (28).	2023	MajesTEC-2 NCT04722146	Open-label, multi-arm, phase 1b study	Tec+ Dara + Len	TEC 0.72/1.5 mg/kg with step-up dosing+ Dara 1800 mg+ LEN 25 mg	32	62	5.78 (1.0-10.4)	4/28	NR	NR	NR	NR	NR	Median 2 prior LOT	Not allowed
Du juan (32)	2024	MajesTEC-1 China cohort	Open-label, single-arm, phase 1-2 study	Tec	SC 1.5mg/kg	26	66	15	19/7	Triple-class refractory: 16	NR	NR	High: 15	III:7	Median 5 prior LOT	Not allowed
Garfall, A. L (29).	2024	MajesTEC-1	MajesTEC-1Update	Tec	SC 1.5mg/kg	165	64.0 (33.0-84.0)	30.4	69/96	50/78/37	6 (0.8-22.7)	55/110	High: 38	85/57/20	Median 5 prior LOT	Not allowed
J Costa, L (30).	2024	MajesTEC-1	Subgroup analysis	Tec	SC 1.5mg/kg	165	64.0 (33.0-84.0)	30	69/96	50/78/37	6 (0.8-22.7)	55/110	High: 38	85/57/20	Median 5 prior LOT	Not allowed
Touzeau, C (10).	2024	MajesTEC-1 Cohort C	Open-label, single-arm, phase1-2 study	Tec	SC 1.5mg/kg	40	64 (32–82)	28 (0.7-31.1)	15/25	Triple-class refractory: 34	6.5 (1.1-24.1)	NR	High: 12	21/9/10	Median 6 prior LOT	100%
Donk, N (31).	2024	NCT05972135	Phase 2, multicenter, prospective OPTec study	Tec +Toci	SC 1.5mg/kg +IV Toci 8 mg/kg	24	72 (50-82)	8.1 (0.9-13.2)	NR	Triple-class refractory: 14	NR	NR	Standard:18	I/II: 23	Median 4 prior LOT	Not allowed

10.3389/fimmu.2025.1565407

C)

Real world experiences

Author	Year	Country	Article type	Patient (n)	Median age (range)	Sex (F/M, n)	Refractory status (n)	Time to onset (years)	ECOG scores (n)	Cytogenic risk status (%)	ISS stage (I/II/III, n)	Lines of previous therapy	Anti-BCMA exposed (%)
Uttervall, K. (33)	2021	Sweden	Conference abstract	17	62 (43-83)	7/10	Triple-class refractory: 15	NR	NR	NR	NR	Median 9 prior LOT	NR
Asoori, S (34).	2023	USA	Conference abstract	37	71 (50-89)	20/17	NR	NR	NR	NR	NR	NR	NR
Dima, D (35).	2023	USA	Conference abstract	102	75 (71-87)	NR	Triple-class refractory: 99	NR	NR	High: 58%	NR	Median 6 prior LOT	58%
Gordon, B (36).	2023	USA	Conference abstract	45	66 (45-88)	24/21	NR	4.9 (1.1-25.8)	0: 14 1: 19 ≥2: 12	High: 42.2%	11/13/12	Median 6 prior LOT	42.2%
Grajales-Cruz, A. F (37).	2023	USA	Conference abstract	22	66 (48-81)	9/13	Penta-class refractory: 11	NR	≥2: 3	High: 50%	III: 10	Median 8 prior LOT	100%
Maringanti, S. A (38).	2023	US, Greece, Spain	Conference abstract	80	69 (38–91)	36/44	Triple-class refractory: 49	NR	NR	High: 25%	NR	Median 6 prior LOT	50%
Dima, D (39).	2024	USA	Article	106	66.5 (35-87)	57/49	Triple-class refractory: 97	5.4 (0.5-20)	0-1: 71 2-4: 35	High: 59%	NR	Median 6 prior LOT	53%
Firestone, R. S (40).	2024	USA	Article	52	70 (39-88)	NR	Penta-class refractory: 35	6.3 (0.7-29)	0: 8 ≥1: 44	High: 33%	NR	Median 7 prior LOT	52%
Ghamsari, F (41).	2024	USA	Conference abstract	18	67 (50-83)	NR	Triple-class refractory: 18	NR	NR	High: 72%	NR	Median 6.5 prior LOT	39%
Graf, K. C (42).	2024	USA	Article	25	66 (37-78)	12/13	Penta-class refractory: 12	NR	NR	High: 36%	NR	Median 5 prior LOT	44%
Kawasaki, Y (43).	2024	USA	Article	All:27	69	12/15	NR	NR	1: 13	NR	NR	Median 5 prior LOT	NR
				1, 3, 5 days:23	69	9/14			1: 12				
				1, 4, 7 days:4	64	3/1			1: 1				
Mohan, M. (44)	2024	USA	Article	110	68 (37–89)	54/56	Penta-class refractory: 84	NR	NR	High: 62%	NR	Median 6 prior LOT	35%
Riedhammer, C (45).	2024	Germany	Article	123	67 (35-87)	53/70	Penta-class refractory: 74	6.5 (0.5-18.7)	NR	High: 36.8%	25/35/31	Median 6 prior LOT	37.4%
Tan, C. R (46).	2024	USA	Conference abstract	77	70 (63-77)	35/42	NR	NR	NR	High: 42%	NR	NR	NR

Sel, selinexor; Dex, dexamethasone; Tec, teclistamab; RWPC, real-world physician's choice; LOT, lines of therapy; Dara, daratumumab; Pom, pomalidomide; BM, belantamab mafodotin; CAR-T, chimeric antigen receptor T cell; LEN, lenalidomide; Tal, talquetamab; Toci, tocilizumab; SC, subcutaneous; IV, intravenous; NR, not reported.

10.3389/fimmu.2025.1565407

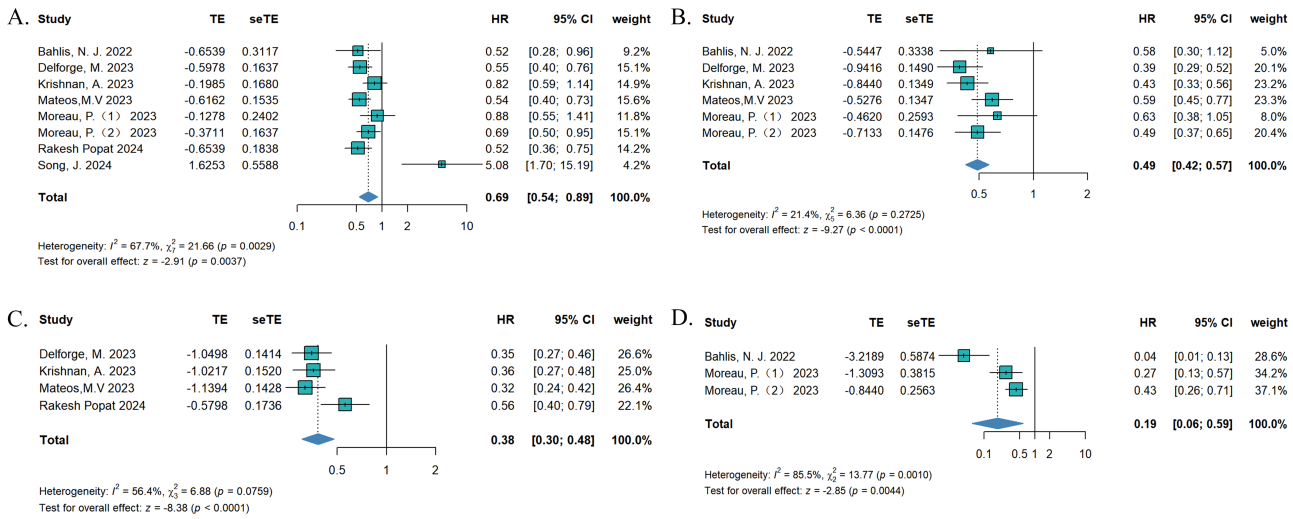

FIGURE 2
The pooled **(A)** OS, **(B)** PFS, **(C)** TTNT, and **(D)** DOR in patients treated with teclistamab in the compared studies.

cohort experienced a higher rate of any-grade anemia (88% vs 60%, p = 0.0078), any-grade CRS (96% vs 60%, p < 0.0001), any-grade infection (96% vs 53%, p < 0.0001), and any-grade neutropenia (96% vs 55%, p < 0.0001). The forest plots are listed in Supplementary Figure S9.

Fourth, five studies reported the outcomes of teclistamab treatment in populations previously exposed to BCMA-targeted therapies (10, 38–40, 45), and six studies reported the outcomes of populations with no prior BCMA exposure (9, 32, 38–40, 45). The non-BCMA-exposed group displayed a higher ORR than the anti-BCMA-exposed group (67% vs 56%, p = 0.0205). For the anti-BCMA exposed group, the pooled ≥VGPR, ≥CR, VGPR, and PR were 46% (95%CI: 38%–55%), 28% (95%CI:19%–38%), 25% (95%CI: 11%–43%), and 23% (95%CI: 2%–55%), respectively. For the non-BCMA exposed group, the pooled ≥VGPR, ≥CR, VGPR and PR were 59% (95%CI: 42%–75%), 41% (95%CI: 30%–52%), 19% (95%CI: 14%–25%) and 4% (95%CI: 0%–12%), respectively. The results are shown in Supplementary Figure S10. No statistical differences were observed for AEs (Supplementary Figure S11).

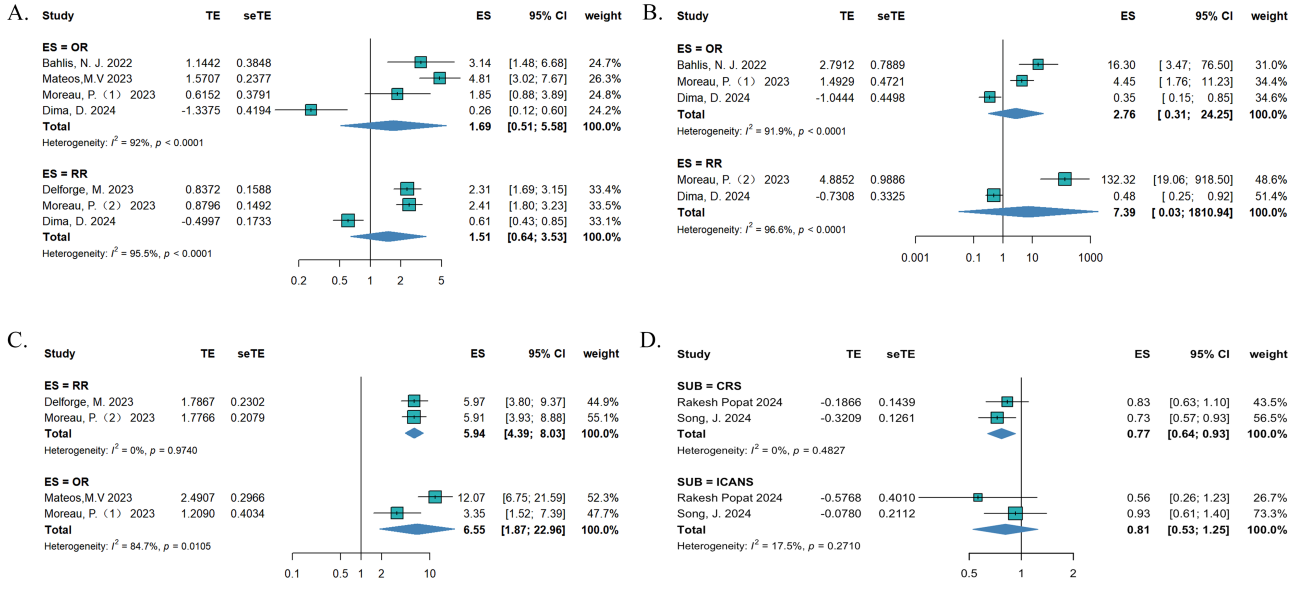

FIGURE 3
The pooled **(A)** ORR, **(B)** ≥CR, **(C)** ≥VGPR, and **(D)** AE in patients treated with teclistamab in the compared studies.

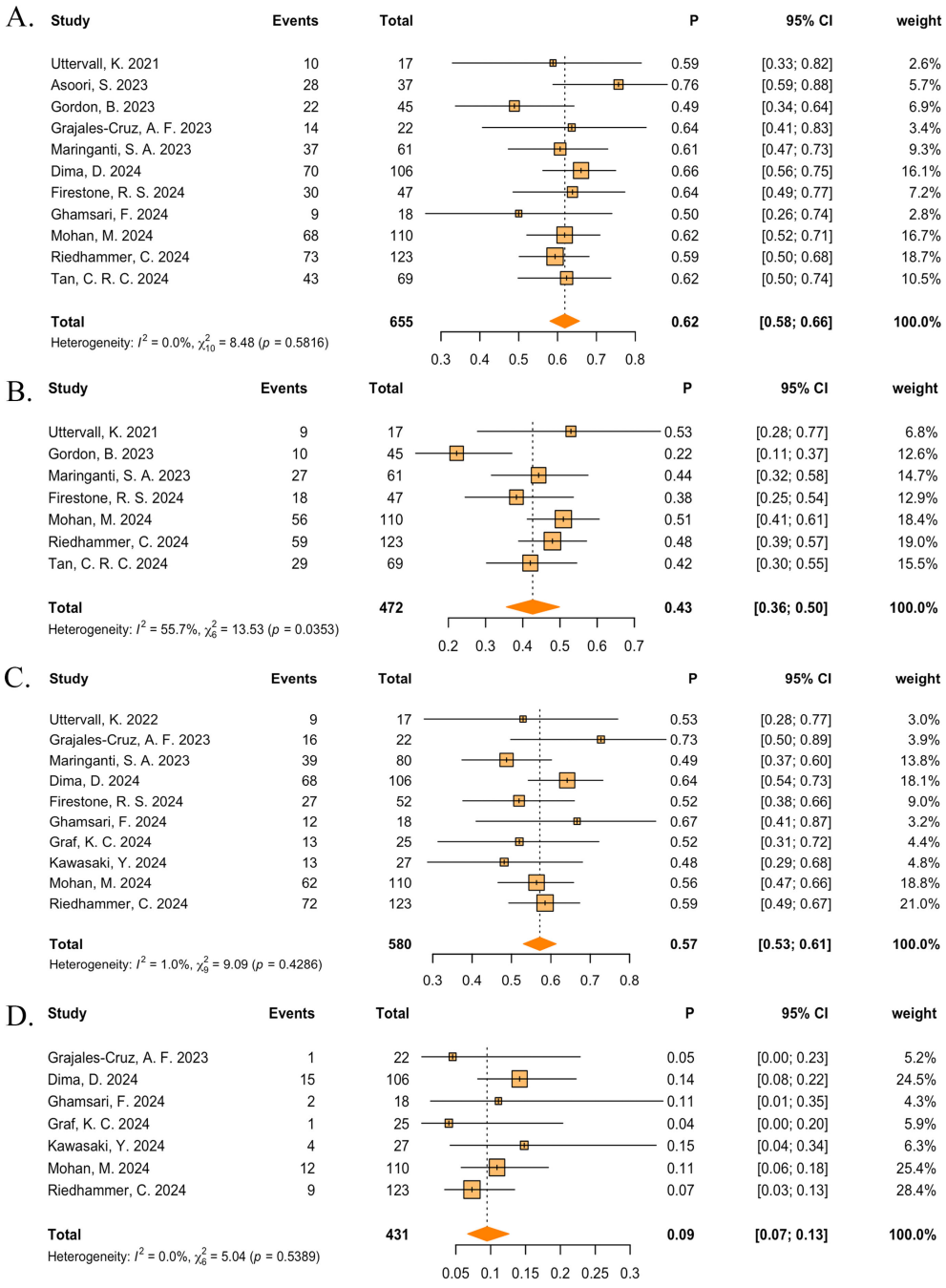

FIGURE 4
The pooled **(A)** ORR, **(B)** ≥VGPR, **(C)** any-grade CRS, and **(D)** any-grade ICANS in patients treated with teclistamab in the real-world studies.

3.5 Sensitivity analysis and publication bias

The sensitivity analysis of OS in the compared studies confirmed that when Song, J. (2024) was individually excluded, I^2 changed to 23.8% (Supplementary Figure S12). For PFS, when each trial was individually excluded, only minimal changes were observed. Egger's test showed no indication of publication bias for OS (p = 0.0751) and PFS (p = 0.4676) (Supplementary Figure S13).

4 Discussion

MM is the second most common hematological malignancy, and during its course, almost all patients experience one or more relapses (47). Patients with RRMM frequently face the challenges of undergoing multiple lines of treatment with limited clinical success, underscoring the need to explore innovative and effective therapeutic options (48). Teclistamab, a BCMA × CD3-directed bispecific antibody, showed high response rates and durable

remissions in the MajesTEC-1 trial in patients with RRMM. In this large-scale systematic review and meta-analysis, we quantified the reported efficacy and safety of teclistamab in RRMM.

In the pairwise meta-analysis, compared with existing treatment options for RRMM, teclistamab demonstrated superior efficacy, except for two articles comparing teclistamab with CAR-T therapy (21, 23). The inferior responses and survival outcomes of the teclistamab group may have been due to the variations in baseline characteristics across populations and can be explained by the more aggressive disease biology, as evidenced by poorer performance status, and higher rates of high-risk cytogenetics. Regarding AEs, CRS was only reported with CAR-T cell therapies. Despite the more aggressive disease biology observed in the teclistamab group, the incidence of CRS was still lower compared to the CAR-T group, suggesting that teclistamab offers better tolerability, even in patients in poorer physical condition. According to preliminary results from the KarMMa study, idecabtagene vicleucel (ide-cel) demonstrated an ORR of 73% in patients who had received at least three prior lines of therapy (8). In the CARTITUDE-1 trial, ciltacabtagene autoleucel (cilta-cel) showed an ORR of 98% in patients treated with at least three prior lines of therapy (49). Although CAR-T therapy has shown impressive response rates, the interval between leukapheresis and CAR-T cell infusion can pose challenges, especially for patients with rapidly progressing disease who may experience worsening cytopenia, progressive organ dysfunction, and declining functional status. In contrast, teclistamab offers the advantage of rapid treatment initiation in cases of rapidly progressing disease and demonstrates better tolerability in patients in a compromised physical condition (45). Therefore, given that both CAR-T and T-cell engagers (TCEs) have their respective advantages and disadvantages, and in the absence of direct head-to-head comparisons, it is recommended that CAR-T therapy be prioritized for eligible candidates when both CAR-T and TCE are equally accessible. However, TCEs, due to their greater accessibility and quicker initiation, should be preferred for patients with rapidly progressing disease who are unlikely to tolerate leukapheresis or bridging therapies. This recommendation is based on the activity data of TCEs following CAR-T treatment, and the longer treatment-free interval after CAR-T therapy, which provides more time for the administration of additional treatment options when relapse occurs (50).

In the real-world study analysis, the pooled ORR for the entire cohort was 62%, which was nearly equal to the ORR of 63% in the MajesTEC-1 trial (9). It is noteworthy that almost half of the real-world studies' patients did not meet the key inclusion criteria of the clinical trial and also had high-risk features such as ISS 3, high-risk cytogenetic aberrations, extramedullary disease (EMD), or high bone marrow infiltration. This could explain why the median PFS in the real-world studies ranged from 5.4 to 12.7 months, with most results slightly lower than the 11.3 months observed in MajesTEC-1. Additionally, the lower rates of ≥VGPR (43%) and ≥CR (22%) observed in the real-world studies could also be attributed to these baseline differences, as patients with more high-risk features tend to have poorer responses. Other factors contributing to these differences could include the shorter median follow-up time in real-world settings, as responses have been shown to deepen over time, and differences in treatment adherence between real-world patients and those in clinical trials. Common AEs of BsAbs therapy included CRS, infections, and neutropenia. In the real-world studies, same as MajesTEC-1, CRS and ICANS were predominantly low-grade and effectively manageable in most cases. The pooled any-grade CRS rate was 57%, lower than that reported in the MajesTEC-1 trial (72%), and could be well managed by antipyretics, analgesics, corticosteroids, and tocilizumab. However, our results demonstrate that the risk of severe CRS and ICANS (grade ≥3) with teclistamab in the real-world setting is higher compared to that noted in clinical trials (1.9% vs 0.6%; 2% vs 0.6%). This is mainly because of the higher tumor burden, which is an important predictor of severe CRS with BsAbs and CAR-T therapy (51). Moreover, cytopenia in real-world studies, such as neutropenia and anemia, were mainly high-grade, which may lead to an increased risk of serious opportunistic infections. Though the any-grade infection rate was lower than MajesTEC-1 (47% vs 76.4%), this may have been associated with the shorter follow-up time in the real-world studies or the primary intravenous immunoglobulin (IVIG) prophylaxis administration (44, 52). Our analysis showed that grade ≥3 infections occurred in 24% of patients treated with teclistamab. The common infections were COVID-19, pneumonia, and upper respiratory tract infection. Dima and colleagues reported three deaths from severe infection while on teclistamab without any evidence of disease progression (39), hence, there is a need for close surveillance and adequate preventive measures for the high rates of infections (53). Better infection risk management is highly suggested for the future use of teclistamab to prevent patients from serious or even fatal outcomes.

This study also presented interesting findings in the subgroup analysis. First, compared to teclistamab monotherapy, the ORR rate increased from 63% to 78% when combined with DARA and further rose to 90% when combined with both DARA and lenalidomide (LEN). Both DARA and LEN possess immunomodulatory effects that may enhance the activity of teclistamab. This might be explained by the immunomodulatory effects of LEN when combined with DARA. The combination can enhance T and NK cell-mediated cytotoxicity and induce *in vivo* T cell proliferation (54). Furthermore, teclistamab can recruit CD3+ T cells to the vicinity of BCMA-positive clonal plasma cells, enhancing targeted cytotoxicity against myeloma cells (6). As for AEs, the combination therapy shows no statistic differences in any-grade anemia, any-grade CRS, any-grade infection, any-grade neutropenia, grade ≥3 anemia, grade ≥3 CRS, grade ≥3 ICANS, grade ≥3 infection, and grade ≥3 neutropenia, and an even lower rate of any-grade ICANS was observed in the pooled studies. These results indicate that the combination therapy had tolerable safety, no overlapping toxicities, and promising efficacy. Further studies are warranted to evaluate the potential role of teclistamab combination therapy on enhanced early disease control or newly diagnosed MM.

Second, another clinically relevant observation was the efficacy of teclistamab in patients previously treated with anti-BCMA therapies. Median PFS in this population was 4.5 months, which

is lower than the 11.3 months observed in BCMA-naïve patients in the MajesTEC-1 RP2D cohort (10). However, our study showed that even ORRs with BCMA-targeted therapies were generally lower in patients who had prior anti-BCMA therapies as compared with BCMA-naive patients (56% vs 67%), however, the ≥VGPR and ≥CR rates showed no statistical differences. It is important to note that prior anti-BCMA-treated patients may present with more severe disease compared to BCMA-naive patients, as they are typically in a more refractory state due to the progression of the disease. As such, the outcomes of prior BCMA-treated patients were generally less favorable. For patients who achieved ≥CR after prior anti-BCMA-targeted therapy, the median duration of response (DOR) was 16.7 months, demonstrating the durability of deep responses. Additionally, in cohort C, the efficacy outcomes of patients who had previously received anti-BCMA ADC therapy were similar to those of patients who had received CAR-T therapy (ORR: 55.2% vs 53.3%) (10). A similar finding was reported in a real-world study by Dima et al. (ORR: 50% vs 57%) (39). This finding suggests that teclistamab can achieve good responses even in patients who have previously undergone T-cell redirection therapies. Furthermore, the safety profile of teclistamab in anti-BCMA-exposed patients was generally consistent with that of BCMA-naïve patients. Overall, our data suggest that teclistamab remains a viable treatment option following BCMA-targeted ADC or CAR-T therapy. BCMA loss may be a potential mechanism of primary resistance to teclistamab after BCMA-directed treatments (55). Therefore, combining teclistamab with agents such as talquetamab (a bispecific antibody targeting the novel myeloma antigen GPRC5D) may improve outcomes by overcoming resistance mechanisms, such as antigen escape, and enhancing survival in this subgroup of patients.

Furthermore, in July 2024, Johnson & Johnson announced that the marketing application for a teclistamab injection had been approved by the National Medical Products Administration (NMPA) of China, therefore, our study included the only reported Asian (China) cohort to evaluate the differences in the efficacy of teclistamab across ethnicities. Compared to the pivotal recommended phase 2 dose (RP2D) cohorts, while the baseline characteristics of the China cohort were generally consistent, some numerical differences were observed (56).The China cohort included fewer patients aged ≥75 years (7.7% vs 14.5%), fewer penta-exposed patients (53.8% vs 70.3%), and fewer patients with prior transplantation (11.5% vs 81.8%). In contrast, a higher proportion of patients in the China cohort presented with baseline features associated with a poorer prognosis, including high-risk cytogenetics (57.7% vs 25.7%), ≥1 extramedullary plasmacytoma (34.6% vs 17.0%), and ISS stage 3 disease (26.9% vs 12.3%). Despite these differences, the China cohort demonstrated a higher ORR rate (77%), and all patients achieved ≥VGPR. With a median follow-up of 15 months, the median DOR, PFS, and OS were not reached. The 12-month DOR, PFS, and OS rates were 78.5%, 68%, and 83.5%, respectively, demonstrating that Chinese patients treated with teclistamab can achieve deep and durable responses (32). Although the AE rate was higher than in the Western populations, no patients experienced a dose reduction or discontinuation due to AEs. The AEs decreased over time and were clinically managed with supportive care. Although some PIs, IMiDs, and monoclonal antibody drugs have been approved in China, unmet treatment needs still exist for patients with RRMM. Older MM patients, those with comorbidities such as renal impairment, patients with extramedullary involvement, and high-risk patients who relapse after transplantation require innovative treatments like teclistamab. However, studies in Asian populations remain limited, and more robust clinical research is needed to confirm the efficacy of teclistamab. In the future, we look forward to the publication of more data on teclistamab in Asian populations to further support its feasibility as a treatment option for RRMM.

In addition, compared with a recently published systematic review and meta-analysis by Qureshi et al., our current meta-analysis includes more studies, encompassing 4,064 patients (57). This notable difference in the number of included studies and patients, despite only a 4-month difference in search cut-off dates, can be attributed to the broader scope of our review. We systematically searched ClinicalTrials.gov and included relevant conference abstracts to capture the most recent and comprehensive evidence. Furthermore, our analysis also incorporated studies investigating teclistamab in combination regimens, providing a more extensive overview of its clinical potential. Therefore, our work not only complements the findings of Qureshi et al. but also further supports the growing body of evidence that highlights teclistamab as a promising and increasingly studied therapeutic option for patients with RRMM.

Our study had some limitations. First, the data for teclistamab in the pairwise meta-analysis mainly came from the MajesTEC-1, so there was unavoidable data redundancy. Second, due to the relatively short time since the approval of the drug, the follow-up periods in all real-world studies were relatively brief, which may have imposed certain limitations on our findings. Third, the heterogeneity in the results largely stemmed from differences in sample sizes and baseline characteristics among studies. At this stage, there is still a lack of large-scale, head-to-head randomized controlled trials to definitively establish the therapeutic advantages of teclistamab. Although this study did not fully meet all the above limitations, the overall risk of bias in study quality was considered acceptable.

5 Conclusion

Teclistamab has demonstrated favorable efficacy in real-world studies and clinical trials and remains a viable and effective treatment option for patients with RRMM previously exposed to BCMA-targeted therapy. Additionally, teclistamab combination therapies can improve response rates and maintain a favorable safety profile, offering new hope for overcoming BCMA resistance. Additionally, compared to Western populations, the China cohort showed better clinical benefits, although they were associated with a higher incidence of AEs. Therefore, we eagerly anticipate the future application of teclistamab in Asian RRMM populations, with the hope of bringing more treatment options and hope to patients in need. Our research indirectly supports the potential of teclistamab

in clinical applications. However, there is still a lack of direct head-to-head studies to demonstrate the efficacy, therefore, we call for more direct comparative clinical trials or real-world studies in the future to validate this conclusion.

Data availability statement

The original contributions presented in the study are included in the article/Supplementary Material. Further inquiries can be directed to the corresponding author.

Author contributions

WL: Conceptualization, Investigation, Methodology, Software, Validation, Writing – original draft. DZ: Conceptualization, Data curation, Investigation, Software, Visualization, Writing – original draft. YJ: Methodology, Project administration, Visualization, Writing – original draft. WD: Conceptualization, Supervision, Visualization, Writing – review & editing. ZW: Data curation, Formal analysis, Methodology, Supervision, Writing – original draft. XY: Conceptualization, Funding acquisition, Investigation, Methodology, Resources, Supervision, Validation, Visualization, Writing – review & editing.

Funding

The author(s) declare that financial support was received for the research and/or publication of this article. This work was supported by the Translational Research Grant of HCRCH (2020ZKMB06), the Xingliao Talents Program (xlyc1807265) and Liaoning Province Central Guidance Special Project for Local Science and Technology Development (2023JH6/100200006). They thank all the faculty members who participated in this study.

Acknowledgments

We would like to thank all authors who provided published data for our meta-analysis and thank International Science Editing (http://www.internationalscienceediting.com) for editing this manuscript.

Conflict of interest

The authors declare that the research was conducted in the absence of any commercial or financial relationships that could be construed as a potential conflict of interest.

Generative AI statement

The author(s) declare that no Generative AI was used in the creation of this manuscript.

Publisher's note

Supplementary material

The Supplementary Material for this article can be found online at: https://www.frontiersin.org/articles/10.3389/fimmu.2025.1565407/full#supplementary-material

References

1. Zhang N, Wu J, Wang Q, Liang Y, Li X, Chen G, et al. Global burden of hematologic Malignancies and evolution patterns over the past 30 years. *Blood Cancer J.* (2023) 13:82. doi: 10.1038/s41408-023-00853-3

2. Kumar SK, Rajkumar V, Kyle RA, van Duin M, Sonneveld P, Mateos MV, et al. Multiple myeloma. *Nat Rev Dis Primers.* (2017) 3:17046. doi: 10.1038/nrdp.2017.46

3. Yong K, Delforge M, Driessen C, Fink L, Flinois A, Gonzalez-McQuire S, et al. Multiple myeloma: patient outcomes in real-world practice. *Br J Haematol.* (2016) 175:252–64. doi: 10.1111/bjh.14213

4. Mateos MV, Weisel K, De Stefano V, Goldschmidt H, Delforge M, Mohty M, et al. LocoMMotion: a prospective, non-interventional, multinational study of real-life current standards of care in patients with relapsed and/or refractory multiple myeloma. *Leukemia.* (2022) 36:1371–6. doi: 10.1038/s41375-022-01531-2

5. Dimopoulos MA, Moreau P, Terpos E, Mateos MV, Zweegman S, Cook G, et al. Multiple myeloma: EHA-ESMO clinical practice guidelines for diagnosis, treatment and follow-up. *Hemasphere.* (2021) 5:e528. doi: 10.1016/j.annonc.2020.11.014

6. Guo Y, Quijano Cardé NA, Kang L, Verona R, Banerjee A, Kobos R, et al. Teclistamab: Mechanism of action, clinical, and translational science. *Clin Transl Sci.* (2024) 17:e13717. doi: 10.1111/cts.13717

7. Pillarisetti K, Powers G, Luistro L, Babich A, Baldwin E, Li Y, et al. Teclistamab is an active T cell-redirecting bispecific antibody against B-cell maturation antigen for multiple myeloma. *Blood Adv.* (2020) 4:4538–49. doi: 10.1182/bloodadvances.2020002393

8. Munshi NC, Anderson LD Jr., Shah N, Madduri D, Berdeja J, Lonial S, et al. Idecabtagene vicleucel in relapsed and refractory multiple myeloma. *N Engl J Med.* (2021) 384:705–16. doi: 10.1056/NEJMoa2024850

9. Moreau P, Garfall AL, van de Donk NWCJ, Nahi H, San-Miguel JF, Oriol A, et al. Teclistamab in relapsed or refractory multiple myeloma. *New Engl J Med.* (2022) 387:495–505. doi: 10.1056/NEJMoa2203478

10. Touzeau C, Krishnan AY, Moreau P, Perrot A, Usmani SZ, Manier S, et al. Efficacy and safety of teclistamab in patients with relapsed/refractory multiple myeloma after BCMA-targeting therapies. *Blood.* (2024) 144:2375–88. doi: 10.1182/blood.2023023616

11. MedCalc Software Ltd. Relative risk calculator. Available online at: https://www.medcalc.org/calc/relative_risk.php (Accessed January 6, 2025).

12. Gioia F, Walti LN, Orchanian-Cheff A, Husain S. Risk factors for COVID-19-associated pulmonary aspergillosis: a systematic review and meta-analysis. *Lancet Respir Med.* (2024) 12:207–16. doi: 10.1016/S2213-2600(23)00408-3

13. Higgins JP, Thompson SG, Deeks JJ, Altman DG. Measuring inconsistency in meta-analyses. *BMJ*. (2003) 327:557–60. doi: 10.1136/bmj.327.7414.557

14. Lin L, Chu H. Quantifying publication bias in meta-analysis. *Biometrics*. (2018) 74:785–94. doi: 10.1111/biom.12817

15. Bahlis NJ, Usmani SZ, Rosiñol L, Krishnan AY, Nooka AK, Rocafiguera AO, et al. Matching-adjusted indirect comparison (MAIC) of teclistamab (tec) versus selinexordexamethasone (sel-dex) for the treatment of patients (pts) with triple-class exposed (TCE) relapsed/refractory multiple myeloma (RRMM). *J Clin Oncol*. (2022) 40, e20028-e20028. doi: 10.1200/JCO.2022.40.16_suppl.e20028

16. Delforge M, Anguille S, Depaus J, Meuleman N, De Velde AV, Broek IV, et al. Teclistamab versus Belgian real-world clinical practice in triple-class exposed relapsed and refractory multiple myeloma patients using adjusted comparison. *Clin Lymphoma Myeloma Leukemia*. (2023) 23:S170–0. doi: 10.1016/S2152-2650(23)01862-1

17. Krishnan A, Nooka AK, Chari A, Garfall AL, Martin TG, Nair S, et al. Teclistamab versus real-world physician's choice of therapy in triple-class exposed relapsed/refractory multiple myeloma. *J Of Comp Effectiveness Res*. (2023) 12 (6). doi: 10.57264/cer-2022-0186

18. Mateos MV, Chari A, Usmani SZ, Goldschmidt H, Weisel K, Qi K, et al. Comparative efficacy of teclistamab versus physician's choice of therapy in the long-term follow-up of APOLLO, POLLUX, CASTOR, and EQUULEUS clinical trials in patients with triple-class exposed relapsed or refractory multiple myeloma. *Clin Lymphoma Myeloma Leuk*. (2023) 23:385–93. doi: 10.1016/j.clml.2023.02.006

19. Moreau P, Usmani SZ, van de Donk NWCJ, Garfall AL, Delforge M, Oriol A, et al. Matching-adjusted indirect treatment comparison (MAIC) of teclistamab vs belantamab mafodotin for the treatment of patients with triple-class exposed (TCE) relapsed/refractory multiple myeloma (RRMM). *Value Health*. (2023) 26:S5–6. doi: 10.1016/j.jval.2023.09.028

20. Moreau P, van de Donk NWCJ, Delforge M, Einsele H, De Stefano V, Perrot A, et al. Comparative efficacy of teclistamab versus current treatments in real-world clinical practice in the prospective LocoMMotion study in patients with triple-class-exposed relapsed and/or refractory multiple myeloma. *Adv Ther*. (2023) 40:2412–25. doi: 10.1007/s12325-023-02480-7

21. Dima D, Davis J, Ahmed N, Sannareddy A, Shaikh H, Shune L, et al. Outcomes of BCMA-directed chimeric antigen receptor T-cell (CART) therapy and teclistamab in patients with relapse-refractory multiple myeloma with extramedullary disease: A real-world experience of the US myeloma innovations research collaborative (USMIRC). *Transplant Cell Ther*. (2024) 30:S384–5. doi: 10.1016/j.jtct.2023.12.538

22. Popat CPR, Jenner M, Ghilotti F, van Nimwegen K, Lied-Lied A, Ming T, et al. *Comparative Efficacy Of Teclistamab Versus Pomalidomide Plus Dexamethasone For Patients With Triple-Class Exposed Relapsed Refractory Multiple Myeloma In England* Vol. Abstract: PB2811. EHA Library (2024) 8:e104. doi: 10.1002/hem3.104

23. Song J, Kim G, Memon RS, Chi KY, Chang Y, Mehta A. 802MO Real-world comparison of overall survival between BCMA - bispecific and CAR-T therapies in multiple myeloma. *Annals of Oncology*. (2024) 35:S597. doi: 10.1016/j.annonc.2024.08.853

24. Rodríguez-Otero P, D'Souza A, Reece DE, Van De Donk NWCJ, Chari A, Krishnan AY, et al. A novel, immunotherapy-based approach for the treatment of relapsed/refractory multiple myeloma (RRMM): Updated phase 1b results for daratumumab in combination with teclistamab (a BCMA x CD3 bispecific antibody). *J Clin Oncol*. (2022) 40(16_suppl):8032–8032. doi: 10.1200/JCO.2022.40.16_suppl.8032

25. Cohen YC, Morillo D, Gatt ME, Sebag M, Kim K, Min CK, et al. First results from the RedirecTT-1 study with teclistamab (tec) + talquetamab (tal) simultaneously targeting BCMA and GPRC5D in patients (pts) with relapsed/refractory multiple myeloma (RRMM). *J Clin Oncol*. (2023) 41:8002. doi: 10.1200/JCO.2023.41.16_suppl.8002

26. Donk N, Popat R, Rosiol L, Besemer B, Lopez JM, Trancucci D, et al. Teclistamab in relapsed or refractory multiple myeloma (Rrmm): majestec-1 subgroup analysis by lines of therapies. *Hematology Transfusion Cell Ther*. (2023) 45:S397–8. doi: 10.1016/j.htct.2023.09.753

27. Donk V, Moreau P, Garfall AL, Bhutani M, Oriol A, Nooka AK, et al. Long-term follow-up from MajesTEC-1 of Teclistamab, a B-cell Maturation Antigen (BCMA) x CD3 Bispecific Antibody, in patients with Relapsed/Refractory Multiple Myeloma (RRMM). *Oncol Res And Treat*. (2023) 46:124–4. doi: 10.1200/JCO.2023.41.16_suppl.8011IF: 42.1

28. Searle E, Quach H, Wong S, Costa L, Hulin C, Janowski W, et al. Single cohort results from majestec-2: teclistamab (Tec) in combination with subcutaneous daratumumab (Dara) and lenalidomide (Len) in patients with multiple myeloma (Mm). *HemaSphere*. (2023) 7:27. doi: 10.1097/01.HS9.0000936248.01150.e8

29. Garfall AL, Nooka AK, van de Donk NW, Moreau P, Bhutani M, Oriol A, et al. MM-336 Long-Term Follow-Up From the Phase 1/2 MajesTEC-1 Trial of Teclistamab in Patients With Relapsed/Refractory Multiple Myeloma (RRMM). *Clinical Lymphoma, Myeloma and Leukemia*. Philadelphia, PA, USA: Elsevier Inc. (2024) 24: S548. doi: 10.1016/S2152-2650(24)01666-5

30. Costa LJ, Bahlis NJ, Usmani SZ, van de Donk NW, Nooka AK, Perrot A, et al. Efficacy And Safety Of Teclistamab In Patients With Relapsed/Refractory Multiple Myeloma With High-Risk Features: A Subgroup Analysis From The Phase 1/2 Majestec-1 Study. *Clinical Lymphoma, Myeloma and Leukemia*. Philadelphia, PA, USA: Elsevier Inc. (2024) 24(Supplement 1):S546–S547. doi: 10.1016/S2152-2650(24)01666-1

31. van de Donk N, Garfall AL, Benboubker L, Uttervall K, Groen K, Rosiñol L, et al. Longer-term follow-up of patients (pts) receiving prophylactic tocilizumab (toci) for the reduction of cytokine release syndrome (CRS) in the phase 1/2 MajesTEC-1 study of teclistamab in relapsed/refractory multiple myeloma (RRMM). *J Of Clin Oncol*. (2024) 42:7517–7517. doi: 10.1200/JCO.2024.42.16_suppl.7517

32. X. Z-j, Cai Z, He Ai–Li, Dong Y, Wang Y, Liao A, et al. *Results From The CHINA Cohort Of The Phase 1/2 Majestec-1 Study Of Teclistamab (Tec) Treatment In Patients (Pts) With Triple-Class Exposed Relapsed/Refractory Multiple Myeloma (RRMM)* Vol. PB2717. EHA2024 Hybrid Congress. HemaSphere (2024) 8:e104. doi: 10.1002/hem3.104

33. Uttervall K, Nahi H, Kashif M, Lemonakis K, Rosengren S, Brolin J, et al. Teclistamab for relapsed/refractory multiple myeloma: real-world experience in an early access program. *Blood*. (2022) 140:12605–6. doi: 10.1182/blood-2022-158801

34. Asoori S, Martin T, Wolf J, Chung A, Arora S. Real world evaluation of teclistamab: A focus on infections in patients with relapsed refractory multiple myeloma (RRMM). *Clin Lymphoma Myeloma Leukemia*. (2023) 23:S536–7. doi: 10.1016/S2152-2650(23)01527-6

35. Dima D, Sannareddy A, Ahmed N, Davis JA, Shaikh H, Mahmoudjafari Z, et al. Toxicity and efficacy outcomes of teclistamab in patients with relapsed-refractory multiple myeloma (RRMM) above the age of 70 years: A multicenter study. *Blood*. (2023) 142:3330. doi: 10.1182/blood-2023-180458

36. Gordon B, Fogel L, Varma G, Saldarriaga MM, Ahn J, Aleman A, et al. Teclistamab demonstrates clinical activity in real-world patients ineligible for the pivotal majestec-1 trial. *Blood*. (2023) 142:4741. doi: 10.1182/blood-2023-181304

37. Grajales-Cruz AF, Castaneda O, Hansen DK, Vazquez-Martinez MA, Blue B, Khadka S, et al. Teclistamab induces favorable responses in patients with relapsed and refractory multiple myeloma after prior BCMA-directed therapy. *Blood*. (2023) 142:3351. doi: 10.1182/blood-2023-184928

38. Maringanti SA, Lin Y, Estritis S, Martinez-Lopez J, Bansal R, Fotiou D, et al. Real world evaluation of teclistamab for the treatment of relapsed or refractory multiple myeloma (RRMM). *Clin Lymphoma Myeloma Leukemia*. (2023) 23:S506–7. doi: 10.1016/S2152-2650(23)01466-0

39. Dima D, Davis JA, Ahmed N, Jia XF, Sannareddy A, Shaikh H, et al. Safety and efficacy of teclistamab in patients with relapsed/refractory multiple myeloma: A real-world experience. *Transplant Cell Ther*. (2024) 30:308.e1–308.e13. doi: 10.1016/j.jtct.2023.12.016

40. Firestone RS, McAvoy D, Shekarkhand T, Serrano E, Hamadeh I, Wang A, et al. CD8 effector T cells enhance teclistamab response in BCMA-exposed and -naïve multiple myeloma. *Blood Adv*. (2024) 8:1600–11. doi: 10.1182/bloodadvances.2023011225

41. Ghamsari F, Trando A, Medley K, Martino J, Block S, Doan T, et al. Real-world outcomes of teclistamab for the treatment of relapsed or refractory multiple myeloma at UC San Diego Health: A single-institution experience. *J Clin Oncol*. (2024) 42:e19504–e19504. doi: 10.1200/JCO.2024.42.16_suppl.e19504

42. Graf KC, Davis JA, Cendagorta A, Granger K, Gaffney KJ, Green K, et al. Fast but not so furious": A condensed step-up dosing schedule of teclistamab for relapsed/refractory multiple myeloma. *EJHaem*. (2024) 5:793–7. doi: 10.1002/jha2.v5.4

43. Kawasaki Y, Steele AP, Rosenberg A, Guglielmo J. Safety outcomes of teclistamab accelerated dose escalation. *J Oncol Pharm Pract*. (2024), 10781552241268429. doi: 10.1177/10781552241268429

44. Mohan M, Monge J, Shah NS, Luan DY, Forsberg M, Bhatlapenumarthi V, et al. Teclistamab in relapsed refractory multiple myeloma: multi-institutional real-world study. *Blood Cancer J*. (2024) 14:35. doi: 10.1038/s41408-024-01003-z

45. Riedhammer C, Bassermann F, Besemer B, Bewarder M, Brunner F, Carpinteiro A, et al. Real-world analysis of teclistamab in 123 RRMM patients from Germany. *Leukemia*. (2024) 38:365–71. doi: 10.1038/s41375-024-02154-5

46. Tan CRC, Derkach A, Maclachlan K, Hultcrantz M, Hassoun H, Mailankody S, et al. Real-world schedule de-escalation of teclistamab in patients with relapsed/refractory multiple myeloma. *J Clin Oncol*. (2024) 42:7536. doi: 10.1200/JCO.2024.42.16_suppl.7536

47. Gengenbach L, Graziani G, Reinhardt H, Rösner A, Braun M, Möller MD, et al. Choosing the right therapy for patients with relapsed/refractory multiple myeloma (RRMM) in consideration of patient-, disease- and treatment-related factors. *Cancers (Basel)*. (2021) 13:4320. doi: 10.3390/cancers13174320

48. Bazarbachi AH, Al Hamed R, Malard F, Harousseau JL, Mohty M. Relapsed refractory multiple myeloma: a comprehensive overview. *Leukemia*. (2019) 33:2343–57. doi: 10.1038/s41375-019-0561-2

49. Lin Y, Martin TG, Usmani SZ, Berdeja JG, Jakubowiak AJ, Agha ME, et al. CARTITUDE-1 final results: Phase 1b/2 study of ciltacabtagene autoleuc el in heavily pretreated patients with relapsed/refractory multiple my eloma. *J Clin Oncol*. 41:8009–9. doi: 10.1200/JCO.2023.41.16_suppl.8009

50. Costa LJ, Banerjee R, Mian H, Weisel K, Bal S, Derman BA, et al. International myeloma working group immunotherapy committee recommendation on sequencing immunotherapy for treatment of multiple myeloma. *Leukemia*. (2025) 39:543–54. doi: 10.1038/s41375-024-02482-6

51. Shimabukuro-Vornhagen A, Gödel P, Subklewe M, Stemmler HJ, Schlößer HA, Schlaak M, et al. Cytokine release syndrome. *J Immunother Cancer*. (2018) 6:56. doi: 10.1186/s40425-018-0343-9

52. Lancman G, Parsa K, Kotlarz K, Avery L, Lurie A, Lieberman-Cribbin A, et al. IVIg use associated with ten-fold reduction of serious infections in multiple myeloma patients treated with anti-BCMA bispecific antibodies. *Blood Cancer Discovery*. (2023) 4:440–51. doi: 10.1158/2643-3230.BCD-23-0049

53. Raje N, Anderson K, Einsele H, Efebera Y, Gay F, Hammond SP, et al. Monitoring, prophylaxis, and treatment of infections in patients with MM receiving bispecific antibody therapy: consensus recommendations from an expert panel. *Blood Cancer J.* (2023) 13:116. doi: 10.1038/s41408-023-00879-7

54. D'Souza C, Prince HM, Neeson PJ. Understanding the role of T-cells in the antimyeloma effect of immunomodulatory drugs. *Front Immunol.* (2021) 12:632399. doi: 10.3389/fimmu.2021.632399

55. Rasche L, Vago L, Mutis T. Tumour escape from CAR-T cells. In: Kröger N, Gribben J, Chabannon C, Yakoub-Agha I, Einsele H, editors. *The EBMT/EHA CAR-T Cell Handbook*. Springer Copyright 2022, The Author(s, Cham (CH (2022). p. 15–22.

56. Cai Z, Xia Z, He AL, Dong YJ, Wang Y, Liao A, et al. Efficacy, safety, and pharmacokinetics of teclistamab in Chinese patients with relapsed/refractory multiple myeloma from the China cohort of MajesTEC-1. *Cancer*. (2025) 131: e35665. doi: 10.1002/cncr.v131.1

57. Qureshi Z, Jamil A, Altaf F, Siddique R, Ahmed F. Efficacy and safety of teclistamab in relapsed or refractory multiple myeloma: a systematic review and meta-analysis. *Ann Hematol.* (2024) 103:4901–12. doi: 10.1007/s00277-024-06078-z

frontiers | Frontiers in Immunology

TYPE Review
PUBLISHED 29 May 2025
DOI 10.3389/fimmu.2025.1572802

OPEN ACCESS

EDITED BY
Renata Pacholczak-Madej,
Maria Skłodowska-Curie National Institute of Oncology, Poland

REVIEWED BY
Rosendo Luria-Perez,
Children's Hospital of Mexico Federico Gomez, Mexico
Moshe Elkabets,
Ben-Gurion University of the Negev, Israel

*CORRESPONDENCE
Yunfeng Zhou
yunf_zhou_hxsy@163.com

RECEIVED 07 February 2025
ACCEPTED 09 May 2025
PUBLISHED 29 May 2025
CORRECTED 17 July 2025

CITATION
Chen W, Zhou A and Zhou Y (2025) Bispecific antibody for lung cancer: mechanisms and clinical insights. *Front. Immunol.* 16:1572802. doi: 10.3389/fimmu.2025.1572802

Bispecific antibody for lung cancer: mechanisms and clinical insights

Wei Chen[1], Afang Zhou[2] and Yunfeng Zhou[1*]

[1]Department of Thoracic Surgery, West China School of Public Health and West China Fourth Hospital, Sichuan University, Chengdu, Sichuan, China, [2]State Key Laboratory of Biotherapy, Sichuan University, Chengdu, Sichuan, China

Lung cancer is a refractory malignancy. Although various therapeutic options, including targeted therapies, immune checkpoint inhibitors, and systemic chemotherapy, have significantly improved the prognosis of lung cancer patients, five-year survival rates are still low. Bispecific antibodies have attracted much attention because of their ability to bind different antigens or epitopes on the same antigen at once and because of their multiple novel functional mechanisms. Recently, three bispecific antibodies have been successively approved for lung cancer treatment, demonstrating the potential of bispecific drugs in lung cancer therapy. Various bispecific antibodies are currently under clinical trials to evaluate their safety and efficacy in lung cancer. In this review, we provide an overview of these antibodies' structure and mechanism of action, summarize their clinical progress in lung cancer treatment, and discuss and analyze the challenges and future directions of bsAbs application in lung cancer.

KEYWORDS

bispecific antibodies, lung cancer, novel therapies, immunotherapy, targeted therapy

1 Introduction

Lung cancer is one of the world's most common cancers and the leading cause of cancer-related deaths, with an estimated 2.2 million new cases and 1.79 million deaths annually (1). In most parts of the world, the 5-year survival rate for lung cancer patients is only 10-20% (2). Non-small cell lung cancer (NSCLC) is one of the most common types of lung cancer, accounting for about 85% of lung cancers (1). The treatment landscape for NSCLC has changed dramatically over the past decade by introducing several new targeted and immunotherapeutic agents. Patients treated with protein kinase inhibitors [especially tyrosine kinase inhibitors (TKIs)] and monoclonal antibodies [e.g., immune checkpoint inhibitors (ICIs)] may have a relatively good prognosis. However, although the above treatment strategies significantly prolong the overall survival of patients, a common problem is drug resistance (3, 4). Small cell lung cancer (SCLC) is another type of lung cancer that accounts for 10-15% of all lung cancers (5–7). It is even a tumor type with an inferior prognosis and limited therapeutic options, with a median survival of 2 years for

most patients with early-stage disease and 1 year for patients with metastatic disease (8). Therefore, there is still a significant unmet medical need in the field of lung cancer.

Bispecific antibodies (bsAbs) have been described as "next-generation antibodies" that overcome the limitation of natural monoclonal antibodies to bind only a single epitope (9). Amivantamab is the first bispecific antibody approved for the treatment of lung cancer. The drug was initially approved for treating adult patients with locally advanced or metastatic NSCLC harboring epidermal growth factor receptor (*EGFR*) Exon 20 insertion mutations whose disease has progressed on or after platinum-based chemotherapy (10). Several bsAbs with potential for lung cancer therapy are currently undergoing clinical trials, and many have produced exciting results. This review provides an overview of the bsAbs that have shown promise in treating lung cancer.

2 Bispecific antibody formats and mechanisms

One of the significant challenges of dual antibodies, which took about half a century to move from concept to the clinic, is that only 12.5% of the target molecules can be obtained by conventional production means, with the rest being mostly nonfunctional or monospecific molecules (11, 12). To address this challenge, researchers have developed various strategies based on natural antibodies such as IgG and heavy-chain antibodies (Figure 1A). These strategies aim to increase the proportion of the target molecule and facilitate its separation and purification, while enabling the modular combination of distinct antibody functional domains as required. Today, more than 100 types of bsAbs are known (9) and can be briefly classified into three categories: no IgG-like bsAbs (Figure 1B), asymmetric IgG-based bsAbs (Figure 1C), and symmetric IgG-based bsAbs (Figure 1D). No IgG-like bsAbs consist of combinations of partial structures of antibodies. Among them, bsAbs designed based on single-chain variable fragment (scFv) (e.g., BiTE, DART, etc.) are the simplest and the least difficult to generate. Moreover, due to their low molecular weight, they have better tissue permeability. However, the absence of fragment crystallizable (Fc) structure results in a short plasma half-life of these molecules and a lack of Fc-mediated effector function [e.g., antibody-dependent cell cytotoxicity (ADCC) or antibody-dependent cell phagocytosis (ADCP)]. To extend the half-life of such bsAbs, a common strategy is to fuse Fc fragments (including HEL-BiTE, Tetravalent DART Fc, VHH-Fc, etc.) or conjugate fragments of anti-human serum albumin (HSA) antibodies (e.g., TRACTr, TriTAC) with the bsAbs protein. IgG-based bsAbs retain Fc and have a longer half-life, and Fc function can be adjusted to enhance the therapeutic effect of the molecule according to specific needs. However, there will be more factors to consider in the molecular design of the protein. For example, asymmetric IgG-based antibodies are closer in form to natural IgG. However, as mentioned above, the target molecule content is only 12.5% when produced by conventional means, and it is not easy to purify the target molecule from the system to obtain a high-purity target molecule. Therefore, a series of molecular modifications are needed to promote the correct pairing of light and heavy chains to increase the target molecule content, and these strategies include knob-into-hole, DEKK mutation, common light chain, and the addition of alternative interchain disulfide. Symmetric IgG-based bsAbs are made by fusing another antigen-binding fragment to the conventional antibody (e.g., Tetrabody, IgG-VHH, FIT-Ig, etc.) or by mutating Fc to form a new antigen-binding site (e.g., mAb2) and thus do not need to consider the correct pairing of light and heavy chains. However, such modifications can change physicochemical properties such as antibody stability and solubility (13, 14). In addition, antigen-antibody binding is affected by the position of the fused fragment (15).

3 The mechanisms of action of bispecific antibodies in lung cancer

Unlike the simple mixing of antibodies, bsAbs have become a primary focus of drug developers because they have new mechanisms of action (MOA) different from those of the parent antibody combination. Currently, bsAbs used in lung cancer therapy include three main mechanisms: dual inhibition (Figure 2A), engaging immune cells and tumor cells (Figure 2B), and immune cytokines (Figure 2C).

By targeting two antigens at the same time, dual-inhibition bsAbs inhibited the pathways of two signals that are related to each other, exerting the effect of 1 + 1>2. More than half of the bsAbs currently applied in lung cancer treatment mainly exert anti-tumor effects by this mechanism of action. They can be further categorized into three types according to the difference in the signals they block: (i) simultaneous targeting of two surface receptors with specific signaling and functional overlap associated with tumorigenesis and progression, mainly ErbB family proteins; (ii) dual immune checkpoint molecule blockade; (iii) simultaneous inhibition of immune checkpoints and tumor microenvironmental pro-tumor growth factors.

Immune cell engagers (ICEs) redirect cytotoxic immune cells to disease-associated target cells that play a key role in the disease process to achieve direct killing of these cells by immune cells. Among them, T cell engagers (TCEs) are the typical application of bsAb, and about half of the bsAbs currently evaluated in clinical trials are TCEs (16). Recently, researchers have also been experimenting with Natural Killer cell engagers (NKCEs) based on the recruitment of cytotoxic NK cells (17, 18).

Immunocytokines are a type of antibody-cytokine fusion protein. Mechanistically, immunocytokines fuse a therapeutic cytokine to one end of an antibody. Through the specific targeting function of the antibody, the cytokine is specifically delivered near tumor cells, allowing it to bind to specific cytokine receptors on the surface of surrounding immune cells, thus significantly reducing non-specific toxicity (19, 20). Structurally, immunocytokines have a symmetric or asymmetric structure based

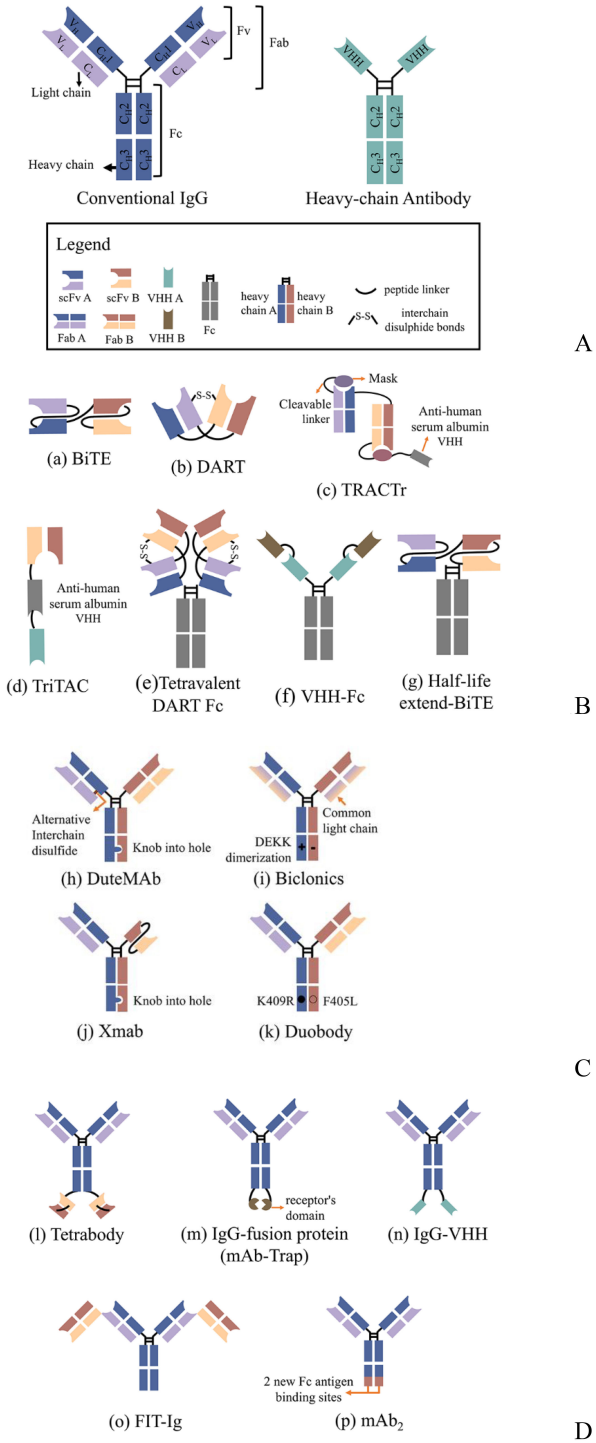

FIGURE 1
Schematic overview of the antibody structure and representations of several classical bsAbs formats; **(A)** Conventional IgG consists of 2 heavy chains and two light chains, while heavy-chain antibodies are only comprised of heavy chains; **(B)** No IgG-like bsAbs; those bsAb consist of antibody-based fragments, such as scFv, VHH, Fab, Fc; **(C)** Asymmetric IgG-based bsAbs; the molecules may contain mutations, knob-into-hole or DEKK for example, that affect chain pairing and other manufacturability parameters. **(D)** Symmetric IgG-based bsAbs; Symmetric bispecific antibodies are generated by a fusion of an additional binding site to the heavy/light chains or by making differential but overlapping use of the light and heavy complementarity determining regions as primary contacts for each antigen. scFv, single-chain variable fragment; Fab, antigen-binding fragments; VHH, variable heavy domain of heavy chain; Fc, fragment crystallizable.

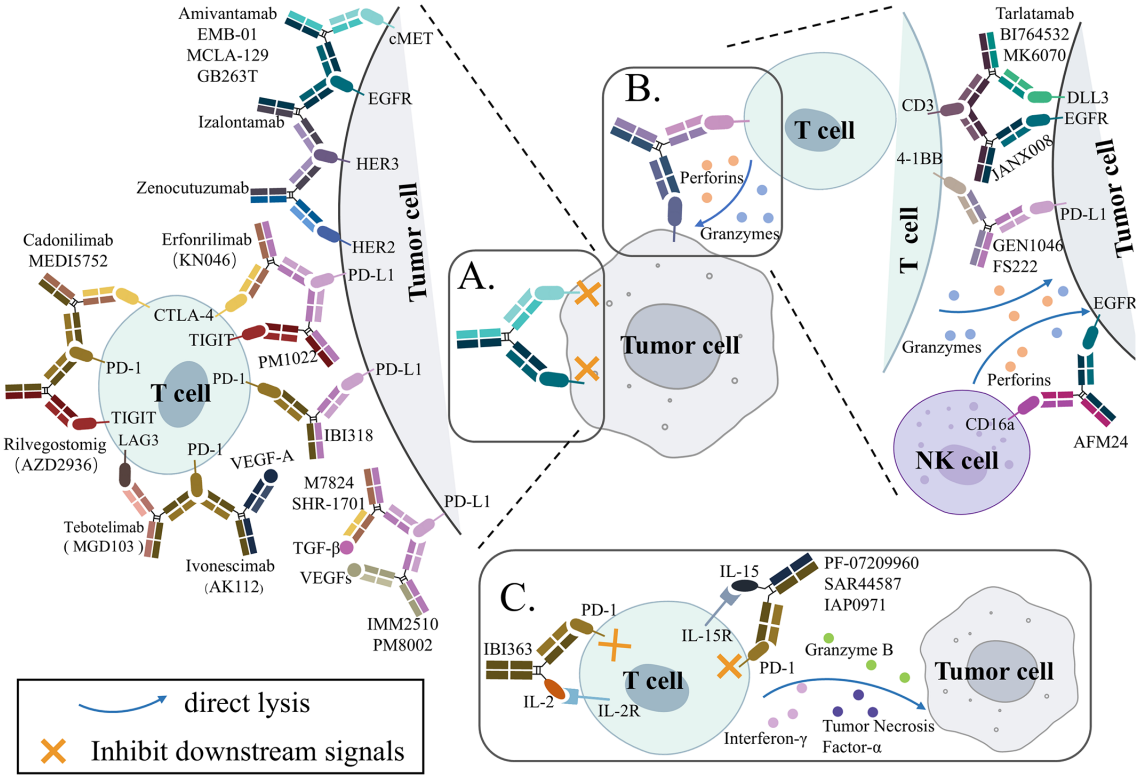

FIGURE 2
Simplified schematic overview of the proposed mechanisms of action for bispecific antibodies (bsAbs) in clinicals for lung cancer treatment. **(A)** Blocking signaling. Two targets are being disrupted by the bsAb. **(B)** Engagement of immune cells to the tumor cell. Immune cells can be engaged to tumor cells by bsAbs. **(C)** Immunocytokine. Increase cytokine accumulation within the tumor and block immune checkpoint. cMET, mesenchymal-epithelial transition; EGFR, epidermal growth factor receptor; HER2, human-epidermal growth factor receptor 2; HER3, human-epidermal growth factor receptor 3; PD-1, programmed cell death protein 1; PD-L1, programmed death-ligand 1; CTLA-4, cytotoxic T-lymphocyte-associated protein 4; TIGIT, T cell immunoglobulin and ITIM domain; LAG-3, lymphocyte activation gene 3; VEGF, vascular endothelial growth factor; TGF-β, transforming growth factor β; DLL3, Delta-like ligand 3; IL-2, interleukin-2.

on IgG (21). Therefore, in some literature and this article, immunocytokines are classified as a type of bispecific antibody with a special mechanism (22, 23).

The following is a further discussion and analysis of bispecific antibodies in lung cancer according to the different mechanisms of action described previously.

4 Dual inhibition bispecific antibodies

4.1 Dual receptors inhibition bispecific antibodies

The ErbB family of transmembrane receptor tyrosine kinases consist of four members: EGFR/ErbB1/HER1, ErbB2/Neu/HER2, ErbB3/HER3, ErbB4/HER4. ErbB receptors are activated upon homo-or heterodimerization, which activates many downstream signaling pathways, primarily the mitogen-activated protein kinase (MAPK), phosphatidylinositol 3-kinase (PI3K)/protein kinase B (PKB/AKT), and Janus kinase (JAK) and signal transducer/activator of transcription (STAT) signaling pathways (24). Moreover, all these pathways regulate cell metabolism, growth, and survival. Overexpression and overactivation of ErbB receptors are associated with poor prognosis, drug resistance, tumor metastasis, and lower survival in a variety of cancers, including lung cancer. There are two clinically important ErbB inhibitors: humanized antibodies targeting the extracellular structural domains of EGFR or HER2 and small-molecule TKIs that compete with adenosine triphosphate in the structural domain of the receptor tyrosine kinase. Eventually, however, a significant proportion of tumor cells develop resistance through the activation of another ErbB receptor signal or the activation of bypass pathways (25, 26). BsAbs inhibit tumor growth more effectively by simultaneously targeting two ErbB members or related bypass pathways, thereby blocking overlapping downstream signals.

4.1.1 EGFR × cMET

EGFR mutations exist in approximately 50% of Asian NSCLC patients and 11-16% of European NSCLC patients (27–29). Currently, the US Food and Drug Administration (FDA) has approved six EGFR TKIs, as well as a fully humanized monoclonal antibody targeting EGFR, as the standard of care for the first-line treatment of NSCLC patients with *EGFR* mutations (30). However, the selection pressure exerted by the above drugs

inevitably leads to treatment resistance. Among cases of acquired resistance to EGFR TKIs, 5-10% are mesenchymal-epithelial transition factor (*MET*) amplified, which activates the EGFR-independent PI3K-AKT signaling pathway by driving ErbB3 dimerization and signal transduction (31, 32). Drug-resistant tumors are also able to activate the cMET pathway through increased cMET expression and/or increased cMET ligand expression, which provides an alternative mechanism for tumor cells to bypass the TKI blockade of EGFR and promote cancer cell survival (33–36). Due to the signaling crossover between EGFR and cMET, combined inhibition of both receptors may limit the activation of the compensatory pathway and improve overall efficacy.

Amivantamab (JNJ-61186372; Rybrevant™) is a fully humanized bsAb targeting EGFR and cMET and is the first approved therapeutic agent for NSCLC patients with *EGFR* exon 20 insertion (*EGFR* ex20ins) after failure of platinum-containing chemotherapy. In addition to its ability to block both EGFR- and cMET-mediated downstream signaling, the antibody exerts its anti-tumor effects through various Fc-mediated mechanisms, such as ADCC and ACDP (37, 38). The CHRYSALIS (NCT02609776) analyses the efficacy and safety of amivantamab in post-platinum NSCLC patients with *EGFR* Exon20ins. In the efficacy population, the reported overall response rate (ORR) was 40%, the median duration of response (mDOR) was 11.1 months, and the median overall survival (mOS) was 22.8 months, respectively (10, 39, 40). Besides, the drug has a favorable safety profile, with the most common side effects including rash (89%) and infusion-related events (67%). Based on the above data, the FDA approved the new drug application of amivantamab in 2021 (41). In a subsequent clinical trial called PAPILLON (NCT04538664), researchers analyzed the anti-tumor activity of amivantamab in combination with carboplatin-pemetrexed. Among treatment-naïve NSCLC patients with *EGFR* ex20ins, the progression-free survival (PFS) in the amivantamab plus chemotherapy group was significantly longer than that of the chemotherapy group (median, 11.4 months and 6.7 months, respectively) (42). Based on this clinical result, the FDA approved amivantamab plus chemotherapy as a first-line therapy for advanced NSCLC with *EGFR* ex20ins mutation (43).

The efficacy of amivantamab is not limited to *EGFR* ex20ins mutation. However, it has shown positive clinical benefits for the larger population of patients with other *EGFR* and *MET* mutations. For patients with locally advanced or metastatic NSCLC with *EGFR* mutations (Ex19del or L858R) (NCT06120140), compared to those receiving osimertinib, patients treated with amivantamab plus lazertinib had longer mPFS (23.7 months vs. 16.6 months, HR=0.7) and longer mDoR (25.8 months vs. 16.8 months) (44, 45). For primary *MET*ex14 patients with advanced NSCLC treated with amivantamab (NCT02609776), an ORR of 33% (56% in the treatment-naïve population) with a mDOR of 11.2 months was observed (46). In addition, a subcutaneous formulation of amivantamab, based on human hyaluronidase, was developed to improve patient tolerability and reduce administration time (47). It was shown (NCT05388669) that when administered subcutaneously, the drug was not only pharmacokinetically non-inferior to intravenous administration, but fewer patients in the subcutaneous group experienced infusion-related reactions (13% vs. 66%) and venous thromboembolism (9% vs. 14%). Concurrently subcutaneously administered patients had prolonged mPFS (6.1 months vs. 4.3 months, HR=0.84), prolonged mDOR (11.2 months vs. 8.3 months), and significantly prolonged OS (HR=0.62).

EMB-01 is an EGFR- and cMET-targeted bispecific antibody based on the FIT-Ig technology platform, which fuses the Fab of an anti-cMET antibody to the variable region of an anti-EGFR antibody to form a tetravalent bispecific antibody. EMB-01 induces endocytosis of EGFR and cMET receptors on the cell surface and their degradation. Preliminary clinical (NCT03797391) data suggest an ORR of 5.3% and a DCR of 42.1% in 38 evaluable patients with advanced NSCLC (48).

MCLA-129 is a 1 + 1 form of asymmetric Ig-G-like bispecific antibody designed based on the biclonics common light chain platform (49). It targets both EGFR and cMET and has a mechanism of action similar to amivantamab. Preliminary clinical data (NCT04930432) on fortnightly intravenous administration of 1,500 mg MCLA-129 in different NSCLC patients were recently published: for patients with *MET*ex14 mutation, the ORR was 43.5%, and the DCR was 95.7%; for *EGFR*20ins-mutated patients, the ORR was 28.6% and DCR of 84.1%; for patients with sensitized *EGFR*-mutated, ORR was 21.8% and DCR was 69.1% (50). In addition, this bispecific antibody in combination with osimertinib was observed in treatment-naïve patients with advanced *EGFR*mut NSCLC (NCT04868877) with an ORR of 75.0% and a DCR of 93.8%; in patients who progressed on osimertinib, the ORR was 35.3%, and the DCR was 73.5% (51).

4.1.2 HER2 × HER3

As a member of the ERBB receptor family, HER2 alterations are involved in the oncogenic process in a variety of solid tumors, mainly including *HER2* mutation, *HER2* amplification, and HER2 overexpression, with corresponding incidence rates of 1%-6.7%, 2%-22%, and 7.7%-23%, respectively, in NSCLC and all of them are associated with poor prognosis (52–55). HER3 is overexpressed in 83% of primary NSCLC tumors and is associated with advanced disease, shorter time to metastasis, and lower survival (56). HER2 is activated by dimerization or with other ERBB family members and further activates downstream signaling pathways. Of all possible EGFR family dimers, the HER2:HER3 heterodimer has the highest translational capacity (57–59). When HER3 binds to its ligands (neuregulin1-4, NRG1-4), its conformation is altered, exposing its dimerization sites with other proteins of the EGFR family, predominantly EGFR and HER2, which induces phosphorylation events downstream of the protein (60). Notably, NRG1 can form fusion proteins with various membrane proteins, which provide a transmembrane structural domain to anchor NRG1 to the membrane, thus enabling NRG1 to bind to HER3 in its own or neighboring cells (61). NRG1 fusions have been detected in a wide

range of tumors, with the highest number of cases reported in NSCLC (62). Early reports observed relatively poor NRG1 fusion-positive ($NRG1^+$) lung therapy outcomes. The ORR of those patients treated with platinum-doublet and taxane-based (post-platinum-doublet) chemotherapy was only 13% and 14%, with mPFS of 5.8 and 4.0 months, respectively (63).

Zenocutuzumab (MCLA-128) is an IgG-like asymmetric bsAb targeting HRE2 and HER3. The antibody preferentially binds to more abundant HER2 proteins on the cell surface via the higher affinity HER2-targeting arm, providing a high concentration of local antibody while at the same time positioning the HER3-targeting arm to block NRG1 or NRG1 fusion proteins binding to HER3 (64). Thereby, the formation of HER2:HER3 heterodimers is potently inhibited, preventing subsequent phosphorylation of the HER3 cytoplasmic structural domain and downstream oncogenic signaling. In addition, glycoengineering modifications enhanced the antibody's ADCC activity (64). The FDA recently granted accelerated marketing approval for zenocutuzumab based on clinical results from a study called eNRGy (NCT02912949) (65). In 64 evaluable patients with $NRG1^+$ advanced NSCLC, the confirmed ORR was 34% (22/64; [95% CI] 23-47), and the mDOR was 12.9 months, with responses ongoing in 11/22 (50%) patients (66). The drug's safety profile was favorable, with <4% of patients experiencing grade ≥3 adverse events (66).

4.1.3 EGFR × HER3

In addition to HER3 forming dimers with HER2 to deliver proliferation and survival signals to the cells, another important dimerization partner is EGFR. It has been found that regardless of the type of EGFR-TKIs resistance mechanisms, such as *EGFR* T790M mutation, *MET* amplification, and *HER2* amplification, *HER3* amplification is observed in *EGFR*-mutated NSCLC tumors that progress after EGFR-TKI treatment (67). HER3 can also be activated independently of ligand binding through dysregulation of other tyrosine kinase receptors. For example, in NSCLC carrying activating *EGFR* mutations, EGFR can transactivate HER3 via heterodimers (68). In the presence of EGFR-TKIs, *MET* amplification activates HER3, thereby initiating a downstream PI3K/AKT survival mechanism (31).

Izalontamab (SI-B001) is a tetravalent symmetric bsAb targeting EGFR and HER3. The antibody is cetuximab-based and contains an anti-HER3 scFv at the end of the constant region of cetuximab (69). Since the antibody has a significantly lower affinity for the HER3 arm than the EGFR arm, the antibody can only bind to HER3 after definitive binding to the EGFR (69). As a result, it effectively inhibits tumor cells that express both EGFR and HER3, minimizing the effect on functioning HER3 in normal tissues. In a phase II clinical trial (NCT04603287), researchers enrolled 55 patients with locally advanced or metastatic *EGFR*/anaplastic lymphoma kinase (*ALK*) wild-type NSCLC who had failed first-line anti-PD-1/L1 therapy with or without platinum-based chemotherapy (PBC) to receive SI-B001 combined with docetaxel (70). Of the 48 evaluable patients, the ORR and the DCR were 31.3% and 77.1%, respectively (63). Among the patients in Cohort B who failed first-line anti-PD-1/L1 combined with PBC, 22 of the evaluable patients in this cohort were on a regimen of 16 + 9 mg/kg/week. These patients' reported ORR and DCR were 45.5% and 68.2%. Among all, the most common≥grade 3 treatment-related adverse events (TRAEs) were myelosuppression (17%), decreased neutrophil count (15%), and decreased white blood cell count (12%).

4.2 Dual immune checkpoints inhibition bispecific antibodies

The immune system is an elaborate and complex network of multiple signals that activate immune cells to accurately recognize and eliminate pathogenic microorganisms and mutated cells in the body. At the same time, to avoid damage to normal tissues and organs by excessive immune response, the immune system has evolved a series of checkpoints to modulate the duration and amplitude of the immune response. However, tumor cells will hold these checkpoints hostage to escape immune surveillance (71). Reactivating or enhancing the immune system's innate or adaptive immune response to strengthen the attack on cancer cells is an important strategy for cancer treatment.

4.2.1 PD-1/L1 × CTLA-4

Programmed cell death protein 1 (PD-1), programmed death-ligand 1(PD-L1), and cytotoxic T-lymphocyte-associated protein 4 (CTLA-4) are the relatively well-studied and most maturely applied immune checkpoints. Currently, immune checkpoint inhibitors are approved for treating various solid and hematological malignancies (72). Despite the success of anti-CTLA-4 and anti-PD-1/L1 therapies, only 10-25% of patients benefit from such treatments (73). Because of the similarities and differences between the CTLA-4 and PD-1 pathways and some complementarity between them (74), combination therapy with anti-PD-1/L1 and anti-CTLA-4 clinically improves overall survival. The combination of these two classes of antibodies has been approved for the treatment of various tumors, including non-small cell lung cancer. However, at the same time, the toxicities of the combination are more intense than those of the single agent (75–79). On the other hand, PD-1 and CTLA-4 are co-expressed in a high percentage of tumor-infiltrating lymphocytes (80). Therefore, it is possible to maximize clinical benefit and minimize additional toxicity by designing bispecific antibodies that can specifically target such tumor-infiltrating lymphocytes and avoid activation of immune cells in other normal tissues by the bsAbs.

Cadonilimab (AK104; 开坦尼®) is a humanized tetravalent symmetric bispecific antibody incorporating an anti-CTLA-4 scFv fragment at the C-terminus of each of the two heavy chains of the anti-PD-1 antibody (81). Also, to avoid T-cell depletion and adverse immune responses caused by Fc-mediated immune cell activation, the Fc segment was mutated to completely remove ADCC, ADCP, and CDC effects (81). Cadonilimab has a higher affinity at high PD-1 concentrations and a relatively low binding capacity at lower PD-1

concentrations (82). As a result, the antibody has higher activity in high PD-1-expressing tumor microenvironments and weaker activity in normal tissues. It received conditional approval for marketing in China in June 2022 for the treatment of patients with recurrent or metastatic cervical cancer who have failed prior treatment with platinum-containing chemotherapy (83). Several clinical trials of cadonilimab alone or combined with other drugs for treating NSCLC and SCLC are underway (83). A clinical trial called AK104-208 (NCT04646330) evaluated the efficacy of cadonilimab in combination with anilotinib, an anti-angiogenic drug, in treatment-naïve patients with NSCLC. In 69 evaluable patients, the overall ORR was 53.6% (95% CI, 41.2-65.7), the DCR was 92.8% (95% CI, 83.9-97.6), and grade 3^+ TRAEs occurred in 49.3% of patients (84). Another study called AK104-IIT-018 (NCT05816499) included patients with histologically or cytologically confirmed stage IIIB/IIIC or IV NSCLC without sensitizing *EGFR/ALK/ROS1* mutations, who must have progressed during or after a PD-1/L1 inhibitor and platinum-based chemotherapy and were treated with three-drug combination therapy (cadonilimab plus anilotinib plus docetaxel) (85). Among 33 evaluable patients, the overall ORR was 30.3% (95% CI:15.6-48.7%), the DCR was up to 94.0% (95% CI:79.8-99.3%), the mPFS was 6.5 months, and the proportion of ≥ grade 3 TRAEs was only 17.4% (85). Patients with advanced driver-negative NSCLC have limited therapeutic options after progression on first-line immune-combination chemotherapy (86). The standard of care recommended by the NCCN guidelines is chemotherapy monotherapy, such as docetaxel, gemcitabine, and albumin-conjugated paclitaxel. However, the efficacy was minimal, with ORR of 14%-17% and mPFS of 4.0-5.4 months (87–89). Therefore, combining cadonilimab with anlotinib and docetaxel offers a potentially attractive treatment option for this group of patients. The LungCadX study (NCT06424821)evaluated the efficacy and safety of cadonilimab in combination with chemotherapy as first-line treatment for patients with driver-negative, PD-L1-negative advanced NSCLC (90). Among 30 evaluable patients, the overall ORR was 66.7%, with an ORR of 93.3% in squamous cancer, 40% in non-squamous cancer, and a DCR of 100% (90). The drug safety was good, with an overall TRAE incidence of 61.4%, including 34.1% of ≥ grade 3 TRAEs (90). The above results indicate that the first-line treatment of PD-L1-negative advanced NSCLC with cadonilimab in combination with chemotherapy shows an auspicious therapeutic effect, especially in patients with squamous carcinoma.

MEDI5752 is a 1 + 1 form of an asymmetric bispecific antibody that preferentially binds CTLA-4 from $PD\text{-}1^+$ T cells by reducing the affinity to the CTLA-4 (80). In a head-to-head comparative trial with Keytruda, patients treated with carboplatin plus pemetrexed plus MEDI5752 had better DOR, PFS, and OS than those treated with carboplatin plus pemetrexed plus Keytruda (mDOR: 20.5% vs. 9.9%, mPFS: 15.1 vs. 8.9 months, mDOR: NR vs. 16.5 months) (91). In addition, bsAbs based on PD-1 and CTLA-4 targeting include XmAb20717, SI-B003, and MGD019, some of which have published preliminary clinical data (Table 1). These bispecific antibodies, although not aligned with AK104 as well as MEDI5752 in terms of the specific protein sequences and format, are all designed to target both PD-1 and CTLA-4 and to bind PD-1/CTLA-4 double-positive cells to reduce CTLA-4 toxicity preferentially (124–126).

Erfonrilimab (KN046) is a tetravalent symmetric bsAb targeting PD-L1 and CTLA-4, consisting of two identical chains, each consisting of a PD-L1 single-domain antibody, a CTLA-4 single-domain antibody, and a Fc domain (87). By design, the antibody has a higher affinity for PD-L1 and, therefore, can preferentially target the tumor microenvironment with high PD-L1 expression to reduce toxicities (96). At the same time, the antibody retains the function of Fc to remove CTLA-4-expressing Treg in the tumor microenvironment (127). In the study named KN046-201 (NCT03838848), a total of 26 advanced NSCLC patients with EGFR sensitivity mutation who had failed EGFR-TKI(s) and without platinum-based chemotherapy were enrolled and were given KN046 in combination with pemetrexed and carboplatin as a second-line treatment (95). The reported ORR was 26.9%, mPFS was 5.5 months, and mOS was 20.2 months (95). And 57.7% of the patients experienced grade 3 or higher TRAEs (95). In another phase II study evaluating KN046 in combination with chemotherapy for the first-line treatment of patients with metastatic NSCLC (NCT04054531), the ORR was 46.0%, with a mPFS of 5.8 months and a mOS of 26.6 months (96). In addition, for patients with metastatic NSCLC who had failed previous immunotherapy and platinum-based chemotherapy, the mOS of patients given KN046 was up to 13.3 months (97). In a study evaluating KN046 in combination with axitinib in advanced NSCLC (NCT05420220), for previously untreated patients with PD-L1 TPS ≥1% and patients treated with CPIs, the ORR after receiving the combination therapy was 56.8% and 9.4% respectively, and the DCR was 90.9% and 81.3%, showing promising efficacy (98).

4.2.2 PD-1 × PD-L1

IBI318/LY3434172 is an IgG-like dual antibody targeting PD-L1 and PD-1, and preclinical data suggest that it has significant tumor-suppressive effects and is superior to equivalent doses of monoclonal antibodies, as well as the combination of PD-1 and PD-L1 monoclonal antibodies (128). Preliminary phase Ib clinical (NCT03875157) data suggests that this drug has significant efficacy in immunotherapy-naïve NSCLC patients who had failed or were intolerant to first-line chemotherapy. Its ORR in patients with PD-L1 scores of 1-49% and ≥50% was 12.5% (1/8) and 45.5% (5/11), respectively, and its DCR was 50% (4/8) and 81.8% (9/11), respectively (99).

4.2.3 PD-1/(L)1 × TIGIT

T cell immunoglobulin and ITIM domain (TIGIT) is an immune checkpoint that has recently attracted attention. TIGIT interacts with CD155 (poliovirus receptor, PVR, or NECL-5) on the surface of antigen-presenting cells or tumor cells and inhibits the anti-tumor response of T cells and NK cells (129). TIGIT is expressed in various lung cancers, including NSCLC, and overexpression of TIGIT/CD155 is an unfavorable prognostic factor in lung adenocarcinoma (130). TIGIT is generally co-

TABLE 1 Clinical results of bsAbs in lung cancer.

bsAb	Targets	INN	Sponsor	Format	Phase	Pts characteristics and intervention	Key results	ref
JNJ-61186372	EGFR cMET	Amivantamab	Janssen	Duobody (1 + 1)	approved (American)	Pts with *EGFR* Exon20ins advanced NSCLC who progressed after platinum-based chemo; Amiv mono; N=81;	ORR: 40%; mDOR: 11.1 mos.; mPFS: 8.3 mos.; mOS: 22.8 mos; TRAEs: 99%; Grade 3^+ TRAEs: 35%;	(39)
						Pts with *EGFR* Exon20ins advanced NSCLC who had not received previous systemic therapy; Amiv + Chemo, N=151; Chem, N=155;	mPFS: 11.4 mos. vs. 6.7 mos.; PFS reported at 18 mos.: 31% vs. 3%; mOS: NR vs. 24.4 mos. (HR=0.67, 95% CI, 0.42–1.09); TRAEs: 100% vs. 98% Grade 3^+ TRAEs: 75% vs. 54% (Amiv + Chem vs. Chemo)	(42)
						Pts with treatment-naïve, *EGFR*-mutated (Ex19del or L858R) locally advanced or metastatic NSCLC; Amiv + Lazertinib, N=429; Osimertinib, N=429;	ORR: 86% vs. 85%; mDoR: 25.8 mos.vs. 16.8 mos.; mPFS: 23.7 mos. vs. 16.6 mos. (HR=0.70, 95% CI, 0.58-0.85); Grade 3^+ TRAEs: 75% vs. 43% (Amiv + Lazertinib vs. osimertinib)	(44) (45)
						Pts with relapsed or refractory NSCLC with *MET* exon 14 skipping mutation; Amiv mono; N=97;	ORR: 33%; mDoR: 11.2 mos.; CBR: 69%; Grade 3^+ TRAEs: 42%;	(46)
						Pts with *EGFR*-mutated advanced NSCLC who progressed after osimertinib and platinum-based chem; Amiv subcutaneous combined with Lazertinib, N=206; Amiv intravenous combined with Lazertinib, N=212;	ORR: 30% vs. 33%; mPFS: 6.1 mos. vs. 4.3 mos.; mDoR:11.2 vs 8.3 mos.; OS: significantly longer (HR 0.62, 95% CI, 0.42- 0.92); IRRs: 13% vs. 66%; VTE: 9% vs. 14%;	(47)
EMB-01	EGFR cMET	Bafisontamab	EpimAb	FIT-Ig (2 + 2)	II	Pts with advanced solid tumors; EMB-01 mono; N=38;	ORR: 5.3%; SD: 36.8%; DCR: 42.1%; Grade 3^+ TRAEs: 8.3% (rash); 1.7%(others);	(48)
MCLA-129	EGFR cMET	/	Merus	Biclonics (1 + 1)	II	Pts with relapsed or refractory NSCLC; MCLA-129 mono; *MET*ex14 mutation,	ORR: 43.5%; 28.6%; 21.8%; DCR: 95.7%; 84.1%; 69.1%;	(50)

(Continued)

TABLE 1 Continued

bsAb	Targets	INN	Sponsor	Format	Phase	Pts characteristics and intervention	Key results	ref
						N=23; *EGFR* Exon20ins, N=63; sensitized *EGFR*-mutated, N=55;	mDoR: 6.3 mos.; 7.2 mos.; 9.8 mos.; Grade 3^+ TRAEs: 51.6%;	
						Pts with advanced/ metastatic *EGFR*mut NSCLC who were treatment-naïve or progressed on osimertinib; MCLA-129 + Osimertinib; treatment-naïve, N=16; progressed on Osimertinib, N=34;	ORR: 75.0%; 35.3%; DCR: 93.8%; 73.5%; Grade 3^+ TRAEs: 23%; 38%;	(51)
MCLA-128	HER2 HER3	Zenocutuzumab	Merus	Biclonics (1 + 1)	II	Pts with relapsed or refractory advanced $NRG1^+$ NSCLC; MCLA-128 mono; N=64;	ORR: 34%; mDoR: 12.9 mos.; Grade 3^+ TRAEs: <4%;	(66)
SI-B001	EGFR HER3	Izalontamab	Baili	IgG1-$scFv_2$ (2 + 2)	III	Patients with locally advanced or metastatic *EGFR/ALK* wild-type NSCLC who had failed first-line anti-PD-1/L1 therapy; SI-B001+ PBC/ docetaxel; N=48;	ORR: 31.3%; DCR: 77.1%; Grade 3^+ TRAEs: 17% (myelosuppression); 15% (decreased neutrophil count); 12% (decreased white blood cell count);	(70)
AK104	PD-1 CTLA-4	Cadonilimab	Akeso	Tetrabody (2 + 2)	approved (China)	Pts who had failed previous platinum-based doublet chemo and were immunotherapy naïve; AK104 mono; N=30;	ORR: 10%; DCR: 40%; mOS: 19.6 mos.; Grade 3^+ TRAEs: 11.3%;	(92)
						Pts with advanced NSCLC; AK104 + anlotinib; treatment naïve, N=17; anti-PD-1/L1 resistant, N=6;	ORR: 70.6%; 16.7%; DCR: 94.1%; 100%; Grade 3^+ TRAEs: 14.3%; 5.9%;	(93)
						Treatment naive Pts with advanced NSCLC; AK104 + anlotinib; N=69;	ORR: 53.6%; DCR: 92.8; mDoR: NR; Grade 3^+ TRAEs: 49.3%;	(84)
						Pts with histologically or cytologically confirmed stage IIIB/ IIIC or IV NSCLC without sensitizing EGFR/ALK/ROS1 mutations must had progressed during or after a PD-1/L1	ORR: 30.3%; DCR: 94.0%; mPFS: 6.5 mos.; Grade 3^+ TRAEs: 17.4%;	(85)

(Continued)

10.3389/fimmu.2025.1572802

TABLE 1 Continued

bsAb	Targets	INN	Sponsor	Format	Phase	Pts characteristics and intervention	Key results	ref
						inhibitor and a platinum-based chemotherapy; AK104 + anlotinib + docetaxel; N=33;		
MEDI5752	PD-1 CTLA-4	Volrustomig	AstraZeneca	DuetMab (1 + 1)	III	Pts with NSCLC who were treatment-naïve; carboplatin/ pemetrexed + MEDI5752, N=20; carboplatin/ pemetrexed + pem, N=21;	ORR: 50%; 47.6%; ORR in PD-L1<1%: 55.6%; 30.0%; mPFS: 15.1 mos.; 8.9 mos.; mPFS in PD-L1<1%: 13.4 mos.; 9.0 mos.; mOS: NR; 16.5 mos.; Grade 3^+ TRAEs: 32%, TEAE-D/C: 20%	(91)
SI-B003	PD-1 CTLA-4	/	Baili	IgG1-$scFv_2$ (2 + 2)	I	Pts with recurrent or metastatic solid tumors who had failed standard therapy; SI-B003 mono; N=56)	ORR: 16.1%; DCR: 50.0%;	(94)
KN046	PD-L1 CTLA-4	Erfonrilimab	Alphamab	VHH-Fc (2 + 2)	III	Pts with *EGFR* sensitizing mutation (Ex19del or L858R), and failed from prior EGFR-TKI(s) without platinum-based chemo; KN046 + Pemetrexed + carboplatin AUC5; N=26;	ORR: 26.9%; DCR: 84.6%; CB: 38.5%; mPFS: 5.5 mos.; mOS: 20.2 mos.; Grade 3^+ TRAEs: 19.2% (infusion reaction); 15.4% (decreased platelet count); 11.5% (anemia);	(95)
						Pts with advanced NSCLC; KN046+ chemo; non-squamous NSCLC, N=51; squamous NSCLC, N=36;	ORR: 43.1%; 52.9% CBR: 50%; 61.1%; mDOR: 9.1 mos.; 7.3 mos.; mPFS: 5.8 mos.; 5.7 mos.; mOS: 27.2 mos.; 26.6 mos.; Grade 3^+ TRAEs: 66.7%;	(96)
						Pts had NSCLC that had progressed after ICI(s) and platinum-based chemotherapy, excluding *EGFR* mutation and/or *ALK* translocation; KN046 mono; N=31;	ORR: 3.2%; DCR: 38.7%; mPFS: 2.8 mos.; mOS: 13.3 mos.; Grade 3^+ TRAEs: 9.7% (anemia); 3.2% (febrile neutropenia); 3.2% (fatigue);	(97)
						Pts with stage IIIB-IV NSCLC and without	ORR: 56.8%; 73.3%; 9.4%;	(98)

(Continued)

TABLE 1 Continued

bsAb	Targets	INN	Sponsor	Format	Phase	Pts characteristics and intervention	Key results	ref
						EGFR activating mutation and *ALK* rearrangement; KN046 +axitinib; treatment-naive and PD-L1 expression ≥1%, N=44; treatment-naive and PD-L1 expression ≥50%, N=15; progressed on CPIs, N=32);	DC: 90.9%; 93.3%; 81.3%; mDOR: 13.2 mos.; NE; 7.4 mos.; mPFS: 8.3 mos.; 12.4 mos.; 5.6 mos.; Grade 3^+ TRAEs: 58.5%; 59.4%; 58.8%;	
IBI318/LY3434172	PD-1 PD-L1	/	Innovent/Lilly	IgG like (1 + 1)	II	Pts with advanced NSCLC; IBI318/LY3434172 mono;IO-failed NSCLC, N= 10; immunotherapy-naïve NSCLC pts with a PD-L1 TPS of 1–49%, N=8; treatment-naïve NSCLC pts with a PD-L1 TPS ≥ 50%, N=11;	ORR: 0%; 12.5%; 45.5%; DCR: 30%; 50%; 81.8%; Grade 3^+ TRAEs: 8.2%;	(99)
AZD2936	PD-1 TIGIT	Rilvegostomig	AstraZeneca	DuetMab (1 + 1)	III	Pts with advanced NSCLC who had prior CPIs treatment and a PD-L1 tumor proportion score ≥1%; AZD2936 mono; PD-L1 TPS=1-49%, 750mg, N=31; PD-L1 TPS≥50%, 750mg, N=34; PD-L1 TPS≥50%, 1500mg, N=30;	ORR:29%; 61.8%; 36.7%; DCR:64.5%; 88.3%; 66.7%; mDoR (all confirmed responders): 10.5 mos.; discontinued due to TRAEs: 4.2%; Grade 3^+ TRAEs: 10.5%	(100)
PM1022	PD-L1 TIGIT	/	Biotheus	IgG-VHH (2 + 2)		Pts with advanced solid tumors; PM1022 mono; N=15;	ORR: 7.1%; DCR: 35.7%; TRAEs: 53.3%;	(101)
MDG103	PD-1 LAG-3	Tebotelimab	MacroGenics	DART-Fc (2 + 2)	III	Pts with advanced or metastatic NSCLC; MDG103 mono; CPIs naive, N=14; post-CPI, N=15;	ORR: 14.3%; 0; DCR: 64.3%; 53.3%; Grade 3 + TRAEs: 50.5%;	(102)
AK112	PD-1 VEGF-A	Ivonescimab	Akeso/Summit	Tetrabody (2 + 2)	approved (China)	NSCLC pts with *EGFR* mutations who had failed prior EGFR-TKIs therapies; Ivon + chemo, N=161; placebo + chemo, N=161;	ORR: 50.6% vs. 35.4%; mPFS: 7.06 mos. vs. 4.80 mos.; mDOR: 6.6 mos. vs. 4.2 mos.; PFS: significantly improved (HR 0.46, 0.34-0.62); OS: significantly improved(HR 0.8, 95% CI, 0.59-1.08)	(103)

(Continued)

TABLE 1 Continued

bsAb	Targets	INN	Sponsor	Format	Phase	Pts characteristics and intervention	Key results	ref
							Grade 3$^+$ TEAEs: 61.5% vs. 49.1%; (Ivon + chemo vs. placebo + chemo)	
						Pts with previous untreated stage IIIB to IV advanced NSCLC (*EGFR/ALK* wild-type and PD-L1≥1%); Ivon, N=198; Pemb, N=200;	ORR: 50.0% vs. 38.5%; DCR: 89.9% vs. 70.5%; mPFS: 11.14 mos. vs. 5.82 mos.; (HR 0.51; 0.38-0.69) TEAEs: 89.8% vs. 81.9% Grade 3$^+$ TEAEs: 29.4% vs. 15.6%; (Ivonescimab vs Pembrolizumab)	(104)
PM8002	PD-L1 VEGF-A	/	Biotheus/ BioNTech	IgG-VHH (2 + 2)	III	Pts with advanced NSCLC; PM8002 mono; Treatment-naïve no-sq-NSCLC with *EGFR/ALK* wild-type and PD-L1$^+$, N=17; EGRF-TKI treated no-sq-NSCLC, N=36; IO and PBC treated NSCLC with *EGFR/ALK* wild-type, N=8;	ORR: 47.1%; 19.4%; 12.5%; mPFS: 10.9 mos.; 4.9 mos.; 6.7 mos.; 6 mos. PFS: 82.4%; 43.8%; 62.5%; Grade 3$^+$ TEAEs: 18%;	(105)
						Pts with advanced SCLC who failed first-line platinum-based chemo with or without CPIs therapy; PM8002 mono; N=22;	ORR: 72.7%; DCR: 81.8%; mPFS: 5.5 mos.; Grade 3$^+$ TEAEs: 18%	(106)
IMM2510	PD-L1 VEGFs	/	ImmuneOnco/ Instil Bio	IgG-fusion protein (2 + 2)	Ib/II	Pts with advanced solid tumors; IMM2510 mono; N=25;	ORR: 12% (3/25); DOR: 40% (10/25); Grade 3+ TEAEs: 33.3%;	(107)
SHR-1701	PD-L1 TGF-β	Retlirafusp alfa	Suzhou Suncadia	IgG-fusion protein (2 + 2)	III	Pts with advanced/ metastatic NSCLC; SHR-1701 mono; Treatment-naïve NSCLC with PD-L1$^+$, N=57; EGFR TKIs treated or no standard EGFR TKIs were available NSCLC, N=41; CPIs treated pts who had received up to 3 previous lines of treatments, N=33;	ORR: 36.8%; 19.5%; 9.1% DCR: 66.7%; 46.3%; 54.5% mPFS: 5.3 mos.; 1.4 mos.; 2.1 mos.; mOS: 24.2 mos.; 14.4 mos.; 16.1 mos.; Grade 3$^+$ TEAEs: 22.9%;	(108)
						Pts with unresectable stage III NSCLC; SHR-1701 plus chem followed by surgery	post-induction ORR: 58%; 18-month EFS: 56.6%;	(109)

(Continued)

TABLE 1 Continued

bsAb	Targets	INN	Sponsor	Format	Phase	Pts characteristics and intervention	Key results	ref
						or radiotherapy, and then consolidation SHR-1701; N=107;	Pts underwent surgery: 25%; Pts achieved R0 resection: 25%; mPR: 12%; cPR: 6.5%;	
AMG757	DLL3 CD3	Tarlatamab	Amgen	HEL-BiTE (1 + 1)	approved (American)	Pts with advanced SCLC previously treated with two or more lines of therapy; Tarl mono; 10mg-group, N=100; 100mg-group, N=88;	ORR:40%; 32%; mPFS: 4.9 mos; 3.9 mos.; mOS: 14.3 mos.; NE; CRS: 51%; 61% Grade 3$^+$ TEAEs: 59.4%; 64%; Fatal: 5.3%; 6%;	(110)
						Pts with previously treated SCLC; Tarl mono; Tarl≥10mg, N=152; 10 mg Tarl Q2W, n=17;)	ORR:25%; 35.3%; mDOR: 11.2 mos.; 19.4 mos.; mOS: 17.5 mos.; 20.3 mos.; Intracranial DCR (all): 87.5% (14/16);	(111)
BI-764532 / OBT-620	DLL3 CD3	/	Boehringer Ingelheim/ Oxford Bio Therapeutics	IgG like (1 + 1)	I	Pts with locally advanced/metastatic DLL3$^+$ (confirmed centrally) solid tumors; BI-764532 mono; SCLC, N=39; epNEC, N=27; LCNEC, N=5; ALL, N=71;	PR: 26%; 19%; 60%; 25%; DCR: 51%; 44%; 100%; 52%; Grade 3$^+$ TEAEs: 27% Discontinued due to TRAEs: 4%;	(112)
HPN328/MK6070	DLL3 CD3 HSA	/	Harpoon/ Merck	TriTAC (1 + 1+1)	I/II	Pts with relapsed/ refractory, metastatic SCLC and other NEN associated with DLL3 expression; HPN328 mon; SCLC, N=28; other NEN, N=13;	ORR: 39%; 46%; DCR:71%; 46%; Grade 3$^+$ TEAEs: 26%; discontinued due to TRAEs: 4%; death due to TRAEs: 2%;	(113)
						Pts with relapsed/ refractory, metastatic SCLC; HPN328 mono; Brain metastases, N=28; No brain metastases, N=21;	ORR:37%; 19%; DCR: 78%; 48%;	(114)
JANX008	EGFR CD3	/	Janux	TRACTr (1 + 1+1)	I	Pts with advanced or metastatic solid tumors known to express high levels of the EGFR target JANX008 mono; N=11;	one Pt with NSCLC had a confirmed PR with 100% reduction of the target lung lesion and elimination of liver metastasis; Grade 1 CRS in 2 Pts;	(115)
GEN1046	PD-L1 4-1BB	Acasunlimab	Genmab	Duobody (1 + 1)	III	Pts with advanced solid tumors;	DCR: 65.6%; Grade 3$^+$ TEAEs:	(116)

(Continued)

TABLE 1 Continued

bsAb	Targets	INN	Sponsor	Format	Phase	Pts characteristics and intervention	Key results	ref
						GEN1046 mono; N=61;	21.3%; DLT: 9.8%	
						Pts with PD-L1$^+$ metastatic NSCLC who had disease progression following one or more prior lines of anti-PD-1/L1-containing treatment; arm A, GEN1046 100 mg Q3W x 2 cycles then 500 mg Q6W, N=16; arm B, GEN1046 100 mg + pemb 200 mg Q3W, N=22; arm C, GEN1046 100 mg + pemb 400 mg Q6W, N=24;	ORR: 12.5%; 18.2%; 16.7%; DCR: 50%; 59.1%; 75%; mDOR: 2.0 mos.; 5.2mos.; NR mos.; mOS: 5.5 mos.; 8.6 mos.; 17.5 mos.; Grade 3$^+$ TEAEs: liver reated events (9.1%; 16.7%; 12.2%); anemia (4.5%; 2.4%; 0%);	(117)
FS222	PD-L1 4-1BB	/	F-star	mAb2 (2 + 2)	I	Pts with pretreated advanced solid tumors; FS222 mono; N=90;	ORR: 15.7% (include NSCLC); Grade 3$^+$ TEAEs (≥10% of pts): AST (13.3%); ALT (11.1%);	(118)
AFM24	EGFR CD16	/	Affimed	IgG1-scFv$_2$ (2 + 2)	III	Pts with *EGFR* mutant NSCLC, relapsed or refractory to ≥1 prior lines of therapy; AFM24 mono, N=10;	DCR: 50%; Grade 3$^+$ TEAEs: 40%; Grade 5 pneumonitis: 1/10	(119)
						Pts with advanced or metastatic *EGFR*-WT NSCLC who progressed on ≥1 prior line of therapy, including at least a platinum doublet and a CPI; AFM24 +atezolizumab, n=15;	ORR: 26.7%; DCR: 73.3% Grade 3+ TEAEs: 13.3%	(120)
IBI363	PD-1 IL-2	/	Innovent	IgG-fusion protein (1 + 1)	II	Pts with advanced non-small cell lung cancer IBI363 mono, N=79;	ORR: 24.1%; DCR: 68.4%; Grade 3$^+$ TEAEs: 19.1%; discontinued due to TRAEs: 4.5%; death due to TRAEs: 1.1%;	(22)
PF-07209960	PD-1 IL-15	/	Pfizer	IgG-fusion protein (2 + 1)	I	Pts with advanced or metastatic solid tumors, N=29;	ORR: 6.9%; DCR: 48.3% Grade 3$^+$ TEAEs: 778.4%;	(121)
SAR44587/KD055	PD-1 IL-15/IL15-Rα	/	Sanofi	IgG-fusion protein (2 + 1)	I	/	/	(122)

(Continued)

TABLE 1 Continued

bsAb	Targets	INN	Sponsor	Format	Phase	Pts characteristics and intervention	Key results	ref
IAP0971	PD-1 IL-15/IL15-Rα		SunHo Bio	IgG-fusion protein (2 + 1)	I	/	/	(123)

bsAb, bispecific antibody; INN, international nonproprietary name; pts, patients; ref, reference; EGFR, epidermal growth factor receptor; cMET, c-mesenchymal-epithelial transition factor; NSCLC, no small cell lung cancer; chemo, chemotherapy; amiv, amivantamab; mono, monotherapy; N, number of efficacy population; ORR, objective response rate; CI, confidence interval; mDOR, median duration of response; mos., months; NR, not reached; mPFS, median progression-free survival; mOS, median overall survival; TRAE, treatment-related adverse events; CBR, clinical benefit ratio; VTE, venous thromboembolism; SD, stable disease; DCR, disease control rate; NRG1, neuregulin 1; PD-1, programed cell death protein 1; PD-L1, programed death-ligand 1; PBC, platinum-based chemotherapy; CTLA-4, cytotoxic T lymphocyte-associated antigen-4; HER2, human epidermal growth factor receptor-2; HER3, human epidermal growth factor receptor-3; pemb, pembrolizumab; ICI, immune checkpoint inhibitor; TIGIT, T cell immunoreceptor with Ig and ITIM domains; CPIs, checkpoint inhibitors; LAG3, lymphocyte activation gene-3; VEGF-A, vascular endothelial growth factor A; Ivon, Ivonescimab; no-sq-NSCLC, non-squamous NSCLC; TGF-β, transforming growth factor-β; DLL3, delta-like protein 3; SCLC, small cell lung cancer; Tarl, tarlatamab; Q2W, once every two weeks; CRS, cytokine-release syndrome; epNEC, extrapulmonary neuroendocrine carcinoma; LCNEC, large cell neuroendocrine carcinoma; NEN, neuroendocrine neoplasms; PR, partial response.

expressed with immunosuppressive molecules, such as PD-1, on various T cells, and both inhibit $CD8^+$ T cell activity through different mechanisms (131, 132). TIGIT blockade is a promising immunotherapy in terms of molecular mechanisms. However, vibostolimab and tiragolumab, two monoclonal antibody drugs targeting TITGI, are ineffective as monotherapy (133, 134). However, tiragolumab in combination with atezolizumab had an overall ORR of 37% and an ORR of 66% in the PD-L1 TPS>50% subgroup, which exceeded atezolizumab monotherapy (21% and 24%, respectively) (135). Therefore, developing bsAb targeting PD-1 and TIGIT is also interesting to researchers.

Rilvegostomig (AZD2936) is an asymmetric dual antibody targeting PD-1 and TIGIT. The initial efficacy of rilvegostomig in patients with advanced NSCLC treated with CPIs has been published (NCT04995523). Patients with PD-L1 TPS ≥50% treated with rilvegostomig 750mg had an ORR of 61.8% and a DCR of 88.3%, and the drug had a favorable safety profile, with a grade 3 or higher adverse events rate of 10.5% (100). The company developing the drug is currently conducting a head-to-head clinical trial with Keytruda, which shows the drug developer's confidence in this drug.

PM1022 is a bispecific antibody targeting PD-L1 and TIGIT, with VHH targeting PD-L1 fused to the C-terminus of the anti-TIGIT antibody. The antibody is currently undergoing a dose extension clinical study (NCT05867771), and preliminary results show an ORR of 7.1%, a DCR of 35.7%, and an overall TRAE rate of 53.3% in treated patients (101). One of the NSCLC patients had received prior treatment, including chemotherapy and anti-PD-1 therapy, and had a 56.8% reduction in lesion size (101).

4.2.4 PD-1 × LAG-3

Lymphocyte activation gene 3 (LAG-3), the third-generation immune checkpoint receptor, is highly up-regulated on exhausted T cells in the tumor microenvironment (136). The binding of LAG-3 to its classical ligand, the major histocompatibility complex-II, leads to the down-regulation of T cell activation, proliferation, and cytokine production, ultimately causing T cell dysfunction (137). Immunohistochemistry analysis revealed that LAG-3 is expressed in various cancer tissues, with 90% of NSCLC and 52% of SCLC samples having detectable positive LAG-3 expression (102). In NCSLC, co-expression of PD-1 and LAG-3 was detectable in 59% of samples (102). Moreover, it was found that LAG-3 and PD-1 synergize on $CD8^+$ T cells to drive T cell exhaustion (138). Currently, the FDA approved Opdualag (consisting of a fixed-dose combination of relatlimab and nivolumab) for treating unresectable or metastatic melanoma in 2022 (139). In addition, it was shown that compared to nivolumab combination chemotherapy, Opdualag combination chemotherapy improved ORR (53.2% vs. 40.8%), prolonged mPFS (9.8 vs. 6.1 months), and had an HR of 0.63 in this group of NSCLC patients with PDL1 ≥ 1%; and, for non-squamous NSCLC (non-sq-NSCLC) patients with PD-L1 TPS≥1%, the ORR improved to 58%, the mPFS increased to 11.6 months, and the HR was further reduced to 0.55 (140). The above study demonstrated that dual immune checkpoint therapy with LAG-3 and PD-1 has a better prospect in lung cancer treatment.

MGD103 (Tebotelimab) is a tetravalent DART-Fc (IgG4κ) fusion protein that blocks PD-1 and LAG-3. *In vitro* studies have shown that this bsAbs is significantly more potent than the combination of nivolumab and relatlimab in stimulating IFN-γ secretion (102). Tebotelimab had an ORR of 14.3% and a DCR of 64.3% in NSCLC patients who did not receive CPIs; however, no remission was observed in NSCLC patients who had previously received CPIs (NCT03219268) (102). Interestingly, there was a correlation between objective response to tebotelimab and LAG-3 expression ($P < 0.05$), but no statistical association between PD-1 and clinical response was observed (102).

In addition to the aforementioned immunomodulatory targets with more basic and clinical studies, some new immune checkpoint molecules (e.g., OX40, TIM3) have also attracted the attention of researchers in the past decade (141, 142). Moreover, there is much clinical or preclinical evidence that these new immune checkpoints synergize with anti-PD-1/L1 and/or anti-CTLA-4 monoclonal antibodies (143). Therefore, it is worth waiting for the final clinical outcome based on these newly discovered immune checkpoints combined with PD-1/L1 or anti-CTLA -4 to form a bsAbs.

4.3 Dual inhibition of tumor microenvironment and immune checkpoints

A tumor is a heterogeneous complex of tumor cells, various non-malignant cells (e.g., immune cells, stromal cells, endothelial cells, cancer-associated fibroblasts), and various non-cellular components (e.g., vascularised extracellular matrix, exosomes, cytokines) (144). The tumor microenvironment (TME) influences tumor growth, metastatic spread, and response to therapy. It has become common knowledge that TME-mediated immunosuppression impairs beneficial responses.

4.3.1 PD-1/L1 × VEGF

In NSCLC, high vascular endothelial growth factor (VEGFs) expression is associated with tumor recurrence, low survival, metastasis, and death in patients (145, 146). Overexpression of VEGF induces a reduction in the expression of endothelial cell adhesion molecules, which severely impairs T-cell homing and reduces the number of T lymphocytes entering the TME (147). It has been shown that VEGF-A also enhances the expression of PD-1 and other inhibitory checkpoints, such as CTLA-4, on the surface of T cells and inhibits the activity of $CD8^+$ T cells, leading to a blockade of the effector function of T cells (148–150). Therefore, combining anti-angiogenic drugs with immunotherapy, which normalizes tumor vasculature through anti-angiogenic drugs and promotes the increase of tumor immune cells (e.g., tumor-infiltrating lymphocytes) in NSCLC, and utilizing immune checkpoint inhibitors which can unlock the functional inhibition of T cells by PD-1 and PD-L1, both act synergistically with each other thus showing better therapeutic effects within solid tumors (151–153). In the IMpower-150 trial, researchers tested atezolizumab plus bevacizumab plus chemotherapy as a first-line treatment for non-squamous NSCLC (non-sq-NSCLC), with an ORR and PFS of 63.5% and 8.3 months, respectively (154). Still, the incidence of adverse events in grades 3 or higher was as high as 58.5% (154). The FDA has approved atezolizumab, bevacizumab, and chemotherapy as first-line treatment for advanced non-squamous NSCLC (155).

AK112 (Ivonescimab) is a humanized anti-PD-1/VEGF-A bispecific monoclonal antibody in which an anti-PD-1 scFv fused to the end of each of the two heavy chains of the anti-VEGF-A antibody (bevacizumab) to form a tetravalent bis-antibody. This bispecific antibody can accumulate in the tumor microenvironment, effectively blocking both the PD-1 and VEGF pathways, inhibiting PD-1-mediated immunosuppression, and blocking tumor angiogenesis in the microenvironment (156, 157). In May 2024, China approved AK112 in combination with chemotherapy (pemetrexed + carboplatin) for patients with locally advanced or metastatic non-sq-NSCLC who are EGFR mutation-positive and have progressed after treatment with EGFR TKIs (158). The approval was based on a phase III clinical trial called HARMONi-A (NCT05184712), which showed that in patients resistant to EGFR TKIs, AK112 in combination with chemotherapy was sufficient to significantly prolong mPFS compared to placebo combination chemotherapy (7.06 months vs. 4.08 months; HR 0.46) and patients had a higher ORR (50.6% vs. 35.4%) (103). The primary results of HARMONi-2 (NCT05499390), a trial comparing the efficacy of ivonescimab with that of pembrolizumab, were also presented. It showed that in patients with previously untreated stage IIIB to IV advanced NSCLC who were *EGFR/ALK* wild-type and with PD-L1 TPS≥1%, AK112 significantly prolonged their mPFS compared to pembrolizumab (11.14 vs. 5.82 months; HR, 0.51; $p<0.0001$), increasing their ORR (50.0% vs. 38.5%) and DCR (89.9% vs. 70.5%) (104). Although the rate of serious adverse events in patients treated with AK112 was slightly higher than with pembrolizumab (Grade 3^+ TRAEs: 29.4% vs. 15.6%), the results of HARMONi-2 are still encouraging (104). It is expected that AK112 will become a potential clinical option in the first-line treatment of lung cancer.

PM8002 is a humanized anti-PD-L1/VEGF-A bispecific antibody with the variable region of a humanized anti-PD-L1 nanobody fused at the end of the two heavy chains of the anti-VEGF-A antibody. Preliminary published data (NCT05918445) showed that in untreated *EGFR/ALK* wild-type and PD-$L1^+$ patients who received PM8002, the ORR is 47.1%, the mPFS is 10.9 months, and the incidence of grade ≥3 TRAEs was 18% (105). In addition, another study (ChiCTR2200059911) demonstrated the efficiency of PM8002 combined with paclitaxel for second-line treatment of SCLC. It was reported that the ORR was 72.7% (16/22), the DCR was 81.8% (18/22), and the mPFS was 5.5 months (106). Notably, the recommended drug for second-line treatment of SCLC is topotecan, with an ORR of 22% and a mDoR of 7.6 months (159). Therefore, further observing the subsequent clinical efficacy of PM8002 in SCLC is worthwhile.

IMM2510 is a bispecific antibody targeting PD-L1 and VEGFs that incorporates a VEGF receptor 1 domain 2 (VEGFR1-D2) at the C-terminus of each of the two heavy chains of the anti-PD-L1 antibody, forming a VEGF trap capable of binding a wide range of VEGF receptor ligands in addition to VEGF-A (160). IMM2510 is currently in the preliminary phase I clinical studies (NCT05972460). As of 21 December 2023, 33 patients with advanced solid tumors were treated with IMM2510 at nine doses (0.007-20.0 mg/kg) (107). Among the 25 patients whose conditions were evaluable, 3 patients had achieved confirmed partial response, and 7 patients had stable disease (107). Among the PR patients, one patient with sq-NSCLC (onco-driver gene negative, previous IO treatment failure) who was treated with 3 mg/kg IMM2510 achieving tumor shrinkage of 46% and still on the treatment with treatment duration over 20 months; one sq-NSCLC treated with 10 mg/kg showed a tumor shrinkage of about 32% and a treatment duration of 9.4 months (107). TRAEs occurred in 32 pts (97.0%), and most were grade 1 or 2. Grade ≥3 TRAEs occurred in 11 pts (33.3%), and no DLT occurred (107).

4.3.2 PD-L1 × TGF-β

A central factor in tumor immune resistance is immunosuppressive cytokines in the tumor microenvironment, a major component of which is transforming growth factor β (TGF-

β). It has been shown that TGF-β upregulates PD-L1 transcription in tumors (161). Besides, TGF-β-mediated T-cell rejection is one of the mechanisms by which tumors become resistant to anti-PD-L1 therapy (162). TGF-β also induces the release of PD-L1-containing exosomes by tumor cells, and PD-L1 exosomes in tumor regions hamper the effector activity of $CD8^+$ T cells (163). In addition, there is a bidirectional interaction between TGF-β and tumor-area hypoxia, where hypoxia is considered a key inducer of TGF-β, and the activity of the latter further enhances tumor-area hypoxia (164). Hypoxia induces upregulation of PD-L1 expression on tumor cells and upregulation of PD-1 expression on immune cells (e.g., TAMs, DCs, Tregs) in the tumor microenvironment (165, 166). Aberrant TGF-β activity is associated with immunosuppressive TME, promoting progression and metastasis in NSCLC (167). Several companies have developed drug molecules with dual inhibitory effects on PD-1/L1 and TGF-β, among which M7824 and SHR1701 were developed earlier and have more preclinical and clinical data.

M7824 is a bifunctional fusion protein, a molecule that fuses a TGF-β receptor II (a TGF-β 'trap' which is capable of trapping all TGF-β) to the end of the constant region of avelumab via a flexible linker (168). M7824 has been noticed and given high expectations based on its phase I clinical (NCT02517398) results released in 2018. Among 40 patients with advanced NSCLC who relapsed after standard therapy treated with 1200 mg of M7824, the ORR was 40.7% for PD-L1-positive patients and 71.4% for patients with high PD-L1 expression (169). However, the subsequent publication of several clinical data has overshadowed M7824's prospects. In the phase III clinical trial (NCT03631706) using either M7824 or pembrolizumab as first-line treatment for patients with advanced PD-L1 high-expression (TPS ≥80%) NSCLC, the results showed that first-line treatment with M7824 did not demonstrate superior efficacy compared to pembrolizumab and had a higher frequency of associated adverse events (170). Combined with unsatisfactory results from multiple other clinical trials, the outlook for M7824 is troubling, and clinical trials for the drug have now primarily been terminated.

SHR-1701 is also a bifunctional fusion protein that fuses an extracellular TGF-β receptor II structure to the C-terminus of a monoclonal antibody against PD-L1 (171). At the ESMO 2023 meeting, researchers preliminarily presented the results of SHR-1701 in 3 NSCLC clinical expansion cohorts (NCT03774979). For patients who had not received systemic chemotherapy and had a PD-L1 TPS ≥1%, ORR was 36.8%, DCR was 66.7%, and mOS was 24.2 months; for patients with an EGFR mutation who had failed prior treatment with standard EGFR TKIs or had no standard EGFR TKIs available, ORR was 19.5%, DCR was 46.3%, and mOS was 14.4 months; for patients who experienced disease progression after recent anti-PD-1/PD-L1 therapy and had received up to 3 lines of prior therapy ORR was 9.1%, DCR was 54.5%, mOS was 16.1 months (108). In this trial, 76.3% of patients treated with SHR-1701 experienced TRAEs, including 22.9% with grade ≥3 TRAEs (108). In addition, a trial (NCT04580498) was conducted to assess neoadjuvant SHR-1701 with or without chemotherapy, followed by surgery or radiotherapy, and then consolidation SHR-1701 in unresectable stage III NSCLC, and preliminary clinical results were recently published. Of the 97 evaluable patients treated with SHR-1701 plus chemotherapy, the postinduction ORR was 58%, and the 18-month event-free survival rate was 56.6% (109). Regarding safety, the rate of patients with grade ≥3 TRAEs was 75% in the SHR1701 plus chemotherapy arm (109). The drug is currently undergoing multiple multi-center phase III clinics, and there is much interest in the final outcome, especially as M7824 has been terminated from the clinic.

5 Immune cell engagement bispecific antibodies

5.1 T cell engagement

TCE is a typical application of bsAbs, with one targeting arm of most TCEs designed to bind specifically to selected tumor-associated antigen (TAA) on the surface of tumor cells and the other targeting arm designed to target the CD3ε chain in the TCR complex. Due to the signaling capacity of the CD3ε chain, TCEs can bypass the major histocompatibility complex restriction and, independently of the epitope specificity of the TCR, elicit T-cell activation and proliferation, as well as the subsequent release of transient inflammatory cytokines induced by the TCR and trigger tumor apoptosis via perforin and granzyme release (172). In addition, bsAbs targeting TAA and co-stimulatory receptors on T cells (e.g., 4-1BB, CD40, CD28, etc.) have a mechanism similar to that of a TCE.

5.1.1 DLL3 × CD3

Delta-like ligand 3 (DLL3) is a TAA highly expressed on the surface of tumor cells in patients with SCLC, with high expression detected in approximately 85%-94% of SCLC patients (173, 174). Under normal conditions, DLL3 is mainly localized in the Golgi apparatus and cytoplasmic vesicles and is hardly expressed on the surface of normal cells (175). In contrast, in cells of SCLC and other high-grade neuroendocrine tumors, DLL3 is highly up-regulated and aberrantly expressed on the cell surface, leading to abnormal growth of neuroendocrine tumor cells (176). Thus, DLL3 has become a potential target for treating SCLC.

Tarlatamab (AMG757) is a DLL3-based TCE. According to published data from the clinical trial called Delphi -301 (NCT05060016), patients with SCLC who had received two or more systemic therapies benefited significantly from fortnightly intravenous treatment with Tarlatamab (110, 177). This study demonstrated a more significant benefit in patients treated with 10 mg of Tarlatamab compared to 100 mg, with an ORR of 40.0%, mPFS of 4.9 months, and mOS of 14.3 months (110, 177). The most common adverse events were cytokine release syndrome (in 51% of the patients in the 10-mg group), decreased appetite (29%), pyrexia (35%), constipation (27%), and anemia (26%) (110, 177). Grade 3 or higher adverse events occurred in 59% of the patients in the 10-mg group (110, 177). Based on the clinical data published in Delphi-301, the FDA granted tarlatamab accelerated approval in May 2024

for the treatment of extensive-stage SCLC, where disease progression occurs during or after platinum-based chemotherapy (178). In addition, newly published long-term follow-up data from Delphi-300 (NCT03319940) showed that the overall ORR for patients treated with more than 10 mg of tarlatamab was 25%, with an mDOR of 11.2 months (111). Patients with brain metastases also showed significant benefits after treatment with tarlatamab, with intracranial disease control occurring in 87.5% (111). Safety data were consistent with Delphi -301, with no new safety signals (111). TCEs in solid tumors have long been considered challenging (172), and tarlatamab is the first TCE therapy to be approved for treating a solid tumor, marking a critical step forward.

BI764532 is an IgG-like TCE that induces strictly DLL3-dependent tumor killing (179). BI764532 is currently in phase I clinical trial (NCT04429087), and preliminary clinical data have been published. Of 71 evaluable patients treated with no less than 90ug/kg of BI764532, 25% achieved partial response, with a DCR of 52%, and tumor shrinkage was observed in all patients (112). A total of 86% of patients experienced adverse events of any grade, with 37% experiencing grade 3^+ TRAEs and four non-Asian patients discontinuing due to TRAEs (112).

PN328/MK6070 is a TCE targeting DLL3 and CD3. In addition, to prolong the half-life of this TCE as well as to maintain its most substantial direct T-cell killing ability, an anti-HSA single-domain antibody was fused in the middle of the DLL3 and CD3 targeting arms (see Figure 1) (180). It is currently enrolling participants with SCLC, neuroendocrine prostate cancer, and other high-grade neuroendocrine neoplasms in a phase I/II clinical trial (NCT04471727). The data showed that in the dose-optimized cohort (1-mg priming dose and a 12- or 24-mg target dose), patients with SCLC had an ORR of 39% and a DCR of 71% (113). In addition, the data showed that SCLC patients with brain metastases also responded well to HPN328 (ORR of 37% and DCR of 78%) (114). In terms of the safety of the drug, the incidence of TRAEs at any grade was 93%, with grade 3^+ TRAEs occurring in 26%, with four patients discontinuing the drug due to TRAEs and two patients dying (113).

5.1.2 EGFR × CD3

As mentioned earlier, EGFR is highly expressed in a variety of tumors. Meanwhile, EGFR regulates the development and homeostasis of regulated epithelial tissues in normal tissues and plays a key role in epithelial cell physiology (181). Therefore, a variety of drugs targeting EGFR have some skin toxicity (182, 183). In contrast, TCE-induced tumor cell killing is highly efficient, as TCE enables individual T cells to connect with multiple tumor cells, resulting in sequential killing (184). In addition, cytokines released from activated T cells can generate a cascade amplification effect to achieve a more excellent range of tumor cell killing (185). Therefore, TCEs targeting EGFR face more severe on-target off-tumor toxicity, resulting in a limited therapeutic window. However, suppose TCEs are engineered with a modified design to specifically recognize EGFR on tumor cells and bind no or less EGFR on normal tissues. In that case, they can significantly enhance the efficacy and expand the drug's therapeutic window.

JANX008 is a prodrug form of TCE that targets EGFR and contains an EGFR-binding domain, a CD3-binding domain, and a HAS-binding domain that serves to extend the half-life of the molecule (see Figure 1c) (186). In addition, a mask is fused to each of the EGFR and CD3 binding domains through tumor protease cleavable linkers, and only when the molecule enters the tumor site and is recognized by the tumor protease can the peptide masks be released, ultimately generating the active molecules (186). The drug currently enrolls patients with advanced or metastatic cancers with high EGFR expression in a clinical phase Ia trial. It has been observed to achieve partial remission in one NSCLC subject, with a 100% reduction in targeted lung lesions and the elimination of liver metastases (115). Notably, JANX008 had a favorable safety profile, with grade 1 CRS observed in only 2 of 11 subjects at doses up to 1.25 mg (significantly higher than the expected maximum tolerated dose of the parental T-cell articulator) (115).

5.1.3 PDL-1 × 4-1BB

4-1BB [also known as CD137 or TNF receptor superfamily member 9 (TNFRSF9)] is an inducible co-stimulatory receptor expressed on activated T cells and NK cells (187, 188). The agonism of 4-1BB avoids tumor-infiltrating lymphocyte exhaustion and enhances the antitumor activity of ICIs (189, 190). Although preclinical results have shown excellent efficacy of anti-4-1BB antibodies in different tumors, the development of 4-1BB-based monoclonal antibodies has successively failed either because of fatal side effects (urelumab) or because of limited efficacy (utomilumab) (191). Therefore, preserving the efficacy of anti-4-1BB antibodies while reducing their toxicity is a priority for subsequent development. One such strategy is the use of bsAb, which minimizes off-target tumor toxicity by designing the antibody to preferentially bind specifically to tumor cells and be enriched in the tumor microenvironment, and then to bind to 4-1BB and achieve activation of 4-1BB signaling. In this strategy, the most studied is the PD-L1/4-1BB bispecific antibody. Because PD-L1 is not only expressed on the surface of a wide range of cancer cells, a variety of host cells in the TME and lymph nodes, including dendritic cells, macrophages, fibroblasts, and T cells, also express PD-L1 to reduce antitumor immunity. In addition, PD-L1 blockade combined with 4-1BB agonistic antibodies has shown enhanced antitumor responses in preclinical cancer models (189, 190, 192). Thus, dual targeting of PD-L1 and 41BB by bispecific antibodies may permit tumor cell-dependent 4-1BB activation of T cells and allow optimal antitumor immunity.

GEN1046 (acasunlimab) is currently the fastest advancing bsAb targeting PD-L1 and 4-1BB. It is an IgG-like bsAb, with one arm targeting PD-L1 to block PD-1/PD-L1 inhibitory signals and another targeting 4-1BB to activate co-stimulatory signals in immune cells (116). A clinical trial (NCT05117242) evaluating acasunlimab monotherapy and acasunlimab in combination with pembrolizumab in metastatic NSCL patients who were resistant to anti-PD-1/L1 antibodies is currently underway, and preliminary results have been published. The data showed that patients treated with GEN1046 100 mg Q6W in combination with pembrolizumab 400 mg Q6W had a favorable treatment outcome (117). This subset of patients had an ORR of 16.7%, a DCR of 75%, a mOS of 17.5 months, and a 12-month OS rate of 69% (117). The most common adverse events (all grades; grade ≥3) in patients treated with the combination therapy included

liver-related events (18.7%; 13.3%), fatigue (14.7%; 0%), malaise (13.3%; 0%), and diarrhea (12%; 0%) (117).

FS222 is a 2 + 2 tetravalent bsAbs constructed on a platform called mAb2. The antibody is based on a PD-L1 antibody, engineered to make its Fc recognize 4-1BB (193). The antibody is, therefore, similar in size to a conventional monoclonal antibody. Additionally, the antibody undergoes Fc mutation to reduce associated effects such as ADCC and CDC. FIH (NCT04740424) is an ongoing phase I clinical trial investigating the efficacy of FS222 in advanced solid tumors. Currently, interim results from the Q4W cohorts have been reported. The cohort had a total of 90 patients enrolled, with a median of 2 (1–7) regimens previously treated. At the cut-off date (05 Dec 2023), 20 (22.2%) patients were still on treatment, and objective remissions (CR, PR) were observed in patients with melanoma, NSCLC, ovarian, triple-negative breast, liposarcoma, and colon cancer with an ORR of 15.7% (118). The most common TRAEs grade ≥3 (≥10% of pts) were increased AST (13.3%) and ALT (11.1%) (118).

5.2 NK cell engagement

NK cells are innate immune cells with cytotoxicity. NKCEs have one targeting arm targeting tumor cell surface-specific antigens and the other targeting arm targeting activating receptors on the surface of NK cells, such as CD16a, NNKG2D (atural Killer Group 2 Member D), NKp30 (Natural Killer cell p30), etc., resulting in the formation of antigen-specific immune synapses between the NK cells and the tumor cells that which in turn triggers NK cell-mediated killing of tumor cells (194). NKCEs are a new exploration, and several drugs of this type are undergoing preclinical or clinical evaluation.

5.2.1 EGFR × CD16a

AFM24 is a tetravalent bispecific antibody in which the anti-EGFR scFv is fused to the c-terminus of the anti-CD16a antibody via a connector, which mediates the killing of tumor cells by NK cells in an EGFR-dependent manner (195). Studies have demonstrated the preliminary efficacy of AMF24 in NSCLC patients with *EGFR* mutant NSCLC, relapsed or refractory to ≥1 prior lines of therapy. Of the 10 evaluable patients, 1 patient suffered a 45% reduction in tumor volume, and 4 had stable disease with a 50% tumor control rate (119). However, a high proportion of patients experienced TRAEs (13/14), with grade ≥3 TRAEs occurring in 4 patients and grade 5 pneumonitis occurring in 1 patient (13/14) (119). In NSCLC patients with *EGFR*-WT who relapsed after one or more first-line therapies, the combination of AFM24 and atezolizumab led to 1 complete response, 3 partial responses, and 7 cases of stable disease among the 15 evaluable patients (120). Moreover, this combination therapy was well tolerated. The main adverse events that occurred in the patients were infusion-related reactions (10/17) (120).

6 Immunocytokines

Cytokines are mediators and modulators of the innate and adaptive immune systems, and immunotherapy based on cytokines such as interferon and interleukin-2 (IL-2) has been used in the treatment of cancer as early as the end of the 20th century (196). However, the short half-life of cytokines results in the need for short periods of high-dose administration, which can lead to severe non-specific toxicity. In addition, the cytokine's inhibitory or activating effect on immune cells is also related to the concentration and the environment of action. Therefore, engineering cytokines to preferentially target disease sites and to activate only specific lymphocyte types can increase the tolerability of cytokine therapy. The specific targeting of antibodies naturally makes them ideal 'carriers' for targeted delivery of therapeutic cytokines. In many mouse models, antibody-cytokine fusion proteins targeting tumor markers increase the selective accumulation of the corresponding cytokines at the tumor site (19, 20). Such antibody-cytokine fusion proteins, also known as immunecytokines, are another significant application of bispecific antibodies and have been called the next generation of cytokine products.

6.1 PD-1 × IL-2

High-dose recombinant IL-2 (Proleukin) was approved by the FDA for treating metastatic renal cell carcinoma in 1992, followed by metastatic melanoma in 1998 (197, 198). However, recombinant natural IL-2 is dose-limited (0.037 mg/kg admitted) and causes severe non-specific extravasation toxicity (197–199). In addition, IL-2 has two opposing functions: at low doses, IL-2 tends to stimulate Treg cells expressing high-affinity trimeric receptors (IL-2Rαβγ), resulting in immunosuppression (200, 201); at high doses, after saturation of the receptor on Treg cells, excess IL-2 also interacts with effector T cells via intermediate affinity receptors (IL-2Rβγ) binds to effector T and NK cells, promoting immune activation and anti-tumour responses (202). To improve the therapeutic index, researchers have engineered IL-2 through various strategies to promote a longer half-life of the modified drug and specific binding to IL2-Rβγ (197) without binding to IL2-Rα (203), expressed on Treg. However, these bias-modified drugs did not achieve better clinical results (204).

IBI363 is a PD-1/IL-2α-bias bispecific antibody fusion protein. Unlike the mainstream IL2-Rβγ-biased design, IBI363 fused an IL-2Rα-biased engineered modified IL-2 at the end of the anti-PD-1 antibody. This design was based on a preclinical correlative study, in which researchers found that newly activated tumor-specific $CD8^+$ T cells expressed PD-1 while upregulating IL-2Rα and that the anti-tumor effect of anti-PD-1 was dependent on the activation of $PD\text{-}1^+$ $CD25^+$ $CD8^+$ T cells via autocrine IL-2/IL2-Rα signaling (205). Thus, through specific guidance of PD-1, PD-1/IL-2α-bias can selectively stimulate and expand T cells expressing both PD-1 and IL-2Rα within the tumor, leading to more precise and effective targeting and activation of this T cell subpopulation. At WCLC 2024, researchers presented a phase I clinical study (NCT05460767) of IBI363 in advanced non-small cell lung cancer. The data showed an ORR of 24.1% and a DCR of 68.4% in 79 patients who received doses higher than 0.3 mg/kg and an ORR of 85.7% (6/7) in the 3 mg/kg dose group (22). The drug's safety profile was good, with

87.6% of patients experiencing any grade of TRAEs and 19.1% of patients experiencing grade 3^+ TRAEs (22). From the preliminary clinical data, it can be seen that IBI363 was administered at an unprecedented dose (3mg/kg) and demonstrated a favorable safety profile, breaking through the safety concerns of IL-2 therapy. Combined with its preliminary published efficacy data, the clinical results of subsequent treatments with IBI363 are promising.

6.2 PD-1 × IL-15

Interleukin 15 (IL-15) is an IL2-related cytokine. Both can bind IL-2Rβγ, but the high-affinity forms of both IL2 and IL15 receptors contain IL2-Rα (CD25) or IL-15Rα (CD215), respectively (206). IL-15 is produced by dendritic cells, macrophages, and stromal cells, and, like IL-2, IL-15 can stimulate T-cell proliferation, induce cytotoxic T lymphocyte production, and promote the maintenance of NK cells (207, 208). In addition, the unique role of IL-15 is to maintain NK cell and $CD8^+CD44^h$ memory T cell function to provide a long-term immune response to pathogen (208). Like IL-2, IL-15 therapy was initially limited by the short molecular half-life and toxicity associated with systemic immune activation (209). Anktiva (N-803) is a recombinant IL-15 superagonist protein complex consisting of a high-affinity IL-15 mutant and IL-15Rα fused to Fc (and thus with an extended half-life). 2024 The FDA approved Anktiva in combination with Bacillus Calmette-Guérin (BCG) for treating adult BCG-naïve patients with non-muscle invasive bladder cancer with carcinoma *in situ* with or without papillary tumors (210). Animal studies have demonstrated that the combination of N-803 and anti-PD-L1 antibody can activate NK and $CD8^+$ T cells and induce the production of immunostimulatory cytokines, demonstrating significant efficacy in various models that do not respond or respond poorly to monotherapy (211). Clinical studies have demonstrated that patients with ≥2nd line NSCLC who failed CPI therapy treated with Anktiva in combination with CPI have an mOS of up to 11.4 months (212).

PF-07209960 is a cytokine fusion protein fused with mutated IL-15 at the end of one of the heavy chains of the anti-PD-1 antibody (213). The mutation in IL-15 is designed so that PF-07209960 does not bind to IL-15Rα and has a significantly reduced affinity for IL-2/15Rβγ. The molecule, therefore, explicitly delivers IL-15 to CD8+ T cells with high PD1 expression in tumors without binding to IL-15Rα-expressing cells and PD1-negative IL-15Rβγ-positive NK cells (213). Preclinical studies demonstrated that PF-07209960 could increase the number of $CD8^+$ TILs within tumors specifically, had excellent anti-tumor activity, and significantly reduced adverse effects (213). Researchers recently published preliminary clinical data on PF-07209960. Of the 29 evaluable patients, two patients, both with microsatellite-stable colorectal cancer, were confirmed to be in partial remission, with an ORR of 6.9% and a DCR of 48.3% (121). Regarding safety, 97.3% of patients experienced one or more adverse events, of which 78.4% experienced grade 3 or higher TRAEs, with a serious adverse events rate of 70.3% (121).

SAR44587, or KD050, consists of an Fc-silenced high-affinity human anti-PD-1 antibody (IgG1 subtype) fused to a mutated IL-15/IL-15Rα sushi domain (122). Through its anti-PD1 portion, SAR44587 binds to PD-1-expressing T cells and NK cells and may result in the specific expansion and activation of $CD8^+$ T cells and NK cells expressing PD-1 and IL-2/15Rβγ (214). In preclinical models of PD-1 resistance, SAR445877 had a stronger tumor suppressive effect compared to pembrolizumab, increasing the ratio of $CD8^+/CD4^+$ T cells in tumors and significantly increasing the percentage of effector memory $CD8^+$ T cells in tumors (215). The drug is currently undergoing a clinical phase I study (NCT05584670), which is planned to enroll 240 adult patients with advanced unresectable or metastatic solid tumors to confirm the safety, tolerability, pharmacokinetics, pharmacodynamics, and antitumor activity (214).

IAP0971 is an immunocytokine that binds specifically to PD-1 and fused IL-15/IL-15Rα complex (123). Mechanistically, IAP0971 can deregulate the immunosuppression of the PD-1/PD-L1 axis while increasing the targeting of IL-15 to the tumor microenvironment and avoiding systemic non-specific activation; furthermore, IAP0971 has an IgG4-based structure, resulting in a weak effect such as ADCC and ADCP, and a long half-life (123). In preclinical studies, IAP0971 can stimulate the proliferation of $CD8^+$ T cells and NKT cells, activate NK cells to kill tumor cells, and significantly inhibit tumor growth in mice at as low as 0.1 mg/kg without affecting their body weights (123). IAP0971 is currently in Phase I/IIa clinical trial (NCT05396391) to evaluate its safety, tolerability, and preliminary efficacy in patients with locally advanced or metastatic malignancies (216). Indications include a variety of malignancies, including lung cancer, cervical cancer, squamous cell carcinoma of the head and neck, hepatocellular carcinoma, and lymphoma.

7 Challenges and limitations

BsAbs show great potential in lung cancer therapy, and several key clinical advances are exciting. However, as described below, the therapeutic use of bsAbs in lung cancer faces many challenges.

7.1 Production challenges

Compared with monoclonal antibodies, the challenges facing the development and industrialization of bsABs are enormous. Unlike the standardized preparation process of monoclonal antibodies, the expression titer of bsABs is usually lower than that of monoclonal antibodies if the traditional process is directly followed (217), and they are prone to the formation of by-products such as aggregation and mismatch products (218–220). Although it is possible to increase the content of target products through various engineering modification strategies, bsAb-specific by-products are generally present at low levels in the cell culture supernatant of bsAb. It is necessary to rely on multiple purification strategies (e.g., a combination of affinity chromatography, ion-exchange chromatography, and size-exclusion chromatography) in order to obtain high purity of the target products, which significantly prolongs the development cycle and increases the cost of production (221).

7.2 Immunogenicity risk

Immunogenicity is one of the key challenges in the development of bsAbs. While some bispecific antibodies, such as amivantamab, have a very low incidence of anti-drug antibodies (ADAs), other bispecific antibodies show a high incidence of ADAs and neutralizing antibody positivity (222). These antibodies, which, due to drug immunogenicity, will directly affect the pharmacokinetics、pharmacodynamics, and safety of the drug (223). How to reduce the ADAs of a drug is a relatively complex issue, which needs to start from the initial molecular design (e.g., optimization of humanized modified epitopes), early *in vitro* immunogenicity assessment (based on in silico algorithms, and *in vitro* T cell-based assays), manufacturing process improvement (e.g., reduction of drug aggregation tendency, reduction of impurity residues), and clinical intervention (e.g., adjustment of drug immunogenicity), production process improvement (e.g., reducing drug aggregation tendency, reducing impurity residues), and clinical interventions (e.g., adjusting drug dosage, dosing regimen, and route of administration) are multifaceted and synergistic, which is complex and time-consuming (224).

7.3 Side effects

The adverse effects of bsAbs are closely related to their mechanism of action. Among them, cytokine release syndrome (CRS) is a common adverse reaction of TCE. For example, 49% of patients receiving AMG757 developed CRS, and 26% of them had severe symptoms (110). BsAbs based on a dual blocking mechanism show adverse reactions that are superimposed on the two targets (although they can be significantly lower than the parent antibody combination). For example, adverse reactions such as rash, pruritus, and diarrhea associated with EGFR and hypoproteinemia and peripheral edema associated with cMET have been observed with amivantamab (42).

Researchers are currently attempting various strategies to reduce the adverse effects of bsAbs and expand the therapeutic window. For example, by lowering the affinity of CD3 to increase the tissue distribution of bispecific antibodies in tumors and significantly reduce the level of cytokine release in normal tissues (225–227); and by restricting the activity of bsAbs in normal tissues through shielding techniques (186, 228); or by using tumor poxviruses as vectors to deliver dual antibodies to tumor sites in a targeted manner (229). However, drugs based on these strategies are currently in the preclinical or early clinical stage, and more clinical data are needed to analyze their safety and efficacy more correctly. Another strategy is to change the mode of administration. Currently, bsAbs are administered mainly by intravenous infusion, but data have shown that subcutaneous administration improves patient compliance and reduces the incidence of adverse events. For example, subcutaneous administration significantly reduced the incidence of infusion-related reactions and venous thromboembolic events with amivantamab compared with intravenous administration (47). Besides, some TCEs have also been shown through clinical studies to have a lower incidence of CRS with subcutaneous administration (230). However, subcutaneous administration is currently not widely used in solid tumors, and adequate subsequent validation is needed before widespread use. Intervention by the clinical therapist is the final barrier against adverse reactions. Real-time monitoring, pretreatment, and symptomatic management can enhance the patient experience (172, 231). However, it then requires clinicians to individualize the assessment of the patient and adjust the treatment regimen, which undoubtedly adds to the widespread use of the drug. Finally, it is worth noting that pneumonia is a particular concern in the lung cancer population, as lung cancer patients often have poor lung reserve due to current or past smoking history (232, 233). Drug-induced pneumonitis can, therefore, severely compromise their already poor lung reserve, which, in some cases, can be fatal.

7.4 Tumour heterogeneity and microenvironmental limitations

The complexity of lung cancer itself also poses a challenge for drug development. Lung cancer, as a very heterogeneous type of solid tumor, has differences in response to the same drug in different patients (as seen in Table 1). Thus, screening the most appropriate target population for bsAbs will be a significant challenge. In addition, the TME plays a central role in the genesis and progression of primary lung cancer, where cancer cells can reprogram tumor-infiltrating stromal cells, thereby promoting carcinogenesis (234, 235). In lung cancer, tumors can reprogram the lung microenvironment, which in turn promotes inflammation, angiogenesis, immunosuppression, and unresponsiveness to therapy, ultimately leading to lung metastasis from both primary and extrapulmonary tumors (236). Moreover, the disturbed and inefficient vascular supply of the TME and the elevated interstitial fluid pressure due to lymphovascular dysfunction greatly limit tumor penetration and T-cell infiltration into the tumor by dual antibodies. Small molecular weight dual antibodies (e.g., BiTE) that have better penetration but short half-lives (e.g., blinatumomab has a half-life of 2-4 hours (172)) require repeated administration. Small molecular weight dual antibodies (e.g., BiTE) that have better penetration but short half-lives (e.g., blinatumomab has a half-life of 2-4 hours (167)) require repeated administration. Fusing the VHH fragment of anti-HSA is a strategy that prolongs the drug's half-life while maintaining high drug penetration, and several such bispecific antibodies are currently under clinical investigation. Finally, the current bsAbs are mainly targeted at some mature targets (e.g., EGFR, PD1, etc.), and breakthroughs are urgently needed in the mining of new lung cancer-specific targets (e.g., c-MET, HER3) and TME regulation strategies (e.g., combining with anti-angiogenic drugs).

7.5 Pharmacoeconomic considerations

In addition to the technical challenges discussed above, pharmacoeconomic considerations are also a key obstacle to the widespread application of bsAbs in treating lung cancer. Compared with conventional antibody drugs, bispecific antibodies have higher production costs and greater clinical development risks, resulting in higher drug prices. Moreover, adverse reactions caused by the drugs

require additional symptomatic medications, which further increase the treatment costs for patients. Therefore, balancing the cost of the drug and its corresponding therapeutic effect is a huge challenge. Some researchers have noted that although the treatment regimens of amivantamab in combination with chemotherapy or amivantamab in combination with lazertinib provide significant benefits to patients, when the economic costs are considered, they are higher than the cost-effectiveness thresholds given current US pricing (237, 238). Therefore, how to balance the cost and pricing to benefit more patients is an issue that needs to be addressed. In addition, the treatment cost can be reduced by further optimising the drug dosage. For example, compared with the recommended treatment regimen, using an optimised alternative dosing regimen can save 16% of the treatment cost of Amivantamab (239).

8 Conclusion

BsAbs have ushered in significant development, with more than 110 in clinical development and nearly 180 in preclinical development (240). There are three drugs approved for lung cancer treatment, of which the launch of AMG757 is a breakthrough in the field of small-cell lung cancer treatment for many years, and AK112 beat Keytruda in head-to-head clinical studies, both of which are of landmark significance. In the next phase of drug development, the therapeutic potential of bsAbs will be further unlocked through research to optimize the production of CMC, reduce the adverse effects, and research into the pathogenesis of lung cancer itself, enhancing the cost-effectiveness of the drugs, which is of great significance, and discovering new therapeutic targets. In conclusion, more new drugs will be developed for more lung cancer patients with unmet needs for quite some time to come.

Author contributions

WC: Conceptualization, Data curation, Writing – original draft, Writing – review & editing, Investigation. AZ: Conceptualization, Data curation, Writing – review & editing, Writing – original draft. YZ: Supervision, Writing – review & editing, Writing – original draft.

Funding

The author(s) declare that no financial support was received for the research and/or publication of this article.

Conflict of interest

The authors declare that the research was conducted without any commercial or financial relationships that could potentially create a conflict of interest.

Generative AI statement

The author(s) declare that no Generative AI was used in the creation of this manuscript.

Correction note

A correction has been made to this article. Details can be found at: 10.3389/fimmu.2025.1656082.

Publisher's note

References

1. Thai AA, Solomon BJ, Sequist LV, Gainor JF, Heist RS. Lung cancer. *Lancet*. (2021) 398:535–54. doi: 10.1016/s0140-6736(21)00312-3

2. Allemani C, Weir HK, Carreira H, Harewood R, Spika D, Wang X-S, et al. Global surveillance of cancer survival 1995–2009: analysis of individual data for 25 676 887 patients from 279 population-based registries in 67 countries (CONCORD-2). *Lancet*. (2015) 385:977–1010. doi: 10.1016/s0140-6736(14)62038-9

3. Rotow J, Bivona TG. Understanding and targeting resistance mechanisms in NSCLC. *Nat Rev Cancer*. (2017) 17:637–58. doi: 10.1038/nrc.2017.84

4. Horvath L, Thienpont B, Zhao L, Wolf D, Pircher A. Overcoming immunotherapy resistance in non-small cell lung cancer (NSCLC) - novel approaches and future outlook. *Mol Cancer*. (2020) 19:141. doi: 10.1186/s12943-020-01260-z

5. Koinis F, Kotsakis A, Georgoulias V. Small cell lung cancer (SCLC): no treatment advances in recent years. *Trans Lung Cancer Res*. (2016) 5(1):39–50. doi: 10.3978/j.issn.2218-6751.2016.01.03

6. Gazdar AF, Bunn PA, Minna JD. Small-cell lung cancer: what we know, what we need to know and the path forward. *Nat Rev Cancer*. (2017) 17:725–37. doi: 10.1038/nrc.2017.87

7. Rudin CM, Giaccone G, Ismaila N. Treatment of small-cell lung cancer: american society of clinical oncology endorsement of the american college of chest physicians guideline. *J Oncol Pract*. (2016) 12:83–6. doi: 10.1200/jop.2015.008201

8. Rudin CM, Brambilla E, Faivre-Finn C, Sage J. Small-cell lung cancer. *Nat Rev Dis Primers*. (2021) 7(1):3. doi: 10.1038/s41572-020-00235-0

9. Brinkmann U, Kontermann RE. The making of bispecific antibodies. *MAbs*. (2017) 9:182–212. doi: 10.1080/19420862.2016.1268307

10. Syed YY. Amivantamab: first approval. *Drugs*. (2021) 81:1349–53. doi: 10.1007/s40265-021-01561-7

11. Krah S, Sellmann C, Rhiel L, Schröter C, Dickgiesser S, Beck J, et al. Engineering bispecific antibodies with defined chain pairing. *N Biotechnol*. (2017) 39:167–73. doi: 10.1016/j.nbt.2016.12.010

12. Krah S, Kolmar H, Becker S, Zielonka S. Engineering igG-like bispecific antibodies-an overview. *Antibodies (Basel)*. (2018) 7(3):28. doi: 10.3390/antib7030028

13. Chames P, Baty D. Bispecific antibodies for cancer therapy. *Curr Opin Drug Discovery Devel*. (2009) 12:276–83. doi: 10.4161/mabs.1.6.10015

14. Chan AC, Carter PJ. Therapeutic antibodies for autoimmunity and inflammation. *Nat Rev Immunol*. (2010) 10:301–16. doi: 10.1038/nri2761

15. Wu C, Ying H, Bose S, Miller R, Medina L, Santora L, et al. Molecular construction and optimization of anti-human IL-1alpha/beta dual variable domain immunoglobulin (DVD-Ig) molecules. *MAbs*. (2009) 1:339–47. doi: 10.4161/mabs.1.4.8755

16. Labrijn AF, Janmaat ML, Reichert JM, Parren P. Bispecific antibodies: a mechanistic review of the pipeline. *Nat Rev Drug Discovery*. (2019) 18:585–608. doi: 10.1038/s41573-019-0028-1

17. Demaria O, Gauthier L, Debroas G, Vivier E. Natural killer cell engagers in cancer immunotherapy: Next generation of immuno-oncology treatments. *Eur J Immunol*. (2021) 51:1934–42. doi: 10.1002/eji.202048953

18. Whalen KA, Rakhra K, Mehta NK, Steinle A, Michaelson JS, Baeuerle PA. Engaging natural killer cells for cancer therapy via NKG2D, CD16A and other receptors. *MAbs*. (2023) 15:2208697. doi: 10.1080/19420862.2023.2208697

19. Carnemolla B, Borsi L, Balza E, Castellani P, Meazza R, Berndt A, et al. Enhancement of the antitumor properties of interleukin-2 by its targeted delivery to the tumor blood vessel extracellular matrix. *Blood*. (2002) 99:1659–65. doi: 10.1182/blood.v99.5.1659

20. Gillies SD, Lan Y, Williams S, Carr F, Forman S, Raubitschek A, et al. An anti-CD20-IL-2 immunocytokine is highly efficacious in a SCID mouse model of established human B lymphoma. *Blood*. (2005) 105:3972–8. doi: 10.1182/blood-2004-09-3533

21. Shi W, Liu N, Lu H. Advancements and challenges in immunocytokines: A new arsenal against cancer. *Acta Pharm Sin B*. (2024) 14:4649–64. doi: 10.1016/j.apsb.2024.07.024

22. Zhou J, Xu N, Shan J, Wang Y, Fang W, Wang H, et al. MA11.04 first-in-class PD-1/IL-2 bispecific antibody IBI363 in patients with advanced non-small cell lung cancer in a phase I study. *J Thorac Oncol*. (2024) 19:S97. doi: 10.1016/j.jtho.2024.09.176

23. Polonskaya Z, Chang T-P, Martomo S, Luna X, Zhang Z, Ng S, et al. Abstract 5215: MOA study of KD050, an anti-PD-1/IL-15 bi-functional antibody selectively targeted PD-1 positive tumor-infiltrating lymphocytes resulted in robust anti-tumor activity and low systemic toxicity. *Cancer Res*. (2022) 82:5215–5. doi: 10.1158/1538-7445.Am2022-5215

24. Wang Z. ErbB receptors and cancer. *Methods Mol Biol*. (2017) 1652:3–35. doi: 10.1007/978-1-4939-7219-7_1

25. Wu SG, Shih JY. Management of acquired resistance to EGFR TKI-targeted therapy in advanced non-small cell lung cancer. *Mol Cancer*. (2018) 17:38. doi: 10.1186/s12943-018-0777-1

26. Lim SM, Syn NL, Cho BC, Soo RA. Acquired resistance to EGFR targeted therapy in non-small cell lung cancer: Mechanisms and therapeutic strategies. *Cancer Treat Rev*. (2018) 65:1–10. doi: 10.1016/j.ctrv.2018.02.006

27. Shi Y, Au JS, Thongprasert S, Srinivasan S, Tsai CM, Khoa MT, et al. A prospective, molecular epidemiology study of EGFR mutations in Asian patients with advanced non-small-cell lung cancer of adenocarcinoma histology (PIONEER). *J Thorac Oncol*. (2014) 9:154–62. doi: 10.1097/jto.0000000000000033

28. Rosell R, Moran T, Queralt C, Porta R, Cardenal F, Camps C, et al. Screening for epidermal growth factor receptor mutations in lung cancer. *N Engl J Med*. (2009) 361:958–67. doi: 10.1056/NEJMoa0904554

29. Barlesi F, Mazieres J, Merlio JP, Debieuvre D, Mosser J, Lena H, et al. Routine molecular profiling of patients with advanced non-small-cell lung cancer: results of a 1-year nationwide programme of the French Cooperative Thoracic Intergroup (IFCT). *Lancet*. (2016) 387:1415–26. doi: 10.1016/s0140-6736(16)00004-0

30. Wu Q, Qian W, Sun X, Jiang S. Small-molecule inhibitors, immune checkpoint inhibitors, and more: FDA-approved novel therapeutic drugs for solid tumors from 1991 to 2021. *J Hematol Oncol*. (2022) 15:143. doi: 10.1186/s13045-022-01362-9

31. Engelman JA, Zejnullahu K, Mitsudomi T, Song Y, Hyland C, Park JO, et al. MET amplification leads to gefitinib resistance in lung cancer by activating ERBB3 signaling. *Science*. (2007) 316:1039–43. doi: 10.1126/science.1141478

32. Yu HA, Arcila ME, Rekhtman N, Sima CS, Zakowski MF, Pao W, et al. Analysis of tumor specimens at the time of acquired resistance to EGFR-TKI therapy in 155 patients with EGFR-mutant lung cancers. *Clin Cancer Res*. (2013) 19:2240–7. doi: 10.1158/1078-0432.Ccr-12-2246

33. Sequist LV, Waltman BA, Dias-Santagata D, Digumarthy S, Turke AB, Fidias P, et al. Genotypic and histological evolution of lung cancers acquiring resistance to EGFR inhibitors. *Sci Transl Med*. (2011) 3:75ra26. doi: 10.1126/scitranslmed.3002003

34. Pao W, Miller VA, Politi KA, Riely GJ, Somwar R, Zakowski MF, et al. Acquired resistance of lung adenocarcinomas to gefitinib or erlotinib is associated with a second mutation in the EGFR kinase domain. *PloS Med*. (2005) 2:e73. doi: 10.1371/journal.pmed.0020073

35. Yano S, Yamada T, Takeuchi S, Tachibana K, Minami Y, Yatabe Y, et al. Hepatocyte growth factor expression in EGFR mutant lung cancer with intrinsic and acquired resistance to tyrosine kinase inhibitors in a Japanese cohort. *J Thorac Oncol*. (2011) 6:2011–7. doi: 10.1097/JTO.0b013e31823ab0dd

36. Turke AB, Zejnullahu K, Wu YL, Song Y, Dias-Santagata D, Lifshits E, et al. Preexistence and clonal selection of MET amplification in EGFR mutant NSCLC. *Cancer Cell*. (2010) 17:77–88. doi: 10.1016/j.ccr.2009.11.022

37. Neijssen J, Cardoso RMF, Chevalier KM, Wiegman L, Valerius T, Anderson GM, et al. Discovery of amivantamab (JNJ-61186372), a bispecific antibody targeting EGFR and MET. *J Biol Chem*. (2021) 296:100641. doi: 10.1016/j.jbc.2021.100641

38. Vijayaraghavan S, Lipfert L, Chevalier K, Bushey BS, Henley B, Lenhart R, et al. Amivantamab (JNJ-61186372), an fc enhanced EGFR/cMet bispecific antibody, induces receptor downmodulation and antitumor activity by monocyte/macrophage trogocytosis. *Mol Cancer Ther*. (2020) 19:2044–56. doi: 10.1158/1535-7163.Mct-20-0071

39. Park K, Haura EB, Leighl NB, Mitchell P, Shu CA, Girard N, et al. Amivantamab in EGFR exon 20 insertion-mutated non-small-cell lung cancer progressing on platinum chemotherapy: initial results from the CHRYSALIS phase I study. *J Clin Oncol*. (2021) 39:3391–402. doi: 10.1200/jco.21.00662

40. Vyse S, Huang PH. Amivantamab for the treatment of EGFR exon 20 insertion mutant non-small cell lung cancer. *Expert Rev Anticancer Ther*. (2022) 22:3–16. doi: 10.1080/14737140.2022.2016397

41. US Food & Drug Administration. *FDA grants accelerated approval to amivantamab-vmjw for metastatic non-small cell lung cancer [media release]*. (2021). Available at: https://www.fda.gov/.

42. Zhou C, Tang KJ, Cho BC, Liu B, Paz-Ares L, Cheng S, et al. Amivantamab plus chemotherapy in NSCLC with EGFR exon 20 insertions. *N Engl J Med*. (2023) 389:2039–51. doi: 10.1056/NEJMoa2306441

43. US Food & Drug Administration. *FDA approves amivantamab-vmjw for EGFR exon 20 insertion-mutated non-small cell lung cancer indications [media release]*. (2024). Available at: https://www.fda.gov/.

44. Cho BC, Felip E, Spira AI, Girard N, Lee JS, Lee SH, et al. LBA14 Amivantamab plus lazertinib vs osimertinib as first-line treatment in patients with EGFR-mutated, advanced non-small cell lung cancer (NSCLC): Primary results from MARIPOSA, a phase III, global, randomized, controlled trial. *Ann Oncol*. (2023) 34:S1306. doi: 10.1016/j.annonc.2023.10.062

45. Cho BC, Lu S, Felip E, Spira AI, Girard N, Lee JS, et al. Amivantamab plus lazertinib in previously untreated EGFR-mutated advanced NSCLC. *N Engl J Med*. (2024). doi: 10.1056/NEJMoa2403614

46. Leighl N, Cho BC, Hiret S, Han JY, Lee KH, Llacer Perez C, et al. OA21.04 amivantamab in patients with advanced NSCLC and MET exon 14 skipping mutation: results from the CHRYSALIS study. *J Thorac Oncol*. (2023) 18:S93–4. doi: 10.1016/j.jtho.2023.09.105

47. Leighl NB, Akamatsu H, Lim SM, Cheng Y, Minchom AR, Marmarelis ME, et al. Subcutaneous versus intravenous amivantamab, both in combination with lazertinib, in refractory epidermal growth factor receptor-mutated non-small cell lung cancer: primary results from the phase III PALOMA-3 study. *J Clin Oncol*. (2024) 42:3593–605. doi: 10.1200/jco.24.01001

48. Qing Z, Gabrail N, Uprety D, Rotow J, Han B, Jänne PA, et al. 22P EMB-01: An EGFR-cMET bispecific antibody, in advanced/metastatic solid tumors phase I results. *Ann Oncol*. (2022) 33:S39–40. doi: 10.1016/j.annonc.2022.02.031

49. Geuijen C, d. Matteo M, Gallenne T, Cafarello ST, Nijhuis R, Visser T, et al. Abstract LB-C07: Preclinical evaluation of MCLA-129: A bispecific antibody targeting c-MET and EGFR. *Mol Cancer Ther*. (2019) 18:LB–C07-LB-C07. doi: 10.1158/1535-7163.Targ-19-lb-c07

50. Wang J, Zhong J, Wu L, Chen B, Wang Z-H, Yao Y, et al. Ding: Efficacy and safety of MCLA-129, an EGFR/c-MET bispecific antibody, in advanced non-small cell lung cancer (NSCLC). *J Clin Oncol*. (2024) 42:8604–4. doi: 10.1200/JCO.2024.42.16_suppl.8604

51. Cappuzzo F, Moreno Garcia V, Ou SHI, Brandão M, Sanmamed MF, Helissey C, et al. 516MO Efficacy and safety of MCLA-129, an anti-EGFR/c-MET bispecific antibody, combined with osimertinib, as first-line therapy or after progression on osimertinib in non-small cell lung cancer (NSCLC). *Ann Oncol*. (2023) 34:S1671. doi: 10.1016/j.annonc.2023.10.595

52. Pillai RN, Behera M, Berry LD, Rossi MR, Kris MG, Johnson BE, et al. HER2 mutations in lung adenocarcinomas: A report from the Lung Cancer Mutation Consortium. *Cancer*. (2017) 123:4099–105. doi: 10.1002/cncr.30869

53. Kim EK, Kim KA, Lee CY, Shim HS. The frequency and clinical impact of HER2 alterations in lung adenocarcinoma. *PloS One*. (2017) 12:e0171280. doi: 10.1371/journal.pone.0171280

54. Tomizawa K, Suda K, Onozato R, Kosaka T, Endoh H, Sekido Y, et al. Prognostic and predictive implications of HER2/ERBB2/neu gene mutations in lung cancers. *Lung Cancer*. (2011) 74:139–44. doi: 10.1016/j.lungcan.2011.01.014

55. Li BT, Ross DS, Aisner DL, Chaft JE, Hsu M, Kako SL, et al. HER2 amplification and HER2 mutation are distinct molecular targets in lung cancers. *J Thorac Oncol*. (2016) 11:414–9. doi: 10.1016/j.jtho.2015.10.025

56. Trinder A, Ding K, Zhang J. The therapeutic significance of HER3 in non-small cell lung cancer (NSCLC): A review study. *Curr Med Chem*. (2024). doi: 10.2174/0109298673269305231115102542

57. Lee-Hoeflich ST, Crocker L, Yao E, Pham T, Munroe X, Hoeflich KP, et al. A central role for HER3 in HER2-amplified breast cancer: implications for targeted therapy. *Cancer Res*. (2008) 68:5878–87. doi: 10.1158/0008-5472.Can-08-0380

58. Hsieh AC, Moasser MM. Targeting HER proteins in cancer therapy and the role of the non-target HER3. *Br J Cancer*. (2007) 97:453–7. doi: 10.1038/sj.bjc.6603910

59. Wallasch C, Weiss FU, Niederfellner G, Jallal B, Issing W, Ullrich A. Heregulin-dependent regulation of HER2/neu oncogenic signaling by heterodimerization with HER3. *EMBO J*. (1995) 14:4267–75. doi: 10.1002/j.1460-2075.1995.tb00101.x

60. Haikala HM, Jänne PA. Thirty years of HER3: from basic biology to therapeutic interventions. *Clin Cancer Res*. (2021) 27:3528–39. doi: 10.1158/1078-0432.Ccr-20-4465

61. Dimou A, Camidge DR. Detection of NRG1 fusions in solid tumors: rare gold? *Clin Cancer Res*. (2019) 25:4865–7. doi: 10.1158/1078-0432.Ccr-19-1219

62. Jonna S, Feldman RA, Swensen J, Gatalica Z, Korn WM, Borghaei H, et al. Detection of NRG1 gene fusions in solid tumors. *Clin Cancer Res*. (2019) 25:4966–72. doi: 10.1158/1078-0432.Ccr-19-0160

63. Drilon A, Duruisseaux M, Han JY, Ito M, Falcon C, Yang SR, et al. Clinicopathologic features and response to therapy of NRG1 fusion-driven lung cancers: the eNRGy1 global multicenter registry. *J Clin Oncol*. (2021) 39:2791–802. doi: 10.1200/jco.20.03307

64. Geuijen CAW, De Nardis C, Maussang D, Rovers E, Gallenne T, Hendriks LJA, et al. Unbiased combinatorial screening identifies a bispecific igG1 that potently inhibits HER3 signaling via HER2-guided ligand blockade. *Cancer Cell*. (2018) 33:922–936.e10. doi: 10.1016/j.ccell.2018.04.003

65. US Food & Drug Administration. *FDA grants accelerated approval to zenocutuzumab-zbco for non-small cell lung cancer and pancreatic adenocarcinoma [media release]*. (2024). Available at: https://www.fda.gov/.

66. Schram A, Goto K, Kim DW, Hollebecque A, Rha SY, Nishino K, et al. 1315MO Durable efficacy of zenocutuzumab, a HER2 x HER3 bispecific antibody, in advanced NRG1 fusion-positive (NRG1+) non-small cell lung cancer (NSCLC). *Ann Oncol*. (2023) 34:S756–7. doi: 10.1016/j.annonc.2023.09.2349

67. Yonesaka K, Tanizaki J, Maenishi O, Haratani K, Kawakami H, Tanaka K, et al. HER3 augmentation via blockade of EGFR/AKT signaling enhances anticancer activity of HER3-targeting patritumab deruxtecan in EGFR-mutated non-small cell lung cancer. *Clin Cancer Res*. (2022) 28:390–403. doi: 10.1158/1078-0432.Ccr-21-3359

68. Engelman JA, Jänne PA, Mermel C, Pearlberg J, Mukohara T, Fleet C, et al. ErbB-3 mediates phosphoinositide 3-kinase activity in gefitinib-sensitive non-small cell lung cancer cell lines. *Proc Natl Acad Sci U.S.A*. (2005) 102:3788–93. doi: 10.1073/pnas.0409773102

69. Goulet DR, Tsai TI, Khalili J, Mak NSA, Zhu H, Zhu Y. *SPECIFICITY ENHANCED BISPECIFIC ANTIBODY (SEBA) WO 2022/061255 A1*. (2022).

70. Zhao Y, Zhang L, Fang W, Yang Y, Huang Y, Zou W, et al. SI-B001 plus chemotherapy in patients with locally advanced or metastatic EGFR/ALK wild-type non-small cell lung cancer: A phase II, multicenter, open-label study. *J Clin Oncol*. (2023) 41:9025–5. doi: 10.1200/JCO.2023.41.16_suppl.9025

71. Kubli SP, Berger T, Araujo DV, Siu LL, Mak TW. Beyond immune checkpoint blockade: emerging immunological strategies. *Nat Rev Drug Discovery*. (2021) 20:899–919. doi: 10.1038/s41573-021-00155-y

72. Darvin P, Toor SM, Sasidharan Nair V, Elkord E. Immune checkpoint inhibitors: recent progress and potential biomarkers. *Exp Mol Med*. (2018) 50:1–11. doi: 10.1038/s12276-018-0191-1

73. Schoenfeld AJ, Hellmann MD. Acquired resistance to immune checkpoint inhibitors. *Cancer Cell*. (2020) 37:443–55. doi: 10.1016/j.ccell.2020.03.017

74. Buchbinder EI, Desai A. CTLA-4 and PD-1 pathways: similarities, differences, and implications of their inhibition. *Am J Clin Oncol*. (2016) 39:98–106. doi: 10.1097/coc.0000000000000239

75. Valsecchi ME. Combined nivolumab and ipilimumab or monotherapy in untreated melanoma. *N Engl J Med*. (2015) 373:1270. doi: 10.1056/NEJMc1509660

76. Hellmann MD, Paz-Ares L, Bernabe Caro R, Zurawski B, Kim SW, Carcereny Costa E, et al. Nivolumab plus ipilimumab in advanced non-small-cell lung cancer. *N Engl J Med*. (2019) 381:2020–31. doi: 10.1056/NEJMoa1910231

77. Motzer RJ, Tannir NM, McDermott DF, Arén Frontera O, Melichar B, Choueiri TK, et al. Nivolumab plus Ipilimumab versus Sunitinib in Advanced Renal-Cell Carcinoma. *N Engl J Med*. (2018) 378:1277–90. doi: 10.1056/NEJMoa1712126

78. Larkin J, Chiarion-Sileni V, Gonzalez R, Grob JJ, Rutkowski P, Lao CD, et al. Five-year survival with combined nivolumab and ipilimumab in advanced melanoma. *N Engl J Med*. (2019) 381:1535–46. doi: 10.1056/NEJMoa1910836

79. Reck M, Borghaei H, O'Byrne KJ. Nivolumab plus ipilimumab in non-small-cell lung cancer. *Future Oncol*. (2019) 15:2287–302. doi: 10.2217/fon-2019-0031

80. Dovedi SJ, Elder MJ, Yang C, Sitnikova SI, Irving L, Hansen A, et al. Design and efficacy of a monovalent bispecific PD-1/CTLA4 antibody that enhances CTLA4 blockade on PD-1(+) activated T cells. *Cancer Discovery*. (2021) 11:1100–17. doi: 10.1158/2159-8290.Cd-20-1445

81. Huang Z, Pang X, Zhong T, Chen N, He X, Xia D, et al. 289 Cadonilimab, an anti-PD1/CTLA4 bi-specific antibody with Fc effector null backbone. *J ImmunoTherapy Cancer*. (2021) 9:A313–4. doi: 10.1136/jitc-2021-SITC2021.289

82. Pang X, Huang Z, Zhong T, Zhang P, Wang ZM, Xia M, et al. Cadonilimab, a tetravalent PD-1/CTLA-4 bispecific antibody with trans-binding and enhanced target binding avidity. *MAbs*. (2023) 15:2180794. doi: 10.1080/19420862.2023.2180794

83. Keam SJ. Cadonilimab: first approval. *Drugs*. (2022) 82:1333–9. doi: 10.1007/s40265-022-01761-9

84. Chen B, Yao W, Li X, Lin G, Chu Q, Liu H, et al. A phase Ib/II study of cadonilimab (PD-1/CTLA-4 bispecific antibody) plus anlotinib as first-line treatment in patients with advanced non-small cell lung cancer. *Br J Cancer*. (2024) 130:450–6. doi: 10.1038/s41416-023-02519-0

85. Han B, Zhang Y. 647P A phase Ib/II study of second-line cadonilimab, anlotinib and docetaxel in patients with checkpoint inhibitor (CPI)-experienced advanced non-small cell lung cancer. *Ann Oncol*. (2024) 35:S1646. doi: 10.1016/j.annonc.2024.10.680

86. Insa A, Martín-Martorell P, Di Liello R, Fasano M, Martini G, Napolitano S, et al. Which treatment after first line therapy in NSCLC patients without genetic alterations in the era of immunotherapy? *Crit Rev Oncol Hematol*. (2022) 169:103538. doi: 10.1016/j.critrevonc.2021.103538

87. Neal J, Pavlakis N, Kim SW, Goto Y, Lim SM, Mountzios G, et al. CONTACT-01: A randomized phase III trial of atezolizumab + Cabozantinib versus docetaxel for metastatic non-small cell lung cancer after a checkpoint inhibitor and chemotherapy. *J Clin Oncol*. (2024) 42:2393–403. doi: 10.1200/jco.23.02166

88. Paz-Ares L, Goto Y, Wan-Teck Lim D, Halmos B, Chul Cho B, Cobo M, et al. Canakinumab in combination with docetaxel compared with docetaxel alone for the treatment of advanced non-small cell lung cancer following platinum-based doublet chemotherapy and immunotherapy (CANOPY-2): A multicenter, randomized, double-blind, phase 3 trial. *Lung Cancer*. (2024) 189:107451. doi: 10.1016/j.lungcan.2023.107451

89. Borghaei H, de Marinis F, Dumoulin D, Reynolds C, Theelen W, Percent I, et al. SAPPHIRE: phase III study of sitravatinib plus nivolumab versus docetaxel in advanced nonsquamous non-small-cell lung cancer. *Ann Oncol*. (2024) 35:66–76. doi: 10.1016/j.annonc.2023.10.004

90. Wang L, Su C. EP.11D.01 A phase II study of cadonilimab plus chemotherapy as first-line treatment for PD-L1-negative advanced non-small cell lung cancer: lungCadX. *J Thorac Oncol*. (2024) 19:S614. doi: 10.1016/j.jtho.2024.09.1152

91. Ahn MJ, Kim SW, Costa EC, Rodríguez LM, Oliveira J, Insa Molla MA, et al. LBA56 MEDI5752 or pembrolizumab (P) plus carboplatin/pemetrexed (CP) in treatment-na&xef;ve (1L) non-small cell lung cancer (NSCLC): A phase Ib/II trial. *Ann Oncol*. (2022) 33:S1423. doi: 10.1016/j.annonc.2022.08.058

92. Zhao Y, Ma Y, Fan Y, Zhou J, Yang N, Yu Q, et al. A multicenter, open-label phase Ib/II study of cadonilimab (anti PD-1 and CTLA-4 bispecific antibody) monotherapy in previously treated advanced non-small-cell lung cancer (AK104-202 study). *Lung Cancer*. (2023) 184:107355. doi: 10.1016/j.lungcan.2023.107355

93. Wu L, Chen B, Yao W, Li X, Xiao Z, Liu H, et al. 1300P A phase Ib/II trial of AK104 (PD-1/CTLA-4 bispecific antibody) in combination with anlotinib in advanced NSCLC. *Ann Oncol*. (2021) 32:S1006. doi: 10.1016/j.annonc.2021.08.1902

94. Wang Y, Li Y, Liu J, S.-x. Luo Q, Zou W, Wang Z, et al. Shen: SI-B003 (PD-1/CTLA-4) in patients with advanced solid tumors: A phase I study. *J Clin Oncol*. (2023) 41:e14668–8. doi: 10.1200/JCO.2023.41.16_suppl.e14668

95. Zhou C, Xiong A, Fang J, Li X, Xie Q, Yu Q, et al. 1330P Updated results of the efficacy and safety of KN046 (a bispecific anti-PD-L1/CTLA-4) in patients with metastatic non-small cell lung cancer (NSCLC) who failed prior EGFR-TKI(s). *Ann Oncol*. (2023) 34:S767–8. doi: 10.1016/j.annonc.2023.09.2363

96. Zhao Y, Chen G, Li X, Wu J, Chang B, Hu S, et al. KN046, a bispecific antibody against PD-L1 and CTLA-4, plus chemotherapy as first-line treatment for metastatic NSCLC: A multicenter phase 2 trial. *Cell Rep Medicine 5(3)*. (2024). doi: 10.1016/j.xcrm.2024.101470

97. Zhou C, Xiong A, Li X, Fan Y, Zhuang W, Yu Q, et al. 1459P Preliminary efficacy and safety of KN046 (a bispecific anti-PD-L1/CTLA-4) in patients with metastatic non-small cell lung cancer who previously treated with immune checkpoint inhibitor(s). *Ann Oncol*. (2023) 34:S829. doi: 10.1016/j.annonc.2023.09.2490

98. Zhang L, Zhao Y, Meng X, Huang Y, Fang W, Yang Y, et al. 133P The efficacy and safety of KN046 combined with axitinib for previously untreated and checkpoint inhibitor treated advanced non-small cell lung cancer: A single-arm, open-label, multicenter phase II clinical trial. *Immuno-Oncology Technol*. (2024) 24:100762. doi: 10.1016/j.iotech.2024.100762

99. Ruan D-Y, Wei X-L, Liu F-R, Hu X-C, Zhang J, Ji D-M, et al. The first-in-class bispecific antibody IBI318 (LY3434172) targeting PD-1 and PD-L1 in patients with advanced tumors: a phase Ia/Ib study. *J Hematol Oncol*. (2024) 17:118. doi: 10.1186/s13045-024-01644-4

100. Hiltermann TJN, Izumi H, Cho BC, Cunha S, Danchaivijitr P, Felip E, et al. OA11.03 efficacy and safety of rilvegostomig, an anti-PD-1/TIGIT bispecific, for CPI-naïve metastatic NSCLC with PD-L1 1-49% or ≥50%. *J Thorac Oncol*. (2024) 19:S33. doi: 10.1016/j.jtho.2024.09.061

101. Xue J, Zhang Y, Hu X, Zhao W, Sun Y, Li Q, et al. Phase I/II safety and preliminary efficacy of PM1022, a bispecific antibody targeting PD-L1 and TIGIT, in patients with advanced solid tumors. *J Clin Oncol*. (2024) 42:e14694–4. doi: 10.1200/JCO.2024.42.16_suppl.e14694

102. Luke JJ, Patel MR, Blumenschein GR, Hamilton E, Chmielowski B, Ulahannan SV, et al. The PD-1- and LAG-3-targeting bispecific molecule tebotelimab in solid tumors and hematologic cancers: a phase 1 trial. *Nat Med*. (2023) 29:2814–24. doi: 10.1038/s41591-023-02593-0

103. Zhang L, Fang W, Zhao Y, Luo Y, Yang R, Huang Y, et al. Ivonescimab combined with chemotherapy in patients with EGFR-mutant non-squamous non-small cell lung cancer who progressed on EGFR tyrosine-kinase inhibitor treatment (HARMONi-A): A randomized, double-blind, multi-center, phase 3 trial. *J Clin Oncol*. (2024) 42:8508–8. doi: 10.1200/JCO.2024.42.16_suppl.8508

104. Zhou JCC, Wu L, Wang L, Xiong A, Yao B, Zhong H, et al. Phase 3 Study of Ivonescimab (AK112) vs. Pembrolizumab as First-line Treatment for PD-L1 positive Advanced NSCLC: HARMONi-2. *In WCLC*. (2024). doi: 10.1016/j.jtho.2024.09.012

105. Wu C, Lv D, Cui J, Wang Z, Zhao H, Duan H, et al. A phase Ib/IIa trial to evaluate the safety and efficacy of PM8002, a bispecific antibody targeting PD-L1 and VEGF-A, as a monotherapy in patients with advanced NSCLC. *J Clin Oncol*. (2024) 42:8533–3. doi: 10.1200/JCO.2024.42.16_suppl.8533

106. Cheng Y, Qin Z, Meng X, Xu F, Wang Y, Yao Y, et al. 1992P A phase II safety and efficacy study of PM8002 (anti-PD-L1 x VEGF-A bispecific) combined with paclitaxel as a second-line therapy for small cell lung cancer (SCLC). *Ann Oncol*. (2023) 34:S1062. doi: 10.1016/j.annonc.2023.09.1223

107. Liu R, Hu X, Song Z, Zhang J, Jin J, Gao S, et al. IMM2510, an anti-PD-L1/VEGF bispecific antibody fusion protein, in patients with advanced solid tumors: A phase I dose-escalation study. *J Clin Oncology 42(16_suppl) e14506-e14506*. (2024). doi: 10.1200/JCO.2024.42.16_suppl.e14506

108. Feng J, Shi M, Chen J, Li K, Li X, Sun M, et al. 511MO A phase I study of SHR-1701, a bifunctional fusion protein targeting PD-L1 and TGF-&x3b2;, in patients with advanced non-small cell lung cancer (NSCLC). *Ann Oncol*. (2023) 34:S1667. doi: 10.1016/j.annonc.2023.10.590

109. Zhou Q, Pan Y, Yang X, Zhao Y, Han G, Pang Q, et al. Neoadjuvant SHR-1701 with or without chemotherapy in unresectable stage III non-small-cell lung cancer: A proof-of-concept, phase 2 trial. *Cancer Cell*. (2024) 42(7):1258–67.e2. doi: 10.1016/j.ccell.2024.05.024

110. Ahn MJ, Cho BC, Felip E, Korantzis I, Ohashi K, Majem M, et al. Tarlatamab for patients with previously treated small-cell lung cancer. *N Engl J Med*. (2023) 389:2063–75. doi: 10.1056/NEJMoa2307980

111. Dowlati A, Hummel H-D, Champiat S, Olmedo ME, Boyer M, He K, et al. Sustained clinical benefit and intracranial activity of tarlatamab in previously treated small cell lung cancer: deLLphi-300 trial update. *J Clin Oncol*. 42(29):3392–9. doi: 10.1200/jco.24.00553

112. Wermke M, Felip E, Kuboki Y, Morgensztern D, Sayehli C, Sanmamed MF, et al. First-in-human dose-escalation trial of BI 764532, a delta-like ligand 3 (DLL3)/CD3 IgG-like T-cell engager in patients (pts) with DLL3-positive (DLL3+) small-cell lung cancer (SCLC) and neuroendocrine carcinoma (NEC). *J Clin Oncol*. (2023) 41:8502–2. doi: 10.1200/JCO.2023.41.16_suppl.8502

113. Beltran H, Johnson ML, Jain P, Schenk EL, Sanborn RE, Thompson JR, et al. Updated results from a phase 1/2 study of HPN328, a tri-specific, half-life (T1/2) extended DLL3-targeting T-cell engager in patients (pts) with small cell lung cancer (SCLC) and other neuroendocrine cancers (NEC). *J Clin Oncol*. (2024) 42:8090–0. doi: 10.1200/JCO.2024.42.16_suppl.8090

114. Choudhury NJ, Beltran H, Johnson ML, Schenk EL, Sanborn RE, Thompson JR, et al. OA10.06 impact of brain metastases on safety and efficacy of MK-6070, a DLL3-targeting T cell engager, in small cell lung cancer. *J Thorac Oncol*. (2024) 19:S32–3. doi: 10.1016/j.jtho.2024.09.060

115. Yingling J. Interim clinical data for EGFR-TRACTr JANX008 in solid tumors as of February 12, 2024. *In: Janux Ther News*. (2024).

116. Muik A, Garralda E, Altintas I, Gieseke F, Geva R, Ben-Ami E, et al. Preclinical characterization and phase I trial results of a bispecific antibody targeting PD-L1 and 4-1BB (GEN1046) in patients with advanced refractory solid tumors. *Cancer Discovery*. (2022) 12:1248–65. doi: 10.1158/2159-8290.Cd-21-1345

117. Aerts J, Paz-Ares LG, Helissey C, Cappuzzo F, Quere G, Kowalski D, et al. Acasunlimab (DuoBody-PD-L1x4-1BB) alone or in combination with pembrolizumab (pembro) in patients (pts) with previously treated metastatic non-small cell lung cancer (mNSCLC): Initial results of a randomized, open-label, phase 2 trial. *J Clin Oncol*. (2024) 42:2533–3. doi: 10.1200/JCO.2024.42.16_suppl.2533

118. Garralda E, Oberoi A, de Velasco G, Victoria I, Pesantez D, Eguren Santamaría I, et al. First-in-human study (FIH) of FS222, a next-generation tetravalent PD-L1/CD137 bispecific antibody: Safety, pharmacodynamics (PD), and antitumor activity in patients (pts) with advanced solid tumors including PD-1 refractory melanoma. *J Clin Oncol*. (2024) 42:2505–5. doi: 10.1200/JCO.2024.42.16_suppl.2505

119. El-Khoueiry AB, Rivas D, Lee S-H, Thomas JS, Kim YJ, Cervantes A, et al. Leveraging innate immunity with AFM24, a novel CD16A and epidermal growth factor receptor (EGFR) bispecific innate cell engager: Interim results for the non-small cell lung cancer (NSCLC) cohort. *J Clin Oncol*. (2023) 41:2533–3. doi: 10.1200/JCO.2023.41.16_suppl.2533

120. Kim HR, Saavedra O, Cervantes A, Lugowska IA, Oberoi A, El-Khoueiry AB, et al. Preliminary results from the phase 2 study of AFM24 in combination with atezolizumab in patients with EGFR wild-type (EGFR-WT) non-small cell lung cancer (NSCLC). *J Clin Oncol*. (2024) 42:2522–2. doi: 10.1200/JCO.2024.42.16_suppl.2522

121. Naing A, McKean M, Rosen LS, Sommerhalder D, Shaik NM, Wang IM, et al. First-in-human phase I study to evaluate safety, tolerability, pharmacokinetics, pharmacodynamics, immunogenicity, and antitumor activity of PF-07209960 in patients with advanced or metastatic solid tumors. *ESMO Open*. (2025) 10:104291. doi: 10.1016/j.esmoop.2025.104291

122. Pratumchai I, Bernardo M, Marquardt KL, Zhu C, Menas F, Carrio R, et al. Abstract 4063: SAR445877, an anti-PD-1 antibody-IL-15 mutein fusion protein restores function to exhausted T cells. *Cancer Res*. (2024) 84:4063–3. doi: 10.1158/1538-7445.Am2024-4063

123. Chen J, Shen Z, Jiang X, Huang Z, Wu C, Jiang D, et al. Preclinical evaluation of IAP0971, a novel immunocytokine that binds specifically to PD1 and fuses IL15/IL15Rα complex. *Antib Ther*. (2023) 6:38–48. doi: 10.1093/abt/tbac031

124. Shum E, Reilley M, Najjar Y, Daud A, Thompson J, Baranda J, et al. 523 Preliminary clinical experience with XmAb20717, a PD-1 x CTLA-4 bispecific antibody, in patients with advanced solid tumors. *J Immuno Therapy of Cancer*. (2021) 8(3):A553–3. doi: 10.1136/jitc-2021-SITC2021.523%

125. Burton EM, Tawbi HA. Bispecific antibodies to PD-1 and CTLA4: doubling down on T cells to decouple efficacy from toxicity. *Cancer Discovery*. (2021) 11:1008–10. doi: 10.1158/2159-8290.CD-21-0257%

126. Berezhnoy A, Sumrow BJ, Stahl K, Shah K, Liu D, Li J, et al. Development and preliminary clinical activity of PD-1-guided CTLA-4 blocking bispecific DART molecule. *Cell Rep Med*. (2020) 1:100163. doi: 10.1016/j.xcrm.2020.100163

127. Coward J, Ganju V, Behzadigohar R, Kwong K, Xu J, Van H, et al. Preliminary safety, efficacy, and pharmacokinetics (PK) results of KN046 (bispecific anti-PD-L1/CTLA4) from a first-in-human study in subjects with advanced solid tumors. *JCO*. (2019) 37:2554–4. doi: 10.1200/JCO.2019.37.15_suppl.2554

128. Kotanides H, Li Y, Malabunga M, Carpenito C, Eastman SW, Shen Y, et al. Bispecific targeting of PD-1 and PD-L1 enhances T-cell activation and antitumor immunity. *Cancer Immunol Res*. (2020) 8:1300–10. doi: 10.1158/2326-6066.Cir-20-0304

129. Tang W, Chen J, Ji T, Cong X. TIGIT, a novel immune checkpoint therapy for melanoma. *Cell Death Dis*. (2023) 14:466. doi: 10.1038/s41419-023-05961-3

130. Rousseau A, Parisi C, Barlesi F. Anti-TIGIT therapies for solid tumors: a systematic review. *ESMO Open*. (2023) 8:101184. doi: 10.1016/j.esmoop.2023.101184

131. Chu X, Tian W, Wang Z, Zhang J, Zhou R. Co-inhibition of TIGIT and PD-1/PD-L1 in cancer immunotherapy: mechanisms and clinical trials. *Mol Cancer*. (2023) 22:93. doi: 10.1186/s12943-023-01800-3

132. Banta KL, Xu X, Chitre AS, Au-Yeung A, Takahashi C, O'Gorman WE, et al. Mechanistic convergence of the TIGIT and PD-1 inhibitory pathways necessitates co-blockade to optimize anti-tumor CD8(+) T cell responses. *Immunity*. (2022) 55:512–526.e9. doi: 10.1016/j.immuni.2022.02.005

133. Niu J, Maurice-Dror C, Lee DH, Kim DW, Nagrial A, Voskoboynik M, et al. First-in-human phase 1 study of the anti-TIGIT antibody vibostolimab as monotherapy or with pembrolizumab for advanced solid tumors, including non-small-cell lung cancer(☆). *Ann Oncol*. (2022) 33:169–80. doi: 10.1016/j.annonc.2021.11.002

134. Bendell JC, Bedard P, Bang Y-J, LoRusso P, Hodi S, Gordon M, et al. Abstract CT302: Phase Ia/Ib dose-escalation study of the anti-TIGIT antibody tiragolumab as a single agent and in combination with atezolizumab in patients with advanced solid tumors. *Cancer Res*. (2020) 80:CT302–2. doi: 10.1158/1538-7445.Am2020-ct302

135. Cho BC, Abreu DR, Hussein M, Cobo M, Patel AJ, Secen N, et al. Tiragolumab plus atezolizumab versus placebo plus atezolizumab as a first-line treatment for PD-L1-selected non-small-cell lung cancer (CITYSCAPE): primary and follow-up analyses of a randomised, double-blind, phase 2 study. *Lancet Oncol*. (2022) 23:781–92. doi: 10.1016/s1470-2045(22)00226-1

136. Aggarwal V, Workman CJ, Vignali DAA. LAG-3 as the third checkpoint inhibitor. *Nat Immunol*. (2023) 24:1415–22. doi: 10.1038/s41590-023-01569-z

137. Mariuzza RA, Shahid S, Karade SS. The immune checkpoint receptor LAG3: Structure, function, and target for cancer immunotherapy. *J Biol Chem*. (2024) 300. doi: 10.1016/j.jbc.2024.107241

138. Andrews LP, Butler SC, Cui J, Cillo AR, Cardello C, Liu C, et al. LAG-3 and PD-1 synergize on CD8(+) T cells to drive T cell exhaustion and hinder autocrine IFN-γ-dependent anti-tumor immunity. *Cell*. (2024) 187:4355–4372.e22. doi: 10.1016/j.cell.2024.07.016

139. US Food & Drug Administration. *FDA approves Opdualag for unresectable or metastatic melanoma [media release]* (2022). Available at: https://www.fda.gov/.

140. Girard N, Burotto M, Paz-Ares LG, Reck M, Schenker M, Lingua A, et al. LBA53 Nivolumab (NIVO) plus relatlimab with platinum-doublet chemotherapy (PDCT) vs NIVO + PDCT as first-line (1L) treatment (tx) for stage IV or recurrent NSCLC: Results from the randomized phase II RELATIVITY-104 study. *Ann Oncol*. (2024) 35:S1243–4. doi: 10.1016/j.annonc.2024.08.2295

141. De Giglio A, Di Federico A, Nuvola G, Deiana C, Gelsomino F. The landscape of immunotherapy in advanced NSCLC: driving beyond PD-1/PD-L1 inhibitors (CTLA-4, LAG3, IDO, OX40, TIGIT, vaccines). *Curr Oncol Rep*. (2021) 23:126. doi: 10.1007/s11912-021-01124-9

142. Sun Q, Hong Z, Zhang C, Wang L, Han Z, Ma D. Immune checkpoint therapy for solid tumours: clinical dilemmas and future trends. *Signal Transduct Target Ther*. (2023) 8:320. doi: 10.1038/s41392-023-01522-4

143. Qin S, Xu L, Yi M, Yu S, Wu K, Luo S. Novel immune checkpoint targets: moving beyond PD-1 and CTLA-4. *Mol Cancer*. (2019) 18:155. doi: 10.1186/s12943-019-1091-2

144. Anderson NM, Simon MC. The tumor microenvironment. *Curr Biol 30(16) R921-r925*. (2020). doi: 10.1016/j.cub.2020.06.081

145. Eguchi R, Wakabayashi I. HDGF enhances VEGF–dependent angiogenesis and FGF–2 is a VEGF–independent angiogenic factor in non–small cell lung cancer. *Oncol Rep*. (2020) 44:14–28. doi: 10.3892/or.2020.7580

146. Jung WY, Min KW, Oh YH. Increased VEGF-A in solid type of lung adenocarcinoma reduces the patients' survival. *Sci Rep*. (2021) 11:1321. doi: 10.1038/s41598-020-79907-6

147. Bellone M, Calcinotto A. Ways to enhance lymphocyte trafficking into tumors and fitness of tumor infiltrating lymphocytes. *Front Oncol*. (2013) 3:231. doi: 10.3389/fonc.2013.00231

148. Voron T, Colussi O, Marcheteau E, Pernot S, Nizard M, Pointet AL, et al. VEGF-A modulates expression of inhibitory checkpoints on CD8+ T cells in tumors. *J Exp Med*. (2015) 212:139–48. doi: 10.1084/jem.20140559

149. Martino EC, Misso G, Pastina P, Costantini S, Vanni F, Gandolfo C, et al. Immune-modulating effects of bevacizumab in metastatic non-small-cell lung cancer patients. *Cell Death Discov 2 16025*. (2016). doi: 10.1038/cddiscovery.2016.25

150. de Almeida PE, Mak J, Hernandez G, Jesudason R, Herault A, Javinal V, et al. Anti-VEGF treatment enhances CD8(+) T-cell antitumor activity by amplifying hypoxia. *Cancer Immunol Res*. (2020) 8:806–18. doi: 10.1158/2326-6066.Cir-19-0360

151. Kudo M. Scientific rationale for combined immunotherapy with PD-1/PD-L1 antibodies and VEGF inhibitors in advanced hepatocellular carcinoma. *Cancers (Basel)*. (2020) 12. doi: 10.3390/cancers12051089

152. Georganaki M, van Hooren L, Dimberg A. Vascular targeting to increase the efficiency of immune checkpoint blockade in cancer. *Front Immunol*. (2018) 9:3081. doi: 10.3389/fimmu.2018.03081

153. Meder L, Schuldt P, Thelen M, Schmitt A, Dietlein F, Klein S, et al. Combined VEGF and PD-L1 blockade displays synergistic treatment effects in an autochthonous mouse model of small cell lung cancer. *Cancer Res*. (2018) 78:4270–81. doi: 10.1158/0008-5472.Can-17-2176

154. Socinski MA, Jotte RM, Cappuzzo F, Orlandi F, Stroyakovskiy D, Nogami N, et al. Atezolizumab for first-line treatment of metastatic nonsquamous NSCLC. *N Engl J Med*. (2018) 378:2288–301. doi: 10.1056/NEJMoa1716948

155. US Food & Drug Administration. *FDA approves atezolizumabas adjuvant treatment for non-small cell lung cancer [media release]*. (2021). Available at: https://www.fda.gov/.

156. Hu X, Song Z, Zhang J, Jin J, Gao S, Sun Y, et al. IMM2510, an anti-PD-L1/VEGF bispecific antibody fusion protein, in patients with advanced solid tumors: A phase I dose-escalation study. *J Clin Oncol*. (2024) 42:e14506–e14506. doi: 10.1200/JCO.2021.39.15_suppl.2515

157. Coward J, Lemech CR, Mislang ARA, Parakh S, Underhill C, Nagrial A, et al. A phase I study of AK112, a bispecific antibody that targets PD-1 and VEGF co-expressing T cells, in patients with advanced solid tumors. *J Clin Oncol*. (2020) 38: TPS3155–TPS3155. doi: 10.1200/JCO.2020.38.15_suppl.TPS3155

158. Dhillon S. Ivonescimab: first approval. *Drugs*. (2024). doi: 10.1007/s40265-024-02073-w

159. Ardizzoni A, Hansen H, Dombernowsky P, Gamucci T, Kaplan S, Postmus P, et al. Topotecan, a new active drug in the second-line treatment of small-cell lung cancer: a phase II study in patients with refractory and sensitive disease. The European Organization for Research and Treatment of Cancer Early Clinical Studies Group and New Drug Development Office, and the Lung Cancer Cooperative Group. *J Clin Oncol*. (1997) 15:2090–6. doi: 10.1200/jco.1997.15.5.2090

160. Cheng X, Song Z, Zhang J, Jin J, Gao S, Liu R, et al. Preliminary results of a phase I dose escalation study of IMM2510, a PD-L1 and VEGF bispecific fusion protein, in patients with advanced tumors. *J Clin Oncol*. (2023) 41:2535–5. doi: 10.1200/JCO.2023.41.16_suppl.2535

161. David JM, Dominguez C, McCampbell KK, Gulley JL, Schlom J, Palena C. A novel bifunctional anti-PD-L1/TGF-β Trap fusion protein (M7824) efficiently reverts mesenchymalization of human lung cancer cells. *Oncoimmunology*. (2017) 6:e1349589. doi: 10.1080/2162402x.2017.1349589

162. Mariathasan S, Turley SJ, Nickles D, Castiglioni A, Yuen K, Wang Y, et al. Powles: TGFβ attenuates tumour response to PD-L1 blockade by contributing to exclusion of T cells. *Nature*. (2018) 554:544–8. doi: 10.1038/nature25501

163. Chatterjee S, Chatterjee A, Jana S, Dey S, Roy H, Das MK, et al. Transforming growth factor beta orchestrates PD-L1 enrichment in tumor-derived exosomes and mediates CD8 T-cell dysfunction regulating early phosphorylation of TCR signalome in breast cancer. *Carcinogenesis*. (2021) 42:38–47. doi: 10.1093/carcin/bgaa092

164. Mortezaee K. Normalization in tumor ecosystem: Opportunities and challenges. *Cell Biol Int*. (2021) 45:2017–30. doi: 10.1002/cbin.11655

165. Karami Z, Mortezaee K, Majidpoor J. Dual anti-PD-(L)1/TGF-β inhibitors in cancer immunotherapy - Updated. *Int Immunopharmacol*. (2023) 122:110648. doi: 10.1016/j.intimp.2023.110648

166. Tschernia NP, Gulley JL. Tumor in the crossfire: inhibiting TGF-β to enhance cancer immunotherapy. *BioDrugs*. (2022) 36:153–80. doi: 10.1007/s40259-022-00521-1

167. Eser P, Jänne PA. TGFβ pathway inhibition in the treatment of non-small cell lung cancer. *Pharmacol Ther*. (2018) 184:112–30. doi: 10.1016/j.pharmthera.2017.11.004

168. Grenga I, Donahue RN, Gargulak ML, Lepone LM, Roselli M, Bilusic M, et al. Anti-PD-L1/TGFβR2 (M7824) fusion protein induces immunogenic modulation of human urothelial carcinoma cell lines, rendering them more susceptible to immune-mediated recognition and lysis. *Urol Oncol*. (2018) 36:93.e1–93.e11. doi: 10.1016/j.urolonc.2017.09.027

169. Paz-Ares LG, Kim TM, Baz DV, Felip E, Lee DH, Lee KH, et al. Results from a second-line (2L) NSCLC cohort treated with M7824 (MSB0011359C), a bifunctional fusion protein targeting TGF-β and PD-L1. *J Clin Oncol*. (2018) 36:9017–7. doi: 10.1200/JCO.2018.36.15_suppl.9017

170. Cho BC, Lee JS, Wu YL, Cicin I, Dols MC, Ahn MJ, et al. Bintrafusp alfa versus pembrolizumab in patients with treatment-naive, programmed death-ligand 1-high advanced NSCLC: A randomized, open-label, phase 3 trial. *J Thorac Oncol*. (2023) 18:1731–42. doi: 10.1016/j.jtho.2023.08.018

171. Liu D, Zhou J, Wang Y, Li M, Jiang H, Liu Y, et al. Bifunctional anti-PD-L1/TGF-βRII agent SHR-1701 in advanced solid tumors: a dose-escalation, dose-expansion, and clinical-expansion phase 1 trial. *BMC Med*. (2022) 20:408. doi: 10.1186/s12916-022-02605-9

172. van de Donk N, Zweegman S. T-cell-engaging bispecific antibodies in cancer. *Lancet*. (2023) 402:142–58. doi: 10.1016/s0140-6736(23)00521-4

173. Giffin MJ, Cooke K, Lobenhofer EK, Estrada J, Zhan J, Deegen P, et al. AMG 757, a half-life extended, DLL3-targeted bispecific T-cell engager, shows high potency and sensitivity in preclinical models of small-cell lung cancer. *Clin Cancer Res*. (2021) 27:1526–37. doi: 10.1158/1078-0432.Ccr-20-2845

174. Rojo F, Corassa M, Mavroudis D, Öz AB, Biesma B, Brcic L, et al. International real-world study of DLL3 expression in patients with small cell lung cancer. *Lung Cancer*. (2020) 147:237–43. doi: 10.1016/j.lungcan.2020.07.026

175. Chapman G, Sparrow DB, Kremmer E, Dunwoodie SL. Notch inhibition by the ligand DELTA-LIKE 3 defines the mechanism of abnormal vertebral segmentation in spondylocostal dysostosis. *Hum Mol Genet*. (2011) 20:905–16. doi: 10.1093/hmg/ddq529

176. Saunders LR, Bankovich AJ, Anderson WC, Aujay MA, Bheddah S, Black K, et al. A DLL3-targeted antibody-drug conjugate eradicates high-grade pulmonary neuroendocrine tumor-initiating cells *in vivo*. *Sci Transl Med*. (2015) 7:302ra136. doi: 10.1126/scitranslmed.aac9459

177. Paz-Ares L, Ahn MJ, Felip E, Handzhiev S, Korantzis I, Izumi H, et al. LBA92 Tarlatamab for patients (pts) with previously treated small cell lung cancer (SCLC): Primary analysis of the phase II DeLLphi-301 study. *Ann Oncol*. (2023) 34:S1333–4. doi: 10.1016/j.annonc.2023.10.094

178. US Food & Drug Administration. *FDA grants accelerated approval to tarlatamab-dlle for extensive stage small cell lung cancer [media release]*. (2024). Available at: https://www.fda.gov/.

179. Hipp S, Voynov V, Drobits-Handl B, Giragossian C, Trapani F, Nixon AE, et al. A bispecific DLL3/CD3 igG-like T-cell engaging antibody induces antitumor responses in small cell lung cancer. *Clin Cancer Res*. (2020) 26:5258–68. doi: 10.1158/1078-0432.Ccr-20-0926

180. Molloy ME, Aaron WH, Barath M, Bush MC, Callihan EC, Carlin K, et al. HPN328, a trispecific T cell–activating protein construct targeting DLL3-expressing solid tumors. *Mol Cancer Ther*. (2024) 23:1294–304. doi: 10.1158/1535-7163.Mct-23-0524

181. Sigismund S, Avanzato D, Lanzetti L. Emerging functions of the EGFR in cancer. *Mol Oncol*. (2018) 12:3–20. doi: 10.1002/1878-0261.12155

182. Soria JC, Ohe Y, Vansteenkiste J, Reungwetwattana T, Chewaskulyong B, Lee KH, et al. Osimertinib in untreated EGFR-mutated advanced non-small-cell lung cancer. *N Engl J Med*. (2018) 378:113–25. doi: 10.1056/NEJMoa1713137

183. Vermorken JB, Mesia R, Rivera F, Remenar E, Kawecki A, Rottey S, et al. Platinum-based chemotherapy plus cetuximab in head and neck cancer. *N Engl J Med*. (2008) 359:1116–27. doi: 10.1056/NEJMoa0802656

184. Hoffmann P, Hofmeister R, Brischwein K, Brandl C, Crommer S, Bargou R, et al. Serial killing of tumor cells by cytotoxic T cells redirected with a CD19-/CD3-bispecific single-chain antibody construct. *Int J Cancer*. (2005) 115:98–104. doi: 10.1002/ijc.20908

185. Arvedson T, Bailis JM, Britten CD, Klinger M, Nagorsen D, Coxon A, et al. Targeting solid tumors with bispecific T cell engager immune therapy. *Annu Rev Cancer Biology 6(Volume 6*. (2022) 2022):17–34. doi: 10.1146/annurev-cancerbio-070620-104325

186. DiRaimondo TR, Budimir N, Ma L, Shenhav S, Cicchini V, Wu H, et al. Abstract B04: Preclinical activity and safety profile or JANX008, a novel EGFR-targeting tumor-activated T cell engager for treatment of solid tumors. *Cancer Immunol Res*. (2022) 10:B04–4. doi: 10.1158/2326-6074.Tumimm22-b04

187. Kwon BS, Weissman SM. cDNA sequences of two inducible T-cell genes. *Proc Natl Acad Sci U.S.A*. (1989) 86:1963–7. doi: 10.1073/pnas.86.6.1963

188. Schwarz H, Valbracht J, Tuckwell J, von Kempis J, Lotz M. ILA, the human 4-1BB homologue, is inducible in lymphoid and other cell lineages. *Blood*. (1995) 85:1043–52. doi: 10.1182/blood.V85.4.1043.bloodjournal8541043

189. Kim HD, Park S, Jeong S, Lee YJ, Lee H, Kim CG, et al. 4-1BB delineates distinct activation status of exhausted tumor-infiltrating CD8(+) T cells in hepatocellular carcinoma. *Hepatology*. (2020) 71:955–71. doi: 10.1002/hep.30881

190. Woroniecka KI, Rhodin KE, Dechant C, Cui X, Chongsathidkiet P, Wilkinson D, et al. 4-1BB agonism averts TIL exhaustion and licenses PD-1 blockade in glioblastoma and other intracranial cancers. *Clin Cancer Res*. (2020) 26:1349–58. doi: 10.1158/1078-0432.Ccr-19-1068

191. Claus C, Ferrara-Koller C, Klein C. The emerging landscape of novel 4-1BB (CD137) agonistic drugs for cancer immunotherapy. *MAbs*. (2023) 15:2167189. doi: 10.1080/19420862.2023.2167189

192. Vezys V, Penaloza-MacMaster P, Barber DL, Ha SJ, Konieczny B, Freeman GJ, et al. 4-1BB signaling synergizes with programmed death ligand 1 blockade to augment CD8 T cell responses during chronic viral infection. *J Immunol*. (2011) 187:1634–42. doi: 10.4049/jimmunol.1100077

193. Lakins MA, Koers A, Giambalvo R, Munoz-Olaya J, Hughes R, Goodman E, et al. FS222, a CD137/PD-L1 tetravalent bispecific antibody, exhibits low toxicity and antitumor activity in colorectal cancer models. *Clin Cancer Res*. (2020) 26:4154–67. doi: 10.1158/1078-0432.Ccr-19-2958

194. Zhang M, Lam KP, Xu S. Natural Killer Cell Engagers (NKCEs): a new frontier in cancer immunotherapy. *Front Immunol*. (2023) 14:1207276. doi: 10.3389/fimmu.2023.1207276

195. Wingert S, Reusch U, Knackmuss S, Kluge M, Damrat M, Pahl J, et al. Preclinical evaluation of AFM24, a novel CD16A-specific innate immune cell engager targeting EGFR-positive tumors. *MAbs*. (2021) 13:1950264. doi: 10.1080/19420862.2021.1950264

196. Kontermann RE. Antibody-cytokine fusion proteins. *Arch Biochem Biophys*. (2012) 526:194–205. doi: 10.1016/j.abb.2012.03.001

197. Fyfe G, Fisher RI, Rosenberg SA, Sznol M, Parkinson DR, Louie AC. Results of treatment of 255 patients with metastatic renal cell carcinoma who received high-dose recombinant interleukin-2 therapy. *J Clin Oncol*. (1995) 13:688–96. doi: 10.1200/jco.1995.13.3.688

198. Atkins MB, Lotze MT, Dutcher JP, Fisher RI, Weiss G, Margolin K, et al. High-dose recombinant interleukin 2 therapy for patients with metastatic melanoma: analysis of 270 patients treated between 1985 and 1993. *J Clin Oncol*. (1999) 17:2105–16. doi: 10.1200/jco.1999.17.7.2105

199. Rosenberg SA, Lotze MT, Muul LM, Chang AE, Avis FP, Leitman S, et al. A progress report on the treatment of 157 patients with advanced cancer using lymphokine-activated killer cells and interleukin-2 or high-dose interleukin-2 alone. *N Engl J Med*. (1987) 316:889–97. doi: 10.1056/nejm198704093161501

200. Rosenzwajg M, Lorenzon R, Cacoub P, Pham HP, Pitoiset F, El Soufi K, et al. Immunological and clinical effects of low-dose interleukin-2 across 11 autoimmune diseases in a single, open clinical trial. *Ann Rheum Dis*. (2019) 78:209–17. doi: 10.1136/annrheumdis-2018-214229

201. Hartemann A, Bensimon G, Payan CA, Jacqueminet S, Bourron O, Nicolas N, et al. Low-dose interleukin 2 in patients with type 1 diabetes: a phase 1/2 randomised, double-blind, placebo-controlled trial. *Lancet Diabetes Endocrinol*. (2013) 1:295–305. doi: 10.1016/s2213-8587(13)70113-x

202. Rosenberg SA, Yang JC, Topalian SL, Schwartzentruber DJ, Weber JS, Parkinson DR, et al. Treatment of 283 consecutive patients with metastatic melanoma or renal cell cancer using high-dose bolus interleukin 2. *Jama*. (1994) 271:907–13. doi: 10.1001/jama.1994.03510360033032

203. Hernandez R, Pöder J, LaPorte KM, Malek TR. Engineering IL-2 for immunotherapy of autoimmunity and cancer. *Nat Rev Immunol*. (2022) 22:614–28. doi: 10.1038/s41577-022-00680-w

204. Bempeg failure unlikely to affect other IL2 drugs. *Cancer Discovery*. (2022) 12:1604–5. doi: 10.1158/2159-8290.Cd-nb2022-0036

205. Wu W, Chia T, Lu J, Li X, Guan J, Li Y, et al. IL-2Rα-biased agonist enhances antitumor immunity by invigorating tumor-infiltrating CD25(+)CD8(+) T cells. *Nat Cancer*. (2023) 4:1309–25. doi: 10.1038/s43018-023-00612-0

206. Ring AM, Lin JX, Feng D, Mitra S, Rickert M, Bowman GR, et al. Mechanistic and structural insight into the functional dichotomy between IL-2 and IL-15. *Nat Immunol*. (2012) 13:1187–95. doi: 10.1038/ni.2449

207. Cheever MA. Twelve immunotherapy drugs that could cure cancers. *Immunol Rev*. (2008) 222:357–68. doi: 10.1111/j.1600-065X.2008.00604.x

208. Waldmann TA. The shared and contrasting roles of IL2 and IL15 in the life and death of normal and neoplastic lymphocytes: implications for cancer therapy. *Cancer Immunol Res*. (2015) 3:219–27. doi: 10.1158/2326-6066.Cir-15-0009

209. Conlon KC, Lugli E, Welles HC, Rosenberg SA, Fojo AT, Morris JC, et al. Redistribution, hyperproliferation, activation of natural killer cells and CD8 T cells, and cytokine production during first-in-human clinical trial of recombinant human interleukin-15 in patients with cancer. *J Clin Oncol*. (2015) 33:74–82. doi: 10.1200/jco.2014.57.3329

210. Keam SJ. Nogapendekin alfa inbakicept: first approval. *Drugs*. (2024) 84:867–74. doi: 10.1007/s40265-024-02060-1

211. Knudson KM, Hicks KC, Alter S, Schlom J, Gameiro SR. Mechanisms involved in IL-15 superagonist enhancement of anti-PD-L1 therapy. *J Immunother Cancer*. (2019) 7:82. doi: 10.1186/s40425-019-0551-y

212. Wrangle J, Reddy S, Soon-shiong P. OA06.05 IL15 superagonist (N-803, anktiva) + Checkpoint inhibitor (CPI) prolongs OS in 2ndline or greater NSCLC patients failing CPI. *J Thorac Oncol*. (2024) 19:S21. doi: 10.1016/j.jtho.2024.09.043

213. Xu Y, Carrascosa LC, Yeung YA, Chu ML, Yang W, Djuretic I, et al. An engineered IL15 cytokine mutein fused to an anti-PD1 improves intratumoral T-cell function and antitumor immunity. *Cancer Immunol Res*. (2021) 9:1141–57. doi: 10.1158/2326-6066.Cir-21-0058

214. Gutierrez M, Garralda E, Calvo E, van Dongen M, Eskens FA, Finlay M, et al. 1074TiP A phase I/II, open label, first-in-human, dose escalation and expansion study of SAR445877 administered as monotherapy in adults with advanced solid tumors. *Ann Oncol*. (2023) 34:S646–7. doi: 10.1016/j.annonc.2023.09.2213

215. Bernardo M, Y.-a. Zhang D, Martomo S, Menas F, Zhu C, Perez R, et al. Li: Abstract 2972: Preclinical characterization of SAR445877, an anti-PD-1 antibody-IL-15 mutein fusion protein with robust anti-tumor efficacy as monotherapy and in combination with PD-L1 blockade. *Cancer Res*. (2023) 83:2972–2. doi: 10.1158/1538-7445.Am2023-2972

216. Yin L, Jiang X, Wu C, Chen Z. Abstract 1889: IAP0971, A novel PD1/IL15 immunocytokine that binds specifically to PD1 and fuses IL15/IL15Rα complex. *Cancer Res*. (2023) 83:1889–9. doi: 10.1158/1538-7445.Am2023-1889

217. Peltret M, Vetsch P, Farvaque E, Mette R, Tsachaki M, Duarte L, et al. Development of a 10 g/L process for a difficult-to-express multispecific antibody format using a holistic process development approach. *J Biotechnol*. (2024) 389:30–42. doi: 10.1016/j.jbiotec.2024.04.017

218. Lu X, Domingo-Yenes B, Cohen N, Grzincic E. Freezing-induced protein aggregation in a bispecific antibody: Characterization and mechanistic insights. *J Pharm Sci*. (2025), 103711. doi: 10.1016/j.xphs.2025.103711

219. Barzadd MM, Lundqvist M, Harris C, Malm M, Volk AL, Thalén N, et al. Autophagy and intracellular product degradation genes identified by systems biology analysis reduce aggregation of bispecific antibody in CHO cells. *N Biotechnol*. (2022) 68:68–76. doi: 10.1016/j.nbt.2022.01.010

220. Wang S, Zhang W, Yang B, Zhang X, Fang J, Rui H, et al. A case study of a bispecific antibody manufacturability assessment and optimization during discovery stage and its implications. *Antib Ther*. (2024) 7:189–98. doi: 10.1093/abt/tbae013

221. Chen SW, Zhang W. Current trends and challenges in the downstream purification of bispecific antibodies. *Antib Ther*. (2021) 4:73–88. doi: 10.1093/abt/tbab007

222. Lim K, Zhu XS, Zhou D, Ren S, Phipps A. Clinical pharmacology strategies for bispecific antibody development: learnings from FDA-approved bispecific antibodies in oncology. *Clin Pharmacol Ther*. (2024) 116:315–27. doi: 10.1002/cpt.3308

223. Lim EA, Schweizer MT, Chi KN, Aggarwal R, Agarwal N, Gulley J, et al. Phase 1 study of safety and preliminary clinical activity of JNJ-63898081, a PSMA and CD3 bispecific antibody, for metastatic castration-resistant prostate cancer. *Clin Genitourinary Cancer*. (2023) 21:366–75. doi: 10.1016/j.clgc.2023.02.010

224. Zhou Y, Penny HL, Kroenke MA, Bautista B, Hainline K, Chea LS, et al. Immunogenicity assessment of bispecific antibody-based immunotherapy in oncology. *J Immunother Cancer*. (2022) 10. doi: 10.1136/jitc-2021-004225

225. Haber L, Olson K, Kelly MP, Crawford A, DiLillo DJ, Tavaré R, et al. Generation of T-cell-redirecting bispecific antibodies with differentiated profiles of cytokine release and biodistribution by CD3 affinity tuning. *Sci Rep*. (2021) 11:14397. doi: 10.1038/s41598-021-93842-0

226. Mandikian D, Takahashi N, Lo AA, Li J, Eastham-Anderson J, Slaga D, et al. Relative target affinities of T-cell-dependent bispecific antibodies determine biodistribution in a solid tumor mouse model. *Mol Cancer Ther*. (2018) 17:776–85. doi: 10.1158/1535-7163.Mct-17-0657

227. Valdes CR, Voorhees PM, D'Souza A, Chung A, Tuchman S, Safah H, et al. Efficacy, safety, and determination of RP2D of ABBV-383, a BCMA bispecific antibody, in patients with relapsed/refractory multiple myeloma (RRMM). *J Clin Oncol*. (2024) 42:7531–1. doi: 10.1200/JCO.2024.42.16_suppl.7531

228. To M, Yeung P, Fox M, Hammond M, Cattaruzza F, Nazeer A, et al. Abstract P193: AMX-818, a novel prodrug HER2-XPAT T-cell engager (TCE) with potent T cell activation, proteolytic cleavage and efficacy in xenograft tumors, and wide safety margins in NHP (Non Human Primate). *Mol Cancer Ther*. (2021) 20:P193–3. doi: 10.1158/1535-7163.Targ-21-p193

229. Wang Y, Cheng P. Arming oncolytic viruses with bispecific T cell engagers: The evolution and current status. *Biochim Biophys Acta Mol Basis Dis*. (2024) 1870:166962. doi: 10.1016/j.bbadis.2023.166962

230. Carlo-Stella C, Mazza R, Manier S, Facon T, Yoon S-S, Koh Y, et al. RG6234, a GPRC5DxCD3 T-cell engaging bispecific antibody, is highly active in patients (pts) with relapsed/refractory multiple myeloma (RRMM): updated intravenous (IV) and first subcutaneous (SC) results from a phase I dose-escalation study. *Blood 140 (Supplement)*. (2022) 1):397–9. doi: 10.1182/blood-2022-157988

231. Girard N, Li W, Spira A, Feldman J, Mak M, Sauder MB, et al. 10MO: Preventing moderate to severe dermatologic adverse events in first-line EGFR-mutant advanced NSCLC treated with amivantamab plus lazertinib: Early success of the COCOON trial. *J Thorac Oncol*. (2025) 20:S14–6. doi: 10.1016/S1556-0864(25)00205-9

232. Shepshelovich D, Barda N, Goldvaser H, Dagan N, Zer A, Diker-Cohen T, et al. Incidence of lung cancer following pneumonia in smokers: a population-based study. *Qjm*. (2022) 115:287–91. doi: 10.1093/qjmed/hcab030

233. Zhang Q, Tang L, Zhou Y, He W, Li W. Immune checkpoint inhibitor-associated pneumonitis in non-small cell lung cancer: current understanding in characteristics, diagnosis, and management. *Front Immunol*. (2021) 12:663986. doi: 10.3389/fimmu.2021.663986

234. Chen Z, Fillmore CM, Hammerman PS, Kim CF, Wong KK. Non-small-cell lung cancers: a heterogeneous set of diseases. *Nat Rev Cancer*. (2014) 14:535–46. doi: 10.1038/nrc3775

235. Hanahan D, Coussens LM. Accessories to the crime: functions of cells recruited to the tumor microenvironment. *Cancer Cell*. (2012) 21:309–22. doi: 10.1016/j.ccr.2012.02.022

236. Altorki NK, Markowitz GJ, Gao D, Port JL, Saxena A, Stiles B, et al. The lung microenvironment: an important regulator of tumour growth and metastasis. *Nat Rev Cancer*. (2019) 19:9–31. doi: 10.1038/s41568-018-0081-9

237. Yue P, Zhang M, Feng Y, Gao Y, Sun C, Chen P. Cost-effectiveness analysis of amivantamab plus chemotherapy versus chemotherapy alone in NSCLC with EGFR Exon 20 insertions. *Front Oncol.* (2024) 14:1368804. doi: 10.3389/fonc.2024.1368804

238. Wu Q, Li Q, Qin Y. A cost-effectiveness analysis of amivantamab plus lazertinib versus osimertinib in the treatment of US and Chinese patients with EGFR-mutated advanced non-small cell lung cancer. *Lung Cancer.* (2025) 203:108533. doi: 10.1016/j.lungcan.2025.108533

239. Ter Heine R, van den Heuvel MM, Piet B, Deenen MJ, van der Wekken AJ, Hendriks LEL, et al. A systematic evaluation of cost-saving dosing regimens for therapeutic antibodies and antibody-drug conjugates for the treatment of lung cancer. *Target Oncol.* (2023) 18:441–50. doi: 10.1007/s11523-023-00958-6

240. Nie S, Wang Z, Moscoso-Castro M, D'Souza P, Lei C, Xu J, et al. Biology drives the discovery of bispecific antibodies as innovative therapeutics. *Antib Ther.* (2020) 3:18–62. doi: 10.1093/abt/tbaa003

frontiers | Frontiers in Immunology

TYPE Correction
PUBLISHED 17 July 2025
DOI 10.3389/fimmu.2025.1656082

OPEN ACCESS

EDITED AND REVIEWED BY
Renata Pacholczak-Madej,
Maria Skłodowska-Curie National Institute of Oncology, Poland

*CORRESPONDENCE
Yunfeng Zhou
yunf_zhou_hxsy@163.com

RECEIVED 29 June 2025
ACCEPTED 01 July 2025
PUBLISHED 17 July 2025

CITATION
Chen W, Zhou A and Zhou Y (2025) Correction: Bispecific antibody for lung cancer: mechanisms and clinical insights. *Front. Immunol.* 16:1656082. doi: 10.3389/fimmu.2025.1656082

Correction: Bispecific antibody for lung cancer: mechanisms and clinical insights

Wei Chen[1], Afang Zhou[2] and Yunfeng Zhou[1]*

[1]Department of Thoracic Surgery, West China School of Public Health and West China Fourth Hospital, Sichuan University, Chengdu, Sichuan, China, [2]State Key Laboratory of Biotherapy, Sichuan University, Chengdu, Sichuan, China

KEYWORDS

bispecific antibodies, lung cancer, novel therapies, immunotherapy, targeted therapy

A Correction on

Bispecific antibody for lung cancer: mechanisms and clinical insights

By Chen W, Zhou A and Zhou Y (2025). *Front. Immunol.* 16:1572802. doi: 10.3389/fimmu.2025.1572802

In the published article, there was an error. The first sentence of the **Introduction** section contained erroneous data for the annual new lung cancer cases. The original text incorrectly stated "22 million new cases," which should be "2.2 million new cases" as cited in Reference 1.

A correction has been made to the section **Introduction**, Paragraph 1. This sentence previously stated:

"Lung cancer is one of the world's most common cancers and the leading cause of cancer-related deaths, with an estimated 22 million new cases and 1.79 million deaths annually (1)."

The corrected sentence appears below:

"Lung cancer is one of the world's most common cancers and the leading cause of cancer-related deaths, with an estimated 2.2 million new cases and 1.79 million deaths annually (1)."

The original version of this article has been updated.

Publisher's note

All claims expressed in this article are solely those of the authors and do not necessarily represent those of their affiliated organizations, or those of the publisher, the editors and the reviewers. Any product that may be evaluated in this article, or claim that may be made by its manufacturer, is not guaranteed or endorsed by the publisher.

frontiers | Frontiers in Immunology

TYPE Original Research
PUBLISHED 18 June 2025
DOI 10.3389/fimmu.2025.1612547

OPEN ACCESS

EDITED BY
Miroslawa Puskulluoglu,
Maria Sklodowska-Curie National Research Institute of Oncology, Poland

REVIEWED BY
Christian Augsberger,
GSK, Germany
Tianye Li,
Zhejiang University School of Medicine, China

*CORRESPONDENCE
Shihua Lin
Shihua_lin@topalliancebio.com
Sheng Yao
Sheng_yao@topalliancebio.com

†These authors share first authorship

RECEIVED 15 April 2025
ACCEPTED 28 May 2025
PUBLISHED 18 June 2025

CITATION
Lin S, Hong M, Zhang J, Zhao W, Li K, Wu C, Yang Q, Xiao Y, Huang L, Wang J, Jia A, Wang X and Yao S (2025) Characterization and functional evaluation of JS207, a novel bispecific antibody against human PD-1 and VEGFA. *Front. Immunol.* 16:1612547. doi: 10.3389/fimmu.2025.1612547

Characterization and functional evaluation of JS207, a novel bispecific antibody against human PD-1 and VEGFA

Shihua Lin[1*†], Min Hong[2†], Jing Zhang[2†], Wenting Zhao[2], Ke Li[1], Chun Wu[2], Qiuyun Yang[2], Yi Xiao[1], Lanqing Huang[1], Jing Wang[2], Aijuan Jia[2], Xujia Wang[2] and Sheng Yao[1*]

[1]The R&D Department of Topalliance Biosciences, Inc., Rockville, MD, United States, [2]R&D Department, Suzhou Union Biopharm Co., Ltd., Suzhou, Jiangsu, China

Introduction: Cancer immunotherapy has been revolutionized by targeting PD-1 to restore antitumor T-cell activity and blocking VEGF to attenuate immunosuppressive tumor angiogenesis. While combining PD-1 and VEGF inhibition has shown promise in enhancing antitumor responses, co-administration of two or more monoclonal antibodies face several challenges, including distinct pharmacokinetics, complex dosing, and toxicity. A bispecific antibody (BsAb) targeting both PD-1 and VEGF pathways could overcome these limitations by enabling simultaneous, localized blockades of PD-1 and VEGF signaling within the tumor microenvironment (TME) as both PD-1 and VEGF are usually co-expressed in the TME.

Methods: Here, we describe the in vitro characterization, functional and preclinical evaluation of JS207, a novel BsAb targeting PD-1 and VEGFA with high antigen binding affinity. JS207 matched or surpassed the activity of benchmarks antibodies in several in vitro binding assessments, T cell activation, VEGF signaling inhibition, cytokines (IL-2 and IFN-γ) release.

Results: JS207 showed significant anti-tumor efficacy in mouse MC38 colon cancer model and A375 melanoma tumor model. Investigation into the mechanism of action revealed that VEGFA could significantly promote JS207's antigen binding activity, T cell activation potency, and internalization of cell surface PD-1. *In vivo* results demonstrated that JS207 was well-tolerated and presented remarkable anti-tumor efficacy. In addition, JS207 showed enhanced thermal stability as evidenced by retained potency under heat stress, a critical factor for CMC (Chemistry, manufacturing and control) manufacture, storage and drug shelf life.

Conclusion: JS207 is a promising therapeutic candidate that may address unmet clinical needs in cancer immunotherapy.

KEYWORDS

PD-1/PD-L1, vascular endothelial growth factor A (VEGFA), tumor microenvironment (TME), bispecific antibody, JS207, internalization, thermal stability

1 Introduction

Cancer persists as a leading cause of global mortality, with conventional therapies often failing to control advanced or metastatic diseases. The immune checkpoint inhibitors (ICIs)-based cancer immunotherapies have achieved remarkable success across cancers (1). Among these, targeting programmed cell death protein 1 (PD-1) and its ligand (PD-L1), have shown remarkable efficacy in various cancers (2). Yet, intrinsic, and adaptive resistance limits the efficacy of ICIs, with only 20–40% of patients achieving long-term remission (3, 4). A key driver of this resistance is the immunosuppressive tumor microenvironment (TME), a dynamic ecosystem comprising cancer cells, stromal cells, immune infiltrates, endothelial cells and aberrant vasculature that collaboratively foster immune evasion, angiogenesis, and metastatic spread (5, 6).

Within the TME, vascular endothelial growth factor (VEGF) plays a dual role, promoting tumor angiogenesis while suppressing antitumor immunity, such as, inhibiting dendritic cell maturation, recruiting regulatory T cells, and impairing cytotoxic T-cell activity (7). Vascular endothelial growth factor A (VEGFA) is a key member of the VEGF family proteins that can be secreted by various types of cells, including endothelial cells and tumor cells (8). VEGFA promotes angiogenesis mainly by binding to VEGF receptor-2 (VEGFR2). The engagement of VEGFR2 by VEGFA causes dimerization and intracellular autophosphorylation of VEGFR2, thereby activating downstream signaling pathways (9). This signaling cascade drives endothelial cell proliferation, migration, and survival, establishing a chaotic vascular network that sustains tumor growth and metastasis (6, 10). In solid tumors, angiogenesis plays a key role in tumor uptake of nutrients and oxygen, followed by proliferation and metastasis (11). Therapeutic antibodies against VEGFA specifically block the binding of VEGFA to VEGFR2 and exert anti-tumor effects (10).

Despite the success of PD-1 inhibitors and anti-VEGF therapies, significant challenges persist in monotherapies resulting in limited efficacy due to the complex and adaptive nature of tumors (12). Resistance mechanisms, such as upregulation of alternative angiogenic pathways or immune evasion tactics, frequently diminish the long-term effectiveness of these treatments (13). Additionally, the heterogeneity of tumors and TME mean that a single therapeutic target may not be sufficient to achieve comprehensive tumor control (14). The need for combination therapies has become evident, yet the concurrent administration of multiple agents can lead to increased toxicity and adverse effects (AEs), complicating patient management and reducing quality of life (15, 16).

PD-(L)1 and VEGF have been shown to be co-expressed in the TME of various tumor types. The expression of PD-(L)1 and VEGF could be used as biomarkers for selecting patients who may benefit from PD-(L)1 and VEGF inhibitors (17, 18). The concentration of VEGF is significant higher in the TME than in plasma (17, 19). This elevated concentration is due to the increased secretion of VEGF by tumor cells, which promotes angiogenesis and supports tumor growth (20, 21). Numerous studies have demonstrated that blocking VEGFA/VEGFR signal pathway could induce tumor regression by not only inhibiting the proliferation of endothelial cells and the formation of new blood vessels in the TME but also improving the infiltration of cytotoxic lymphocytes into the TME, while PD-1/PD-L1 pathway blockade could activate the infiltrated cytotoxic lymphocytes by removing the immunosuppressive effect mediated by this pathway (22). Dual targeting-PD-1 and VEGFR2 significantly inhibited primary tumor growth and doubled survival in murine models of hepatocellular carcinoma (23). Combining anti-VEGFA and anti-PD-1/L1 agents has shown promise in clinical beneficials, as seen in clinical trials pairing bevacizumab with atezolizumab (24, 25). However, conventional combination therapies face challenges, including discordant pharmacokinetics, overlapping toxicities, and dosing complexities (26, 27). The Food and Drug Administration AEs reporting system database showed that the combination of PD-(L)1 inhibitors with bevacizumab provided a survival benefit but significantly increased the risk of various AEs, including fever, neutropenia, nephritis, and thrombocytopenic purpura, which were attributed to the combination therapy as an independent risk factor for these AEs (27). Bispecific antibodies (BsAb), engineered to simultaneously target two antigens, represent a promising solution to these challenges by simultaneously targeting two distinct pathways (28). This dual-targeting approach can enhance therapeutic efficacy while potentially reducing toxicity and the likelihood of resistance development (29). In the context of cancer therapy, particularly in solid tumors, BsAbs provide a multifaceted approach to immunotherapy by simultaneously targeting PD-(L)1 and other immune regulatory molecules, such as anti-CD47/PD-L1, anti-PD-1/CTLA-4, and anti-4-1BB/PD-L1. This strategy could enhance antitumor immunity, mitigate immune evasion, and overcome the limitations of monotherapy approaches (19). BsAb that combine immune checkpoint inhibition with anti-angiogenic effects hold particular promise (28). Combinations of anti-PD-(L)1 and VEGFA inhibition have been clinically validated and approved for the treatment of solid tumors (30). For example, AK112, also known as ivonescimab, is the first-in-class humanized IgG1 bispecific antibody that targets PD-1 and VEGFA by inhibiting PD-1-mediated immunosuppression and simultaneously blocking tumor angiogenesis in the TME (31). By concurrently blocking PD-1-mediated immune evasion and VEGFA-driven angiogenesis, AK112 has demonstrated potent anti-tumor efficacy in both preclinical and clinical settings (31–33). Thus, through dual targeting PD-1-expressing T cells and VEGF-rich vasculature, dual target approach via BsAb could exert a more comprehensive anti-tumor effect.

Here, we describe a novel BsAb, JS207, designed to overcome resistance mechanisms in cancer therapy. JS207 is a recombinant humanized anti-PD-1 and VEGFA bispecific antibody of IgG4 κ subtype constructed in a tetravalent IgG-VHH format combining full-length anti-PD-1 IgG with VEGFA-targeting Variable domain of Heavy chain-only (VHH) antibody. This study characterized the physiochemical and biological properties of JS207 and evaluated the therapeutic potential of this novel anti-PD-1/anti-VEGF BsAb through assessing antigen binding affinity, T cell activation, HUVEC proliferation inhibition, and *in vivo* anti-tumor efficacy. Through these studies, we seek to establish a foundation for the clinical translation of this promising therapeutic approach,

contributing to more effective and durable cancer treatments. In addition to extensive characterization studies, we compared JS207 with AK112 to assess the similarities and differences of these two BsAbs using a variety of methods to delineate the structural–functional relationships and antitumor activities. Our results demonstrated that engaging PD-1 and VEGFA by JS207 can significantly enhance antigen binding and PD-1 internalization, T cell activation, and anti-tumor activities.

2 Materials and methods

2.1 Materials, cell lines, and animals

The list of materials, cell lines and animals used in this study is available in the Supplementary Materials in Supplementary Data Sheet.

2.2 Enzyme-linked immunosorbent assay

Binding to PD-1: To assess the binding of JS207 to PD-1 and related proteins, 0.3 μg/mL of target protein (PD-1, BTLA, PD-L1, PD-L2 and ICOS, all from human) was coated onto 96-well plates. After blocking with 2%BSA, test samples were then added. Bound antibody was detected using an HRP-goat anti-human IgG (Fc-specific) antibody. Absorbance was measured at 450 nm/620 nm. To assess the species cross-reactivity, PD-1 proteins from rat, mouse, Cynomolgus monkey and human were used (Supplementary Data Sheet).

Binding to VEGFA: To evaluate the binding of JS207 to VEGFA and related proteins, 0.3 μg/mL of target protein (VEGFA, VEGFB, VEGFC, VEGFD, VEGFE and PLGF, all from human) was coated onto 96-well plates. After blocking with 2% BSA, test samples were added. Detection was carried out using an HRP-goat anti-human IgG (Fc-specific) antibody. To assess the species cross-reactivity, VEGFA proteins from rat, mouse, human and Cynomolgus monkey were used (Supplementary Data Sheet).

Blocking the interaction between human PD-1 with PD-L1/PD-L2: Inhibition of the interaction between human PD-1 and its ligands (PD-L1 and PD-L2) was assessed using blocking ELISAs. Human PD-1 protein (1.5 μg/mL) was coated on the plate and blocked with 2% BSA. Test samples were prepared in assay buffer containing biotin-PD-L1 hFc (4.0 μg/mL). After detection with HRP-streptavidin, absorbance was read at 450 nm/620 nm (Supplementary Data Sheet).

Blocking the interaction between human VEGFA and VEGFR2: To assess JS207's competitive inhibition of the VEGFA–VEGFR2 interaction, 0.5 μg/mL of human VEGFA was coated on 96-well plates and blocked with 2% BSA. Test samples (JS207, VEGF-DotAb, AK112) were added in assay buffer containing biotin-VEGFR2 (0.3 μg/mL). After detection with HRP-streptavidin, absorbance was read at 450 nm/620 nm (Supplementary Data Sheet).

2.3 Surface plasma resonance binding assays

Binding to human PD-1: The binding affinity of JS207 to human PD-1 was measured by Biacore T200. 40 μg/mL of anti-human Fc antibody was coated to CM5 chip, and then 2 μg/mL of JS207 were captured. Serially diluted human PD-1 was then applied, and the kinetic model was analyzed, and the binding affinity (K_D value) was calculated (Supplementary Data Sheet).

Binding to human VEGFA: The binding affinity of JS207 to human VEGFA was determined by the Biacore T200. 40 μg/mL of anti-human Fc antibody was coated to CM5 chip, and test samples were added. The kinetic model was analyzed, and the binding affinity (K_D value) was calculated (Supplementary Data Sheet).

Binding of JS207/VEGFA complex to human PD-1: The binding of pre-formed JS207/VEGFA complex to human PD-1 was assessed using the Octet RED96e system. 20 μg/mL of human PD-1-mFc was immobilized on an AMC biosensor, then incubated with JS207/VEGFA complex. Kinetic parameters were analyzed using Data Analysis 11.1 software (Supplementary Data Sheet).

Simultaneous binding of JS207 to human PD-1 and VEGFA: The ability of JS207 to simultaneously bind to human PD-1 and human VEGFA was measured using the Biacore T200. Two different experimental formats were used: (1) PD-1 first, then VEGFA, and (2) VEGFA first, then PD-1 (Supplementary Data Sheet).

2.4 Luciferase reporter gene assays

PD-1 reporter gene assay: Jurkat/PD-1-NAFT-Luc (Jurkat/PD-1) cells and PD-L1 aAPC/CHO-K1 (CHO/PD-L1) cells were used in this assay. JS207 inhibits the binding of PD-1 in Jurkat/PD-1 cells to PD-L1 in CHO/PD-L1 cells leading to NFAT/luciferase reporter gene activation, and the anti-PD-1 potency was determined via bioluminescent measurement (Supplementary Data Sheet). The signal to noise (S/N) ratio was generated by dividing the Top response by Bottom response. EC_{50} or IC_{50} is the concentration of an antibody required to achieve 50% of its maximum biological effect.

VEGF reporter gene assay: H293/VEGFR2 cell that was engineered to express VEGFR2/NFAT-luciferase was used in this assay. When VEGFA binds to VEGFR2 to initiate the signaling pathway, the NFAT-luciferase reporter gene is activated. The anti-VEGFA potency of JS207 was determined via bioluminescent measurement (Supplementary Data Sheet).

2.5 HUVEC proliferation inhibition assay

VEGFA at 10 ng/mL and the test antibody solutions at 0.004 nM-10 nM were added to 96-well plate and incubated at 37°C for 30 minutes. Then, HUVECs at 3×10^3 cells/well were seeded and incubated at 37°C for 96 hours. Cell counting-Lite luciferase assay

reagent was added and chemiluminescence signals were measured (Supplementary Data Sheet).

2.6 Flow cytometry binding experiments

Internalization assay using cell surface residual PD-1 quantification method: H293/PD-1 cells were seeded at 1×10^5 cells/well in a 96-well plate. Serially diluted test samples were added in the absence or presence of VEGFA. After incubation at 4°C for 30-minutes, the cells were divided into two aliquots and incubated at 37°C and 4°C for 0.5, 1, 2, and 4 hours, respectively. All cells were stained with an anti-human IgG-PE antibody for 30 minutes at 4°C. The samples were then analyzed by flow cytometry. The mean fluorescence intensity (MFI) was determined, and the internalization index was calculated using the following formula (Supplementary Data Sheet):

$$\text{Internalization Index} = [1 - (\text{MFI at } 37°C)/(\text{MFI at } 4°C)] \times 100.$$

Internalization assay using intracellular fluorescence method: JS207 and other test antibodies were conjugated with CypHer5E follow manufacture's instruction (GE Healthecare). The conjugated antibodies were serially diluted and incubated with or without VEGFA, then incubated with Jurkat/PD-1 cells for 4 hours at either 4°C or 37°C. Cells were washed with cold medium and subsequently stained with a PE-labeled noncompetitive anti-PD-1 antibody (MIH4 PD-1 PE, BD Biosciences). Samples were then analyzed on a BD FACSCanto II flow cytometer (Supplementary Data Sheet).

Cell-based PD-1 binding: To assess the effect of VEGFA on cell-based PD-1 binding, H293/PD-1 cells were seeded at 1×10^5 cells/well in a 96-well plate. Test samples were added in the absence or presence of VEGFA. The cells were incubated at 4°C for 30 minutes, stained with mouse anti-human Fc-PE antibody for 30 minutes at 4°C and then analyzed by flow cytometry. Data analysis was performed using FlowJo (Supplementary Data Sheet).

2.7 Mixed lymphocyte reaction assays

The effect of JS207 on IL-2 and IFN-γ release was evaluated using a mixed lymphocyte reaction (MLR) system. Peripheral blood mononuclear cells (PBMCs) resuspended in EasySep buffer and $CD4^+$ T cells were isolated. Mature dendritic cells (mDCs) and purified $CD4^+$ T cells were then seeded into 96-well plates at densities of 10,000 mDCs/well and 100,000 $CD4^+$ T cells/well, respectively. Test samples were added with a final concentration ranging from 150 nM to 15 pM. The cells were incubated at 37 °C for 5 days. Supernatants were collected on days 3 and 5 for IL-2 and IFN-γ measurement (Supplementary Data Sheet).

2.8 Thermal stability assessment

Test samples were first diluted to 2 mg/mL in cell culture medium and then subjected to heat stress at 40°C for 0–96 hr, 55°C for 0 – 48hr, and 65°C for 0–4 hr to assess the impact of heat-stress on anti-PD-1 activity. To assess the impact of heat-stress on anti-VEGFA activity, samples were stressed at 40°C and 50°C for 0–6 days. The potency values of stressed samples was compared with the respective control samples (Time 0).

2.9 Anti-tumor activity studies

Mouse colon cancer MC38 model in B-hPD-1 humanized mice: MC38 cells were implanted subcutaneously in the right flank of C57BL/6-Pdcd1$^{tm1(PDCD1)Bcgen/Bcgen}$ mice (B-hPD-1 humanized mice) at 1×10^5 cells/mouse. When the mean tumor volume reached approximately 115 mm^3, mice were randomly assigned into seven groups (n = 8 per group): (1) saline, (2) toripalimab 0.6 mg/kg, (3) VEGF-DotAb 0.33 mg/kg, (4) toripalimab 0.6 mg/kg + VEGF-DotAb + 0.33 mg/kg, (5) JS207 0.75 mg/kg, (6) JS207 1.5 mg/kg, and (7) JS207 4.5 mg/kg. Treatments were administered intraperitoneally twice weekly for a total of 6 doses. Tumor volumes and animal body weights were recorded (Supplementary Data Sheet).

Malignant melanoma A375 model in NDG mice: A375 cells at 5×10^6 cells/mouse were suspended mixed with Matrigel and implanted subcutaneously into NDG mice. When the average tumor volume reached approximately 137 mm^3, 10×10^6 PBMCs in 0.2 mL were injected intravenously. Two days after PBMC administration, the tumor-bearing mice were randomly assigned to five groups (n = 8 per group): (1) saline control group, (2) AK112 11.1 mg/kg, (3) JS207 1.0 mg/kg), (4) JS207 3.0 mg/kg, and (5) JS207 10.0 mg/kg. All the treatments were administered intraperitoneally twice a week for a total of 6 doses (Supplementary Data Sheet). Tumor volumes and animal body weights were recorded, and tumor growth inhibition rate (TGI_{TV}) was calculated as:

$$TGI_{TV}(\%) = [1 - (Ti - T0)/(Vi - V0)] \times 100\,\%$$

Where: Ti = mean tumor size of the treatment group on the i-th day of administration, T0 = mean tumor size of the treatment group on day 0 of administration; Vi = mean tumor size of the negative control group on the i-th day of administration, V0 = mean tumor size of the negative control group on day 0 of administration.

All animals of the above *in vivo* studies were housed in an SPF-grade facility of Suzhou Junmeng Biopharmaceuticals. The housing conditions were maintained at a temperature of 20–26 °C, relative humidity of 40%-70%, with 12-hour light/dark cycle. All protocols and procedures are approved by the local Institutional Animal Care and Use Committee (IACUC) under permit number YTSYDWIACUC202401.

2.10 Statistical analysis

Statistical significance was determined using Microsoft Excel and GraphPad Prism software. Comparisons between groups were performed using a two-tailed Student's t-test. Data are presented as the mean ± standard deviation, and differences between groups were considered statistically significant when $p < 0.05$ (*$p < 0.05$; **$p < 0.01$, ***$p < 0.001$, ****$p < 0.0001$).

3 Results

3.1 Structure and antigen binding profile of JS207

JS207 is a recombinant humanized bispecific antibody that targets both PD–1 and VEGFA and belongs to the IgG4 κ subtype. It was independently developed by Shanghai Junshi Biosciences Co., Ltd. for the treatment of advanced malignancies. JS207 comprises two identical light chains (LC) and two identical heavy chains (HC), which are linked by intra– and inter–chain disulfide bonds. The molecule incorporates the Fab, hinge, and Fc regions derived from an anti–PD–1 monoclonal antibody, with an anti–VEGFA nanobody fused to the hinge region of the heavy chain via flexible linkers ($(G_4S)_3$ and $(G_4S)_1$) (Figure 1A). The intact molecular weight of JS207 is approximately 180.5 kDa.

3.2 Binding of JS207 to human PD-1 related immune proteins

The binding activity of JS207 to human PD–1 and a panel of related immune proteins was examined by ELISA. As shown in Figures 1B, C, JS207 exhibited concentration–dependent binding to human PD–1. In contrast, it did not bind to human BTLA, CTLA–4, CD28, PD–L1, PD–L2, or ICOS. Comparative analysis using toripalimab (an in–house, commercially approved anti–PD–1 antibody, also known as JS001) and AK112 demonstrated that all three antibodies specifically bound to human PD–1. The calculated EC_{50} values were 10.4 ng/mL (58.6 pM) for JS207, 8.9 ng/mL (60.5 pM) for toripalimab, and 20.1 ng/mL (100.0 pM) for AK112.

3.3 Binding of JS207 to human VEGF family proteins

The binding of JS207 to human vascular endothelial growth factor (VEGF) family proteins, including VEGFA, VEGFB, VEGFC, VEGFD, VEGFE, and placental growth factor (PLGF), was evaluated by ELISA. As shown in Figures 1D, E, JS207 specifically bound to human VEGFA, with no detectable binding to human VEGFB, VEGFC, VEGFD, VEGFE, or PLGF.

3.4 Blocking of PD-1/PD-L1, PD-1/PD-L2 and VEGFA/VEGFR2 by JS207

The ability of JS207 to inhibit the binding of human PD-1 to its ligands (PD-L1 and PD-L2) and to block the interaction between

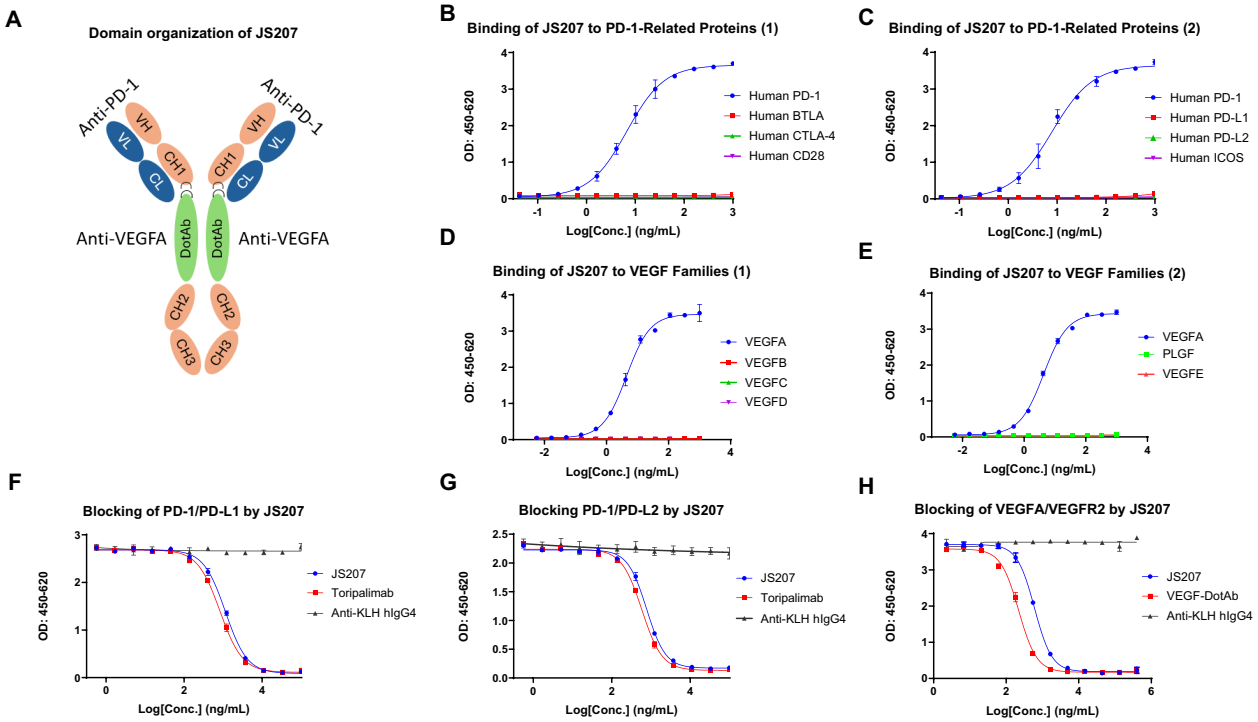

FIGURE 1
Structure and binding profile of JS207. **(A)** Domain organization of JS207. **(B)** JS207 binds to human PD–1 but not to BTLA, CTLA–4, or CD28. **(C)** JS207 binds to human PD–1 but not to PD–L1, PD–L2, or ICOS. **(D)** JS207 binds to human VEGFA but not to VEGFB, VEGFC, or VEGFD. **(E)** No binding of JS207 to human PLGF (placental growth factor) or VEGFE. **(F)** Blocking of PD–1/PD–L1 interaction by JS207 and toripalimab (positive control). **(G)** Blocking of PD–1/PD–L2 interaction by JS207. **(H)** Blocking of VEGFA/VEGFR2 interaction by JS207 and VEGF–DotAb (positive control). An anti–KLH hIgG4 antibody served as the negative control in experiments **(F–H)**.

human VEGFA and VEGFR2 was assessed using blocking ELISA. In these assays, toripalimab and VEGF-DotAb (an in-house anti-VEGFA Dotbody) served as positive controls, while an anti-KLH hIgG4 antibody was used as the negative control.

As presented in Figures 1F, G, JS207 effectively blocked the interaction between human PD-1 and PD-L1 with an IC_{50} of 1149 ng/mL (6.37 nM) and between PD-1 and PD-L2 with an IC_{50} of 776.6 ng/mL (4.3 nM). Moreover, JS207 inhibited the binding of human VEGFA to VEGFR2 with an IC_{50} of 603.9 ng/mL (3.35 nM). In contrast, toripalimab only blocked the PD-1/PD-L1 and PD-1/PD-L2 interactions, with IC_{50} values of 883.7 ng/mL (5.56 nM) and 587.7 ng/mL (3.92 nM), respectively, but did not block the VEGFA/VEGFR2 interaction. VEGF-DotAb specifically inhibited VEGFA binding to VEGFR2, with an IC_{50} of 221.6 ng/mL (1.48 nM) (Figure 1H).

3.5 Species cross-reactivity of JS207

To evaluate the cross-species reactivity, the binding of JS207 to PD-1 proteins from different species was assessed by ELISA. As shown in Figures 2A–C, JS207 bound potently to human PD-1 and cynomolgus (cyno) PD-1 with EC_{50} values of 8.2 ng/mL (45 pM) and 17.2 ng/mL (95 pM), respectively, while no binding was observed for rat or mouse PD-1. The negative control anti-KLH IgG4 exhibited no binding.

Similarly, the cross-species binding of JS207 to VEGFA was examined. As depicted in Figures 2D, E, JS207 bound to human and cyno VEGFA with an EC_{50} of 4.2 ng/mL (23 pM) and also recognized rat and mouse VEGFA with EC_{50} values of 5.3 ng/mL (29 pM) and 4.8 ng/mL (27 pM), respectively.

3.6 Binding affinity to human PD-1 and VEGFA

The binding affinity and kinetics of JS207 toward human PD-1 were characterized using surface plasmon resonance (SPR). Figure 3A shows the binding profile of JS207 to human PD-1, which is similar to that of toripalimab (Figure 3C), a finding that is consistent with the fact that the anti-PD-1 domain of JS207 is derived from toripalimab. In contrast, AK112 displayed a distinct profile (Figure 3B), with slower association and faster dissociation kinetics compared to JS207 and toripalimab. The equilibrium dissociation constant (K_D) for JS207 binding to human PD-1 was determined to be 4.60×10^{-10} M, approximately 11-fold higher affinity than that of AK112 (5.05×10^{-9} M). In addition, the PD-1 binding affinity of JS207 was comparable to that of toripalimab (5.55×10^{-10} M) (Figure 3G).

The binding profile of JS207 to human VEGFA was similarly assessed by SPR. As shown in Figures 3D–F, the binding traces of JS207 were similar to those observed for AK112 and VEGF-DotAb. All three antibodies exhibited very high affinities for human VEGFA, with K_D values of 9.00×10^{-12} M for JS207, $<2.59\times10^{-11}$ M for AK112, and $<7.14\times10^{-12}$ M for VEGF-DotAb (Figure 3H).

3.7 Binding of JS207/VEGFA complex to human PD-1

Because JS207 exhibits high affinity for human VEGFA, intravenous administration is expected to result in the rapid formation of a JS207/VEGFA complex in circulation prior to its

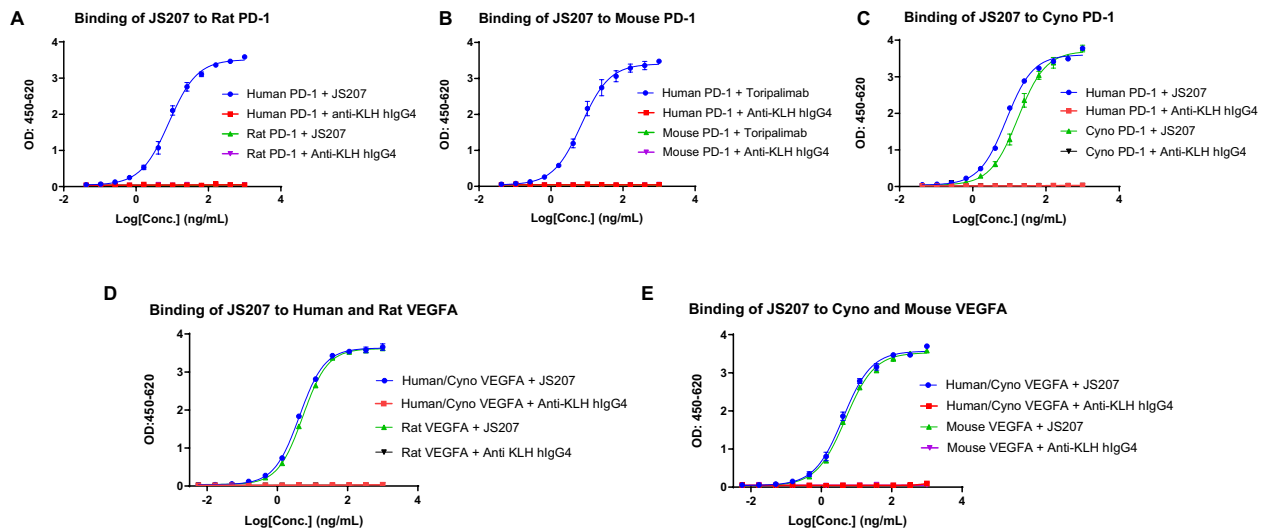

FIGURE 2
Species cross-reactivity of JS207. **(A)** No binding of JS207 to rat PD-1. **(B)** No binding of JS207 to mouse PD-1. **(C)** JS207 binding to human and Cynomolgus Monkey (Cyno) PD-1. **(D)** JS207 binding to human and rat VEGFA. **(E)** JS207 binding to Cyno and mouse VEGFA. Anti KLH hIgG4 was used as negative control.

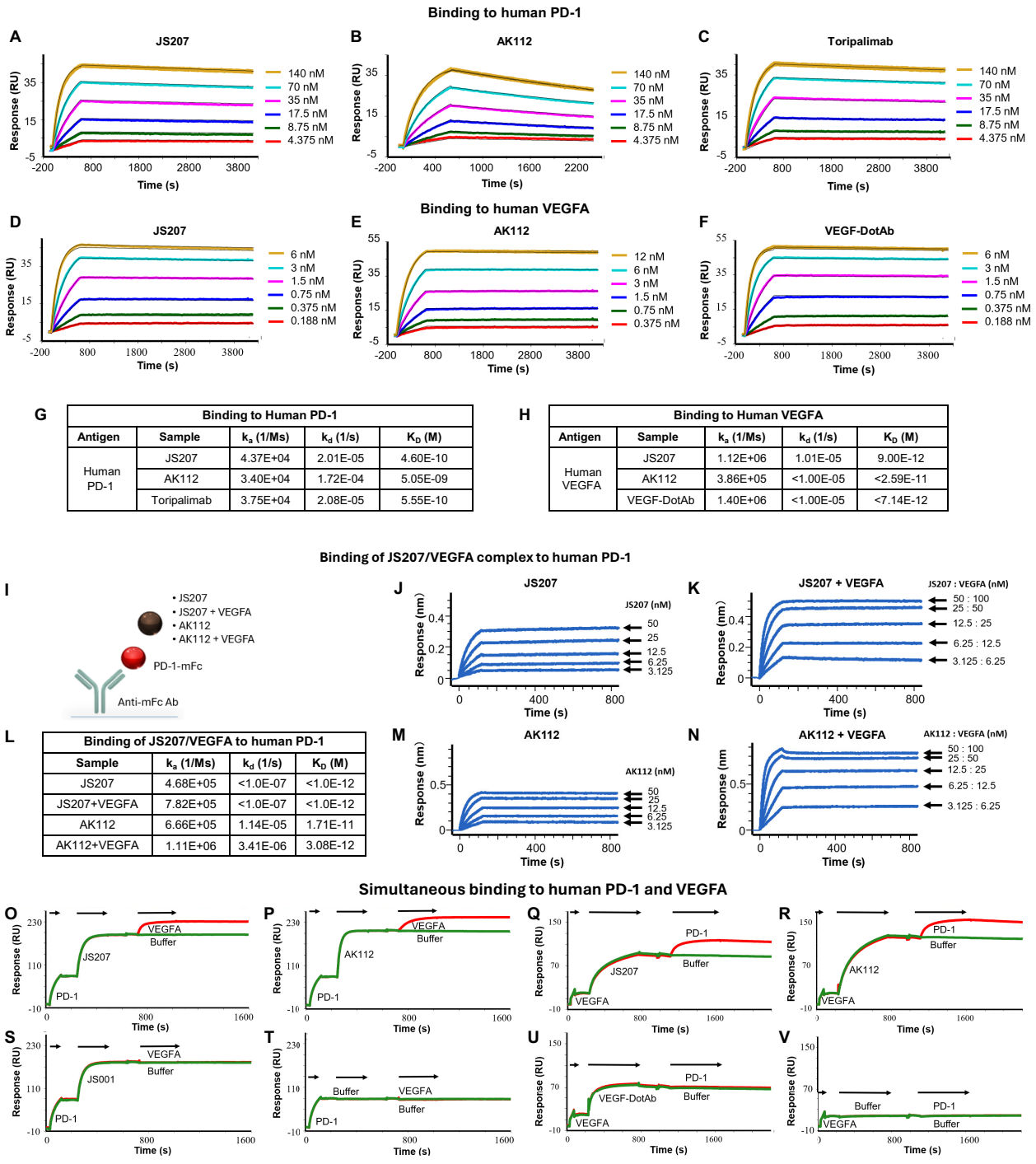

G

Binding to Human PD-1				
Antigen	**Sample**	**k_a (1/Ms)**	**k_d (1/s)**	**K_D (M)**
Human PD-1	JS207	4.37E+04	2.01E-05	4.60E-10
	AK112	3.40E+04	1.72E-04	5.05E-09
	Toripalimab	3.75E+04	2.08E-05	5.55E-10

H

Binding to Human VEGFA				
Antigen	**Sample**	**k_a (1/Ms)**	**k_d (1/s)**	**K_D (M)**
Human VEGFA	JS207	1.12E+06	1.01E-05	9.00E-12
	AK112	3.86E+05	<1.00E-05	<2.59E-11
	VEGF-DotAb	1.40E+06	<1.00E-05	<7.14E-12

L

Binding of JS207/VEGFA to human PD-1			
Sample	**k_a (1/Ms)**	**k_d (1/s)**	**K_D (M)**
JS207	4.68E+05	<1.0E-07	<1.0E-12
JS207+VEGFA	7.82E+05	<1.0E-07	<1.0E-12
AK112	6.66E+05	1.14E-05	1.71E-11
AK112+VEGFA	1.11E+06	3.41E-06	3.08E-12

FIGURE 3
Antigen binding characteristics of JS207 in comparison with AK112, toripalimab and VEGF-DotAb. **(A)** JS207 binding to human PD-1. **(B)** AK112 binding to human PD-1. **(C)** Toripalimab binding to human PD-1. **(D)** JS207 binding to human VEGFA. **(E)** AK112 binding to human VEGFA. **(F)** VEGF-DotAb binding to human VEGFA. **(G)** Binding affinity of JS207, AK112 and toripalimab to human PD-1. **(H)** Binding affinity of JS207, AK112 and VEGF-DotAb to human VEGFA. **(I)** Experimental design for JS207/VEGFA and AK112/VEGFA complex binding to human PD-1. **(J)** JS207 binding to human PD-1. **(K)** JS207/VEGFA complex binding to human PD-1. **(L)** Binding affinity of JS207/VEGFA and AK112/VEGFA complex to human PD-1. **(M)** AK112 binding to human PD-1. **(N)** AK112/VEGFA complex binding to human PD-1. **(O)** JS207 binding to human PD-1, then human VEGFA. **(P)** AK112 binding to human PD-1, then human VEGFA. **(Q)** JS207 binding to human VEGFA, then human PD-1. **(R)** AK112 binding to human VEGFA, then human PD-1. **(S)** Toripalimab binding to human PD-1 but not VEGFA. **(T)** No binding in buffer control. **(U)** VEGF-DotAb binding to human VEGFA but not PD-1. **(V)** No binding signal for buffer control.

engagement with PD-1 within the tumor microenvironment. To determine whether this preformed complex retains its ability to bind human PD-1, we employed an Octet-based assay (Figure 3I). In this experiment, human PD-1 conjugated with a mouse Fc fragment was immobilized on an AMC biosensor. Next, JS207, the preformed JS207/VEGFA complex, AK112, and the AK112/VEGFA complex were injected (Figures 3I–N). As shown in Figure 3K, the JS207/VEGFA complex produced a strong binding signal to human PD-1, with a K_D value of $<1.0\times10^{-12}$ M, comparable to JS207 alone (Figures 3J–L). Similarly, the AK112/VEGFA complex bound to PD-1 with an affinity similar to that of AK112 alone (Figures 3L–N). These results indicate that both JS207/VEGFA and AK112/VEGFA complexes maintain robust binding activity to human PD-1.

3.8 Simultaneous binding of JS207 to human PD-1 and human VEGFA

To assess whether JS207 can bind human PD-1 and human VEGFA simultaneously, we designed an SPR assay. In this experiment, AK112 was used as a comparator, while toripalimab and VEGF-DotAb served as positive controls for PD-1 and VEGFA binding, respectively. In one format, human PD-1 was first captured; subsequent injection of JS207, followed by VEGFA, produced an additional binding response (Figure 3O), demonstrating that JS207 can engage both antigens simultaneously. A similar dual-binding profile was observed for AK112 (Figure 3P). In contrast, toripalimab bound exclusively to PD-1 (Figure 3S), and no binding was detected in the buffer control (Figure 3T). In a complementary approach, when human VEGFA was immobilized first, JS207 was subsequently able to bind human PD-1, further confirming JS207's dual-binding capability (Figures 3Q, R). AK112 exhibited a similar binding pattern as JS207 (Figures 3P, R). As expected, toripalimab bound only to PD-1, while VEGF-DotAb bound exclusively to VEGFA (Figure 3U); no binding signal was observed in the corresponding buffer control (Figure 3V).

3.9 Anti-PD-1 potency of JS207 using PD-1 reporter gene assay

The anti–PD–1 potency of JS207 was evaluated using a PD–1/PD–L1 reporter gene assay (RGA). Jurkat effector cells stably overexpressing human PD–1 and an NFAT–driven luciferase reporter were co–cultured with CHO target cells expressing human PD–L1. JS207 effectively blocked the PD–1/PD–L1 interaction, thereby promoting T cell activation. The EC_{50} value for JS207 was 2.89 nM with a signal-to-noise (S/N) ratio of 4.95. In parallel, the EC_{50} values and S/N ratios for AK112 and toripalimab were 8.34 nM, 4.47 and 3.49 nM, 6.0, respectively. Hence, the anti–PD–1 potency of JS207 is comparable to that of toripalimab and superior to that of AK112 (Figure 4A).

3.10 Anti-VEGFA potency of JS207 in VEGFA reporter gene assay

The anti–VEGFA activity of JS207 was assessed using a VEGFA/VEGFR2 RGA in H293 cells engineered to overexpress VEGFR2. As shown in Figure 4B, JS207, AK112, and VEGF–DotAb effectively inhibited the binding of VEGF to VEGFR2. The IC_{50} value for JS207 was 0.773 nM with an S/N ratio of 4.49; for AK112, the corresponding values were 1.131 nM and 4.79; and for VEGF–DotAb, 0.479 nM and 4.83, respectively. Thus, JS207 exhibited anti–VEGF activity comparable to or slightly better than that of AK112 but was marginally less potent than VEGF–DotAb (Figure 4B).

3.11 HUVEC proliferation inhibition by JS207

The ability of JS207 to inhibit human umbilical vein endothelial cell (HUVEC) proliferation was examined *in vitro*. HUVECs were cultured in the presence of 10 ng/mL VEGFA along with serial dilutions of JS207, AK112, and VEGF–DotAb (0.005–10.0 nM). The IC_{50} values and S/N ratios were determined to be 0.296 nM, 2.76 for JS207, 0.328 nM, 2.41 for AK112, and 0.243 nM, 3.22 for VEGF–DotAb. These data indicate that the inhibitory effect of JS207 on HUVEC proliferation is comparable to or marginally better than that of AK112, albeit somewhat less potent than VEGF–DotAb (Figure 4C).

3.12 VEGFA enhances JS207's cell-based binding and anti-PD-1 potency

The effect of VEGFA on the anti–PD–1 activity of JS207 was investigated using the PD–1 RGA. As indicated in Figure 4D, the presence of 20.8 nM VEGFA markedly enhanced the anti–PD–1 activity of JS207 compared with JS207 alone. Further increasing the VEGFA concentration to 333.3 nM elevated the maximum response (upper asymptote) of JS207's anti–PD–1 potency. VEGFA at 1000 nM also enhanced the anti–PD–1 potency of AK112 with similar extent as JS207, whereas toripalimab remained unaffected (Figure 4E).

Cell–based binding studies using H293/PD–1 cells demonstrated that VEGFA enhanced the binding of both JS207 and AK112 to PD–1, while toripalimab showed no such effect (Figure 4F). Similar results were observed in PD-1 expressing Jurkat/PD–1 cells (Supplementary Figure S1 in Supplementary Data Sheet).

3.13 JS207 induces IL-2 and IFN-γ in the mixed lymphocytes reaction

The mixed lymphocyte reaction (MLR) system was used to assess JS207's effect on T cell activation. In this assay, *in vitro*–

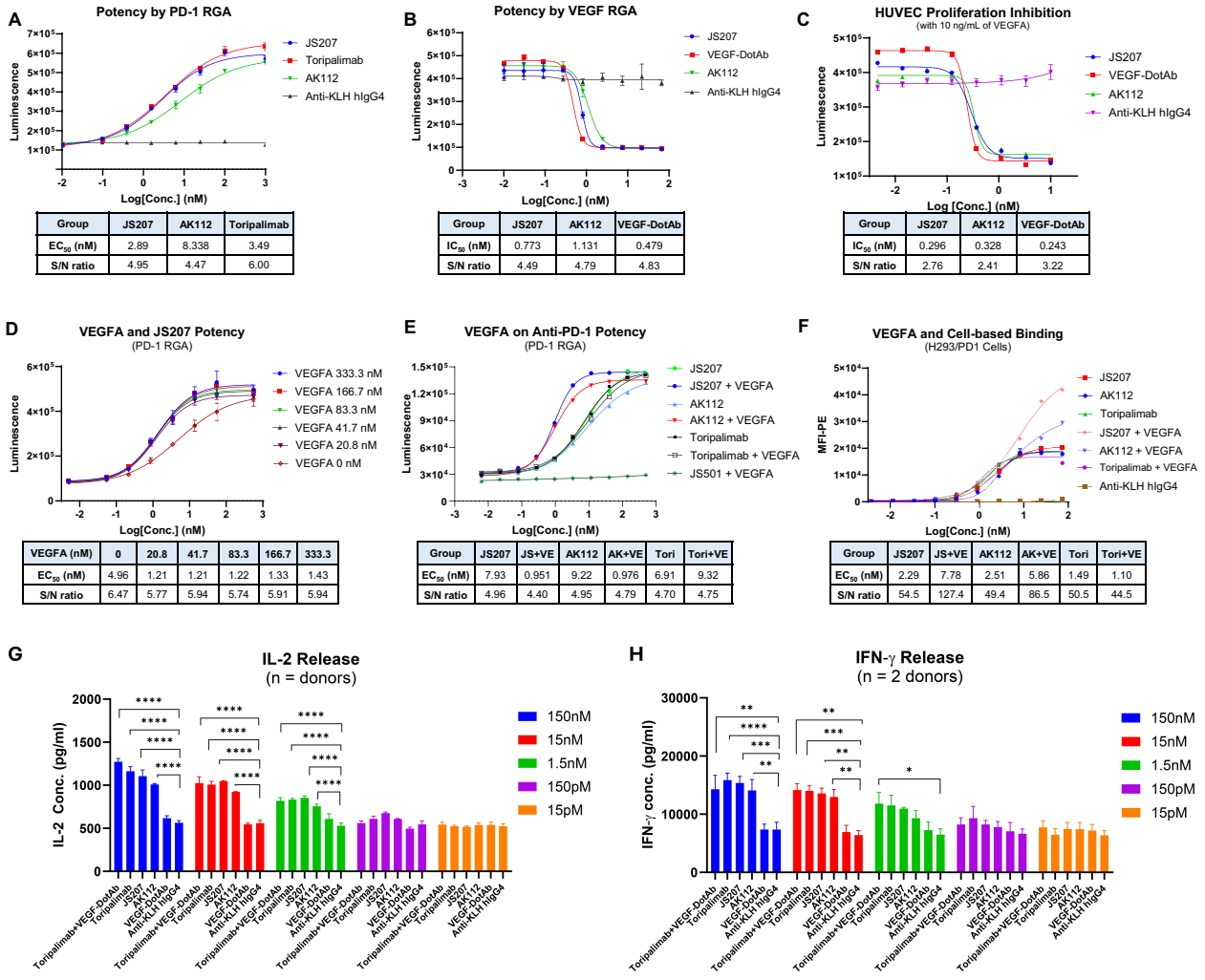

Group	JS207	AK112	Toripalimab
EC_{50} (nM)	2.89	8.338	3.49
S/N ratio	4.95	4.47	6.00

Group	JS207	AK112	VEGF-DotAb
IC_{50} (nM)	0.773	1.131	0.479
S/N ratio	4.49	4.79	4.83

Group	JS207	AK112	VEGF-DotAb
IC_{50} (nM)	0.296	0.328	0.243
S/N ratio	2.76	2.41	3.22

VEGFA (nM)	0	20.8	41.7	83.3	166.7	333.3
EC_{50} (nM)	4.96	1.21	1.21	1.22	1.33	1.43
S/N ratio	6.47	5.77	5.94	5.74	5.91	5.94

Group	JS207	JS+VE	AK112	AK+VE	Tori	Tori+VE
EC_{50} (nM)	7.93	0.951	9.22	0.976	6.91	9.32
S/N ratio	4.96	4.40	4.95	4.79	4.70	4.75

Group	JS207	JS+VE	AK112	AK+VE	Tori	Tori+VE
EC_{50} (nM)	2.29	7.78	2.51	5.86	1.49	1.10
S/N ratio	54.5	127.4	49.4	86.5	50.5	44.5

FIGURE 4
Cell-based biological activity of JS207. **(A)** Anti-PD-1 potency of JS207 in PD-1 reporter gene assay (RGA). **(B)** Anti-VEGFA potency of JS207 in VEGFA RGA. **(C)** HUVEC proliferation inhibition by JS207. **(D)** The impact of VEGFA concentration on JS207's anti-PD-1 potency. **(E)** VEGFA enhanced anti-PD-1 activity of JS207 and AK112 but not toripalimab. **(F)** VEGFA enhanced cell-based PD-1 binding by JS207 and AK112. **(G)** JS207, AK112, toripalimab, and toripalimab plus VEGF-DotAb at 1.5 nM or higher significantly enhanced IL-2 levels. **(H)** JS207, AK112 and toripalimab at 15 nM or higher significantly enhanced IFN-γ levels. Toripalimab plus VEGF-DotAb at 1.5 nM significantly enhanced IFN-γ release in the MLR system. *p < 0.05; **p < 0.01, ***p < 0.001, ****p < 0.0001 vs negative control (anti-KLH IgG4) group.

induced mature dendritic cells and $CD4^+$ T cells from four donors were co–incubated with JS207 and control antibodies over a concentration range of 15 pM to 150 nM. JS207 significantly promoted the release of IL–2 and IFN–γ in a dose–dependent manner. The cytokine responses induced by JS207 were comparable to those observed for AK112, toripalimab, and the combination of toripalimab plus VEGF–DotAb (Figures 4G, H). Notably, VEGF–DotAb alone did not induce IL–2 or IFN–γ release relative to the anti–KLH hIgG4 control.

3.14 JS207 induces PD-1 internalization

To investigate PD–1 internalization, two complementary methods were employed: the cell surface residual PD–1 assay and the intracellular fluorescence assay.

Cell Surface Residual PD-1 Method: Human PD–1–expressing H293 cells were incubated at 4°C with 30 nM of JS207, AK112, or toripalimab for 30 minutes in the presence or absence of VEGFA (60 nM). After washing to remove unbound antibodies, cells were stained with PE–labeled anti–PD–1 human IgG to quantify the residual cell surface–bound PD–1. In the absence of VEGFA, approximately 16–20% of surface PD–1 was internalized within 30 minutes, increasing to 21–32% after 60–240 minutes of incubation for all three antibodies. However, in the presence of VEGFA, JS207– and AK112–treated cells exhibited a marked increase in PD-1 internalization, reaching 46–50% within 30 minutes and up to 65% after 4 hours, while toripalimab was unaffected (Figures 5A–C).

Intracellular Fluorescence Method: JS207, AK112, toripalimab, and JS501 (an anti–VEGFA mAb) were conjugated with CypHer5E, a pH–sensitive cyanine dye that exhibits enhanced fluorescence in

acidic intracellular compartments. Jurkat/PD−1 cells were incubated with serial dilutions of these CypHer5E−conjugated antibodies at 37° C for 4 hours. At the end of incubation, a noncompetitive anti−PD−1 antibody (MIH4 PD−1−PE) was added to measure the remaining cell surface PD−1. As shown in Figures 5D–F, the intracellular fluorescence intensity of CypHer5E−labeled JS207 and AK112 increased in a dose−dependent manner, while the cell surface PD −1 signal detected by MIH4 PD−1−PE concomitantly decreased, providing further evidence of PD−1 internalization. In the presence of VEGFA, both fluorescence intensity and PD−1 internalization were further enhanced for JS207 and AK112. In contrast, toripalimab−induced internalization was not affected by VEGFA (Figure 5F). Only minimal internalization was observed when cells were incubated at 4°C (Figure 5G).

In the absence of VEGFA, JS207 and toripalimab exhibited comparable internalization activities with EC_{50} values of 62.3 ng/mL (0.35 nM) and 58.4 ng/mL (0.39 nM), respectively, both of which were more potent than AK112 (EC_{50} = 322.7 ng/mL, or 1.61 nM). To assess the impact of varying VEGFA concentrations on PD−1 internalization, a PD−1 RGA was performed using a fixed concentration of JS207 (25 nM) and AK112 (25 nM). As shown in Figure 5I, when VEGFA concentrations were low (0.017–1.37 nM), JS207 exhibited higher anti-PD−1 potency than AK112. However, at high VEGFA concentrations (111.1 nM and 333.3 nM), both antibodies demonstrated comparable anti-PD−1 potencies, with EC_{50} values of 11.52 nM for JS207 and 11.62 nM for AK112 (Figure 5I).

3.15 Thermal stability assessment

The thermal stability is an important factor to be considered during antibody CMC manufacturing and storage. In general, due to multiple domain composition, BsAbs tend to have lower thermal stability compared to conventional monoclonal antibodies that add additional challenge during BsAb development (34, 35). The thermal stability of JS207 was evaluated using two potency assays: anti−PD−1 RGA and anti−VEGFA RGA.

At 40°C, neither JS207 nor AK112 exhibited significant changes in anti−PD−1 potency after 24, 48, or 96 hours of heat stress (Figures 6A, B). Similarly, at 40°C, no significant changes in anti −VEGFA potency were observed for JS207 and AK112 after 1, 4, and 6 days of incubation (Figures 6E, F). Under extended periods of high temperature (50°C, up to 6 days), JS207 showed a time-dependent increase in IC50 values (potency decrease) but retained an unchanged S/N ratio for anti-VEGFA potency (Figure 6G). Under the same stress condition (50°C, up to 6 days), AK112 exhibited

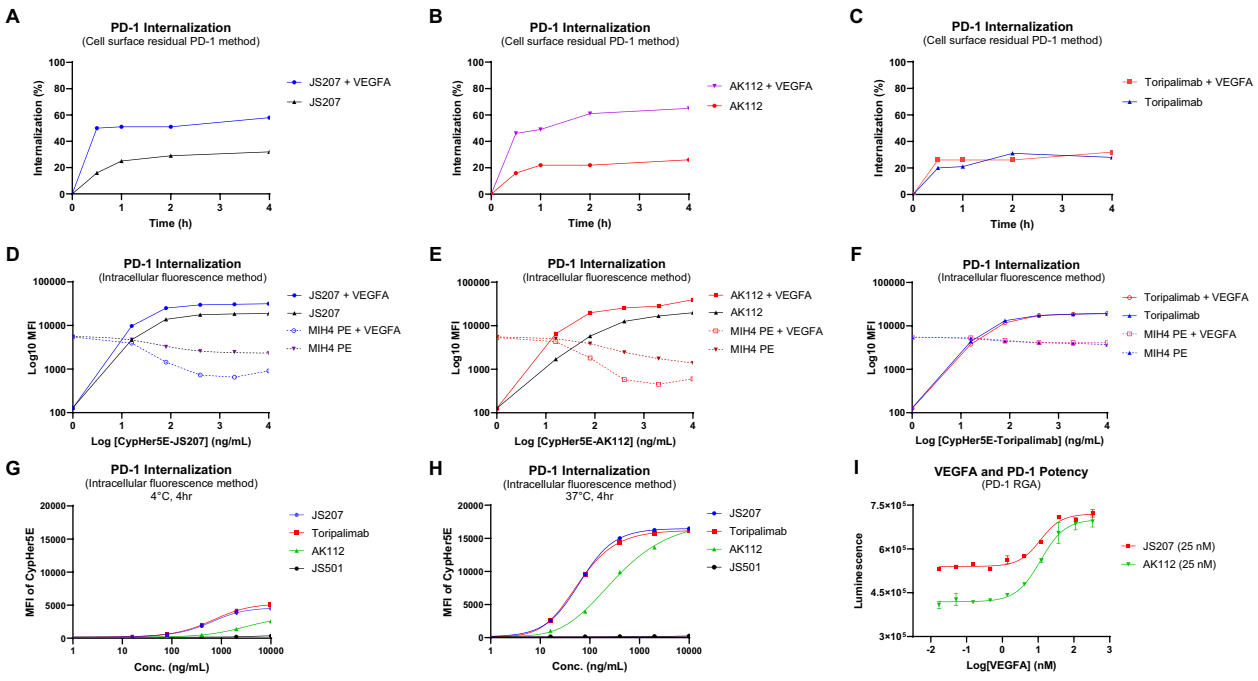

FIGURE 5
PD-1 internalization assessment using the cell surface residual PD-1 method in PD-1 expressing H293 cells **(A-C)** and the intracellular fluorescence method in Jurkat/PD-1 cells **(D-H)**. **(A)** VEGFA enhanced PD-1 internalization induced by JS207. **(B)** VEGFA enhanced PD-1 internalization induced by AK112. **(C)** VEGFA did not impact PD-1 internalization induced by toripalimab. **(D)** VEGFA enhanced JS207-induced PD-1 internalization with increased intracellular fluorescence and decreased cell surface PD-1 signal. **(E)** VEGFA enhanced AK112-induced PD-1 internalization with increased intracellular fluorescence and decreased cell surface PD-1 signal. **(F)** VEGFA did not impact PD-1 internalization induced by toripalimab. **(G)** Minimal PD-1 internalization was seen in cells incubated at 4°C. **(H)** JS207 and toripalimab showed comparable PD-1 internalizations, which are stronger than AK112. **(I)** VEGFA concentration-dependently enhanced anti-PD-1 potency of JS207 and AK112. The concentration of JS207 and AK112 used in this study was 25 nM.

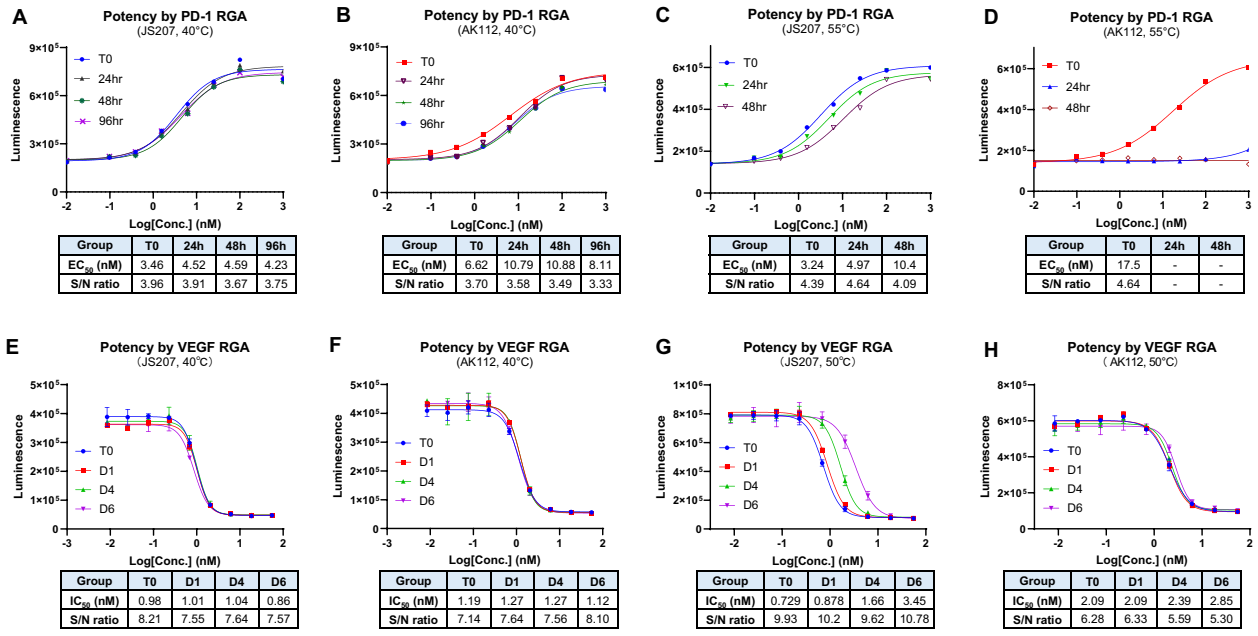

FIGURE 6
Thermal stability assessment for JS207 using PD-1 RGA and VEGFA RGA. **(A)** Anti-PD-1 potency of JS207 after 40°C stress for 24, 48 and 96 hr. **(B)** Anti-PD-1 potency of AK112 after 40°C stress for 24, 48 and 96 hr. **(C)** Anti-PD-1 potency of JS207 after 55°C stress for 24 and 48 hr. **(D)** Anti-PD-1 potency of AK112 after 55°C stress for 24 and 48 hr. **(E)** Anti-VEGFA potency of JS207 after 40°C stress for 1, 4 and 6 days. **(F)** Anti-VEGFA potency of AK112 after 40°C stress for 1, 4 and 6 days. **(G)** Anti-VEGFA potency of JS207 after 50°C stress for 1, 4 and 6 days. **(H)** Anti-VEGFA potency of AK112 after 50°C stress for 1, 4 and 6 days.

increases in IC50 values (potency decrease) and a decrease in the S/N ratio for anti-VEGFA potency (Figure 6H).

At 55°C, AK112 lost nearly all anti-PD–1 activity by 24 hours and completely lost anti-PD-1 activity by 48 hours. In contrast, JS207 maintained relatively strong anti–PD–1 activity, retaining 65% potency at 24 hours and 31% at 48 hours compared to time 0. Furthermore, even after 4 hours at 65°C, JS207 retained 15.5% anti-PD-1 activity while AK112 had no activity at all (Supplementary Figure S2 in Supplementary Data Sheet). These results demonstrate that JS207 possesses enhanced thermal stability in anti-PD-1 potency. These results support previous finding that Fab format (anti-PD-1 domain of JS207) is more stable than scFv format (anti-PD-1 domain of AK112) (36).

3.16 Anti-tumor efficacy in mouse MC38 tumor model in B-hPD-1 humanized mice

To evaluate the *in vivo* anti–tumor activity of JS207, mouse colon cancer MC38 cells were subcutaneously implanted into C57BL/6-Pdcd1$^{tm1(PDCD1)Bcgen}$/Bcgen humanized mice (abbreviated as B-hPD-1 mice). As shown in Figures 7A, C, JS207 significantly inhibited tumor growth in a dose–dependent manner when administered at 0.75, 1.5, and 4.5 mg/kg, achieving tumor growth inhibition (TGI) rates of 76.1%, 78.0%, and 84.4%, respectively, at day 20 post–treatment. At equivalent molar doses, JS207 (0.75 mg/kg) exhibited superior anti–tumor activity compared to toripalimab monotherapy (0.6 mg/kg) or toripalimab plus VEGF–DotAb combination therapy (0.6 mg/kg + 0.33 mg/kg). Notably, none of the treatment groups showed significant body weight loss or other overt side effects, indicating that JS207 was well tolerated (Figure 7E).

3.17 Anti-tumor efficacy in malignant melanoma A375 model in NDG mice

The anti–tumor efficacy of JS207 was further examined in a human malignant melanoma A375 model using human PBMC transplanted NDG mice. In the saline–treated group, the mean tumor volume reached 585 ± 83 mm^3 at day 21. In contrast, mice treated with JS207 at doses of 1, 3, and 10 mg/kg exhibited mean tumor volumes of 362 ± 38 mm^3, 344 ± 32 mm^3, and 262 ± 25 mm^3, corresponding to TGI rates of 49.6%, 53.7%, and 72.0%, respectively (Figures 7B, D). Additionally, mice treated with AK112 at 11.1 mg/kg displayed a mean tumor volume of 349 ± 62 mm^3 with a TGI of 52.7%. At equivalent molar doses (AK112 at 11.1 mg/kg versus JS207 at 10 mg/kg), JS207 demonstrated superior anti–tumor efficacy compared with AK112. Importantly, the body weights of animals in the treatment groups did not significantly differ from those in the saline group, underscoring the favorable tolerability of both JS207 and AK112 (Figure 7F).

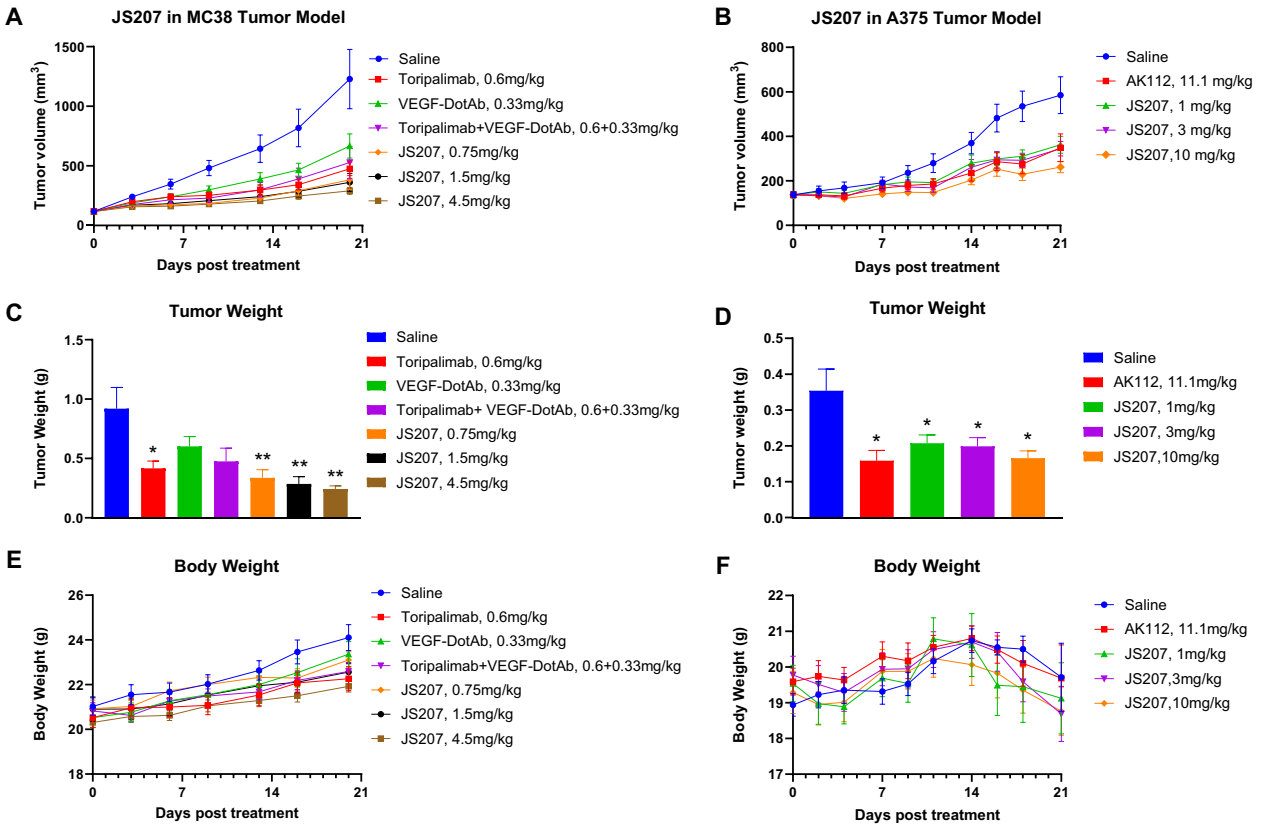

FIGURE 7
Anti–tumor efficacy of JS207 in the MC38 mouse colon cancer model in C57BL/6-Pdcd1$^{tm1(PDCD1)Bcgen}$/^{Bcgen} mice (B–hPD–1 humanized mice) and the A375 malignant melanoma model in NDG mice. **(A)** Tumor growth curves for MC38 hPD–1 tumors treated with JS207, toripalimab, and toripalimab plus VEGF–DotAb. **(B)** Tumor growth curves for A375 hPD–1 tumors in mice treated with JS207 and AK112. **(C)** Significant decrease in MC38 tumor weight in animals treated with JS207, toripalimab, and toripalimab plus VEGF–DotAb (mean ± SEM, n = 8; *p < 0.05, **p < 0.01 vs Saline). **(D)** Significant reduction in A375 tumor weight in animals treated with JS207 and AK112 (mean ± SEM, n = 8; *p < 0.05 vs Saline). **(E)** Average body weight of animals in the MC38 tumor model. **(F)** Average body weight of animals in the A375 tumor model.

4 Discussion

The combination of PD-(L)1 and VEGF inhibition has exhibited considerable potential in amplifying antitumor responses. Nevertheless, the co-administration of monoclonal antibodies poses several challenges, including intricate dosing schedules, distinct pharmacokinetics, and increased toxicity risks. Bispecific antibodies (BsAbs) provide a streamlined solution by facilitating dual targeting within a single molecular construct. Interestingly, investigations into HB0025 (anti-PD-L1/VEGFR1 BsAb), CVL006 (anti-PD-L1/VEGFA BsAb) and AK112 (anti-PD-1/VEGFA BsAb) have demonstrated promising preclinical and clinical efficacy, further underscoring the feasibility and potential of this innovative therapeutic approach (31, 33, 37, 38). As summarized in Table 1, these BsAbs, whether in an anti-PD-L1/VEGFA format or an anti-PD-1/VEGFA format, can enhance T cell activation and *in vivo* antitumor activity, regardless of the Fc region configuration, whether IgG4, or IgG1 with or without ADCC (antibody-dependent cellular cytotoxicity). This study introduces JS207, a novel BsAb targeting PD-1 and VEGFA, engineered to overcome resistance mechanisms in cancer therapy by concurrently inhibiting immunosuppressive and angiogenic pathways. JS207 demonstrated high-affinity binding to human PD-1 (K_D = 4.60×10^{-10} M) and potent inhibition of VEGFA activity (IC_{50} = 0.773 nM), effectively blocking both PD-1/PD-L1 and VEGFA/VEGFR2 interactions. Notably, JS207 exhibited an 11-fold higher PD-1 binding affinity compared to AK112 (K_D = 5.05×10^{-9} M) while maintaining comparable VEGFA binding activity. JS207 could bind to human PD-1 either by itself or as JS207/VEGFA complex. Furthermore, JS207 could simultaneously bind to human PD-1 and VEGFA (Figure 3). Mechanistically, JS207 induced robust PD-1 internalization, a process augmented by VEGFA, and sustained T-cell activation. In preclinical models, JS207 achieved remarkable anti-tumor efficacy, with tumor growth inhibition (TGI) rates of 84.4% in the MC38 colon cancer model and 72.0% in the A375 melanoma model at 10 mg/kg, outperforming AK112 at equivalent molar doses (11.1 mg/kg). Collectively, these findings underscore JS207's dual mechanism of action and its promise as a next-generation therapeutic agent in cancer immunotherapy.

The TME and aberrant angiogenic signaling represent major hurdles to achieving durable responses with current cancer immunotherapies (39). Although ICIs such as PD-1 blockers (e.g.,

TABLE 1 Comparison of JS207, AK112, HB0025 and CVL006.

BsAb	Structural Format	Binding Affinities	Biological Activities
JS207	• PD-1/VEGFA BsAb • IgG4 • M.W. = 180 kDa	• High affinity for PD-1 and VEGFA • KD values by SPR assay [a]: ■ PD-1 = 4.60E-10 M ■ VEGFA = 9.00E-12 M	• Enhances T-cell activation, cytokine release, and PD-1 internalization • Blocks VEGF-induced HUVEC proliferation • Enhances in vivo anti-tumor activities
AK112	• PD-1/VEGFA BsAb • IgG1, ADCC silenced • M.W. = 200 kDa	• High affinity for PD-1 and VEGFA • KD values by SPR assay [a]: ■ PD-1 = 5.05E-09 M ■ VEGFA = <2.59E-11 M	• Enhances T-cell activation, PD-1 internalization and inhibits tumor angiogenesis • Enhances in vivo anti-tumor activities
HB0025	• Fusion protein-based PD-L1/VEGFR1 BsAb • IgG4 • M.W.= 171 kDa	• High affinity for PD-L1 and VEGFR1 • KD values by SPR assay [b]: ■ PD-L1 = 1.76E-9 M ■ VEGFA = 4.72E-12 M	• Enhances T-cell activation • Blocks VEGF-induced HUVEC proliferation and migration • Enhances in vivo anti-tumor activities
CVL006	• PD-L1/VEGFA BsAb • IgG1, ADCC active • M.W. = 150 – 200 kDa [d]	• High affinity for PD-L1 and VEGFA • KD values by SPR assay [c]: ■ PD-L1 = 1.55E-10 M ■ VEGFA = 1.50E-11 M	• Enhances T-cell activation • Blocks VEGF-induced HUVEC proliferation • Enhances in vivo anti-tumor activities

[a] Results of current study; [b] Data from Cui et al., 2021 (Reference 36); [c] Data from Wang et al., 2024 (Reference 37); [d] the exact molecular weight is not publicly available.

pembrolizumab) and anti-VEGFA agents (e.g., bevacizumab) have revolutionized cancer treatment, their efficacy is often compromised by resistance mechanisms, including compensatory angiogenic pathways and immune evasion (2, 40). Several studies using patient-derived xenografts and tumor tissue analyses indicate that tumors with elevated VEGFA levels foster a microenvironment rich in PD-1–positive immune cells. For example, Voron et al. demonstrated that VEGFA modulates inhibitory checkpoint expression on $CD8^+$ T cells, thereby providing a mechanistic basis for combining anti-angiogenic therapy with immune checkpoint blockade (41). Huang et al. showed that anti-angiogenic treatment normalizes tumor vasculature and reprograms the TME to enhance immune cell infiltration (42). Allen et al. reported that pairing antiangiogenic with anti-PD-L1 therapies synergistically stimulates tumor immunity through complementary mechanisms (43). These findings underscore the translational relevance of our work, suggesting that anti-PD-1/VEGFA BsAbs could potentially generate a more effective antitumor response. Moreover, preclinical and clinical evidence supports the rationale for combining PD-1 and VEGFA blockade, as VEGFA not only drives angiogenesis but also impairs dendritic cell maturation and cytotoxic T-cell activity (25, 41). It has been shown that dual PD-1 and VEGFR-2 blockade promotes vascular normalization and enhances anti-tumor immune responses in murine hepatocellular carcinoma models (23). Clinical studies using combinations such as bevacizumab (anti-VEGFA) with atezolizumab (anti-PD-L1) have validated this approach, although challenges related to discordant pharmacokinetics and overlapping toxicities remain (24).

JS207's efficacy arises from its ability to engage PD-1 and VEGFA, disrupting two critical TME pathways. Interestingly, our results revealed that exogenous VEGFA enhanced JS207's cell-based binding (Figure 4F) and anti-PD-1 activity (Figures 4D, E). Several mechanisms may contribute to this phenomenon: (i) Target Upregulation: VEGFA may upregulate PD-1 expression on target cells, amplifying the impact of dual blockade (21). (ii) Avidity Effects: VEGFA binding could stabilize JS207 near PD-1-expressing cells, increasing local antibody concentration and blockade efficiency (44). (iii) Feedback Modulation: Neutralizing VEGFA may reduce immunosuppressive PD-L1 expression, indirectly enhancing PD-1 blockade (45), (iv) Receptor Clustering: Dual binding may facilitate PD-1 cross-linking and sustaining T-cell activation (37), (vi) Enhanced PD-1 Internalization: JS207 achieved 65% PD-1 internalization in the presence of VEGFA (vs. 32% without) (Figures 5A–I), and (vii) Synergistic Pathway Inhibition: Concurrent PD-1/VEGFA blockade elevated IL-2 and IFN-γ secretion in mixed lymphocyte reactions, mirroring effects seen with toripalimab + VEGF-DotAb combination therapy (Figures 4G, H).

While BsAbs offer a versatile platform, selecting the optimal BsAb format is critical because its structural design directly impacts efficacy, safety, and CMC manufacturability by influencing production complexity, yield, and scalability. While scFv is widely used in BsAb development (e.g., IgG-scFv) due to its versatility and compact structure, VHH format (e.g., IgG-VHH) could serve as a good alternative because of its superior chemical and physical properties such as smaller size, higher solubility and lower production cost (46). Previous studies have shown that VHH antibodies have better stability compared to scFv antibodies due to the structural differences in domain composition, hydrophobic interactions, disulfide bonds and evolutionary adaptation (36, 47, 48). Our findings demonstrated that anti-PD-1/VEGFA BsAb in an IgG-VHH form like JS207 could simultaneously block PD-1 and VEGFA with high affinity and biological activities while maintaining good thermal stability. In terms of anti-PD-1 activity, JS207 was extremely stable under heat tress retaining good activity after 48 hours at 55°C (Figure 6C) and measurable activity after 4 hours at 65°C (Supplementary Figure S2). For anti-VEGFA activity, JS207 also showed good heat resistance for extended periods. After

6 days of heat stress, there was no change in its anti-VEGFA potency at 40°C and retained measurable activity at 50°C (Figures 6E, G). Thus, JS207 demonstrates an excellent heat stability profile, a critical factor for CMC manufacture, storage and drug shelf life.

The rationale for using NDG mice in the A375 model and B-hPD-1 mice in the MC38 model for JS207 efficacy studies is based on their distinct immunological characteristics. NDG mice are highly immunocompromised, allowing human tumor cell lines such as A375 melanoma to engraft and proliferate without immune rejection. This model helps isolate the effects of the anti-VEGF/PD-1 bispecific antibody on tumor vascularization and growth while eliminating the confounding influence of an active adaptive immune response. In contrast, B-hPD-1 mice carry a human PD-1 gene and support syngeneic MC38 tumors within a fully functional immune system. This setup more accurately mimics the human TME, enabling the evaluation of immune checkpoint inhibition effects on T cell activation, cytokine secretion, and overall antitumor activity. While NDG mice cannot model immune-mediated responses due to their lack of adaptive immunity, B-hPD-1 mice provide a more physiologically relevant immune setting—though many aspects of their biology remain murine. JS207's preclinical profile positions it as a promising candidate for clinical translation. Delivering dual targeting in a single agent could mitigate toxicity and dosing complexities inherent to combination therapies (28). Key implications include (i) Potency at Lower Doses: JS207 achieved significant TGI at 0.75 mg/kg in the MC38 model, outperforming toripalimab monotherapy (Figure 7A); (ii) Broad Applicability: Cross-reactivity with cynomolgus PD-1/VEGFA supports non-human primate toxicology studies; and (iii) Enhanced Stability simplifies storage and distribution requirements (49). These attributes could address unmet needs in oncology, particularly for tumors with high PD-L1/VEGF co-expression or resistance to single-agent immunotherapies (50).

While this study establishes JS207's therapeutic potential, several limitations warrant attention, such as, (i) Model Constraints: The use of immunocompromised NDG mice limits assessment of adaptive immunity; humanized models with intact immune systems are warranted (51); (ii) Mechanistic Clarity: The structural basis for VEGFA-enhanced PD-1 internalization remains unclear, necessitating crystallography or cryo-EM studies (52). One hypothesis is that VEGFA directly interacts with PD-1 or associated adaptor proteins, triggering conformational changes that promote receptor internalization. Structural studies, such as cryogenic electron microscopy (cryo-EM) and co-crystallization, could elucidate whether VEGFA binds directly to PD-1 or alters the surrounding membrane microenvironment. These methods might reveal specific binding interfaces, conformational shifts, or protein-lipid interactions that facilitate internalization. Future directions include mutagenesis experiments based on structural data to validate these mechanisms, paving the way for targeted therapies that modulate immune checkpoint recycling and optimize the antitumor immune response; and (iii) Biomarker Validation: PD-L1/VEGF co-expression levels should be evaluated as predictive biomarkers in clinical trials (53). Given these encouraging preclinical findings, JS207 is advancing into clinical development to assess safety, pharmacokinetics, and efficacy in cancer patients. Future studies exploring combinations with chemotherapy or immunomodulators (e.g., CTLA-4, BTLA inhibitors) could further enhance therapeutic outcomes (12, 54, 55).

In conclusion, JS207 represents a significant advancement in bispecific antibody therapeutics by integrating potent PD-1 and VEGFA blockade into a single and stable molecule with high affinity for target antigens. Its ability to enhance PD-1 internalization, synergistically inhibit immunosuppressive/angiogenic pathways, and achieve robust anti-tumor efficacy in preclinical models underscores its therapeutic potential. By addressing limitations of existing therapies, such as resistance mechanisms, pharmacokinetic discordance, and formulation instability, JS207 offers a promising strategy for improving outcomes in advanced cancers. Clinical validation is now imperative to translate these preclinical advantages into patient benefits. Given the well-documented toxicity concerns associated with anti-VEGF and anti-PD-(L)1 combination therapy, dual-targeting VEGF/PD-(L)1 BsAb may pose potential immune, vascular, and inflammatory risks. Therefore, careful monitoring, optimized dosing strategies, and rigorous clinical validation are essential to ensuring their safe and effective therapeutic application.

Data availability statement

The original contributions presented in the study are included in the article/Supplementary Material. Further inquiries can be directed to the corresponding authors.

Ethics statement

The animal study was approved by the local Institutional Animal Care and Use Committee (IACUC) under permit number YTSYDWIACUC202401, Suzhou Junmeng Biopharmaceuticals. The study was conducted in accordance with the local legislation and institutional requirements.

Author contributions

SL: Writing – review & editing, Formal Analysis, Conceptualization, Methodology, Writing – original draft, Data curation, Investigation, Visualization. MH: Methodology, Formal Analysis, Data curation, Conceptualization, Writing – original draft, Visualization, Investigation, Writing – review & editing. JZ: Formal Analysis, Writing – original draft, Data curation, Visualization, Methodology, Conceptualization, Investigation, Writing – review & editing. WZ: Methodology, Formal Analysis, Data curation, Visualization, Writing – review & editing. KL: Formal Analysis, Methodology, Visualization, Writing – review & editing, Data curation. CW: Visualization, Formal Analysis, Data curation, Methodology, Writing – review & editing. QY: Formal Analysis,

Writing – review & editing, Methodology, Data curation, Visualization. YX: Writing – review & editing, Formal Analysis, Methodology, Data curation, Visualization. LH: Data curation, Methodology, Writing – review & editing, Formal Analysis. JW: Visualization, Methodology, Data curation, Writing – review & editing, Formal Analysis. AJ: Data curation, Methodology, Writing – review & editing, Visualization, Formal Analysis. XW: Writing – review & editing, Formal Analysis, Methodology, Data curation. SY: Resources, Conceptualization, Project administration, Investigation, Writing – review & editing, Formal Analysis, Supervision.

Funding

The author(s) declare that financial support was received for the research and/or publication of this article. This study is founded by TopAlliance Biosciences and Suzhou Junmeng Biosciences. The funders were not involved in the study design, collection, analysis, interpretation of data, the writing of this article or the decision to submit it for publication.

Acknowledgments

We thank Yuming Zhao and Kefan Han for technical support. The authors would like to thank colleagues in TopAlliance Biosciences Inc. and Suzhou Union Biopharm Co., Ltd.

Conflict of interest

All authors are or were employees of TopAlliance Biosciences Inc. or Suzhou Union Biopharm Co., Ltd., at the time this work was performed.

Generative AI statement

The author(s) declare that no Generative AI was used in the creation of this manuscript.

Publisher's note

Supplementary material

The Supplementary Material for this article can be found online at: https://www.frontiersin.org/articles/10.3389/fimmu.2025.1612547/full#supplementary-material

References

1. Sharma P, Allison JP. Immune checkpoint targeting in cancer therapy: toward combination strategies with curative potential. *Cell*. (2015) 161:205–14. doi: 10.1016/j.cell.2015.03.030

2. Topalian SL, Drake CG, Pardoll DM. Immune checkpoint blockade: A common denominator approach to cancer therapy. *Cancer Cell*. (2015) 27:450–61. doi: 10.1016/j.ccell.2015.03.001

3. Alsaafeen BH, Ali BR, Elkord E. Resistance mechanisms to immune checkpoint inhibitors: updated insights. *Mol Cancer*. (2025) 24:20. doi: 10.1186/s12943-024-02212-7

4. Karasarides M, Cogdill AP, Robbins PB, Bowden M, Burton EM, Butterfield LH, et al. Hallmarks of resistance to immune-checkpoint inhibitors. *Cancer Immunol Res*. (2022) 10:372–83. doi: 10.1158/2326-6066.CIR-20-0586

5. Chen DS, Mellman I. Elements of cancer immunity and the cancer–immune set point. *Nature*. (2017) 541:321–30. doi: 10.1038/nature21349

6. Chen DS, Mellman I. Oncology meets immunology: the cancer-immunity cycle. *Immunity*. (2013) 39:1–10. doi: 10.1016/j.immuni.2013.07.012

7. Ferrara N. VEGF and the quest for tumour angiogenesis factors. *Nat Rev Cancer*. (2002) 2:795–803. doi: 10.1038/nrc909

8. Hicklin DJ, Ellis LM. Role of the vascular endothelial growth factor pathway in tumor growth and angiogenesis. *JCO*. (2005) 23:1011–27. doi: 10.1200/JCO.2005.06.081

9. Olsson A-K, Dimberg A, Kreuger J, Claesson-Welsh L. VEGF receptor signalling ? in control of vascular function. *Nat Rev Mol Cell Biol*. (2006) 7:359–71. doi: 10.1038/nrm1911

10. Ferrara N, Hillan KJ, Gerber H-P, Novotny W. Discovery and development of bevacizumab, an anti-VEGF antibody for treating cancer. *Nat Rev Drug Discov*. (2004) 3:391–400. doi: 10.1038/nrd1381

11. Carmeliet P, Jain RK. Angiogenesis in cancer and other diseases. *Nature*. (2000) 407:249–57. doi: 10.1038/35025220

12. Ribas A, Wolchok JD. Cancer immunotherapy using checkpoint blockade. *Science*. (2018) 359:1350–5. doi: 10.1126/science.aar4060

13. Bergers G, Hanahan D. Modes of resistance to anti-angiogenic therapy. *Nat Rev Cancer*. (2008) 8:592–603. doi: 10.1038/nrc2442

14. Marusyk A, Almendro V, Polyak K. Intra-tumour heterogeneity: a looking glass for cancer? *Nat Rev Cancer*. (2012) 12:323–34. doi: 10.1038/nrc3261

15. Postow MA, Sidlow R, Hellmann MD. Immune-related adverse events associated with immune checkpoint blockade. *N Engl J Med*. (2018) 378:158–68. doi: 10.1056/NEJMra1703481

16. Hegde PS, Chen DS. Top 10 challenges in cancer immunotherapy. *Immunity*. (2020) 52:17–35. doi: 10.1016/j.immuni.2019.12.011

17. Hack SP, Zhu AX, Wang Y. Augmenting anticancer immunity through combined targeting of angiogenic and PD-1/PD-L1 pathways: challenges and opportunities. *Front Immunol*. (2020) 11:598877. doi: 10.3389/fimmu.2020.598877

18. Holder AM, Dedeilia A, Sierra-Davidson K, Cohen S, Liu D, Parikh A, et al. Defining clinically useful biomarkers of immune checkpoint inhibitors in solid tumours. *Nat Rev Cancer*. (2024) 24:498–512. doi: 10.1038/s41568-024-00705-7

19. Li T, Niu M, Zhou J, Wu K, Yi M. The enhanced antitumor activity of bispecific antibody targeting PD-1/PD-L1 signaling. *Cell Commun Signal*. (2024) 22:179. doi: 10.1186/s12964-024-01562-5

20. Finley SD, Popel AS. Effect of tumor microenvironment on tumor VEGF during anti-VEGF treatment: systems biology predictions. *JNCI: J Natl Cancer Institute*. (2013) 105:802–11. doi: 10.1093/jnci/djt093

21. Kang Y, Li H, Liu Y, Li Z. Regulation of VEGF-A expression and VEGF-A-targeted therapy in Malignant tumors. *J Cancer Res Clin Oncol*. (2024) 150:221. doi: 10.1007/s00432-024-05714-5

22. Li Y, Amaladas N, O'Mahony M, Manro JR, Inigo I, Li Q, et al. Treatment with a VEGFR-2 antibody results in intra-tumor immune modulation and enhances anti-tumor efficacy of PD-L1 blockade in syngeneic murine tumor models. *PLoS ONE* (2022) 17(7):e0268244. doi: 10.1371/journal.pone.0268244

23. Shigeta K, Datta M, Hato T, Kitahara S, Chen IX, Matsui A, et al. Dual programmed death receptor-1 and vascular endothelial growth factor receptor-2

blockade promotes vascular normalization and enhances antitumor immune responses in hepatocellular carcinoma. *Hepatology*. (2020) 71:1247–61. doi: 10.1002/hep.30889

24. Socinski MA, Jotte RM, Cappuzzo F, Orlandi F, Stroyakovskiy D, Nogami N, et al. Atezolizumab for first-line treatment of metastatic nonsquamous NSCLC. *N Engl J Med*. (2018) 378:2288–301. doi: 10.1056/NEJMoa1716948

25. Finn RS, Qin S, Ikeda M, Galle PR, Ducreux M, Kim T-Y, et al. Atezolizumab plus bevacizumab in unresectable hepatocellular carcinoma. *N Engl J Med*. (2020) 382:1894–905. doi: 10.1056/NEJMoa1915745

26. Jain RK. Normalizing tumor vasculature with anti-angiogenic therapy: A new paradigm for combination therapy. *Nat Med*. (2001) 7:987–9. doi: 10.1038/nm0901-987

27. Bai S, Tian T, Pacheco JM, Tachihara M, Hu P, Zhang J. Immune-related adverse event profile of combination treatment of PD-(L)1 checkpoint inhibitors and bevacizumab in non-small cell lung cancer patients: data from the FDA adverse event reporting system. *Transl Lung Cancer Res*. (2021) 10:2614–24. doi: 10.21037/tlcr-21-464

28. Labrijn AF, Janmaat ML, Reichert JM, Parren PWHI. Bispecific antibodies: a mechanistic review of the pipeline. *Nat Rev Drug Discov*. (2019) 18:585–608. doi: 10.1038/s41573-019-0028-1

29. Spiess C, Zhai Q, Carter PJ. Alternative molecular formats and therapeutic applications for bispecific antibodies. *Mol Immunol*. (2015) 67:95–106. doi: 10.1016/j.molimm.2015.01.003

30. Dhillon S. Ivonescimab: first approval. *Drugs*. (2024) 84:1135–42. doi: 10.1007/s40265-024-02073-w

31. Zhao Y, Chen G, Chen J, Zhuang L, Du Y, Yu Q, et al. AK112, a novel PD-1/VEGF bispecific antibody, in combination with chemotherapy in patients with advanced non-small cell lung cancer (NSCLC): an open-label, multicenter, phase II trial. *eClinicalMedicine*. (2023) 62:102106. doi: 10.1016/j.eclinm.2023.102106

32. Wang F, Wei X, Zheng Y, Wang J, Ying J, Chen X, et al. Safety, pharmacokinetics, and pharmacodynamics evaluation of ivonescimab, a novel bispecific antibody targeting PD -1 and VEGF, in chinese patients with advanced solid tumors. *Cancer Med*. (2025) 14:e70653. doi: 10.1002/cam4.70653

33. Frentzas S, Austria Mislang AR, Lemech C, Nagrial A, Underhill C, Wang W, et al. Phase 1a dose escalation study of ivonescimab (AK112/SMT112), an anti-PD-1/VEGF-A bispecific antibody, in patients with advanced solid tumors. *J Immunother Cancer*. (2024) 12:e008037. doi: 10.1136/jitc-2023-008037

34. Ingavat N, Dzulkiflie N, Liew JM, Wang X, Leong E, Loh HP, et al. Investigation on environmental factors contributing to bispecific antibody stability and the reversal of self-associated aggregates. *Bioresour Bioprocess*. (2024) 11:82. doi: 10.1186/s40643-024-00796-y

35. Grunert I, Heinrich K, Ernst J, Hingar M, Briguet A, Leiss M, et al. Detailed analytical characterization of a bispecific igG1 crossMab antibody of the knob-into-hole format applying various stress conditions revealed pronounced stability. *ACS Omega*. (2022) 7:3671–9. doi: 10.1021/acsomega.1c06305

36. Miller BR, Demarest SJ, Lugovskoy A, Huang F, Wu X, Snyder WB, et al. Stability engineering of scFvs for the development of bispecific and multivalent antibodies. *Protein Engineering Design Selection*. (2010) 23:549–57. doi: 10.1093/protein/gzq028

37. Cui X, Jia H, Xin H, Zhang L, Chen S, Xia S, et al. A novel bispecific antibody targeting PD-L1 and VEGF with combined anti-tumor activities. *Front Immunol*. (2021) 12:778978. doi: 10.3389/fimmu.2021.778978

38. Wang C, Huang H, Song Z, Li Z, Huang J, Cao L, et al. A novel bispecific antibody CVL006 superior to AK112 for dual targeting of PD-L1 and VEGF in cancer therapy. *Antib Ther*. (2024) tbaf012. doi: 10.1093/abt/tbaf012

39. Sharma P, Allison JP. The future of immune checkpoint therapy. *Science*. (2015) 348:56–61. doi: 10.1126/science.aaa8172

40. Gabrilovich DI, Nagaraj S. Myeloid-derived suppressor cells as regulators of the immune system. *Nat Rev Immunol*. (2009) 9:162–74. doi: 10.1038/nri2506

41. Voron T, Colussi O, Marcheteau E, Pernot S, Nizard M, Pointet A-L, et al. VEGF-A modulates expression of inhibitory checkpoints on CD8+ T cells in tumors. *J Exp Med*. (2015) 212:139–48. doi: 10.1084/jem.20140559

42. Huang Y, Yuan J, Righi E, Kamoun WS, Ancukiewicz M, Nezivar J, et al. Vascular normalizing doses of antiangiogenic treatment reprogram the immunosuppressive tumor microenvironment and enhance immunotherapy. *Proc Natl Acad Sci USA*. (2012) 109:17561–6. doi: 10.1073/pnas.1215397109

43. Allen E, Jabouille A, Rivera LB, Lodewijckx I, Missiaen R, Steri V, et al. Combined antiangiogenic and anti–PD-L1 therapy stimulates tumor immunity through HEV formation. *Sci Transl Med*. (2017) 9:eaak9679. doi: 10.1126/scitranslmed.aak9679

44. Kontermann R. Dual targeting strategies with bispecific antibodies. *mAbs*. (2012) 4:182–97. doi: 10.4161/mabs.4.2.19000

45. Meder L, Schuldt P, Thelen M, Schmitt A, Dietlein F, Klein S, et al. Combined VEGF and PD-L1 blockade displays synergistic treatment effects in an autochthonous mouse model of small cell lung cancer. *Cancer Res*. (2018) 78:4270–81. doi: 10.1158/0008-5472.CAN-17-2176

46. Asaadi Y, Jouneghani FF, Janani S, Rahbarizadeh F. A comprehensive comparison between camelid nanobodies and single chain variable fragments. *biomark Res*. (2021) 9:87. doi: 10.1186/s40364-021-00332-6

47. Wörn A, Plückthun A. Stability engineering of antibody single-chain Fv fragments. *J Mol Biol*. (2001) 305:989–1010. doi: 10.1006/jmbi.2000.4265

48. Ikeuchi E, Kuroda D, Nakakido M, Murakami A, Tsumoto K. Delicate balance among thermal stability, binding affinity, and conformational space explored by single-domain VHH antibodies. *Sci Rep*. (2021) 11:20624. doi: 10.1038/s41598-021-98977-8

49. Jarasch A, Koll H, Regula JT, Bader M, Papadimitriou A, Kettenberger H. Developability assessment during the selection of novel therapeutic antibodies. *J Pharm Sci*. (2015) 104:1885–98. doi: 10.1002/jps.24430

50. Koh YW, Han J-H, Yoon DH, Suh C, Huh J. PD-L1 expression correlates with VEGF and microvessel density in patients with uniformly treated classical Hodgkin lymphoma. *Ann Hematol*. (2017) 96:1883–90. doi: 10.1007/s00277-017-3115-6

51. Chuprin J, Buettner H, Seedhom MO, Greiner DL, Keck JG, Ishikawa F, et al. Humanized mouse models for immuno-oncology research. *Nat Rev Clin Oncol*. (2023) 20:192–206. doi: 10.1038/s41571-022-00721-2

52. Han Z-G, He K, Zheng Y, Qian L. Visualizing the cellular internalization of therapeutic antibodies *via* pH-sensitive release of AIEgen. *Org Biomol Chem*. (2024) 22:4950–7. doi: 10.1039/D4OB00512K

53. Galon J, Bruni D. Approaches to treat immune hot, altered and cold tumours with combination immunotherapies. *Nat Rev Drug Discov*. (2019) 18:197–218. doi: 10.1038/s41573-018-0007-y

54. Andrzejczak A, Karabon L. BTLA biology in cancer: from bench discoveries to clinical potentials. *biomark Res*. (2024) 12:8. doi: 10.1186/s40364-024-00556-2

55. Pardoll DM. The blockade of immune checkpoints in cancer immunotherapy. *Nat Rev Cancer*. (2012) 12:252–64. doi: 10.1038/nrc3239

frontiers | Frontiers in Immunology

TYPE Review
PUBLISHED 23 July 2025
DOI 10.3389/fimmu.2025.1611701

OPEN ACCESS

EDITED BY
Renata Pacholczak-Madej,
Maria Skłodowska-Curie National Institute of Oncology, Poland

REVIEWED BY
Anil Kumar,
City of Hope National Medical Center, United States
Ayça Koca Yozgat,
Yuksek Ihtisas Training and Research Hospital, Türkiye

*CORRESPONDENCE
Aiguo Liu
drliuaiguo@tjh.tjmu.edu.cn
Yifang Cheng
chengyfmedstu@hust.edu.cn

RECEIVED 14 April 2025
ACCEPTED 04 July 2025
PUBLISHED 23 July 2025

CITATION
Cheng Y and Liu A (2025) Blinatumomab in pediatric B-acute lymphoblastic leukemia. *Front. Immunol.* 16:1611701. doi: 10.3389/fimmu.2025.1611701

Blinatumomab in pediatric B-acute lymphoblastic leukemia

Yifang Cheng[1]* and Aiguo Liu[2]*

[1]The Second Clinical School, Tongji Medical College, Huazhong University of Science and Technology, Wuhan, China, [2]Department of Pediatrics, Tongji Hospital, Tongji Medical College, Huazhong University of Science and Technology, Wuhan, China

Blinatumomab, a bispecific T-cell engager, has demonstrated substantial clinical benefits in treating pediatric patients with relapsed or refractory B-cell acute lymphoblastic leukemia (R/R B-ALL). Approved by FDA for several indications, blinatumomab is now integral to therapeutic protocols for specific pediatric cohorts, with real-world applications steadily increasing. As one of the representatives of cutting-edge immunotherapy for pediatric ALL, blinatumomab plays a crucial role in precision medicine against the backdrop of current genetic testing. Clinical efficacy is influenced by factors such as tumor burden, endogenous T-cell function, CD19 antigen loss, and lineage switch. Treatment-related complications, such as cytokine release syndrome (CRS), neurotoxicity (ICANS), and infections, necessitate vigilant monitoring. Administration involves continuous intravenous infusion, with consideration for drug interactions. Despite proven short-term efficacy and tolerability, long-term impacts on pediatric patients warrant further investigation. Current studies refine dosing strategies and combinational approaches to enhance therapeutic precision for pediatric patients. This review synthesizes selected literature related to clinical trials of blinatumomab, emphasizing determinants of clinical efficacy and adverse events associated with treatment.

KEYWORDS

blinatumomab, pediatric B-ALL, immunotherapy, efficacy, toxicity

1 Introduction

Acute lymphoblastic leukemia (ALL) is the most common type of leukemia in children, with precursor B-cell lineage (B-ALL) being the predominant form, accounting for over 75% of all pediatric leukemia (1, 2). As the leading childhood hematologic malignancy, B-ALL is responsible for about one-third of all pediatric cancers. Over the past few decades, the treatment efficacy of pediatric ALL has seen a substantial improvement, largely due to advancements in clinical trials and enhanced supportive care. Survival rates have surged from below 10% in the pre-1970s era to approximately 70% by the 1980s, with current long-term survival exceeding 85% (3–5).

Despite modern therapies achieve cure rates approaching 90%, a subset of pediatric patients continues to encounter challenges such as intrinsic drug resistance or post-remission relapse. For these refractory and relapsed cases, immunotherapy and

hematopoietic stem cell transplantation (HSCT) have become main treatment methods. As a representative of immunotherapy, blinatumomab has demonstrated significant efficacy and safety. Current data indicate that the complete remission (CR) rate for refractory or relapsed patients in children treated with conventional chemotherapy is only 20-30%, with a median overall survival (OS) time of only 2 to 4 months (6). In contrast, the CR rate for R/R ALL treated with blinatumomab monotherapy can reach 43-69%, with a median OS time of 6.1 to 13 months (7), which is significantly better than traditional chemotherapy. The efficacy is better with lower tumor burden, and outcomes are even better for MRD+ patients (7).

Blinatumomab functions as a bispecific T-cell engager (BiTE), targeting tumor cells for destruction by simultaneously blinding to tumor-specific antigens (CD19 antigen on malignant B cells) and patients' own T-cell receptors (typically CD3ε) (8). It not only targets tumor cells but also enhances T-cell activity, modifies the tumor microenvironment to reduce immunosuppression, and improves anti-tumor effects. Since its initial application in 2011 on three pediatric patients, blinatumomab has been found to improve disease remission rates and survival rates, effectively clear minimal residual disease (MRD), and offer higher safety compared to cytotoxic drugs through a series of clinical trials. Currently, the focus of pediatric ALL is on precision medicine. Based on the classification of different subtypes of pediatric ALL through genetic testing methods such as Next-Generation Sequencing (NGS), more targeted therapeutic approaches are then adopted, including blinatumomab. Specifically, in several retrospective assessments, children with R/R ALL have shown treatment response rates to blinatumomab ranging from 34-38% to approximately 60% (9). Up to now, almost all published articles indicate that connecting blinatumomab treatment before or after allo-HSCT will improve the survival rate of pediatric patients (9). Furthermore, for children with poor prognosis who have rare genetic variant subtypes, such as germline TP53 mutations and MYC/BCL2 rearrangements, although there is currently limited reported data, blinatumomab represents another potential option beyond cytotoxic drugs (10). In a report regarding nine pediatric patients with TCF3-HLF positive ALL (11), most children experienced durable remissions after using blinatumomab early in the first consolidation as a bridge to HSCT. This rare subtype of childhood ALL is typically characterized by a high rate of treatment failure.

Notably, since its approval by the US Food and Drug Administration (FDA) for the treatment of pediatric ALL, blinatumomab progressively extended its clinical utility. Its favorable efficacy and relative manageable toxicity profile have reshaped treatment paradigms, offering new hope for pediatric patients with R/R ALL (12).

2 Clinical adaptations

2.1 Official approvals

Blinatumomab (blincyto®) has achieved sequential regulatory milestones since its first accelerated approval in 2014 by the US Food and Drug Administration (FDA) for adult and pediatric (≧1month old) patients with relapsed or refractory CD19+ B-cell precursor acute lymphoblastic leukemia (ALL). Subsequent expansion of its indications include:

2018 Authorization: Approval extended to adult and pediatric (≧1month old) patients with CD19+ B-ALL in first or second complete remission exhibiting minimal residual disease (MRD) greater than or equal to 0.1%.

2024 Update: FDA clearance for incorporation into consolidation therapy protocols targeting adult and pediatric (≧1month old) patients with Philadelphia chromosome-negative CD19+ B-ALL during multiphase chemotherapy.

2.2 Clinical recommendations

Based on the research and real-world data of blinatumomab in pediatric patients, guidelines from different countries have made relevant recommendations for the application of blinatumomab in pediatric B-ALL.

The 2025, 2nd edition NCCN Guidelines (13) suggest that for newly diagnosed Ph-negative children who achieve a complete response (CR) with minimal residual disease (MRD) positivity after induction therapy, blinatumomab treatment can be recommended, followed by a bridge to allogeneic Hematopoietic Stem Cell Transplantation (allo-HSCT). For high-risk Ph-positive children who fail to achieve CR with induction therapy or still have MRD at the end of consolidation therapy, blinatumomab treatment is also recommended, followed by a bridge to allo-HSCT. For infants with newly diagnosed leukemia accompanied by *KMT2A* rearrangements, the Interfant chemotherapy regime can be recommended, either alone or in combination with blinatumomab, followed by continuation of the Interfant intensive chemotherapy consolidation protocol. For those without *KMT2A* rearrangements, blinatumomab treatment is recommended after induction if MRD is positive, followed by a bridge to allo-HSCT. For children with B-ALL experiencing a first relapse, blinatumomab treatment can be used after achieving CR with induction therapy, regardless of MRD status, with consideration given to a bridge to allo-HSCT. For those who relapse after transplantation, as well as those with multiple relapse or refractory disease, blinatumomab can be used for re-induction therapy.

In the 2024 Chinese Expert Consensus (14), the expert panel's treatment recommendations are as follows: For newly diagnosed high-risk, chemotherapy-intolerant, and infant patients with leukemia, the use of blinatumomab in combination with chemotherapy for induction of remission and consolidation therapy is recommended; for patients with relapsed/refractory (R/R), the earlier blinatumomab is used, the greater the benefit. Blinatumomab is recommended for salvage therapy of the first relapse and for consolidation therapy in patients with early relapse and positive MRD after induction, corresponding to patients considered as intermediate to high risk. Following this, a bridge to allo-HSCT can lead to longer survival.

2.3 Real-world supplementary applications

Since the approval by FDA, blinatumomab has gained widespread recognition for its efficacy in several clinical scenarios. Based on instructions and expert consensus, blinatumomab plays an important role in the real-word clinical treatments and also holds clinical significance in other supplementary situations.

2.3.1 First-line treatment for children

Blinatumomab has been explored as a first-line treatment, particularly for infants with *KMT2A* rearrangements (15). The Interfant-06 study demonstrated a significant improvement in 2-year disease-free and OS rates compared to historical controls (15). Additionally, ongoing clinical trials, such as the AIEOP-BFM ALL 2017 (NCT03643276) and the St. Jude protocols (NCT031177510), as well as the recently finished COG AALL1731 (US), are evaluating its efficacy in the high-risk pediatric B-ALL population. In China, collaborative studies have further extended its application to intermediate-risk cases, marking a shift from its original use in relapse/refractory disease to frontline settings. However, critical questions regarding optimal dosing schedules, treatment duration, and synergistic chemotherapy combinations remain under investigation.

2.3.2 Post-HSCT relapse prevention

Blinatumomab has emerged as a valuable adjunct for preventing relapse following HSCT. When combined with donor lymphocyte infusions, it can effectively help children who are MRD-positive after HSCT to become MRD-negative again. However, its efficacy appears limited in preventing relapses in the central nervous system (16).

2.3.3 Bridging therapy for alleviating chemotoxicity

Blinatumomab has been applied in pediatric ALL patients with severe chemotherapy-related toxicities or those who are intolerant to chemotherapy, and this preliminary exploration has shown a promising outlook. A small proportion of pediatric ALL patients experience overwhelming chemotherapy-related toxicities or temporary contraindications to chemotherapy after receiving chemo, leading to interruptions and delays in chemotherapy or prompting changes in chemotherapy dosages, thereby resulting in treatment failure or relapse. Elitzur et al. (17) reported 11 pediatric patients who received blinatumomab treatment due to severe chemotoxicities, and all patients successfully recovered and transitioned to further therapy. Daniel et al. (18) introduced 15 pediatric ALL cases with invasive fungal disease (IFD) caused by chemotherapy, and these patients received blinatumomab as a bridge treatment, allowing for continued targeted treatment for ALL while recovering from IFD. Another study involving a 10-month-old female patient and a 4-year-old female patient (19) also demonstrated that blinatumomab can improve the toxic state to continue chemotherapy and that blinatumomab treatment is safe even in the presence of infectious complications. In a retrospective analysis conducted by Beijing Children's Hospital of 23 children treated with blinatumomab (18), 20 were intolerant to chemotherapy, mainly due to pancreatitis, mucositis, cerebral venous thrombosis, infectious shock, and so on. After 1 to 2 cycles of blinatumomab treatment, all children achieved molecular biological remission with negative MRD. Among them, 4 children with relapse subsequently underwent HSCT, and the remaining children received maintenance therapy. Blinatumomab bridge therapy shortens the duration of chemotherapy interruption and provides a novel treatment option for pediatric ALL patients who cannot tolerate cytotoxic therapy. However, experience and data on the use of blinatumomab in pediatric patients with severe chemotherapy-related toxicities are limited, and prospective clinical studies are needed to determine the exact and optimal role of blinatumomab in improving treatment and reducing treatment-related toxicities.

3 Treatment response across different subtypes

With the continuous advancement of molecular technology and the application of NGS technology, both the International Consensus Classification (ICC) and the World Health Organization (WHO) have conducted detailed molecular subtyping of B-ALL. Although this has increased the complexity of subtyping diagnosis, it has significant implications for personalized precision treatment and prognostic management. Comprehensive genomic analysis of large cohorts of ALL, through the identification of novel clonal, subtype-defining chromosomal alterations, has reduced the proportion of patients previously classified as "others" from 25% to approximately 5% (20), thereby expanding the scope of precision medicine treatment for pediatric ALL. Children with different subtypes of B-ALL harbor distinct abnormal molecular signaling pathways or other biological pathways, which correspond to varying degrees of prognosis. The identification of clear subtypes provides definite abnormal targets, facilitating the selection of targeted drugs and offering the opportunity for preemptive treatment planning for subtypes with poor prognosis. There is currently evidence that ETV6-RUNX1, high hyperdiploidy of chromosomes 4, 10, and 17, or double/triple trisomies are associated with a favorable prognosis, whereas hypodiploidy, BCR-ABL1, KMT2A rearrangements (KMT2AR), TCF3-HLF, and intrachromosomal amplification of chromosome 21 are associated with an adverse prognosis (21). Recently identified novel subtype-defining chromosomal alterations, some of which have prognostic and/or therapeutic implications, may involve multiple rearrangements of a single partner gene, sequence mutations of transcription factors, or a spectrum of genomic alterations within a single group (20), such as the MYC rearrangement subtype, which has an extremely poor prognosis.

Meanwhile, the molecular subtypes also provide a platform for understanding the genetic basis and clonal architecture of R/R B-ALL, contributing to the progress in the mechanisms of relapse. The mutations in relapsed ALL often originate from minor clones that exist at diagnosis, which survive therapy and acquire additional cooperating mutations, thereby becoming the founding clones of relapse (22). These founding clones may arise as a result of chemotherapy-induced selection, and thus are drug-resistant, rendering the original chemotherapy ineffective. Targeted therapies, such as tyrosine kinase inhibitors (TKIs), can effectively inhibit tumor progression and exert antitumor effects by interfering with molecular signaling pathways, but they face the problems of drug resistance and relapse. At this point, immunotherapy, which is not dependent on specific genetic abnormalities, can overcome the chemotherapy-resistant mutations that are enriched in relapsed ALL (22). Specifically, blinatumomab bridging to HSCT has demonstrated high efficacy and low toxicity in children with intermediate and high-risk first relapse of B-ALL (23).

3.1 B-ALL with BCR::ABL1 fusion

The BCR::ABL1 fusion gene is generated by a reciprocal translocation between chromosomes 9 and 22, which results in the formation of the Philadelphia chromosome (Ph). Pediatric Ph+ B-ALL is a subtype with a poor prognosis, accounting for 2%-5% of childhood ALL (24). The BCR-ABL1 fusion event leads to the abnormal activation of tyrosine kinase, which in turn causes the dysregulation of its downstream pathways. Therefore, the application of TKIs has brought significant improvement for children, with the survival rate of pediatric Ph+ ALL achieving a leap from 20% to over 60% (25). At present, the treatment of pediatric Ph+ ALL has formed a comprehensive strategy centered on the combination of TKIs and chemotherapy, and is gradually evolving towards precision stratification and targeted immunotherapy. Blinatumomab has been applied in the consolidation phase of children with Ph+ ALL and in those with relapsed/refractory disease. In patients with relapsed/refractory Ph+ B-ALL, blinatumomab monotherapy has demonstrated a high CR rate and molecular complete remission (CMR) rate. Besides, the RIALTO study showed that blinatumomab had a significant effect on MRD remission, with an MRD remission rate of 79% in children with a baseline blast count of ≥5%, and an MRD remission rate as high as 92% in children with a baseline blast count of <5%.

3.2 B-ALL with BCR::ABL1-like features

BCR::ABL1-like ALL, also termed as Ph-like ALL, is a high-risk B-ALL, which is characterized by adverse clinical features and a poor relapse-free survival rate, even when treated with risk-adapted multi-agent chemotherapy regimens. The advent of NGS technology has unveiled the diversity of kinase-activating genetic drivers in Ph-like ALL, which may be amenable to "personalized" molecularly targeted therapies. Ph-like ALL is characterized by a variety of kinase-activating alterations, leading to a gene expression profile similar to that of Ph+ ALL, but lacking the typical BCR::ABL1 fusion. The proportion of this subtype in pediatric B-ALL is 10-13%. Blinatumomab is primarily used in the treatment of pediatric Ph-like ALL for continuous administration during the consolidation phase until minimal residual disease (MRD) is negative, followed by allogeneic hematopoietic stem cell transplantation (allo-HSCT), which helps to improve the remission rate and survival rate.

3.3 Novel molecular subtypes

The molecular heterogeneity of B-ALL is far more complex than previously recognized. As research continues to delve deeper, an increasing number of novel molecular subtypes are emerging. The discovery of these new subtypes further expands the boundaries of our understanding of the molecular characteristics of B-ALL and also brings new opportunities and challenges for future therapeutic strategies. This review mainly focuses on the rare (with a frequency of only 1- 9%) but extremely poor-prognosis MYC-rearranged subtype. This subtype was initially described in Burkitt lymphoma (BL). In ALL, it represents a rare molecular subtype characterized by MYC rearrangement, positive expression of TdT, optional CD34 expression, frequent absence of surface immunoglobulin (sIg) and CD20, and potential Burkitt-like morphological features (26). In children with this subtype of B-ALL, the MYC gene is typically overexpressed. Studies have shown that intrinsic defects in the B-ALL microenvironment lead to reduced production of type I interferons (IFN-Is) by plasmacytoid dendritic cells and/or autocrine IFN-Is from B cells, resulting in impaired IFN-I-driven immune responses that promote tumor progression in the MYC subtype (27). The abnormality of IFN-Is further diminishes IL-15 transcription, leading to impaired maturation of natural killer (NK) cells in the microenvironment. Consequently, these NK cells cannot lyse NK cell-sensitive targets as efficiently as normal NK cells. An increased frequency of abnormal NK cells is independently associated with heightened disease severity and poor prognosis in patients (28). Meanwhile, MYC overexpression enhances the sensitivity of B-ALL cells to NK cell-mediated cytotoxicity. Thus, NK cells secreting IL-15 may serve as a therapeutic approach for the MYC subtype, a hypothesis validated in *in vitro* experiments (27). Regarding blinatumomab, while current research has not proven its specific efficacy against this subtype, its mechanism of action—promoting the release of various cytokines to modulate the immune microenvironment—suggests that if used during the consolidation phase, it could effectively maintain the activity and quantity of IL-15-secreting NK cells. Blinatumomab has synergistic effects with NK cell therapy, which may enhance treatment tolerance in children and reduce therapy-related toxicity. Ocadlikovad et al. found that after treatment with blinatumomab, there was a persistent increase in NK cells, such as the cytotoxic CD56dim NK cell subset, but this upregulation was only observed in peripheral blood, not in the bone marrow (29). The mechanism behind this upregulation of NK cells is not clear and may be related

to the off-target effects of blinatumomab (29). Blinatumomab, as one of the cutting-edge immunotherapeutic modalities, can be combined with targeted therapy in rare subtypes such as MYC-rearranged to enhance efficacy and treatment safety. However, due to the limited number of clinical samples, further studies are needed to confirm this. International cooperation to design prospective clinical trials can be carried out to achieve this goal.

4 Factors impact on efficacy

Clinical evidence demonstrates superior efficacy of blinatumomab compared to conventional chemotherapy in relapsed/refractory B-ALL. A phase III multicenter randomized clinical trial reported significantly improved outcomes with blinatumomab, including 2-year overall survival (OS) rates of 81% versus 56% with chemotherapy, and MRD remission rates of 93% versus 24% after one treatment cycle (30). Extended follow-up data revealed that patients receiving blinatumomab consolidation therapy maintained event-free survival (EFS) exceeding 50% and OS surpassing 80% at 57 months, with consistent hazard ratios 0.33 for both EFS (95%CI: 0.19 - 0.59) and OS (95% CI: 0.15 - 0.72) compared to chemotherapy controls (30). Blinatumomab provides higher health benefits in treating R/R ALL compared to traditional chemotherapy. Blinatumomab has a clear clinical significance, with prominent therapeutic effects, filling a gap in clinical treatment, achieving rapid and high-quality hematological remission, effectively clearing MRD, offering more HSCT possibilities for patients, and improving their long-term survival. Its efficacy has been verified in adult patients in China.

Blinatumomab treatment responses exhibit interpatient variability influenced by complex multifactorial interactions. However, because of the complex interplay between external environmental factors and leukemia-intrinsic factors, the predication of efficacy remains limited. Unlike conventional chemotherapy regimens where treatment efficacy correlates with established predictors including patient's age, duration of prior remission, chemosensitivity profiles, and post-transplant relapse status, these conventional parameters demonstrate limited predictive value for blinatumomab outcomes (31). The observation that traditional efficacy prediction indicators do not match the response to blinatumomab is consistent with the fact that blinatumomab works by CD3/CD19 bispecific targeting to lyse tumor cells, thereby bypassing many mechanisms associated with chemotherapy resistance (32). Therefore, traditional indicators for predicting chemotherapy efficacy are not applicable for predicting the efficacy of blinatumomab. Currently, new biomarkers are being explored to better predict the efficacy of blinatumomab. Apart from the known T-cell subsets and CD19 status, some new molecular markers (such as specific gene mutation or immune cell surface markers) may help identify patients who are more likely to benefit from the treatment. Tumor burden, the function of endogenous T-cell and status of T-cell subset, loss/decrease of CD19 antigen are important factors affecting the efficacy of blinatumomab. The rare phenomenon of lineage switch can also lead to treatment failure. Moreover, the efficacy may also be influenced by the drug's specific impact on particular patients and individual differences among patients, including genetic background, immune status, and prior treatment history.

4.1 Tumor burden

Tumor burden serves as an important clinical indicator for assessing disease severity and predicting therapeutic outcomes in pediatric B-ALL. This quantitative measure reflects both the absolute number and anatomical distribution of malignant cells within the patient's hematopoietic system. In clinical practice, tumor burden assessment employs a multimodal diagnostic approach incorporating the MICM model (morphological examination, immunophenotypic characterization, cytogenetic analysis, and molecular genetic profiling), complemented by bone marrow aspiration and biopsy procedures, comprehensive immunophenotyping panels, advanced genetic testing methodologies, and sensitive minimal residual disease (MRD) monitoring techniques. These diagnostic tools collectively provide a robust framework for accurate disease quantification and characterization. Current risk stratification protocols universally incorporate tumor burden measurements as a key determinant of disease classification. The National Cancer Institute (NCI) risk stratification system categorizes patients into two distinct groups: standard-risk and high-risk, based on predefined tumor burden thresholds. Alternative classification systems employed by various international cooperative groups further refine this approach by implementing three-tiered stratification schemes (low-risk, intermediate-risk, and high-risk categories). These risk-adapted classifications serve critical functions in clinical management by guiding therapeutic intensity selection, informing prognostic predictions, and facilitating comparative outcome analyses across treatment protocols and clinical trials.

Extensive clinical investigation has established a strong inverse correlation between baseline tumor burden and treatment efficacy. Several prospective studies and retrospective analyses have consistently demonstrated that pediatric patients presenting with lower initial disease burdens achieve significantly higher rates of complete hematological remission following blinatumomab therapy (30, 32, 33). This relationship extends to long-term clinical endpoints in adult patients, with lower tumor burden cohorts exhibiting superior relapse-free survival and overall survival rates compared to their high-burden counterparts (34). The biological underpinnings of this clinical observation involve several interrelated mechanisms. From a pharmacological perspective, the bispecific T-cell engager mechanism of blinatumomab requires adequate T-cell to tumor cell ratios for optimal cytotoxic activity. Excessive leukemic cell populations may overwhelm endogenous T-cell effector capacity through numerical superiority and potential immune exhaustion phenomena, thereby limiting therapeutic effectiveness. Meanwhile, the rapid cytoreduction characteristic of blinatumomab therapy in high tumor burden patients precipitates substantial cellular destruction, triggering massive release of

intracellular contents and proinflammatory cytokines. This pathophysiological cascade manifests clinically as an increased incidence and severity of cytokine release syndrome (CRS), a potentially life-threatening treatment complication (35). Furthermore, the abrupt liberation of cellular metabolites from lysed leukemic cells may overwhelm normal homeostatic mechanisms, resulting in tumor lysis syndrome (TLS) characterized by dangerous electrolyte disturbances and acute kidney injury (36). Adverse reactions have a negative impact on the treatment effect and reduce the safety of treatment. In response to these challenges, contemporary treatment algorithms have incorporated strategic pretreatment approaches for high tumor burden patients in order to make the treatment process safer, enable patients to better tolerate the treatment, and improve treatment compliance and the overall therapeutic effect. Clinical evidence from adult populations demonstrates that preliminary cytoreduction with conventional chemotherapy or targeted debulking regimens prior to blinatumomab initiation significantly reduces the incidence and severity of CRS events while simultaneously improving rates of MRD negativity (37). In pediatric patients, individuals with a higher tumor burden may require more aggressive pretreatment to improve the treatment efficacy. The development of refined tumor burden assessment techniques and corresponding treatment algorithms continues to represent an active area of clinical investigation in pediatric B-ALL management.

4.2 Endogenous T-cell function and T-cell subset impact

Blinatumomab activates T cells by targeting them, thereby attracting leukemic cells. After the use of this frug, the patient's immune system is activated, capable of activating different T-cell subset. Although blinatumomab can activate T cells, the patients' immune status, such as the basal function and number of T cells, will still affect the treatment outcome. Growing evidence suggests that endogenous T-cell function and T-cell subsets influence the response to blinatumomab immunotherapy. The baseline functionality of endogenous T cells, such as their ability to produce cytokines like IFN-γ upon initial exposure to antigens, can significantly impact how well blinatumomab works. T cells with higher pre-treatment IFN-γ production were associated with a more robust anti-leukemia response after blinatumomab treatment (38).

Recent single-cell transcriptomic studies have provided comprehensive insights into the complex immunological mechanisms underlying blinatumomab's therapeutic effects in B-ALL. These investigations have identified four different T-cell subsets activated by blinatumomab, including CD8+ effector memory T cells (TEM), CD4+central memory T cells (TCM), naïve T cells, and regulatory T cells (Tregs). Detailed analysis of gene expression patterns in these activated clusters have revealed significant upregulation of multiple critical pathways, including immune system activation, glycolytic metabolism, interferon-alpha (IFNA) signaling, gap junction communication, and interferon-gamma (IFNG) signaling pathways, reflecting the multifaceted nature of T-cell activation induced by blinatumomab therapy (39). The activation of these T-cell populations following blinatumomab administration leads to substantial production of proinflammatory cytokines, which mediates the drug's therapeutic effects. Among these subsets, CD8+ TEM cells demonstrate particularly robust activation, exhibiting markedly higher expression of cytotoxic factors such as perforin (PRF1), interferon-gamma (IFNG), and FAS ligand (FASLG), along with numerous cytokines and chemokines such as CCL2, CCL3, CCL3L1, CCL4 and TNFSF9 compared to other T-cell subsets (39). This distinct cytokine secretion profile suggests that different T-cell populations contribute variably to target cell lysis, thereby influencing the overall treatment efficacy in a subset-specific manner. CD4+ TCM cells, for example, are crucial for maintaining a long-term immune response. They can rapidly proliferate and differentiate into effector cells upon re-encountering the antigen. Patients with a higher proportion of CD4+ TCM cells at the start of treatment are more likely to achieve long-term remission, suggesting their importance in sustaining the anti-leukemia immune attack (38). Interestingly, transcriptomic analysis of responding patients has revealed enrichment of tumor cell immune response genes, suggesting that the efficacy of blinatumomab-induced T-cell activation may be modulated by leukemia-intrinsic factors (31). Furthermore, clinical observations have identified that increased frequencies of Tregs in peripheral blood can predict *in vitro* response to blinatumomab, likely mediated through interleukin-10-dependent suppression of T-cell activity (31). Additional investigations focusing on Tregs, specifically those identified by CD4, CD25 and FOXP3 expression makers, have demonstrated that blinatumomab-activated Tregs promote immunosuppressive effects through IL-10 production, which subsequently inhibits general T-cell proliferation and reduces CD8+ T-cell-mediated lysis of ALL cells, ultimately impacting treatment outcomes (40). Understanding these complex interactions between different T-cell subsets and blinatumomab can potentially lead to more personalized treatment strategies for patients.

4.3 CD19 antigen loss/decrease

The CD19 antigen is the target site for blinatumomab's action. However, leukemic cells may develop resistance through either complete loss of CD19 expression or significant reduction in antigen density, thereby impairing T-cell recognition and cytotoxic attack against malignant cells. This immune evasion mechanism can manifest as either complete immunological escape or progressive T-cell exhaustion, both of which substantially compromise treatment outcomes. A comprehensive retrospective analysis of real-world data from adult patients receiving blinatumomab revealed that 9.8% of cases experienced relapsed with CD19-negative disease, representing 34.2% of all relapsed events, with similar patterns observed in pediatric patients (41). These findings confirm CD19 antigen loss as a

major pathway for leukemic cells to evade CD19-directed immunotherapies. Analysis of patient samples with antigen loss after blinatumomab treatment conclude that possible mechanisms leading to CD19 antigen loss include acquired mutations in the CD19 gene itself, alterations in CD81 (a crucial chaperone protein required for CD19 membrane expression), and other chromosomal causes (31). In addition, a high tumor burden is independently associated with CD19 loss and is related to a poor EFS (42). This relationship suggests that patients presenting with extensive disease may be at heightened risk for developing this resistance mechanism during treatment. The clinical impact of CD19 loss has been extensively documented across pediatric studies. A comprehensive single-center retrospective analysis incorporating data from multiple trials confirmed that diminished or absent CD19 expression represents a major contributor to treatment failure in pediatric B-ALL (30). Across various pediatric cohorts, a substantial proportion of poor responders exhibited either reduced CD19 antigen density or complete antigen loss, with this phenomenon being strongly associated not only with diminished initial response rates but also with increased risk of disease recurrence. These observations underscore the universal significance of CD19 antigen modulation as a key determinant of treatment outcomes across all age groups. Further complicating this picture, pediatric patients demonstrating poor response to blinatumomab frequently exhibit concurrent upregulation of T-cell exhaustion markers, particularly PD-1 and TIM-3 (43). This dual phenomenon of CD19 loss combined with T-cell exhaustion creates a synergistic immunosuppressive environment that further facilitates leukemic cell escape from immune surveillance. The co-occurrence of these mechanisms suggests a potential feedback loop where CD19 loss reduces antigenic stimulation while exhaustion markers dampen remaining T-cell activity, collectively crippling the anti-leukemic immune response. However, t the clinical consequences of CD19 loss appear somewhat less severe in blinatumomab therapy compared to CD19-directed CAR-T cell treatments (44). This differential impact stems from fundamental mechanistic distinctions between these immunotherapeutic approaches. CAR-T cells rely exclusively on direct CD19 recognition for target cell engagement, making them particularly vulnerable to antigen loss variants. In contrast, bispecific antibody design of blinatumomab may retain partial efficacy even in the face of CD19 modulation, as its T-cell activating capacity persists independently of absolute antigen density. This relative advantage may explain why some patients with partial CD19 loss can still derive clinical benefit from blinatumomab despite suboptimal responses.

4.4 Lineage switch

Lineage switch is a rare phenomenon observed in patients after receiving blinatumomab treatment, where lymphoid tumor cells transdifferentiate into myeloid tumor cells that do not express CD19. The phenomenon is particularly well-documented in cases harboring mixed lineage leukemia (MLL) rearrangements, where the leukemic cells demonstrate inherent lineage plasticity and may undergo myeloid conversion under therapeutic pressure. While lineage switching has been historically associated with conventional chemotherapy regimens, emerging evidence confirms its occurrence following blinatumomab treatment, with the most common transformation being to acute myeloid leukemia (AML) (45). A comprehensive multicenter study involving 182 pediatric BCP-ALL patients treated with blinatumomab provided detailed insights into the incidence and molecular characteristics of this phenomenon (46). The investigation identified six confirmed cases of lineage switch occurring either during active blinatumomab treatment or in the post-therapy period. These cases represented 17.2% (4/23) of all documented treatment-resistant instances and 3.2% (2/63) of relapse events, establishing lineage conversion as an important mechanism of therapeutic failure. The phenotypic manifestations of lineage switch exhibited considerable heterogeneity among affected patients. Approximately half of the cases demonstrated complete conversion from BCP-ALL to CD19-negative AML, while the remainder displayed more complex immunophenotypic patterns characterized by the coexistence of residual CD19-positive B lymphoblasts with newly emergent CD19-negative blast populations of either myeloid or unclassifiable lineage. The transdifferentiated myeloid tumor cells no longer express CD19, thereby evading the targeted therapy of blinatumomab and leading to a decrease in treatment efficacy. The mechanisms of lineage switch are currently unclear and may be related to cytogenetic abnormalities (45).

4.5 Other factors

Several additional clinical considerations also impact the therapeutic effectiveness of blinatumomab in B-ALL management. The drug's pharmacokinetic properties, particularly its central nervous system (CNS) penetration capabilities and activity against extramedullary disease, represent important determinants of clinical outcomes. In the ALL1331 clinical trial, it was indicated that the efficacy of blinatumomab within the CNS may be limited, leading to poorer prognosis for patients with isolated CNS disease. Additionally, the efficacy of blinatumomab in extramedullary sites may be limited, resulting in a poorer prognosis for low-risk patients with isolated extramedullary relapse, especially those with isolated CNS disease. In actual treatment, Patient tolerance represents another critical factor influencing blinatumomab treatment success. Clinical experience has shown that adverse event profiles frequently necessitate dose modifications or temporary treatment interruptions, potentially compromising therapeutic efficacy. Optimizing the dose adjustment strategy and managing adverse reactions, patients' tolerance and treatment compliance can be improved, thus enhancing the overall efficacy. Pediatric and adult patients have different tolerances to the drug. Pediatric patients generally have better tolerance to immunotherapy but this enhanced tolerance coexists with unique vulnerabilities, including increased susceptibility to specific developmental toxicities such as growth impairment and delayed maturation processes (9). Moreover, the strategic positioning of blinatumomab within

comprehensive treatment algorithms represents an additional variable affecting clinical outcomes. Emerging evidence supports multiple effective sequencing approaches for blinatumomab administration in R/R ALL management. The agent has demonstrated significant utility when employed as consolidation therapy following successful induction remission, where it may deepen molecular responses and prolong remission duration. Alternatively, pre-transplant administration has shown efficacy in reducing tumor burden prior to allo-HSCT, thereby potentially enhancing engraftment success rates and reducing post-transplant relapse risk (37). Blinatumomab has also been successfully incorporated as a bridging therapy preceding CAR-T cell interventions, where its tumor-reducing effects can create more favorable conditions for subsequent cellular therapy, improving both safety profiles and treatment success rates (37).

5 Toxicity

Current clinical trials indicate that the toxicity of blinatumomab, the adverse events (AE) produced in clinical applications, is less than that of traditional chemotherapy in general. The most common adverse reactions include fever, headache, infection, and febrile neutropenia, with fever being the most common AE at the recommended dose (80%) (47). Other more common side effects include dizziness, tremors or ataxia, nausea, hypokalemia, fatigue, constipation, and diarrhea. More serious AE include cytokine release syndrome (CRS) and neurological AE, which often require immediate discontinuation of the drug and corresponding treatment. Although blinatumomab is generally well-tolerated, serious adverse reaction such as CRS, immune effector cell-associated neurotoxicity syndrome (ICANS) and infections have been identified in clinical trials and real-world studies, necessitating discontinuation of the drug.

5.1 cytokine release syndrome

CRS is considered a clinically significant systemic inflammatory response associated with blinatumomab immunotherapy (48), mediated by elevated levels of cytokines and other inflammatory markers. CRS is characterized by fever and multi-organ dysfunction. The NCCN 2025 second edition describes CRS as a spectrum of clinical symptoms ranging from fever or hypothermia in mild cases to potentially life-threatening hypotension and end-organ damage in severe manifestations (13). The American Society for Transplantation and Cellular Therapy (ASTCT) has established a standardized five-grade classification system for CRS severity, with grade 1 representing mild febrile reactions and grade 5 indicating fatal complications requiring immediate intervention (49). Clinical management strategies vary according to severity, with grades 1–2 typically managed through symptomatic support, while grades 3–5 necessitate treatment interruption combined with corticosteroids, vasopressors, and IL-6 receptor antagonists such as tocilizumab following manufacturer guidelines. Epidemiological data indicate that CRS occurs in 4-22% of pediatric patients receiving blinatumomab, though high-grade (≥3) events are less frequent (approximately 3%) (29). Interestingly, a 2022 meta-analysis found comparable CRS incidence rates between blinatumomab and conventional chemotherapy groups when evaluating pediatric safety profiles (12).

The pathophysiological mechanisms underlying CRS involve complex cytokine networks activated during blinatumomab therapy. When the bispecific antibody engages T-cells with CD19+ leukemic cells, massive T-cell activation triggers an exaggerated release of proinflammatory mediators including IFN-γ, IL-6 and TNF. These cytokines normally help with immune response, but in CRS, their release far exceeds physiological levels, leading to a systemic inflammatory response. Cytokines such as IFN-γ and GM-CSF can further stimulate macrophages and monocytes to release more IL-1 and IL-6. IL-6 plays a key role in CRS. It nor only directly mediates acute inflammatory response but also induces the expression of Vascular Endothelial Growth Factor (VEGF), increasing vascular permeability and leading to capillary leak and hemodynamic instability (50). CRS is a target phenomenon associated with multiple cytokines, most notably IFN-γ and IL-6, with a lesser association with TNF (51). Several risk factors influence CRS development, with baseline tumor burden representing a particularly important modifiable predictor. Clinical evidence confirms that cytoreductive strategies implemented prior to blinatumomab initiation can mitigate both CRS incidence and severity (51). Most CRS is reversible, and effective prevention can be achieved by identifying high-risk patients before blinatumomab administration, premedication with dexamethasone, and stepwise dose escalation. After CRS occurs, most patients can continue blinatumomab treatment after CRS subsides by interrupting blinatumomab therapy, administering corticosteroids and IL-6 receptor antagonists according to graded assessment, and/or supportive care (50). However, accurate diagnosis remains challenging due to significant symptom overlap with other conditions including infusion reactions, systemic infections, capillary leak syndrome, and hemophagocytic lymphohistiocytosis/macrophage activation syndrome (14). The NCCN 2025 guidelines emphasize the importance of thorough infectious disease evaluation in suspected CRS cases, recommending empirical antimicrobial therapy when appropriate given the potential for concurrent severe infections to mimic CRS presentation (13). This diagnostic complexity underscores the need for comprehensive clinical assessment and multidisciplinary management approaches when addressing potential CRS events during blinatumomab treatment.

5.2 Immune effector cell-associated neurotoxicity syndrome

Immune effector cell-associated neurotoxicity syndrome (ICANS) represents a clinically significant neurological complication observed in patients undergoing T-cell activating immunotherapies such as blinatumomab for B-cell malignancies. This neuropsychiatric syndrome, first formally characterized by the ASTCT in 2019,

typically manifests during the initial treatment cycle with symptom duration varying from transient to prolonged depending on severity (48). The clinical presentation encompasses a spectrum of neurological disturbances including confusion, dysphasia, somnolence, ataxia, tremors, seizures, and syncopal episodes. Neurological adverse events are common in therapies that utilize activated T cells to destroy malignant B-cell tumors, often occurring in the early stages of the first treatment cycle, with short symptom duration and most being reversible. ICANS is a common and potentially life-threatening adverse reaction associated with T-cell involvement in immunotherapy. These symptoms reflect the complex interplay between activated immune effectors and the central nervous system, with pathophysiological mechanisms that may overlap with concurrent cytokine release syndrome (CRS) while maintaining distinct clinical features (52). Blinatumomab, by activating T cells, leads to the release of a large number of cytokines. These cytokines may disrupt the blood-brain barrier, exposing brain tissue to circulating cytokines and thereby inducing neurotoxicity. Cytokines like IL-6 may affect the integrity of the blood-brain barrier, leading to brain tissue edema and neurological dysfunction. Additionally, activated T-cells themselves may transmigrate across the compromised blood-brain barrier, establishing localized inflammatory foci within the CNS parenchyma that further exacerbate neurotoxicity (52). These mechanisms collectively contribute to the diverse neurological manifestations observed in clinical practice. The ASTCT has established a standardized five-tier grading system for ICANS severity assessment (49). Grade 1 events typically involve mild symptoms such as headache or subtle tremors, while grade 5 represents life-threatening complications including status epilepticus or cerebral edema. Clinical management strategies are severity-dependent, with grades 1–2 generally managed through supportive measures and close monitoring, whereas grades 3–5 necessitate immediate treatment interruption combined with high-dose corticosteroids and other neuroprotective interventions. Epidemiological analyses reveal important age-related differences in ICANS presentation and outcomes. Pediatric populations demonstrate lower overall incidence rates (3.7-24%) compared to adults, with severe (grade ≥3) events occurring in only 2-3.6% of cases (29). However, children exhibit distinct clinical characteristics including earlier symptom onset and more rapid progression timelines, potentially increasing acute life-threatening risks despite lower absolute frequencies (33). A comprehensive 2022 systematic review of published clinical trials demonstrated comparable seizure risks between blinatumomab and conventional chemotherapy, but identified significantly higher encephalopathy rates with blinatumomab-based immunotherapy (53). These findings highlight the need for age-specific monitoring protocols and management algorithms. ICANS is one of the common reasons for discontinuing blinatumomab therapy, and the drug should be stopped immediately upon the appearance of grade ≥3 neurological symptoms, followed by appropriate treatment. Due to the short elimination half-life of blinatumomab, most neurotoxic symptoms can disappear after discontinuation of the drug and initiation of steroid therapy. Seizures are a relatively rare symptom, and the use of antiepileptic drugs should be cautious, with routine use of antiepileptic drugs for prophylaxis not recommended. To prevent the occurrence of ICANS, it is first necessary to identify high-risk patients, such as those with a high tumor burden or a history of neurological disease, and to adopt more cautious treatment strategies for these patients. Before treatment, corticosteroids such as dexamethasone can be used for pre-treatment, and a stepwise dose-escalation approach can be employed to reduce the risk of ICANS occurrence.

5.3 Infections

Infections is currently one of the most significant adverse reactions in patients receiving blinatumomab treatment. Patients with leukemia have various risk factors for infection, including immunosuppression, hematological toxicity, concomitant use of immunosuppressants, and catheter-related infection. As an immunomodulatory antibody, blinatumomab may suppress the immune functions of B cells and T cells, leading to hypogammaglobulinemia and immune dysregulation, thereby increasing the risk of infection. Blinatumomab has myelosuppressive effects, causing persistent cytopenia, and may also lead to B-cell aplastic anemia; meanwhile, treatment-related neutropenia is a common phenomenon in immunotherapy, making patients more susceptible to infections. However, blinatumomab's myelosuppressive effect is weaker than traditional chemotherapy, and the suppression is mostly transient. The patient's weakened immune system, coupled with the use of corticosteroids or tocilizumab for infection. Additionally, since blinatumomab is typically administered through long-term continuous infusion, requiring the establishment of a venous infusion pathway, catheter-related infections must also be vigilantly monitored. To prevent severe infections or life-threatening conditions, routine blood tests should be conducted for pediatric patients, and attention should be paid to the emergence of infection-related clinical symptoms. If symptoms and signs of suspected infection appear, empirical antimicrobial treatment should be initiated immediately, and pathogen testing should be completed as soon as possible.

6 Administration

The clinical management of blinatumomab is decisive for its efficacy and the incidence and severity of adverse events. The appropriate route of administration is determines based on pharmacokinetic characteristics and the patient's specific condition, a course of treatment is selected and planned, and adverse events that occur after medication are managed.

6.1 Route of administration and course of treatment selection

In studies conducted over 4~8 hours under continuous intravenous infusion, it was confirmed that blinatumomab exhibits linear pharmacokinetic characteristic, which means that

its clearance rate and distribution volume remain constant across different dosage ranges. The average systemic clearance of 2.92 L/hour reflects rapid elimination from circulation, while the average volume of distribution of 4.52 L confirms predominantly intravascular compartmentalization. These predictable pharmacokinetic parameters contribute significantly to both the therapeutic efficacy and safety profile of blinatumomab in clinical applications. The standard administration protocol for both adult and pediatric patients involves continuous intravenous delivery using precision infusion pumps to maintain constant flow rates. Particular attention must be given to pediatric dosing regimens to minimize adverse events while maintaining therapeutic effectiveness. For pediatric patients with body weight below 45 kg, a carefully titrated dose-escalation approach is implemented, typically progressing through 5, 10, and 15 $\mu g/m^2$ dose levels with close monitoring for toxicity. Patients weighing 45 kg or more receive fixed dosing according to established protocols. The conventional treatment cycle consists of 4 weeks of continuous infusion followed by a 2-week treatment-free interval, a schedule designed to achieve and maintain therapeutic serum concentrations while allowing for physiological recovery. Recent clinical investigations have explored alternative administration routes to potentially improve treatment convenience and accessibility. A multicenter phase 1b trial expansion cohort evaluated subcutaneous blinatumomab administration in adults with relapsed/refractory B-ALL, demonstrating both feasibility and acceptable safety profiles with this delivery method (54). The subcutaneous route offers potential advantages in outpatient management and reduced healthcare resource utilization. However, it is important to note that comparable studies in pediatric populations have not yet been conducted, and intravenous infusion remains the only approved administration method for children at present. This represents an important area for future clinical investigation, particularly given the potential benefits of subcutaneous administration in pediatric oncology care settings.

6.2 Drug interactions

Blinatumomab had drug interactions with other medications, which may affect its efficacy or lead to adverse drug events. Common drug interactions include the following. Blinatumomab can increase blood glucose levels, so when used with glucose-lowering agents or insulin, it is necessary to carefully monitor blood glucose levels and adjust medication doses as needed. The use of white blood cell growth factors (such as filgrastim) in combination with blinatumomab may increase the risk of severe infection during treatment. Sedatives, hypnotics, or anesthetic drugs used in conjunction with blinatumomab may increase the risk of adverse reactions such as somnolence, fatigue, dizziness, and confusion. As an immunotherapy, blinatumomab may interact with other immunosuppressants such as cyclosporine, tacrolimus, and methotrexate. These immunosuppressants may reduce the immunostimulatory effects of blinatumomab, thereby weakening its therapeutic effect. Therefore, when treating with blinatumomab, it is important to carefully consider other medication choices and conduct monitoring.

7 Conclusion

Blinatumomab is the world's first and only approved BiTE therapy drug. One end is bound to CD19 expressed on the surface of B cells, and the other end to CD3 expressed on the surface of T cells, activating T cells and enabling them to exert cytotoxic effects, thus lysing B lymphoid leukemic cells. It is used for the treatment of adult and pediatric B-ALL. As clinical researches continue to advance, the clinical application of blinatumomab is expanding, and the management of its side effects is becoming increasingly refined. Meanwhile, efforts are being made to further clarify the factors affecting efficacy and to optimize treatment plans or adopt combination therapy strategies, in order to better ensure its therapeutic effectiveness. In the application of treating pediatric B-ALL, blinatumomab has shown significant efficacy and safety compared to traditional chemotherapy in treatments such as R/R B-ALL and MRD clearance. However, due to the limitations of pediatric clinical research duration, the long-term effects of treatment in children are currently unclear. Currently, blinatumomab is being explored as part of first-line treatment regimen, especially in "chemotherapy-free" protocols. In the ongoing phase III clinical trials NCT04530565, the efficacy of conventional treatment with chemotherapy and corticosteroids along with a tyrosine kinase inhibitor (TKI) is being compared to that of the same regimen augmented with blinatumomab. The primary objective is to compare OS following induction with corticosteroids + TKI + blinatumomab versus induction with corticosteroids + TKI + chemotherapy. The outcomes of this study may help determine whether the combination of corticosteroids, TKI, and blinatumomab is more effective than the standard of care. Moreover, this "chemotherapy-free" approach may reduce the toxicity and side effects associated with chemotherapy while improving patients' survival rates and quality of life. However, no definitive results have been reported yet, and the study remain in the realm of adult applications. Since the launch of blinatumomab, the timing of drug administration, course of treatment, and scope of application for pediatric patients have all been continuously explores, and methods to reduce drug production costs are also being sought. Research on blinatumomab is continuously being updated, and it is believed that in the future this drug will bring more benefits to pediatric patients.

Author contributions

YC: Writing – original draft, Writing – review & editing. AL: Supervision, Validation, Writing – review & editing.

Funding

The author(s) declare that no financial support was received for the research and/or publication of this article.

Conflict of interest

The authors declare that the research was conducted in the absence of any commercial or financial relationships that could be construed as a potential conflict of interest.

Generative AI statement

The author(s) declare that no Generative AI was used in the creation of this manuscript.

Publisher's note

References

1. Linet MS, Ries LA, Smith MA, Tarone RE, Devesa SS. Cancer surveillance series: recent trends in childhood cancer incidence and mortality in the United States. *J Natl Cancer Inst*. (1999) 91:1051. doi: 10.1093/jnci/91.12.1051

2. Siegel R, Naishadham D, Jemal A. Cancer statistics, 2013. *CA Cancer J Clin*. (2013) 63:11. doi: 10.3322/caac.21166

3. Kersey JH. Fifty years of studies of the biology and therapy of childhood leukemia. *Blood*. (1997) 90:4243. doi: 10.1182/blood.v90.11.4243

4. Hunger SP, Lu X, Devidas M, Camitta BM, Gaynon PS, Winick NJ, et al. Improved survival for children and adolescents with acute lymphoblastic leukemia between 1990 and 2005: a report from the children's oncology group. *J Clin Oncol*. (2012) 30:1663. doi: 10.1200/jco.2011.37.8018

5. Ma H, Sun H, Sun X. Survival improvement by decade of patients aged 0–14 years with acute lymphoblastic leukemia: a SEER analysis. *Sci Rep*. (2014) 4:4227. doi: 10.1038/srep04227

6. Rafei H, Kantarjian HM, Jabbour EJ. Recent advances in the treatment of acute lymphoblastic leukemia. *Leuk Lymphoma*. (2019) 60:2606–21. doi: 10.1080/10428194.2019.1605071

7. Zugmaier G, Gökbuget N, Klinger M, Viardot A, Stelljes M, Neumann S, et al. Long-term survival and T-cell kinetics in relapsed/refractory ALL patients who achieved MRD response after blinatumomab treatment. *Blood*. (2015) 126:2578–84. doi: 10.1182/blood-2015-06-649111

8. Nagorsen D, Kufer P, Baeuerle PA, Bargou R. Blinatumomab: a historical perspective. *Pharmacol Ther*. (2012) 136:334–42. doi: 10.1016/j.pharmthera.2012.07.013

9. Queudeville M, Ebinger M. Blinatumomab in pediatric acute lymphoblastic leukemia— from salvage to first line therapy (A systematic review). *J Clin Med*. (2021) 10. doi: 10.3390/jcm10122544

10. Yin JL, Zhang RD. Research progress of acute lymphoblastic leukemia with TP53 gene mutation. *Chin J Pract Pediatr Clin Med*. (2024) 39:389–393. doi: 10.3760/cma.j.cn101070-20230515-00382

11. Mouttet B, Vinti L, Ancliff P, Bodmer N, Brethon B, Cario G, et al. Durable remissions in TCF3-HLF positive acute lymphoblastic leukemia with blinatumomab and stem cell transplantation. *Haematologica*. (2019) 104:e244–7. doi: 10.3324/haematol.2018.210104

12. Chen B, Zou Z, Zhang Q, Chen K, Zhang X, Xiao D, et al. Efficacy and safety of blinatumomab in children with relapsed/refractory B cell acute lymphoblastic leukemia: a systematic review and meta-analysis. *Front Pharmacol*. (2022) 13:1032664. doi: 10.3389/fphar.2022.1032664

13. National Comprehensive Cancer Network. *NCCN Clinical Practice Guidelines in Oncology: Pediatric Acute Lymphoblastic Leukemia (Version 2.2025)*. PA, USA: National Comprehensive Cancer Network, Plymouth Meeting (2025).

14. Union for China leukemia of Chinese society of clinical oncology, Union for lymphoma investigatios of chinese society of clinical oncology and Chinese society of hematology, chinese medical association, Chinese hematology association, chinese medical doctor association. Chinese consensus for the bispecific T cell engager in the treatment of acute lymphoblastic leukemia (2024). *Zhonghua Xue Ye Xue Za Zhi = Zhonghua Xueyexue Zazhi*. (2024) 45:629–36. doi: 10.3760/cma.j.cn121090-20240528-00194

15. van der Sluis IM, de Lorenzo P, Kotecha RS, Attarbaschi A, Escherich G, Nysom K, et al. Blinatumomab added to chemotherapy in infant lymphoblastic leukemia. *N Engl J Med*. (2023) 388:15721581. doi: 10.1056/NEJMoa2214171

16. Chan WYK, Lee PPW, Cheuk DKL, Yeung EWM, Wong KCW, Li CK, et al. Blinatumomab with donor lymphocyte infusions post haploidentical hematopoietic stem cell transplantation as salvage therapy for relapsed refractory acute lymphoblastic leukemia post chimeric antigen receptor T-cell therapy. *Pediatr Blood Cancer*. (2023) 70:e29852. doi: 10.1002/pbc.29852

17. Elitzur S, Arad-Cohen N, Barzilai-Birenboim S, Ben-Harush M, Bielorai B, Elhasid R, et al. Blinatumomab as a bridge to further therapy in cases of overwhelming toxicity in pediatric B-cell precursor acute lymphoblastic leukemia: Report from the Israeli Study Group of Childhood Leukemia. *Pediatr Blood Cancer*. (2019) 66:e27898. doi: 10.1002/pbc.27898

18. Wu Y, Li Y, Fan J, Qi P, Lin W, Yang J, et al. Blinatumomab for treating pediatric B-lineage acute lymphoblastic leukemia: A retrospective real-world study. *Front Pediatr*. (2022) 10:1034373. doi: 10.3389/fped.2022.1034373

19. Yozgat AK, Bilir Ö.A, Bozkaya İ.O, Yaralı HN. Blinatumomab bridge therapy for mitigating chemotoxicity in children with acute lymphoblastic leukemia. *Indian J Hematol Blood Transfusion*. (2024) 40:1185–9. doi: 10.1007/s12288-024-01791-1

20. Mullighan CG. How advanced are we in targeting novel subtypes of ALL? *Best Pract Res Clin Haematol*. (2019) 32:101095. doi: 10.1016/j.beha.2019.101095

21. Tasian SK, Hunger SP. Genomic characterization of paediatric acute lymphoblastic leukaemia: an opportunity for precision medicine therapeutics. *Br J Haematol*. (2017) 176:867–82. doi: 10.1111/bjh.14474

22. Tran TH, Hunger SP. The genomic landscape of pediatric acute lymphoblastic leukemia and precision medicine opportunities. In: *Seminars in Cancer Biology*, vol. 84. London, United Kingdom: Academic Press (2022). p. 144–52. doi: 10.1016/j.semcancer.2020.10.013

23. Cao W, Li N, Wang G, Xu H, Yang Y, Wang J, et al. Efficacy and safety comparison of CAR-T and blinatumomab immunotherapy as bridge-to-transplant strategies in relapsed/refractory B cell acute lymphoblastic leukemia. *J Trans Med*. (2025) 23:391. doi: 10.1186/s12967-025-06399-1

24. Hunger SP, Mullighan CG. Acute lymphoblastic leukemia in children. *New Engl J Med*. (2015) 373:1541–52. doi: 10.1056/NEJMra1400972

25. Schultz KR, Bowman WP, Aledo A, Slayton WB, Sather H, Devidas M, et al. Improved early event-free survival with imatinib in Philadelphia chromosome - Positive acute lymphoblastic leukemia: A Children's Oncology Group Study. *J Clin Oncol*. (2009) 27:5175–81. doi: 10.1200/JCO.2008.21.2514

26. *WHO Classification of Tumours: Haematolymphoid Tumours. 5th ed*. Lyon, France: International Agency for Research on Cancer (2022). Available online at: https://tumourclassification.iarc.who.int/chapters/63. (Accessed September 17, 2024).

27. Kumar A, Taghi Khani A, Duault C, Aramburo S, Sanchez Ortiz A, Lee SJ, et al. Intrinsic suppression of type i interferon production underlies the therapeutic efficacy of IL-15-producing natural killer cells in B-cell acute lymphoblastic leukemia. *J ImmunoTherapy Cancer*. (2023) 11. doi: 10.1136/jitc-2022-006649

28. Ferrari B, Peyvandi F. Activated natural killer cells predict poor clinical prognosis in high-risk B- and T-cell acute lymphoblastic leukemia. *Blood*. (2020) 136:2125–32. doi: 10.1182/BLOOD.2019000962

29. Ocadlikova D, Lussana F, Fracchiolla N, Bonifacio M, Santoro L, Delia M, et al. Blinatumomab differentially modulates peripheral blood and bone marrow immune cell repertoire: A Campus ALL study. *Br J Haematology*. (2023) 203:637–50. doi: 10.1111/bjh.19104

30. Locatelli F, Zugmaier G, Rizzari C, Morris JD, Gruhn B, Klingebiel T, et al. Effect of blinatumomab *vs* chemotherapy on event-free survival among children with high-risk first-relapse B-cell acute lymphoblastic leukemia: a randomized clinical trial. *JAMA*. (2021) 325:843–54. doi: 10.1001/jama.2021.098741

31. Lyons KU, Gore L. Bispecific T-cell engagers in childhood B-acute lymphoblastic leukemia. In: *Haematologica*, vol. 109. Pavia, Italy: Ferrata Storti Foundation (2024). p. 1668–9. doi: 10.3324/haematol.2023.283818

32. Aldoss I, Song J, Stiller T, Nguyen T, Palmer J, O'Donnell M, et al. Correlates of resistance and relapse during blinatumomab therapy for relapsed/refractory acute lymphoblastic leukemia. *Am J Hematol*. (2017) 92:858–65. doi: 10.1002/ajh.24783

33. von Stackelberg A, Locatelli F, Zugmaier G, Handgretinger R, Trippett TM, Rizzari C, et al. Phase I/phase II study of blinatumomab in pediatric patients with relapsed/refractory acute lymphoblastic leukemia. *J Clin Oncol*. (2016) 34:4381–9. doi: 10.1200/jco.2016.67.3301

34. Cabannes-Hamy A, Brissot E, Leguay T, Huguet F, Chevallier P, Hunault M, et al. High tumor burden before blinatumomab has a negative impact on the outcome of adult patients with B-cell precursor acute lymphoblastic leukemia. A real-world study by the GRAALL. *Haematologica*. (2022) 107:2072–80. doi: 10.3324/haematol.2021.280078

35. Shi YJ, Han Y, Wang Y, Mao DF, Zhang JL, Xi R, et al. Analysis on the clinical efficacy and adverse reactions of blinatumomab for the treatment of relapsed/refractory acute lymphoblastic leukemia. *Zhonghua Xue Ye Xue Za Zhi = Zhonghua Xueyexue Zazhi*. (2023) 44:516–9. doi: 10.3760/cma.j.issn.0253-2727.2023.06.015

36. Li XL, Liu LP, Liu F, Guo Y, Chen XJ, Zhu XF, et al. Safety and short-term effectiveness of blinatumomab in the treatment of childhood relapsed/refractory acute lymphoblastic leukemia. *Chin J Contemp Pediatr*. (2023) 25:374–80. doi: 10.7499/j.issn.1008-8830.2210114

37. Pu Y, Zhou X, Liu Y, Kong X, Han J, Zhang J, et al. Clinical efficacy and safety of blinatumomab bridging CAR- T cell therapy in the treatment of patients with adult acute B-cell lymphoblastic leukemia. *Chin J Hematol*. (2024) 45:339–44. doi: 10.3760/cma.j.cn121090-20231127-00283

38. Huo Y, Sheng Z, Lu DR, Ellwanger DC, Li CM, Homann O, et al. Blinatumomab-induced T cell activation at single cell transcriptome resolution. *BMC Genomics*. (2021) 22:372. doi: 10.1186/s12864-021-07435-2

39. Yin H, Huo Y, Sheng Z, Li CM, Ren R. Blinatumomab-induced t cell activation at single cell transcriptome resolution. *Blood*. (2019) 134:3886–6. doi: 10.1182/blood-2019-124636

40. Duell J, Dittrich M, Bedke, Mueller T, Eisele F, Rosenwald A, et al. Frequency of regulatory T cells determines the outcome of the T-cell-engaging antibody blinatumomab in patients with B-precursor ALL. *Leukemia* 31(10):2181–90. doi: 10.1038/leu.2017.41

41. Aldoss I, Otoukesh S, Zhang J, Mokhtari S, Ngo D, Mojtahedzadeh M, et al. Extramedullary disease relapse and progression after blinatumomab therapy for treatment of acute lymphoblastic leukemia. *Cancer*. (2022) 128:529–35. doi: 10.1002/cncr.33967

42. Myers RM, Taraseviciute A, Steinberg SM, Lamble AJ, Sheppard J, Yates B, et al. Blinatumomab nonresponse and high-disease burden are associated with inferior outcomes after CD19-CAR for B-ALL. *J Clin Oncol*. (2021) 40:932–44. doi: 10.1200/JCO.21

43. Feucht J, Kayser S, Gorodezki D, Hamieh M, Döring M, Blaeschke F, et al. T-cell responses against CD19+ pediatric acute lymphoblastic leukemia mediated by bispecific T-cell engager (BiTE) are regulated contrarily by PD-L1 and CD80/CD86 on leukemic blasts. *Oncotarget*. (2016) 7:76902–19. doi: 10.18632/oncotarget.12357

44. Qi Y, Liu H, Li X, Shi Y, Mu J, Li J, et al. Blinatumomab as salvage therapy in patients with relapsed/refractory B-ALL who have failed/progressed after anti-CD19-CAR T therapy. *Ann Med*. (2023) 55. doi: 10.1080/07853890.2023.2230888

45. Locatelli F, Shah B, Thomas T, Velasco K, Adedokun B, Aldoss I, et al. Incidence of CD19-negative relapse after CD19-targeted immunotherapy in R/R BCP acute lymphoblastic leukemia: a review. *Leuk Lymphoma*. (2023) 64:1515–633. doi: 10.1080/10428194.2023.2232496

46. Semchenkova A, Mikhailova E, Komkov A, Gaskova M, Abasov R, Matveev E, et al. Lineage conversion in pediatric B-Cell precursor acute leukemia under blinatumomab therapy. *Int J Mol Sci*. (2022) 23:4019. doi: 10.3390/ijms23074019

47. Wyatt KD, Bram RJ. Immunotherapy in pediatric B-cell acute lymphoblastic leukemia. In: *Human Immunology*, New York, NY, USA: Elsevier Inc (2019). p. 400–8. doi: 10.1016/j.humimm.2019.01.011

48. Lee DW, Santomasso BD, Locke FL, Ghobadi A, Turtle CJ, Brudno JN, et al. ASTCT consensus grading for cytokine release syndrome and neurologic toxicity associated with immune effector cells. *Biol Blood Marrow Transplant*. (2019) 25:625–38. doi: 10.1016/j.bbmt.2018.12.758

49. Lee DW, Santomasso BD, Locke FL, Ghobadi A, Turtle CJ, Brudno JN, et al. ASTCT consensus grading for cytokine release syndrome and neurologic toxicity associated with immune effector cells. In: *Biology of Blood and Marrow Transplantation*, New York, NY, USA: Elsevier Inc (2019). p. 625–38. doi: 10.1016/j.bbmt.2018.12.758

50. Ojemolon PE, Kalidindi S, Ahlborn TA, Aihie OP, Awoyomi MI. Cytokine release syndrome following blinatumomab therapy. *Cureus*. (2022) 14(2). doi: 10.7759/cureus.21583

51. Topp MS, Gökbuget N, Zugmaier G, Klappers P, Stelljes M, Neumann S, et al. Phase II trial of the anti-CD19 bispecific T cell-engager blinatumomab shows hematologic and molecular remissions in patients with relapsed or refractory B-precursor acute lymphoblastic leukemia. *J Clin Oncol*. (2014) 32:41344140. doi: 10.1200/JCO.2014.56.3247

52. Jain T, Litzow MR. Management of toxicities associated with novel immunotherapy agents in acute lymphoblastic leukemia. *Ther Adv Hematol*. (2020) 11:204062071989989. doi: 10.1177/2040620719899897

53. Marrapodi MM, Mascolo A, di Mauro G, et al. The safety of blinatumomab in pediatric patients with acute lymphoblastic leukemia: a systematic review and meta-analysis. *Front Pediatr*. (2022) 10:929122. doi: 10.3389/fped.2022.929122

54. Jabbour E, Zugmaier G, Agrawal V, Martínez-Sánchez P, Rifón Roca JJ, Cassaday RD, et al. Single agent subcutaneous blinatumomab for advanced acute lymphoblastic leukemia. *Am J Hematol*. (2024) 99:586–95. doi: 10.1002/ajh.27227

frontiers | Frontiers in Immunology

TYPE Original Research
PUBLISHED 12 August 2025
DOI 10.3389/fimmu.2025.1625813

OPEN ACCESS

EDITED BY
Miroslawa Puskulluoglu,
Maria Sklodowska-Curie National Research Institute of Oncology, Poland

REVIEWED BY
Stefano Ugel,
University of Verona, Italy
Ilona Hagelstein,
Tübingen University Hospital, Germany
Dennis Awuah,
City of Hope National Medical Center, United States

*CORRESPONDENCE
Xin Chen
chenxin1990@webmail.hzau.edu.cn
Kangkang Ji
kyrie@mail.ustc.edu.cn

RECEIVED 09 May 2025
ACCEPTED 24 July 2025
PUBLISHED 12 August 2025

CITATION
Ma X, He H, Zhu Y, Zuo D, Wang F, Feng M, Ji K and Chen X (2025) Dual T/NK cell engagement via B7-H6-targeted bispecific antibodies and IL-15 eradicates chemo-resistant solid tumors.
Front. Immunol. 16:1625813.
doi: 10.3389/fimmu.2025.1625813

Dual T/NK cell engagement via B7-H6-targeted bispecific antibodies and IL-15 eradicates chemo-resistant solid tumors

Xuqian Ma[1,2], Huixia He[2], Yuankui Zhu[2], Dianbao Zuo[1,3], FangLin Wang[1], Mingqian Feng[1,2], Kangkang Ji[1,4]* and Xin Chen[2,5]*

[1]College of Life Science and Technology, Huazhong Agricultural University, Wuhan, Hubei, China, [2]College of Biomedicine and Health, Huazhong Agricultural University, Wuhan, Hubei, China, [3]Research Center for Translational Medicine, Xiangyang No.1 People's Hospital, Hubei University of Medicine, Xiangyang, China, [4]Department of Clinical Medical Research, Binhai County People's Hospital, Clinical Medical College of Yangzhou University, Yancheng, Jiangsu, China, [5]School of Life and Health Sciences, Hubei University of Technology, Wuhan, Hubei, China

Introduction: B7-H6, a tumor-specific immune checkpoint molecule within the B7 family, represents a promising therapeutic target due to its selective overexpression in malignancies and negligible expression in normal tissues.
Method: Here, we developed bispecific antibodies (BsAbs) targeting B7-H6 to redirect T and NK cells against solid tumors. Through phage display, 15 high-affinity B7-H6 monoclonal antibodies were generated.
Results: Two optimized BsAbs, B7-H6M4-OKT3 (T cell-engaging) and B7-H6M4-LC21 (NK cell-engaging), were constructed in and scFv-hFc-scFv format. Both demonstrated nanomolar affinity (EC50: 0.04–1.22 nM) and selective cytotoxicity against B7-H6+ cells (H446, Huh-7, HepG2), while showing minimal cytotoxicity against B7-H6-negative cells (A431). B7-H6M4LC21 exhibited enhanced tumor-killing efficacy (IC50: 5 ng/mL) compared to B7H6M4-OKT3(IC50: 1 ng/mL) when combined with an IL-15/IL-15Ra sushi fusion protein, which augmented NK cell proliferation and cytotoxicity. In H446 xenograft models, both BsAbs suppressed tumor growth in a dose-dependent manner (0.1–20 mg/kg) without significant toxicity. Combination therapy with B7-H6M4-LC21 (10 mg/kg) and B7-H6M18/IL-15/IL-15Ra sushi (0.03 mg/kg) achieved synergistic tumor inhibition ($p<0.05$), surpassing the efficacy of T cell-based combinations.
Discussion: These findings establish B7-H6-targeted BsAbs combined with cytokine engineering as a viable strategy for treating refractory solid tumors.

KEYWORDS

B7-H6, bispecific antibodies, NK cells, IL-15Rα sushi, solid tumor

1 Introduction

The B7 family of immune checkpoint proteins plays critical roles in tumor immune evasion, among which B7-H6 (NCR3LG1) has garnered significant attention as a tumor-selective antigen due to its minimal expression in healthy tissues and aberrant overexpression across multiple malignancies, including lung, hepatic, and pancreatic carcinomas (1–3). Distinct from PD-L1 or CTLA-4 that predominantly regulate T cell activity, B7-H6 directly activates natural killer (NK) cell cytotoxicity via NKp30 engagement—a mechanism circumventing T cell-centric immunosuppression (4, 5). This unique biological property positions B7-H6 as a strategic target for bispecific antibody (BsAb) platforms designed to coordinate innate and adaptive immune responses.

Despite the clinical success of CD3-directed BsAbs (e.g., mosunetuzumab, teclistamab) in hematologic malignancies, their efficacy in solid tumors remains constrained by insufficient T cell infiltration, immunosuppressive stromal components, and cytokine depletion (6–8). While CD16-targeted BsAbs (e.g., AFM13) demonstrate enhanced safety and allogeneic potential for NK cell engagement, their therapeutic impact is limited by poor NK cell persistence within hostile tumor microenvironments (TMEs) (9, 10). These challenges highlight the imperative for combinatorial approaches integrating BsAb-mediated tumor targeting with cytokine support to sustain effector cell functionality. IL-15, a pleiotropic cytokine essential for NK and $CD8^+$ T cell homeostasis, holds therapeutic potential but is hampered by systemic toxicity and transient bioavailability (11, 12). Engineered IL-15/IL-15Rα heterodimers (e.g., N-803) mitigate but incompletely resolve these limitations through stabilized receptor interactions, while lacking spatial control over cytokine activity (13–16). Unrestricted IL-15 delivery risks off-target Treg activation, underscoring the necessity for tumor-localized cytokine delivery systems (17).

Recent advances in antibody-cytokine fusion technology, exemplified by PD-L1/IL-12 conjugates, demonstrate enhanced therapeutic precision through tumor-directed cytokine activation (18, 19). However, this paradigm remains unexplored for B7-H6-targeted therapies. To address this gap, we developed a modular immunotherapy platform combining B7-H6-specific BsAbs with a tumor-anchored IL-15/IL-15Rα sushi fusion protein. Through phage display screening, we identified 15 high-affinity B7-H6 monoclonal antibodies and engineered T/NK cell-engaging BsAbs (B7-H6M4-OKT3 and B7-H6M4-LC21, scFv-hFc(N297A)-scFv architecture) with nanomolar binding affinity. The B7-H6M18/IL-15/IL-15Rα sushi fusion protein enables tumor-localized cytokine activation while preserving effector cell specificity. Our findings demonstrate superior synergy between NK cell-redirected BsAbs and IL-15 fusion, achieving >90% tumor lysis *in vitro* and significant regression in xenograft models. This work establishes three key advances: (1) B7-H6-dependent spatial restriction of IL-15 activity, (2) dual T/NK cell engagement to combat effector heterogeneity, and (3) modular designs permitting flexible cytokine pairing. By simultaneously addressing spatial, temporal, and cellular barriers to immune efficacy, this strategy transforms B7-H6 from a passive target into an active orchestrator of precision immunotherapy.

2 Materials and methods

2.1 Cell lines and culture conditions

Human hepatocellular carcinoma (HepG2, Hep3B, Huh-7), pancreatic adenocarcinoma (PANC-1, KLM-1, T3M4, MiaPaCa-2), breast carcinoma (SKBR-3, ZR75, MCF-7, MDA-MB-231), lung carcinoma (H446, H82, H196, H226, H1975, H1299, PC9, H292, H358), and epidermal carcinoma (A431) cell lines were procured from the Cell Bank of the Chinese Academy of Sciences (Shanghai, China). All lines underwent short tandem repeat (STR) authentication and mycoplasma screening (PlasmoTest™, Invivogen). Cells were maintained in DMEM or RPMI-1640 medium (Invitrogen) supplemented with 10% fetal bovine serum (HyClone), 1% L-glutamine, and 1% penicillin-streptomycin at 37°C under 5% CO_2. Lentiviral transduction using a full-length human B7-H6 construct (GeneChem) generated stable B7-H6-expressing A431(B7-H6) cells, with parental A431 serving as negative controls.

2.2 Western blot

Cells were washed twice with PBS and lysed in buffer containing 50 mM Tris–HCl (pH 7.5), 50 mM NaCl, 5 mM EDTA, 1% Triton X-100, and protease inhibitor cocktail (Roche Applied Science). Lysates were agitated at 4°C for 30 min, centrifuged at 12,000 × g for 15 min, and protein concentrations determined via BCA assay (Pierce). Fifty micrograms of total protein per sample was resolved by SDS-PAGE under reducing conditions and transferred to PVDF membranes for immunoblotting.

2.3 Isolation of lymphocyte populations

Human PBMCs were isolated from whole blood of healthy donors (Wuhan Blood Center) by Ficoll separation (Stem Cell Technologies, Vancouver, BC, Canada) according to the manufacturer's instruction. Total T cells were then isolated using a Pan T Cell Isolation Kit II (human, Miltenyi Biotec) through negative selection. Human NK cells were isolated from PBMCs by negative selection using magnetic-activated cell sorting (MACS) with a human NK Cell Isolation Kit (Miltenyi Biotec).

2.4 Dual-color flow cytometry for detection of $CD69^+$ T and NK cells in PBMC co-cultures

Following 24-hour treatments, PBMCs per group were harvested and washed twice by centrifugation (300 × g, 5 min at 4°C), then

resuspended in ice-cold PBS containing 5% BSA. For the purpose of T cell analysis, PBMCs were initially incubated with b12-OKT3 (anti-CD3, 5 μg/mL) in PBS/5% BSA for 30 minutes on ice, followed by a single wash with 2 mL cold PBS via centrifugation (300 × g, 5 minutes, 4°C). Subsequently, the samples were incubated with Cy5-conjugated goat anti-human IgG (1:500; Sangon Biotech, Shanghai) on ice under conditions that protected them from light. Following an additional PBS wash, final staining was performed using mouse anti-human CD69-FITC (1:100 dilution; ZenBio) for 30 minutes on ice prior to flow cytometric analysis. For the purpose of NK cell analysis, PBMCs were initially incubated with CD16M39-HisFlag (20) (5 μg/mL) in PBS/5% BSA for 30 minutes on ice, followed by a single wash with 2 mL cold PBS via centrifugation (300 × g, 5 minutes, 4°C). Subsequently, the samples were subjected to incubation with an Alexa Fluor 647-conjugated anti-Flag antibody (1:500 dilution; BioLegend) for a duration of 30 minutes at 0°C under conditions that provided protection from light. This antibody was designed to target the Flag-tag of bound CD16M39-HF. Following an additional PBS wash, final staining was performed using mouse anti-human CD69-FITC (1:100 dilution; ZenBio) for 30 minutes on ice prior to flow cytometric analysis. Immediate analysis of all samples was conducted on a CytoFLEX S flow cytometer (Beckman Coulter, USA) utilizing a gating strategy that firstly categorized lymphocytes as live singlets, followed by the identification of the CD3 positive population for T cells (CD69 quantification) or the CD16 positive population for NK cells (CD69 quantification). A minimum of 10,000 gated events per sample were collected for the analysis.

2.5 Antibody development

2.5.1 B7-H6 monoclonal antibody production

The extracellular domain of human B7-H6 (NP_001189368.1, a.a. 25-262) was fused with 6 × His tag and expressed in HEK-293F cells and purified using Ni-NTA affinity chromatography (Qiagen). The Amino acid sequence of the B7-H6 extracellular domain: DLKVEMMAGGTQITPLNDNVTIFCNIFYSQPLNITSMGITWF WKSLTFDKEVKVFEFFGDHQEAFRPGAIVSPWRLKSGDASL RLPGIQLEEAGEYRCEVVVTPLKAQGTVQLEVVASPASRLLLD QVGMKENEDKYMCESSGFYPEAINITWEKQTQKFPHPIEISED VITGPTIKNMDGTFNVTSCLKLNSSQEDPGTVYQCVVRHA SLHTPLRSNFTLTAARHSLSETEKTDNFS. BALB/c mice (n=6) were immunized subcutaneously with 50 μg B7-H6-His emulsified in Freund's adjuvant (Sigma) over six weeks. Splenic mRNA was reverse-transcribed, and scFv phage display libraries were constructed for three rounds of panning against immobilized B7-H6-His as previously described (21). Phage display yielded 15 high-affinity mAbs. And the antibody produced as scFv-rFc.

2.5.2 Bispecific antibody construction

Variable domains from B7-H6 mAbs (M4 for NK-targeting BsAbs, Mx for T-cell targeting BsAbs), CD3ε (OKT3), and CD16a (LC21) were cloned into a scFv-hFc(N297A)-scFv backbone. The B7-H6M18/IL-15/IL-15Rα sushi fusion protein was engineered with human Fc(N297A) linking the B7-H6M18 scFv and IL-15/IL-15Rα sushi domain. Anti-HIV scFv b12 (VH and VL sequences are from 2NY7_H and 2NY7_L, respectively) was used to make an irrelevant control. Constructs were transiently transfected into HEK-293F cells using polyethylenimine (PEI, Polysciences), with culture supernatants harvested at 120 h post-transfection. Proteins were purified by Protein A affinity chromatography (Cytiva) and analyzed via non-reducing SDS-PAGE.

2.6 Binding characterization

2.6.1 ELISA

96-well plates (Corning) were coated with 5 μg/mL B7-H6-His overnight at 4°C, blocked with 5% BSA, and incubated with serially diluted antibodies (0.001–100 nM). Binding was detected using HRP-conjugated goat anti-human IgG (1:5,000; Sangon Biotech) and TMB substrate (Thermo Fisher), with absorbance measured at 450 nm (BioTek Synergy H1).

2.6.2 Flow cytometry

Cells (1×10^6/mL) were stained with 5 μg/mL antibodies in PBS/5% BSA for 30 min at 4°C. After washing, samples were incubated with Cy5-conjugated goat anti-human IgG (1:500; Sangon Biotech) and analyzed on a CytoFLEX S flow cytometer (Beckman Coulter). Data processing utilized FlowJo v10 software.

2.7 Functional assays

2.7.1 *In vitro* cytotoxicity

Tumor cells stably expressing firefly luciferase (ffLuc2) were plated in 96-well plates (5×10^3 cells/well). Freshly isolated human PBMCs (Wuhan Blood Center) were added at effector-to-target (E:T) ratios of 10:1. This outcome was attributed to the laboratory's prior publication on bispecific antibodies (22). The findings indicated that an effector-to-target ratio of 10:1 was an optimal choice, as it exhibited substantial tumor-killing capability against positive tumor cells, i.e., antibody dose-dependent cell killing, while concomitantly evading pronounced non-specific killing. Antibodies or fusion proteins were incubated with the cells at variable concentrations starting from 10,000 ng/mL and followed by 1:10 serial dilutions. After 48 h, residual luciferase activity was quantified using the Bright-Glo™ Assay System (Promega) on a SpectraMax M5 microplate reader (Molecular Devices). Cytotoxicity was calculated as: Cytotoxicity (%) = $[(1 - (\text{luminescence}_{\text{sample}}/\text{luminescence}_{\text{control}})] \times 100$.

2.7.2 *In vivo* efficacy

All animal procedures were approved by the Huazhong Agricultural University Animal Care Committee. Female NSG mice (6-week-old, Vital River Laboratories) received subcutaneous injections of 5×10^6 H446 cells. When tumors reached ~100 mm^3, mice were pretreated with intraperitoneal cyclophosphamide (100 mg/kg) for lymphocyte depletion. Weekly intravenous PBMC infusions (1×10^7 cells) and bispecific antibody administration (0.1–20 mg/kg every 4

days) were performed. Tumor volumes were calculated as (length × width^2)/2 using caliper measurements. Body weights were monitored biweekly for toxicity assessment.

2.8 Statistical analysis

Data represent mean ± SEM. Two-group comparisons utilized unpaired Student's t-tests (two-tailed). Multiple groups were analyzed by one-way ANOVA with Tukey's *post hoc* test (GraphPad Prism 9). Statistical significance was defined as $p < 0.05$.

3 Results

3.1 Tumor-selective B7-H6 expression patterns

Western blot and flow cytometry analyses revealed differential B7-H6 expression patterns across solid tumor cell lines (Figure 1). Among lung cancer models, nine cell lines (H446, H82, H196, H226, H1975, H1299, PC9, H358, H292) demonstrated detectable B7-H6 expression, while A549 and H1703 remained negative (Figure 1A). Hepatocellular carcinoma (Hep3B, Huh-7, HepG2), pancreatic adenocarcinoma (PANC-1, KLM-1, T3M4, MiaPaCa-2), and MCF-7 breast cancer cells exhibited strong B7-H6 positivity, contrasting with negative expression in SKBR-3, ZR75, and MDA-MB-231 lines. Lentiviral-transduced A431(B7-H6) cells served as stable overexpression controls, while parental A431 cells confirmed baseline negativity (Figure 1B). This expression profile corroborates previous reports of tumor-restricted B7-H6 distribution (4).

3.2 Development and characterization of B7-H6-specific mAbs

The recombinant B7-H6 extracellular domain (B7-H6-His) expressed in HEK-293F cells showed an apparent molecular weight of ~42 kDa via SDS-PAGE (theoretical 28.1 kDa), consistent with post-translational glycosylation (Figure 2A). The phage display library was subjected to four rounds of panning, with the input and output of each round illustrated in Figure 2B. It was observed that there was an enrichment of specific antibody sequences at various points throughout the panning rounds. Phage display yielded 15 high-affinity mAbs (M4, M9, M14, M18, M26, M39, M44, M49, M53, M56, M59, M65, M73, M88, M90) (Figure 2C). The antibody produced as scFv-rFc fusions with >90% purity (Figure 2C). ELISA quantification revealed sub-nanomolar binding affinities (EC50: 0.02–0.43 nM; Figure 2D). Flow cytometric screening confirmed tumor-specific recognition, with M4 demonstrating superior specificity, while M90 was excluded due to non-specific binding (Figure 2E).

3.3 Bispecific antibody binding characteristics

Ten scFv-hFc(N297A)-scFv format B7-H6/CD3 bispecific antibodies (BsAbs) demonstrated proper assembly and >90% purity by SDS-PAGE (Figures 3A, B). ELISA binding analyses showed nanomolar-range affinity for B7-His (EC50: 0.04–1.22 nM; Figure 3C). Flow cytometry confirmed dual specificity: B7-H6M53-OKT3 selectively bound B7-H6$^+$ tumor cells (A431(B7-H6), H446, Huh-7) and PBMCs, while maintaining specificity against B7-H6-negative controls (Figure 3D).

3.4 T B7-H6/CD3 BsAb cytotoxic activitys

At 10:1 E:T ratio, B7-H6M4-OKT3 induced significant target cell lysis in B7-H6$^+$ lines (H446: 85% ± 3.2%; A431(B7-H6): 78% ± 2.8%; Huh-7: 72% ± 4.1%; HepG2: 68% ± 3.5%), while showing minimal activity against B7-H6-negative A431 cells (Figures 4A–F). Dose-response analyses revealed superior potency of B7-H6M4-OKT3 (IC50: 1.0 nM) compared to other BsAbs (IC50: 2.5–8.0 nM).

3.5 NK cell synergy with IL-15 fusion protein

Purified proteins (>90% purity by SDS-PAGE; Figure 5A) demonstrated high B7-H6-His affinity (EC50: 0.01–0.1 nM), with control b12/CD3 showing no binding (Figure 5B). B7-H6M4-LC21 (NK-engaging BsAb) mediated 60% ± 2.3% H446 lysis at 10 ng/mL (IC50: 5 ng/mL). Co-administration with B7-H6M18/IL-15/IL-15Rα sushi (0.1 nM) enhanced cytotoxicity to 90% ± 1.8% ($p < 0.01$ vs monotherapy; Figures 5D, E). Flow cytometry confirmed simultaneous engagement of B7-H6$^+$ tumors and PBMCs (Figure 5C).

3.6 Bispecific antibodies M4-OKT3 and M4-LC21 mediate targeted engagement and functional activation of T and NK effector cells

Flow cytometry analysis confirmed specific binding of M4-OKT3 to purified T cells and M4-LC21 to purified NK cells (Figure 6A), demonstrating effective target engagement by both bispecific antibodies. To assess functional activation, surface CD69 expression—an early activation marker—was quantified on T cells (gated as CD3$^+$ lymphocytes) and NK cells (gated as CD16$^+$ lymphocytes) in PBMC-tumor co-culture systems using multiparameter staining with anti-CD3/anti-CD69 and anti-CD16/anti-CD69 antibody pairs.B7-H6M4-OKT3 significantly upregulated CD69 on T cells (Figure 6B), while B7-H6M4-LC21 potently induced CD69 expression on NK cells (Figure 6C). The B7-

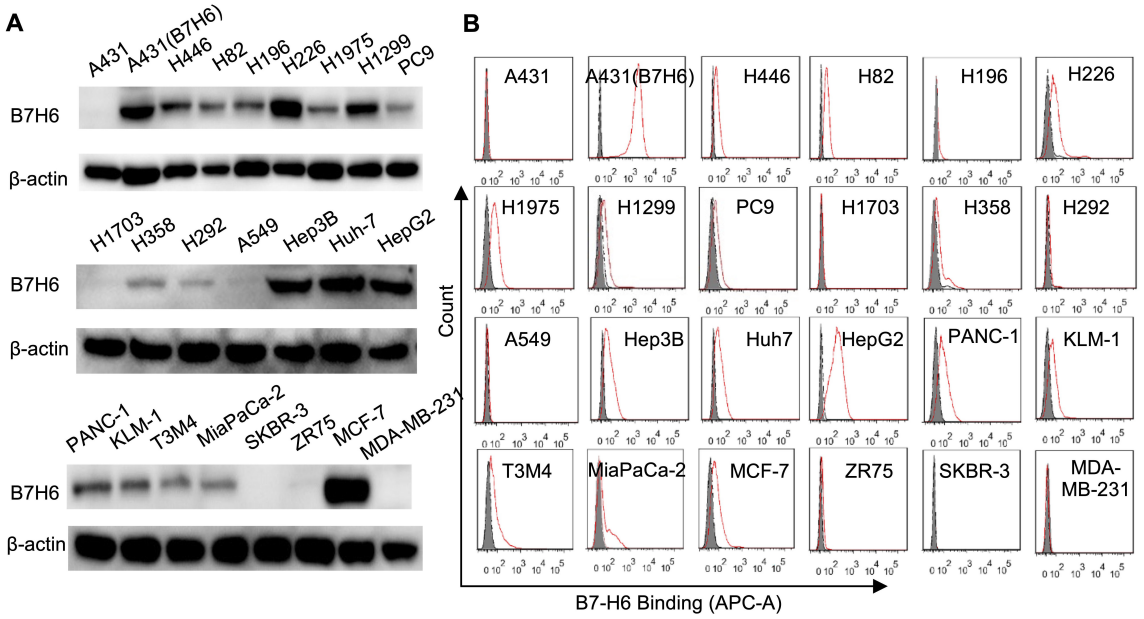

FIGURE 1
Comparative analysis of B7-H6 protein expression across solid tumor cell lines. **(A)** Western blot analysis of B7-H6 protein expression in lung cancer (H446, H82, H196, H226, H1975, H1299, PC9, H1703, H358, H292, A549), hepatocellular carcinoma (Hep3B, Huh7, HepG2), pancreatic adenocarcinoma (PANC-1, KLM-1, T3M4, MiaPaCa-2), and breast carcinoma (SKBR-3, ZR75, MCF-7, MDA-MB-231) cell lines. A431 epidermal carcinoma cells served as B7-H6-negative controls, while lentiviral-transduced A431(B7-H6) stable transfectants were used as positive controls. Total protein lysates (50 μg/lane) were resolved by SDS-PAGE under reducing conditions and probed with HRP-conjugated goat anti-rabbit IgG (1:5,000). β-Actin served as the loading control. **(B)** Flow cytometric quantification of surface B7-H6 expression. Cells were incubated with 5 μg/mL primary B7-H6-specific antibody followed by Cy5-conjugated goat anti-rabbit IgG (1:500). Shaded histograms represent untreated controls; red lines indicate antibody-treated groups.

H6M18/IL-15/IL-15Rα sushi activated both T and NK cell populations (Figures 6C, D). Consistent with these findings, B7-H6M4-OKT3 showed the highest CD69 induction among T cell-targeting agents (Supplementary Figure S1), and B7-H6M4-LC21 demonstrated superior activation of NK cells (Supplementary Figure S2). Collectively, these results establish that M4-OKT3 and M4-LC21 bispecific antibodies selectively engage and activate their respective effector cells (T and NK lymphocytes) within PBMC, enabling potent cytotoxic function against tumor targets.

3.7 Combination therapy efficacy and safety profile

In H446 xenografts, B7-H6M4-OKT3 (1.0 mg/kg) and B7-H6M4-LC21 (10 mg/kg) monotherapies achieved 69.5% ± 10.2% and 66.9% ± 11.2% tumor growth inhibition, respectively, versus PBS ($p < 0.05$; Figures 7A, B). B7-H6M18/IL-15/IL-15Rα sushi demonstrated dose-dependent efficacy (0.06 mg/kg: 25.0% ± 7.4% inhibition; 0.5 mg/kg: 57.5% ± 9.0%) with associated toxicity at higher doses (7.4% ± 2.2% weight loss; $p < 0.05$; Figures 7C, D). The combination regimen (B7-H6M4-LC21 + IL-15 fusion) significantly enhanced tumor suppression versus monotherapies (achieved 76.1% ± 14.8% tumor growth inhibition; $p < 0.05$; Figures 7E, F) without significant weight changes at therapeutic doses.

4 Discussion

This study establishes B7-H6 as a therapeutically actionable immune checkpoint in solid malignancies through three principal advances: (1) development of high-affinity bispecific antibodies (BsAbs) redirecting T/NK cells against B7-H6+ tumors, (2) design of a tumor-localized IL-15/IL-15Rα sushi fusion protein to amplify effector cell activity, and (3) identification of NK cell-redirected therapy as the optimal strategy for overcoming immunosuppressive tumor microenvironments (TMEs). Phage display-derived B7-H6M4-OKT3 (T cell-targeting) and B7-H6M4-LC21 (NK cell-targeting) BsAbs demonstrated tumor-selective cytotoxicity with nanomolar binding affinity (EC50: 0.01–1.22 nM). Notably, B7-H6M4-LC21 combined with IL-15 fusion protein elicited synergistic tumor lysis (>90% at 10 ng/mL *in vitro*) and enhanced *in vivo* antitumor efficacy, surpassing T cell-based modalities. These observations align with emerging evidence supporting NK cell engagement to bypass T cell exhaustion and stromal resistance in solid tumors (9, 23). The effectiveness of our B7-H6/IL-15/IL-15Rα sushi fusion further underscores the value of spatial cytokine regulation—a concept validated in recent PD-L1/IL-12 fusion studies (24, 25). Tumor-restricted IL-15 delivery reduced systemic toxicity while enhancing effector cell persistence, a critical advantage for treating chemoresistant malignancies like small-cell lung cancer (SCLC).

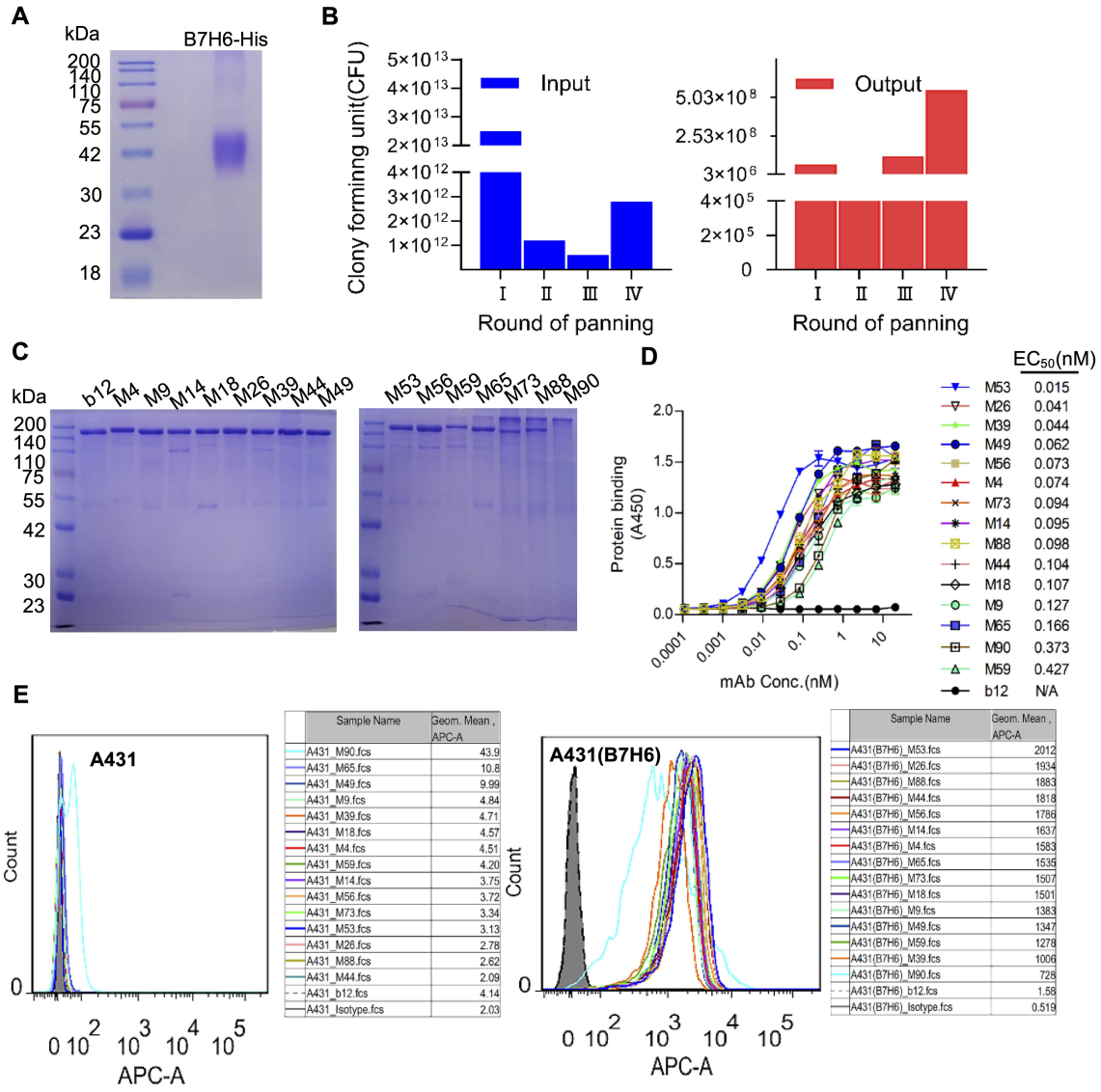

FIGURE 2
Phage display-derived B7-H6-specific monoclonal antibodies show nanomolar affinity. **(A)** SDS-PAGE analysis of purified recombinant B7-H6-His protein under reducing conditions. **(B)** Phage display library screening. Input and output phage titers were quantified via bacterial colony counts. **(C)** Non-reducing SDS-PAGE of scFv-rFc monoclonal antibodies (2 μg/lane), confirming dimeric assembly. **(D)** ELISA-based affinity measurement. Plates coated with 5 μg/mL B7-H6-His were incubated with serially diluted antibodies (0.01–100 nM) and detected using HRP-conjugated goat anti-rabbit IgG (1:5,000). **(E)** Flow cytometric validation of antibody specificity. A431(B7-H6)+ (red line) and A431– (shaded histogram) cells were stained with 5 μg/mL B7-H6 mAbs and Cy5-conjugated goat anti-rabbit IgG (1:500).

4.1 B7-H6 as a tumor-restricted immune checkpoint for solid cancers

B7-H6 has been identified as a marker in various types of cancer, including non-small cell lung cancer (26), small cell lung cancer (2), gastric cancer, pancreatic cancer, colorectal cancer (3), oral squamous cell carcinoma (27), and cervical cancer (28). This finding indicates the possible utilization of B7-H6-targeted therapy in a range of solid tumor indications. Conversely, B7-H6 expression is minimal in normal human tissues. Quantitative RT-PCR analysis of 48 normal human tissues did not detect B7-H6 mRNA expression (4). Immunohistochemistry (IHC) analysis has confirmed that normal pancreatic, colonic, and gastric tissues do not express B7-H6 membrane protein (29). B7-H6/CD3 T cell conjugates (for example, BI 765049) have been shown to bind specifically to tumor cells that express B7-H6. In addition, they have been demonstrated to have no cytotoxic effect on B7-H6-negative cells, thereby reducing off-target toxicity (3).

Systematic analysis of B7-H6 expression confirms its tumor-selective distribution, with negligible detection in normal tissues. Elevated expression in lung (H446, H1299), hepatic (Hep3B, Huh-7), and pancreatic (PANC-1, MiaPaCa-2) carcinomas supports prior associations between B7-H6 and epithelial-mesenchymal transition-driven metastasis (30–32). Heterogeneity observed in breast cancer lines (e.g., MCF-7+ vs. MDA-MB-231–) suggests context-dependent regulation, potentially involving STAT3 or

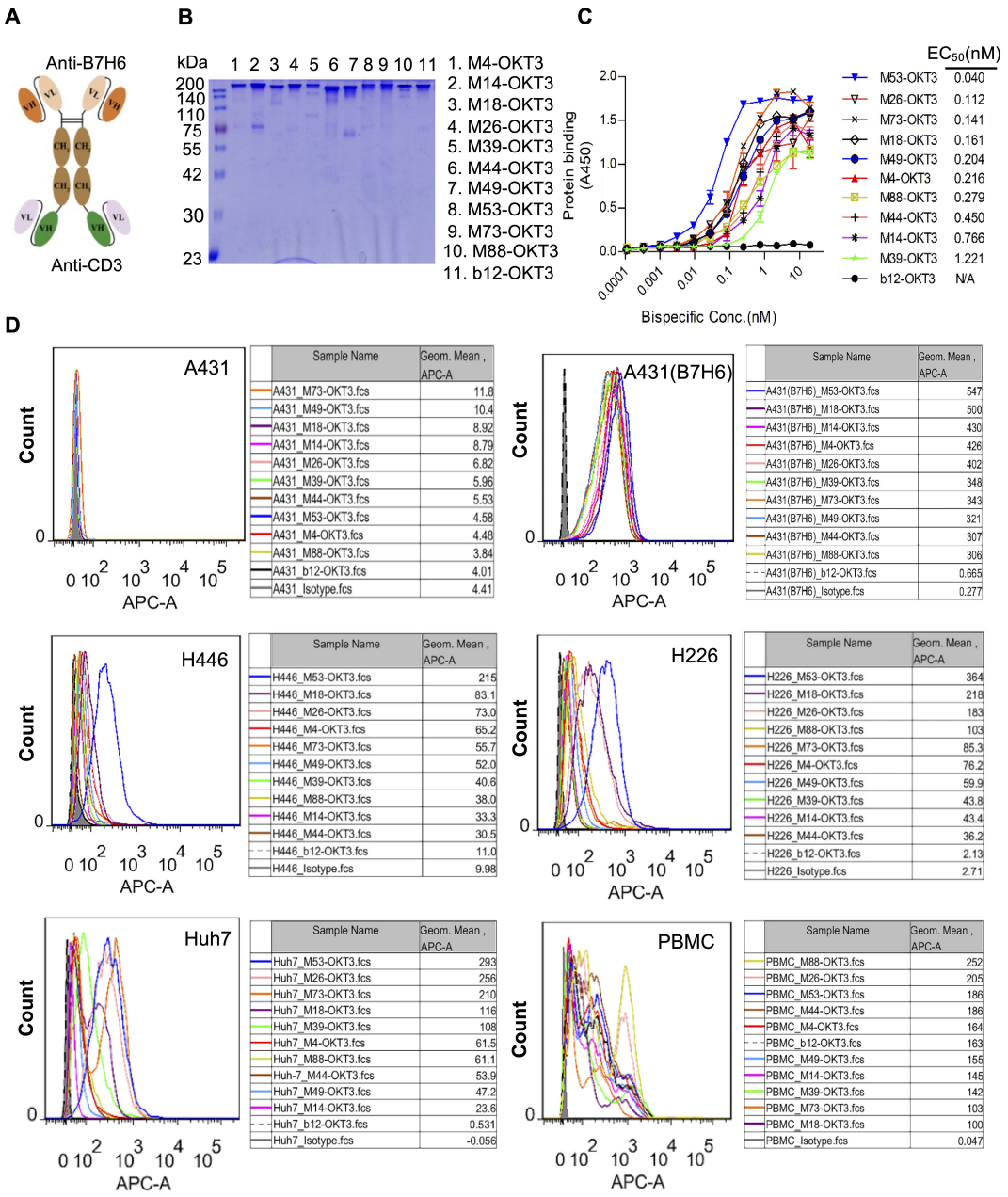

FIGURE 3
Design framework and functional validation of B7-H6/CD3 bispecific antibodies. **(A)** Schematic of the B7-H6/CD3 bispecific antibody (BsAb) architecture. **(B)** Non-reducing SDS-PAGE of purified BsAbs (2 μg/lane), confirming dimeric assembly. **(C)** ELISA affinity assessment. Plates coated with 5 μg/mL B7-H6-His were incubated with serially diluted BsAbs (100 nM starting concentration) and detected using HRP-conjugated goat anti-human IgG (1:5,000). **(D)** Flow cytometric validation of BsAb binding to B7-H6$^+$ tumor cells (A431(B7-H6), H446, H226, Huh7) and healthy donor PBMCs. Cells were stained with 5 μg/mL BsAbs followed by Cy5-conjugated goat anti-human IgG (1:500). Shaded profiles: unstained controls; solid lines: BsAb-treated groups. Isotype control (pooled human IgG).

Wnt/β-catenin signaling (33, 34). This tumor-restricted expression profile, coupled with B7-H6's role in NKp30-mediated NK cell activation (4), establishes its dual utility as both a therapeutic target and diagnostic biomarker. In summary, the low toxicity of B7-H6-targeted therapy is primarily attributable to its tumor-specific expression and precise targeting mechanism, thus rendering it a promising low-toxicity immunotherapy strategy.

4.2 Dual-arm immunotherapy: NK cell engagement outperforms T cell strategies

While T cell-redirecting BsAbs (e.g., B7-H6M4-OKT3) exhibited potent *in vitro* cytotoxicity (IC50: 1 ng/mL), their *in vivo* efficacy plateaued—likely due to limited T cell infiltration, a well-documented challenge in solid tumors (35). In contrast, NK

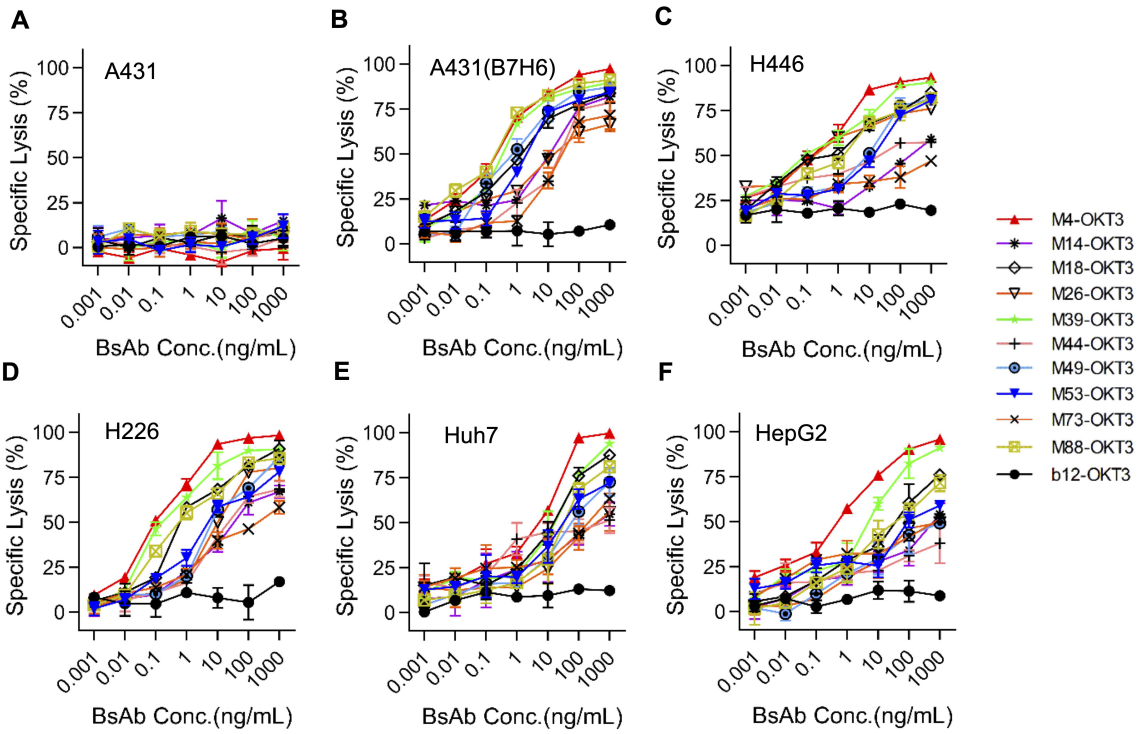

FIGURE 4
B7-H6/CD3 bispecific antibodies induce antigen-dependent cytotoxicity *in vitro*. **(A–F)** Cytotoxic activity of ten B7-H6/CD3 BsAbs against tumor cell lines at an effector-to-target (E:T) ratio of 10:1. Target cells (A431, A431(B7-H6), H446, H226, Huh7, HepG2) stably expressed firefly luciferase (ffLuc2). Residual luminescence inversely correlates with cytotoxicity. A431 (B7-H6^{-}): negative control for antigen-independent killing; *b12*: isotype control. Data represent mean ± SEM.

cell-engaging B7-H6M4-LC21 achieved superior tumor control with reduced cytokine release risk, mirroring outcomes of CD16-targeted BsAbs in lymphoma models (9, 10). This advantage may stem from NK cells' intrinsic ability to lyse MHC-I-deficient tumors and resist TME-mediated suppression (23, 36). Furthermore, IL-15 fusion synergized more robustly with B7-H6M4-LC21 (>90% lysis) than T cell-BsAbs, likely attributable to IL-15's preferential enhancement of NK cell metabolic fitness and granzyme B production (13, 37, 38).

In this study, both T/NK cell-type bispecific antibodies demonstrated significant cytolytic activity and tumor growth inhibition in NSG mice in both *in vitro* experiments and *in vivo* experiments in NSG mice. When the M18 antibody was combined with the IL-15/IL-15Rα fusion protein and the two types of bispecific antibody, significant activity was observed both *in vivo* and *in vitro*. The combination with the NK cell-type bispecific antibody proved to be the most significant. Interleukin-15 (IL-15) is a cytokine that plays a pivotal role in regulating the development, balance, and function of natural killer (NK) cells and T cells (39). The IL-15/IL-15Rα complex signaling pathway is stimulated, thereby promoting the survival, proliferation, and effector functions of NK cells and T cells (39). Consequently, therapeutic IL-15 pathway agonists have the potential to enhance the activity of immunotherapies that induce NK and T cell activity, such as monoclonal antibodies, immune checkpoint inhibitors, and T cell bispecific antibodies, by expanding NK/T cell expansion and enhancing antitumor immune responses.

As demonstrated in previous studies, the combination of XmAb24306 (IL-15/IL-15Rα Fc fusion protein) with T cell bispecific antibodies has been shown to enhance the proliferation and expansion of CD8+ and CD4+ T cells induced by these antibodies (40). The present study hypothesizes that T cell bispecific antibody stimulation can serve as an initiator for XmAb24306, thereby enhancing T cell responsiveness to IL-15. It has been reported that IL-15 can promote TCR sensitization, resulting in stronger T cell responses (41). NK cells have been observed to constitutively overexpress IL-2/15Rβγ (CD122/CD132) on their surface, and it has been demonstrated that IL-15/IL-15Rα can directly bind to this receptor, resulting in the rapid activation of the JAK-STAT5 pathway and the subsequent expression of perforin/granzyme B. In contrast, T cells require higher concentrations of IL-15 and are inhibited by Tregs. Consequently, the combination of NK cell-type bispecific antibodies has been demonstrated to be the most efficacious approach (23, 42).

4.3 Spatial control of IL-15 activity through tumor anchoring

The B7-H6M18/IL-15/IL-15Rα sushi fusion represents an innovative cytokine delivery paradigm. Unlike systemic IL-15

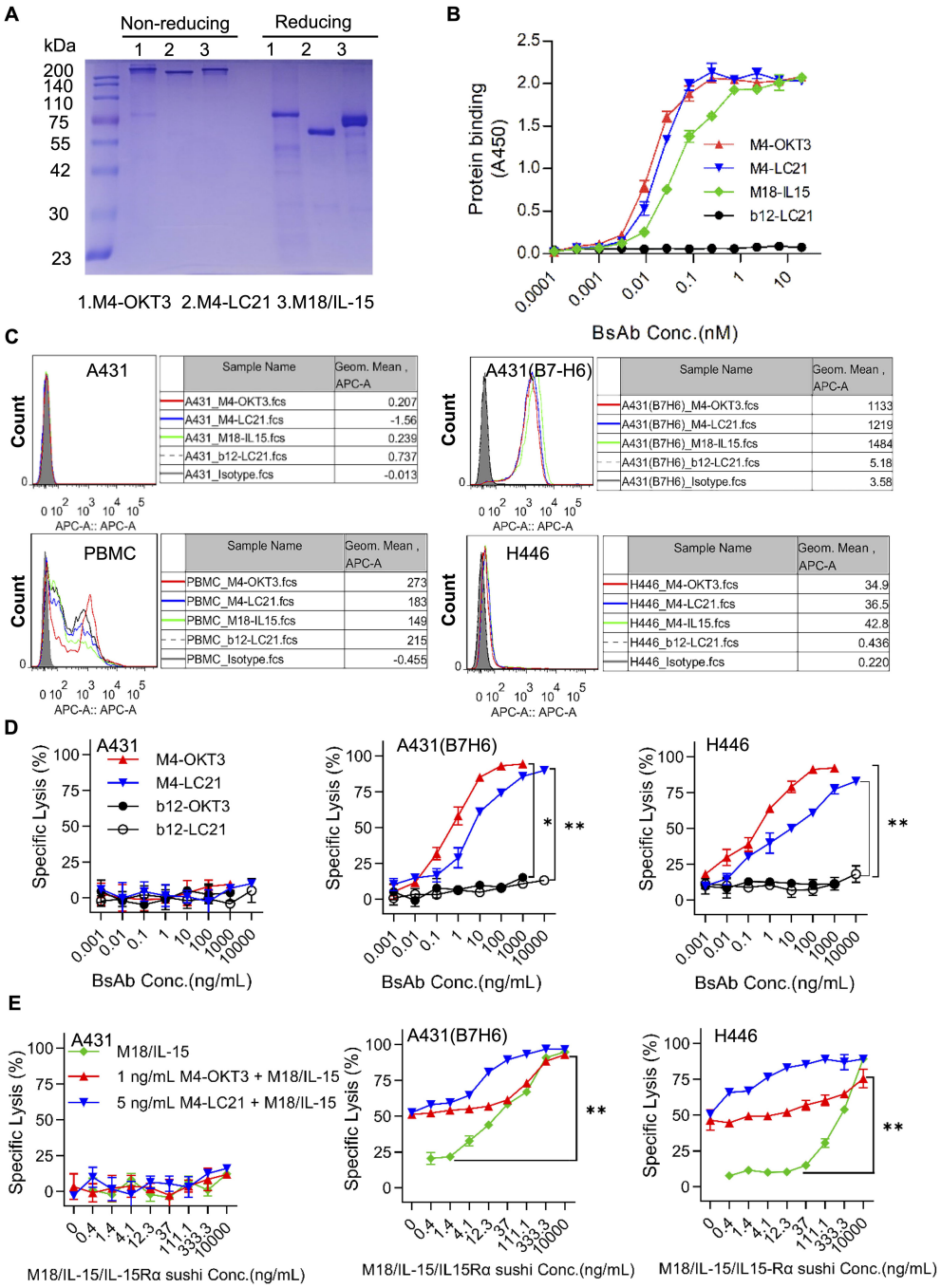

FIGURE 5
Synergistic activity of NK cell-engaging BsAbs and tumor-localized IL-15 delivery. **(A)** SDS-PAGE analysis of B7-H6M4-OKT3, B7-H6M4-LC21, and B7-H6M18/IL-15/IL-15Rα sushi under non-reducing (–βME) and reducing (+βME) conditions (2 μg/lane). The structures of all proteins are scFv (Anti B7H6)-hFc (N297A)-scFv. **(B)** ELISA-based affinity measurement. Plates coated with B7-H6-His (5 μg/mL) were incubated with serially diluted proteins (0.01–100 nM) and detected using HRP-conjugated goat anti-human IgG (1:5,000). **(C)** Flow cytometric validation of BsAb binding to B7-H6+ tumor cells (A431 (B7-H6), H446). PBMC were used to evaluate the binding ability of the bispecific antibodies. Cells were stained with 5 μg/mL antibodies followed by Cy5-conjugated goat anti-human IgG (1:500). Isotype control (pooled human IgG) **(D)** *In vitro* cytotoxicity of B7-H6M4-OKT3 and B7-H6M4-LC21 against tumor cell lines (E:T = 10:1). **(E)** Synergistic cytotoxicity of BsAbs combined with B7-H6M18/IL-15/IL-15Rα sushi. Data: mean ± SEM. Statistical significance determined by unpaired t-test or one-way ANOVA with Tukey's *post hoc* test. *p<0.05, **p<0.01.

therapies (e.g., ALT-803) that promote Treg expansion and hepatotoxicity (14, 43, 44), our design confines IL-15 activity to B7-H6+ tumors, analogous to PD-L1-targeted IL-12 strategies that improve tumor-specific immunity (18, 19). Mechanistically, the sushi domain stabilizes IL-15 binding to CD122/CD132 on NK cells, prolonging STAT5 activation without requiring dendritic cell-mediated trans-presentation (45–47). Dose-dependent toxicity at 0.5 mg/kg underscores the necessity for

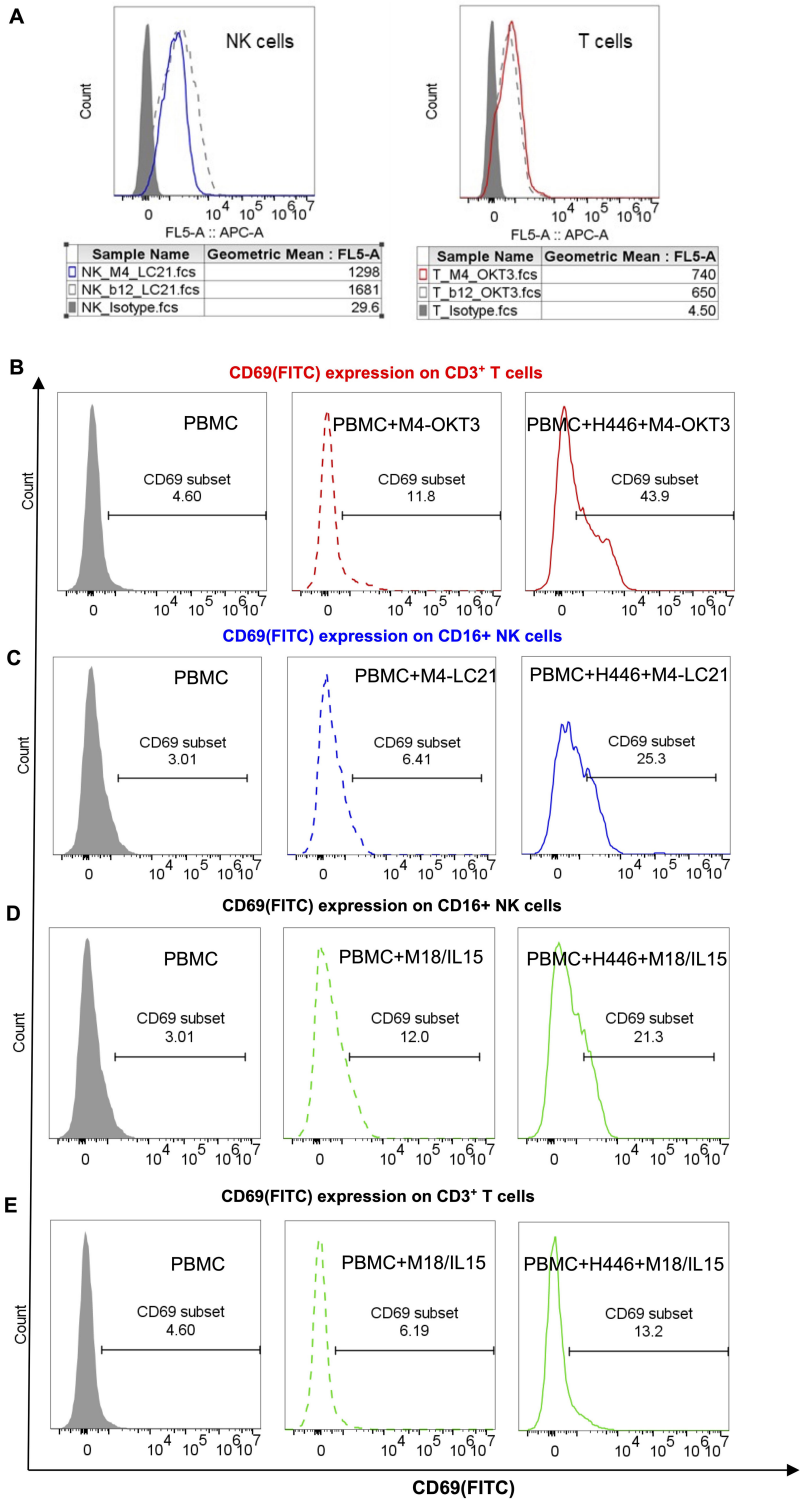

FIGURE 6
Target binding and functional activation of bispecific antibodies. **(A)** Flow cytometric binding specificity of NK/T cells purified from healthy donor PBMCs. NK cells were stained with 5 μg/mL M4-LC21 followed by Cy5-conjugated goat anti-human IgG (1:500). T cells were stained with 5 μg/mL M4-OKT3 followed by Cy5-conjugated goat anti-human IgG (1:500). **(B–E)** CD69 expression after 24-hour treatments: Gray-shaded histogram: PBMC alone (control). Dashed line: PBMC+antibody co-culture. Solid line: PBMC+tumor cells+antibody triple co-culture **(B)** CD69 expression on T cells (gated as $CD3^+$ lymphocytes). **(C)** CD69 expression on NK cells (gated as $CD16^+$ lymphocytes). **(D, E)** CD69 co-expression profiles on T and NK cell subsets.

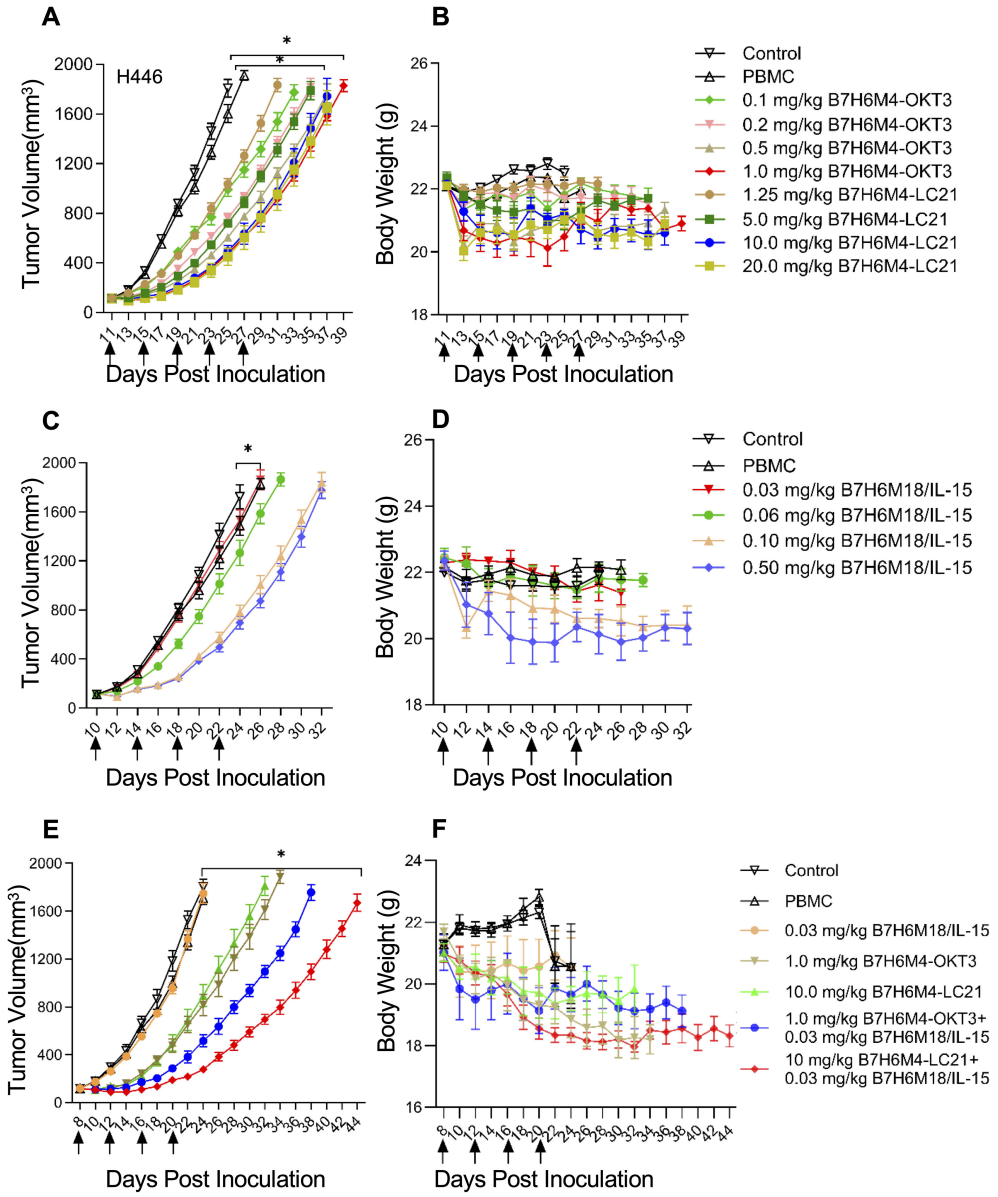

FIGURE 7
Dose-dependent tumor suppression by B7-H6-targeted bispecific antibodies in xenograft models. **(A, B)** Tumor growth curves in H446 xenografts treated with escalating doses of B7-H6M4-OKT3 or B7-H6M4-LC21. Controls: untreated mice and PBMC-only groups. **(C, D)** Dose-dependent efficacy of B7-H6M18/IL-15/IL-15Rα sushi. **(E, F)** Combination therapy (B7-H6M4-OKT3: 1.0 mg/kg; B7-H6M4-LC21: 10.0 mg/kg; IL-15 fusion: 0.03 mg/kg). Arrows: treatment timepoints of antibodies (intravenous injection via tail vein). PBMCs (1×10^7 cells) administered weekly (×2). Tumor volume calculated as $V=\text{length}\times\text{width}^2/2$. Body weight monitored for toxicity. Data: mean ± SEM. Significance determined by unpaired t-test. *p<0.05.

precise cytokine dosing—a challenge mitigated by tumor-localized delivery.

4.4 Clinical translation and therapeutic implications

Our findings position B7-H6 as a pivotal target in refractory solid tumors, particularly cisplatin-resistant SCLC (H446 model). The observed tumor regression parallels PD-1 inhibitor efficacy in similar models (2), suggesting complementary innate-adaptive immune mechanisms. Clinically, this regimen could benefit patients with B7-H6+ tumors identifiable via standard immunohistochemistry—a feasible approach using existing diagnostic antibodies (1). The modular BsAb platform also permits rapid integration with alternative cytokines (e.g., IL-18, IFN-α), costimulatory molecules (4-1BB, OX40), or nanoparticle-based delivery systems such as microrobots, which show promise in enhancing tumor-targeted drug penetration and overcoming biological barriers (48), enabling tailored combination therapies.

4.5 Limitations and future perspectives

Despite promising results, several limitations require resolution. First, validation in patient-derived xenograft (PDX) models of B7-H6+ pancreatic/hepatic cancers is essential. Second, the role of endogenous immune cells in PBMC-humanized NSG mice remains unclear; single-cell RNA sequencing of tumor-infiltrating lymphocytes could clarify NK/T cell interactions. Third, IL-15 fusion dosing optimization demands comprehensive pharmacokinetic studies in non-human primates to balance efficacy and safety. Finally, issues related to treatment safety were explored. With regard to the weight loss phenomenon referenced in Figure 7, it is imperative to elucidate its correlation with cytokine storms. It is regrettable that, owing to an absence of foresight regarding the possibility of toxicity risks during the study design stage, serum or tissue samples were not retained for the purpose of cytokine detection. Nevertheless, the controllability of toxicity is a pivotal focal point of subsequent analyses. The extant data support the hypothesis that toxicity is unrelated to the storm, with limited weight loss: the maximum recorded weight loss was 15% of initial body weight (Figure 7F), consistent with temporary stress responses (e.g. suppression of appetite) rather than the explosive characteristics of a storm (49). No clinical symptoms related to the storm were observed in the subjects. The experimental mice administered the treatment did not display the customary indications of the storm, including hair erection, lethargy, or respiratory distress (50). A review of the clinical data for analogous bispecific antibodies (for example, CD3×CD19 Blinatumomab) yielded the following results: The incidence of weight loss was approximately 18% (CTCAE Grade 1–2) (51). The incidence of cytokine storm was only 3–5% (≥ Grade 3) (51). Therefore, weight loss is not necessarily storm-related and is more likely attributed to energy expenditure caused by T-cell activation.

5 Conclusion

This study establishes an integrative platform for solid tumor immunotherapy combining B7-H6-targeted bispecific antibodies with tumor-anchored cytokine delivery. High-affinity NK cell-engaging B7-H6M4-LC21 (IC50: 5 ng/mL) and T cell-redirecting B7-H6M4-OKT3 (IC50: 1 ng/mL) demonstrate the therapeutic versatility of B7-H6, a tumor-selective immune checkpoint. Co-administration of B7-H6M4-LC21 with IL-15/IL-15Rα sushi fusion achieved synergistic tumor inhibition, outperforming T cell-based strategies and emphasizing NK cells' unique capacity to overcome stromal immunosuppression. Tumor-localized IL-15 delivery minimized systemic toxicity—a critical advancement given the dose-limiting hepatotoxicity of conventional IL-15 therapies.

These results hold immediate clinical relevance for cisplatin-resistant SCLC (H446 model) and other B7-H6+ malignancies where current immunotherapies show limited efficacy. The modular BsAb design facilitates adaptation to alternative cytokines (e.g., IL-18, IFN-α) or costimulatory molecules (4-1BB, OX40), providing a framework for personalized regimens. Future priorities include (1) biomarker-driven patient stratification via B7-H6 IHC, (2) pharmacokinetic optimization of IL-15 fusion dosing, and (3) combinatorial trials with PD-1/CTLA-4 inhibitors to exploit innate-adaptive immune synergy. By unifying targeted antibody engineering with precision cytokine delivery, this work repositions B7-H6 as both a diagnostic marker and therapeutic cornerstone in immuno-oncology.

Data availability statement

The raw data supporting the conclusions of this article will be made available by the authors, without undue reservation.

Ethics statement

Ethical approval was not required for the studies on humans in accordance with the local legislation and institutional requirements because only commercially available established cell lines were used. All animal procedures were approved by the Huazhong Agricultural University Animal Care Committee. The study was conducted in accordance with the local legislation and institutional requirements.

Author contributions

XM: Writing – review & editing, Methodology, Writing – original draft, Investigation, Formal analysis, Resources, Data curation, Project administration, Validation, Conceptualization, Visualization. HH: Writing – original draft, Methodology, Validation, Project administration, Data curation. YZ: Project administration, Writing – original draft, Resources, Formal analysis, Methodology. DZ: Writing – original draft, Validation, Data curation, Methodology. FW: Project administration, Formal analysis, Writing – original draft. MF: Writing – review & editing, Conceptualization, Writing – original draft, Funding acquisition, Resources, Validation. KJ: Writing – review & editing, Software, Validation, Supervision, Methodology, Writing – original draft, Data curation, Investigation, Conceptualization, Visualization. XC: Supervision, Methodology, Conceptualization, Visualization, Investigation, Data curation, Software, Validation, Funding acquisition, Resources, Writing – review & editing, Project administration, Writing – original draft, Formal analysis.

Funding

The author(s) declare financial support was received for the research and/or publication of this article. This work was funded by the National Natural Science Foundation of China (32300783 and 32270992), the Natural Science Foundation of Hubei Province of China (2021CFB155), and the China Postdoctoral Science Foundation (2021M701338).

Acknowledgments

We extend our gratitude to the Public Instrument Platform of the College of Life Science and Technology at Huazhong Agricultural University.

Conflict of interest

The authors declare that the research was conducted in the absence of any commercial or financial relationships that could be construed as a potential conflict of interest.

Generative AI statement

The author(s) declare that no Generative AI was used in the creation of this manuscript.

Publisher's note

Supplementary material

The Supplementary Material for this article can be found online at: https://www.frontiersin.org/articles/10.3389/fimmu.2025.1625813/full#supplementary-material

References

1. Pulanco MC, Madsen AT, Tanwar A, Corrigan DT, Zang X. Recent advancements in the B7/CD28 immune checkpoint families: new biology and clinical therapeutic strategies. *Cell Mol Immunol*. (2023) 20:694–713. doi: 10.1038/s41423-023-01019-8

2. Thomas PL, Groves SM, Zhang YK, Li J, Gonzalez-Ericsson P, Sivagnanam S, et al. Beyond programmed death-ligand 1: B7-H6 emerges as a potential immunotherapy target in SCLC. *J Thorac Oncol*. (2021) 16:1211–23. doi: 10.1016/j.jtho.2021.03.011

3. Zhang W, Auguste A, Liao X, Walterskirchen C, Bauer K, Lin YH, et al. A novel B7-H6-targeted igG-like T cell-engaging antibody for the treatment of gastrointestinal tumors. *Clin Cancer Res*. (2022) 28:5190–201. doi: 10.1158/1078-0432.CCR-22-2108

4. Brandt CS, Baratin M, Yi EC, Kennedy J, Gao Z, Fox B, et al. The B7 family member B7-H6 is a tumor cell ligand for the activating natural killer cell receptor NKp30 in humans. *J Exp Med*. (2009) 206:1495–503. doi: 10.1084/jem.20090681

5. Zhang H, Dai Z, Wu W, Wang Z, Zhang N, Zhang L, et al. Regulatory mechanisms of immune checkpoints PD-L1 and CTLA-4 in cancer. *J Exp Clin Cancer Res*. (2021) 40:184. doi: 10.1186/s13046-021-01987-7

6. June CH, O'Connor RS, Kawalekar OU, Ghassemi S, Milone MC. CAR T cell immunotherapy for human cancer. *Science*. (2018) 359:1361–5. doi: 10.1126/science.aar6711

7. Budde LE, Sehn LH, Assouline S, Flinn IW, Isufi I, Yoon S-S, et al. Mosunetuzumab, a full-length bispecific CD20/CD3 antibody, displays clinical activity in relapsed/refractory B-cell non-hodgkin lymphoma (NHL): interim safety and efficacy results from a phase 1 study. *Blood*. (2018) 132:399–9. doi: 10.1182/blood-2018-99-118344

8. Usmani SZ, Garfall AL, van de Donk N, Nahi H, San-Miguel JF, Oriol A, et al. Teclistamab, a B-cell maturation antigen × CD3 bispecific antibody, in patients with relapsed or refractory multiple myeloma (MajesTEC-1): a multicentre, open-label, single-arm, phase 1 study. *Lancet*. (2021) 398:665–74. doi: 10.1016/S0140-6736(21)01338-6

9. Kerbauy LN, Marin ND, Kaplan M, Banerjee PP, Berrien-Elliott MM, Becker-Hapak M, et al. Combining AFM13, a bispecific CD30/CD16 antibody, with cytokine-activated blood and cord blood-derived NK cells facilitates CAR-like responses against CD30(+) Malignancies. *Clin Cancer Res*. (2021) 27:3744–56. doi: 10.1158/1078-0432.CCR-21-0164

10. Wu J, Fu J, Zhang M, Liu D. AFM13: a first-in-class tetravalent bispecific anti-CD30/CD16A antibody for NK cell-mediated immunotherapy. *J Hematol Oncol*. (2015) 8:96. doi: 10.1186/s13045-015-0188-3

11. Propper DJ, Balkwill FR. Harnessing cytokines and chemokines for cancer therapy. *Nat Rev Clin Oncol*. (2022) 19:237–53. doi: 10.1038/s41571-021-00588-9

12. Patidar M, Yadav N, Dalai SK. Interleukin 15: A key cytokine for immunotherapy. *Cytokine Growth Factor Rev*. (2016) 31:49–59. doi: 10.1016/j.cytogfr.2016.06.001

13. Conlon KC, Lugli E, Welles HC, Rosenberg SA, Fojo AT, Morris JC, et al. Redistribution, hyperproliferation, activation of natural killer cells and CD8 T cells, and cytokine production during first-in-human clinical trial of recombinant human interleukin-15 in patients with cancer. *J Clin Oncol*. (2015) 33:74–82. doi: 10.1200/JCO.2014.57.3329

14. Wrangle JM, Velcheti V, Patel MR, Garrett-Mayer E, Hill EG, Ravenel JG, et al. ALT-803, an IL-15 superagonist, in combination with nivolumab in patients with metastatic non-small cell lung cancer: a non-randomised, open-label, phase 1b trial. *Lancet Oncol*. (2018) 19:694–704. doi: 10.1016/S1470-2045(18)30148-7

15. Guo Y, Luan L, Patil NK, Sherwood ER. Immunobiology of the IL-15/IL-15Rα complex as an antitumor and antiviral agent. *Cytokine Growth Factor Rev*. (2017) 38:10–21. doi: 10.1016/j.cytogfr.2017.08.002

16. Foltz JA, Hess BT, Bachanova V, Bartlett NL, Berrien-Elliott MM, McClain E, et al. Phase I trial of N-803, an IL15 receptor agonist, with rituximab in patients with indolent non-hodgkin lymphoma. *Clin Cancer Res*. (2021) 27:3339–50. doi: 10.1158/1078-0432.CCR-20-4575

17. Klebanoff CA, Finkelstein SE, Surman DR, Lichtman MK, Gattinoni L, Theoret MR, et al. IL-15 enhances the *in vivo* antitumor activity of tumor-reactive CD8+ T cells. *Proc Natl Acad Sci U.S.A*. (2004) 101:1969–74. doi: 10.1073/pnas.0307298101

18. Zou Z, Shen J, Xue D, Li H, Xu L, Cao W, et al. Anti-PD-1 cis-delivery of low-affinity IL-12 activates intratumoral CD8(+)T cells for systemic antitumor responses. *Nat Commun*. (2024) 15:4701. doi: 10.1038/s41467-024-49034-1

19. Liao J, Pan H, Huang G, Gong H, Chen Z, Yin T, et al. T cell cascade regulation initiates systemic antitumor immunity through living drug factory of anti-PD-1/IL-12 engineered probiotics. *Cell Rep*. (2024) 43:114086. doi: 10.1016/j.celrep.2024.114086

20. Chen L, Zhu Y, Feng M, Zuo D, Chen G, Ji K. Targeting CD16A on NK cells and GPC3 in hepatocellular carcinoma: development and functional validation of a therapeutic bispecific antibody. *Front Immunol*. (2025) 16:1599764. doi: 10.3389/fimmu.2025.1599764

21. Xu M, Lei G, Chen M, Wang K, Lv W, Zhang P, et al. Development of a novel, fully human, anti-PCSK9 antibody with potent hypolipidemic activity by utilizing phage display-based strategy. *EBioMedicine*. (2021) 65:103250. doi: 10.1016/j.ebiom.2021.103250

22. Chen X, Chen Y, Liang R, Xiang L, Li J, Zhu Y, et al. Combination therapy of hepatocellular carcinoma by GPC3-targeted bispecific antibody and irinotecan is potent in suppressing tumor growth in mice. *Mol Cancer Ther*. (2022) 21:149–58. doi: 10.1158/1535-7163.MCT-20-1025

23. Myers JA, Miller JS. Exploring the NK cell platform for cancer immunotherapy. *Nat Rev Clin Oncol*. (2021) 18:85–100. doi: 10.1038/s41571-020-0426-7

24. Yang Z, Pietrobon V, Bobbin M, Stefanson O, Yang J, Goswami A, et al. Nanoscale, antigen encounter-dependent, IL-12 delivery by CAR T cells plus PD-L1 blockade for cancer treatment. *J Transl Med*. (2023) 21:158. doi: 10.1186/s12967-023-04014-9

25. Di Trani CA, Cirella A, Arrizabalaga L, Alvarez M, Bella Á, Fernandez-Sendin M, et al. Intratumoral injection of IL-12-encoding mRNA targeted to CSFR1 and PD-L1 exerts potent anti-tumor effects without substantial systemic exposure. *Mol Ther Nucleic Acids*. (2023) 33:599–616. doi: 10.1016/j.omtn.2023.07.020

26. Zhang X, Zhang G, Qin Y, Bai R, Huang J. B7-H6 expression in non-small cell lung cancers. *Int J Clin Exp Pathol*. (2014) 7(10):6936–42.

27. Wang J, Jin X, Liu J, Zhao K, Xu H, Wen J, et al. The prognostic value of B7-H6 protein expression in human oral squamous cell carcinoma. *J Oral Pathol Med*. (2017) 46:766–72. doi: 10.1111/jop.12586

28. Gutierrez-Silerio GY, Franco-Topete RA, Haramati J, Navarrete-Medina EM, Gutierrez-Franco J, Bueno-Topete MR, et al. Positive staining of the immunoligand B7-H6 in abnormal/transformed keratinocytes consistently accompanies the progression of cervical cancer. *BMC Immunol*. (2020) 21:9. doi: 10.1186/s12865-020-0341-9

29. Zhu Z, Teng K-Y, Zhou J, Xu Y, Zhang L, Zhao H, et al. B7H6 serves as a negative prognostic marker and an immune modulator in human pancreatic cancer. *Front Oncol*. (2022) 12. doi: 10.3389/fonc.2022.814312

30. Mohammadi A, Najafi S, Amini M, Mansoori B, Baghbanzadeh A, Hoheisel JD, et al. The potential of B7-H6 as a therapeutic target in cancer immunotherapy. *Life Sci*. (2022) 304:120709. doi: 10.1016/j.lfs.2022.120709

31. Hu Y, Zeng T, Xiao Z, Hu Q, Li Y, Tan X, et al. Immunological role and underlying mechanisms of B7-H6 in tumorigenesis. *Clin Chim Acta*. (2020) 502:191–8. doi: 10.1016/j.cca.2019.12.030

32. Baragaño Raneros A, Rodriguez RM, Bernardo Flórez A, Palomo P, Colado E, Minguela A, et al. Bromodomain protein BRD4 is an epigenetic activator of B7-H6 expression in acute myeloid leukemia. *Oncoimmunology*. (2021) 10:1897294. doi: 10.1080/2162402X.2021.1897294

33. Xu X, Zhang M, Xu F, Jiang S. Wnt signaling in breast cancer: biological mechanisms, challenges and opportunities. *Mol Cancer*. (2020) 19:165. doi: 10.1186/s12943-020-01276-5

34. Ma JH, Qin L, Li X. Role of STAT3 signaling pathway in breast cancer. *Cell Commun Signal*. (2020) 18:33. doi: 10.1186/s12964-020-0527-z

35. Gajewski TF. The next hurdle in cancer immunotherapy: overcoming the non-T-cell-inflamed tumor microenvironment. *Semin Oncol*. (2015) 42:663–71. doi: 10.1053/j.seminoncol.2015.05.011

36. Laskowski TJ, Biederstädt A, Rezvani K. Natural killer cells in antitumour adoptive cell immunotherapy. *Nat Rev Cancer*. (2022) 22:557–75. doi: 10.1038/s41568-022-00491-0

37. Dubois SP, Miljkovic MD, Fleisher TA, Pittaluga S, Hsu-Albert J, Bryant BR, et al. Short-course IL-15 given as a continuous infusion led to a massive expansion of effective NK cells: implications for combination therapy with antitumor antibodies. *J Immunother Cancer*. (2021) 9:e002193. doi: 10.1136/jitc-2020-002193

38. Conlon KC, Potter EL, Pittaluga S, Lee CR, Miljkovic MD, Fleisher TA, et al. IL15 by continuous intravenous infusion to adult patients with solid tumors in a phase I trial induced dramatic NK-cell subset expansion. *Clin Cancer Res*. (2019) 25:4945–54. doi: 10.1158/1078-0432.CCR-18-3468

39. Fehniger TA, Caligiuri MA. Interleukin 15: biology and relevance to human disease. *Blood*. (2001) 97:14–32. doi: 10.1182/blood.V97.1.14

40. Li J, Clark R, Slaga D, Avery K, Liu K, Schubbert S, et al. IL-15/IL-15Rα-fc-fusion protein xmAb24306 potentiates activity of CD3 bispecific antibodies through enhancing T-cell expansion. *Mol Cancer Ther*. (2024) 23:1305–16. doi: 10.1158/1535-7163.MCT-23-0910

41. Deshpande P, Cavanagh MM, Le Saux S, Singh K, Weyand CM, Goronzy JJ. IL-7– and IL-15–mediated TCR sensitization enables T cell responses to self-antigens. *J Immunol*. (2013) 190:1416–23. doi: 10.4049/jimmunol.1201620

42. Cai Y, Han Z, Shen J, Zou Z, Guo J, Liang Y, et al. Concurrent intratumoural Treg cell depletion and CD8+ T cell expansion via a cleavable anti-4-1BB–interleukin-15 fusion protein. *Nat Biomed Eng*. (2024) 9:952–66. doi: 10.1038/s41551-024-01303-6

43. Felices M, Chu S, Kodal B, Bendzick L, Ryan C, Lenvik AJ, et al. IL-15 super-agonist (ALT-803) enhances natural killer (NK) cell function against ovarian cancer. *Gynecol Oncol*. (2017) 145:453–61. doi: 10.1016/j.ygyno.2017.02.028

44. Rosario M, Liu B, Kong L, Collins LI, Schneider SE, Chen X, et al. The IL-15-based ALT-803 complex enhances fcγRIIIa-triggered NK cell responses and *in vivo* clearance of B cell lymphomas. *Clin Cancer Res*. (2016) 22:596–608. doi: 10.1158/1078-0432.CCR-15-1419

45. Gotthardt D, Putz EM, Grundschober E, Prchal-Murphy M, Straka E, Kudweis P, et al. STAT5 is a key regulator in NK cells and acts as a molecular switch from tumor surveillance to tumor promotion. *Cancer Discov*. (2016) 6:414–29. doi: 10.1158/2159-8290.CD-15-0732

46. Monaghan KL, Aesoph D, Ammer AG, Zheng W, Rahimpour S, Farris BY, et al. Tetramerization of STAT5 promotes autoimmune-mediated neuroinflammation. *Proc Natl Acad Sci U.S.A*. (2021) 118:e2116256118. doi: 10.1073/pnas.2116256118

47. Maghsoodi N, Zareinejad M, Ghaderi A, Mahmoudi Maymand E, Irajie C, Ramezani A. Anti-CD8/IL-15 (N72D)/sushi fusion protein: A promising strategy for improvement of cancer immunotherapy. *Cytokine*. (2025) 185:156822. doi: 10.1016/j.cyto.2024.156822

48. Wang J, Liao Z-X. Research progress of microrobots in tumor drug delivery. *Food Med Homol*. (2024) 1:9420025. doi: 10.26599/FMH.2024.9420025

49. Lee DW, Santomasso BD, Locke FL, Ghobadi A, Turtle CJ, Brudno JN, et al. ASTCT consensus grading for cytokine release syndrome and neurologic toxicity associated with immune effector cells. *Biol Blood Marrow Transplant*. (2019) 25:625–38. doi: 10.1016/j.bbmt.2018.12.758

50. Teachey DT, Lacey SF, Shaw PA, Melenhorst JJ, Maude SL, Frey N, et al. Identification of predictive biomarkers for cytokine release syndrome after chimeric antigen receptor T-cell therapy for acute lymphoblastic leukemia. *Cancer Discov*. (2016) 6:664–79. doi: 10.1158/2159-8290.CD-16-0040

51. Neelapu SS, Tummala S, Kebriaei P, Wierda W, Gutierrez C, Locke FL, et al. Chimeric antigen receptor T-cell therapy — assessment and management of toxicities. *Nat Rev Clin Oncol*. (2017) 15:47–62. doi: 10.1038/nrclinonc.2017.148

frontiers | Frontiers in Immunology

TYPE Original Research
PUBLISHED 27 August 2025
DOI 10.3389/fimmu.2025.1642454

OPEN ACCESS

EDITED BY
Renata Pacholczak-Madej,
Maria Skłodowska-Curie National Institute of Oncology, Poland

REVIEWED BY
Longchao Liu,
Chinese Academy of Sciences (CAS), China
Ge Yang,
Rutgers, The State University of New Jersey, United States

*CORRESPONDENCE
Oliver Seifert
oliver.seifert@izi.uni-stuttgart.de

RECEIVED 06 June 2025
ACCEPTED 04 August 2025
PUBLISHED 27 August 2025

CITATION
Löffler A-K, Huber A, Olayioye MA, Kontermann RE and Seifert O (2025) Trispecific eFab-elg T-cell engagers targeting HER2 and HER3.
Front. Immunol. 16:1642454.
doi: 10.3389/fimmu.2025.1642454

Trispecific eFab-elg T-cell engagers targeting HER2 and HER3

Ann-Kathrin Löffler [1], Annika Huber[1], Monilola A. Olayioye [1,2], Roland E. Kontermann [1,2] and Oliver Seifert [1,2]*

[1]Institute of Cell Biology and Immunology, University of Stuttgart, Stuttgart, Germany, [2]Stuttgart Research Center Systems Biology (SRCSB), University of Stuttgart, Stuttgart, Germany

Trispecific antibodies have emerged as molecules for enhanced cancer immunotherapy by addressing the complexity of cancer cell biology and anti-cancer immune responses. Here, we present a novel approach to generate trispecific antibodies based on the previously developed elg technology. These trispecific antibodies comprise one Fab and two eFab moieties, fused to obtain an asymmetric eFab-elg molecule. The design principle employs two different eFab building blocks, characterized by divergent arrangements of heterodimerizing hetEHD2 domains. Specifically, the first (inner) eFab arm comprises the hetEHD2–1 domain in the heavy chain and the corresponding hetEHD2–2 domain in one of the light chains, while in the second eFab (outer) this arrangement is reversed. The feasibility of this approach was demonstrated for a trispecific eFab-elg T-cell engager (TCE) targeting HER2, HER3, and CD3. Importantly, the trispecific TCE retained binding activity for all three antigens and was capable of recruiting T-cells to HER2 and/or HER3-expressing cancer cells and mediating effective cancer cell killing, as shown in 2D and 3D model systems. Due to the modular architecture, this approach should be suitable to generate trispecific antibodies of any specificity and for a multitude of applications.

KEYWORDS

trispecific antibody, T-cell retargeting, antibody engineering, HER2, HER3, CD3, hetEHD2

Introduction

Bispecific antibodies have found increasing applications in cancer therapy (1). The majority of the approved bispecific antibodies is designed as T-cell engagers (TCEs) that simultaneously bind to a tumor-associated antigen (TAA) on the cancer cells and to the CD3 chain of the T-cell receptor (TCR) complex on T-cells. Many of these TCEs utilize a 1 + 1 stoichiometry for the TAA and CD3 chain. However, recently TCEs with a 2 + 1 stoichiometry containing two identical binding sites for the TAA have demonstrated increased tumor cell binding and killing. This superior efficacy can be explained by avidity effects, whereas the monovalent CD3-binding is maintained to prevent systemic T-cell

activation (2–6). For example, avidity-driven activation and killing of solid tumors was shown for the 2 + 1 bispecific TCE, AMG 509 (xaluritamig), targeting STEAP1, which allowed to discriminate between high target expressing cancer cells and normal cells (7). A first 2 + 1 TCE, glofitamab, directed against CD20 and CD3 was approved in 2023 for the treatment of patients with relapsed or refractory diffuse large B-cell lymphoma (DLBCL) (8).

Various formats are utilized to generate bispecific 2 + 1 TCEs (9, 10). Several of these formats have further been adapted for the generation of trispecific 1 + 1 + 1 TCEs targeting two different TAAs (11). From a design point of view, the generation of such 2 + 1 trispecific antibody molecules requires further engineering to allow pairing of the three different V_L domains with their cognate V_H domains. Examples of such engineering approaches include Fab-IgG molecules assembled from half-antibodies (12), Fab-IgGs comprising a common light chain (13), OrthoTsAbs built from orthogonal Fabs (14), trispecific CODV-Igs comprising a Fab moiety and a defined arrangement of V_H and V_L domains fused to C_H1 and C_L domains which assemble into a bispecific binding moiety (15), and scFvs or single-domain antibodies used as building blocks (16, 17).

We have recently developed a novel technology, the eIg technology, to generate bispecific antibodies, including TCEs (18, 19). Central to this technology is the heavy chain domain 2 of the IgE (EHD2) which naturally forms disulfide-stabilized homodimers acting as a hinge-like structure in the IgE. The covalent linkage is based on two disulfide bonds at the interface of the two domains formed between two different cysteine residues. This EHD2 can be used as a versatile building block to generate homodimeric fusion proteins (20). Substitution of one of the two cysteine residues in the first EHD2 (hetEHD2-1) and substitution of the other cysteine residue in the second EHD2 (hetEHD2-2), e.g. by serine residues, results in efficient formation of disulfide-linked hetEHD2–1 x hetEHD2–2 heterodimers, while homodimers lacking disulfide bonds are instable (21). These heterodimerizing hetEHD2–1 and hetEHD2–2 domains were developed further, generating Fab-like moieties (eFab) as versatile building blocks for the generation of bispecific antibody molecules. Thus, bispecific bivalent molecules (eIg) were generated by fusing a natural Fab and an eFab moiety to heterodimerizing Fc-chains (18). Furthermore, trivalent bispecific molecules, so-called 2 + 1 formats, were generated by fusing an additional Fab to one of the eIg chains (i.e. the N- or C-terminus of one of the heavy chains or one of the light chains) (19).

In the present study, we have extended the eIg technology to generate trispecific eFab-eIg molecules comprising one natural Fab arm and two different eFab arms (1 + 1 + 1 format). The first (inner) eFab arm comprises the hetEHD2–1 domain in the heavy chain and the corresponding hetEHD2–2 domain in one of the light chains, while in the second eFab (outer) this arrangement is reversed. Recently, we have published a bivalent bispecific antibody for dual-targeting of HER2 and HER3 and confirmed strong activity against tumor cells *in vitro* and *in vivo* (22). Based on the excellent inhibitory effect of this bispecific antibody, the feasibility was evaluated for a trispecific eFab-eIgs TCE targeting HER2, HER3 and CD3. The Fc part for the generation of bi-or trispecific TCEs is silenced (FcΔab) and is not able to exert Fc-mediated effector functions (23). This trispecific eFab-eIg TCE was compared to bispecific eIgs targeting both HER2 or HER3 with respect to binding of antigen and antigen-expressing tumor cell lines and to CD3 for T-cell engagement. Finally, dual targeting of both antigens and efficient killing of HER2 and HER3 expressing tumor cells was demonstrated using 2D and 3D cell culture models.

Abbreviations: TCE, T-cell engager; TAA, tumor-associated antigen; TCR, T-cell receptor; STEAP1, six transmembrane epithelial antigen of the prostate 1; DLBCL, diffuse large B cell lymphoma; V_L, variable domain of the light chain; V_H, variable domain of the heavy chain; Fab, fragment antigen binding; Ig, immunoglobulin; OrthoTsAbs, orthogonal Fab-based trispecific antibodies; CODV, cross-over dual variable; C_H, constant domain of heavy chain; C_L, constant domain of light chain; scFv, single-chain fragment variable; eIg, bispecific Ig domain containing hetEHD2; hetEHD2, heterodimerized second domain of IgE; DLS, dynamic light scattering; CD, cluster of differentiation; eFab, Fab with hetEHD2; HER2, HER3, epidermal growth factor receptor 2, 3; moFc, mouse fragment crystalline; hetEHD2-1, hetEHD2 domain with C102S; hetEHD2-2, hetEHD2 domain with C14S and N39Q; PBMC, peripheral blood mononuclear cell; R_S, Stokes radius; EHD2, heavy chain domain 2 of IgE; SEC, size-exclusion chromatography; GBM, glioblastoma multiforme; EGFRvIII, epidermal growth factor variant III; DLS, dynamic light scattering; TNF, tumor-necrosis-factor; IL, interleukin.

Materials and methods

Materials

For the different *in vitro* experiments, we used BT474 cells (ATCC HTB-20), LIM1215 (Sigma-Aldrich Cat#10092301), MDA-MB-468 (CLS Cat#C0006003) and Jurkat cells (provided by Dr. Ammon Altman form the La Jolla Institute for Allergy & Immunology) were cultivated in RPMI 1640, 10% FCS. For the production of antibodies, we used HEK293-6E cells provided by National Research Council of Canada (Ottawa, Canada) and cultivated in F17 Freestyle expression medium (ThermoFisher) supplemented with 0.1% Kolliphor P-118 (Sigma), 4 mM GlutaMAX (ThermoFisher), and 25 µg/ml G418. Human peripheral blood mononuclear cells (PBMC) were isolated from buffy coat of healthy donors (Klinikum Stuttgart/Institut für Klinische Transfusionsmedizin und Immungenetik Ulm gemeinnützige GmbH, Germany) by Ficoll density gradient centrifugation (Lymphocyte Separation Medium 1077, Promocell, C-44010) and cultivated in RPMI 1640, 10% FCS.

Antibody production and purification

All antibodies were produced in HEK293-6E cells cultivated in F17 Freestyle medium (ThermoFischer). Transient transfection with pSecTagA vectors carrying the genes for light and heavy chains of the different antibodies was performed with polyethyleneimine (PEI; 25 kDa, linear, Polysciences). 24 h after transfection, 2.5% (v/v) TN1

(20% (w/v) tryptone N1 (Organotechnie S.A.S.) in F17 Freestyle expression medium) was added and cells were incubated for additional four days before supernatant harvest and antibody purification via protein A affinity chromatography (Cytiva). Bound antibodies were eluted using 100 mM glycine pH 3.5 and dialyzed against phosphate-buffered saline at 4°C. A preparative FPLC size-exclusion chromatography (SEC) step was included for the eIg molecules targeting HER2xCD3 and eIg HER3xCD3.

Antibody characterization

Purified antibodies were analyzed by SDS-PAGE (3 µg for non-reducing, 6 µg for reducing conditions) using 12% (v/v) polyacrylamide gels and staining proteins with Coomassie-Brilliant Blue G-250. Analytical SEC was performed using a VANQUISH (Thermo Fisher Scientific GmbH) HPLC in combination with a TSKgel SuperSW mAb HR column (Tosoh Bioscience) at a flow rate of 0.5 or 0.4 mL/min using 0.1 M Na_2HPO_4/NaH_2PO_4, 0.1 M Na_2SO_4, pH 6.7 as mobile phase. Standard proteins: thyroglobulin (669 kDa, R_S 8.5 nm), apoferritin (443 kDa, R_S 6.1 nm), β-amylase (200 kDa, R_S 5.4 nm), bovine serum albumin (67 kDa, R_S 3.55 nm) and carbonic anhydrase (29 kDa, R_S 2.35 nm). For eIg HER2xCD3 and eIg HER3xCD3 we further purified the molecules with a preparative SEC by FPLC. The thermal stability of molecules was analyzed by dynamic light scattering (DLS) using ZetaSizer Nano ZS (Malvern). Purified proteins were exposed to increasing temperature (30°C to 85°C) in 1°C intervals with 2-minute equilibration steps. The aggregation point was defined by the starting point of the increase in the mean count rate.

Enzyme-linked immunosorbent assay

High-binding 96-well plates were coated with 3 µg/mL HER2-moFc and HER3-moFc (22) at 4°C overnight. Residual-binding sites were blocked with 2% (w/v) skim milk in PBS (MPBS). Antibodies were titrated (1:4) in MPBS starting from 400 nM (sequential binding of eFab-eIg) or 100 nM (binding of eFab-eIg and eIg molecules) and incubated for 1 h at RT. A human Fc-specific HRP-conjugated secondary antibody (A0170, Sigma Aldrich) was added for detection of bound antibodies or a mouse anti-His HRP-conjugated secondary antibody (9991, Cell Signaling) for detection of bound receptors and incubated for 1 h at RT. TMB was used as substrate (1 mg/mL TMB; 0.006% (v/v) H_2O_2 in 100 mM Na-acetate buffer, pH 6.0) and reaction was stopped using 50 µL 1 M H_2SO_4 and absorption was measured at a wavelength of 450 nm.

Flow cytometry analysis

Serial dilutions of antibodies in PBA (PBS + 2% (v/v) FCS + 0.02% (w/v) sodium azide) were added to a 96-well U-bottom plate containing $1x10^5$ CD3-expressing Jurkat or HER2- and HER3-expressing tumor cells (BT474, LIM1215, MDA-MB-468) per well. Bound antibodies were detected using a R- phycoerythrin (PE)-labeled anti-human Fc antibody (109-115-098, Jackson ImmunoResearch) diluted in PBA. For the sequential binding of HER2 and HER3 using the trispecific antibody bound to Jukrat cells, we detected the receptors with an FITC-labeled anti-murine IgG antibody (F0257; Sigma Aldrich). Before every step, cells were washed three times via centrifugation at 500 x g/4°C for 3 min and resuspension in 150 µL PBA. Binding of the antibodies to the cells was analyzed using a MACSQuant VYB (Miltenyi Biotec) and FlowJo (BD Biosciences). The relative median fluorescence intensity (MFI) was calculated as followed: relative MFI = $((MFI_{sample}-(MFI_{detection}-MFI_{cells}))/MFI_{cells})$.

2D cytotoxicity assay

Tumor cells (7,500 to 15,000 cells/well) were seeded per 96-well in RPMI containing 10% (v/v) FCS and P/S (1:100) and were incubated 24 h at 37°C/5% (v/v) CO_2. In addition, PBMCs were thawed and cultivated in a cell culture dish (10 cm) in 10 mL RPMI with 10% (v/v) FCS overnight. Serial dilutions of tri- or bispecific antibodies in RPMI containing 10% (v/v) FCS and P/S (1:100) were pre-incubated with the tumor cells for 15 min. Subsequently, PBMCs from different donors were added to the tumor cells in an effector-to-target ratio of 10:1 and incubated for 3 days. Supernatant was then discarded and remaining viable tumor cells were stained with crystal violet and optical density at 550 nm was measured using the Tecan Spark (Tecan).

3D spheroid killing assay

BT474 cells (1,000 cells/well) were seeded on poly-HEMA coated U-bottom 96-well plates to prevent cell attachment in RPMI + 10% (v/v) FCS + P/S (1:100) and left 24 h at 37°C/5% (v/v) CO_2 to form compact spheroids. In addition, PBMCs were thawed and cultivated in a cell culture dish (10 cm) in 10 mL RPMI with 10% (v/v) FCS overnight. The next day, spheroids were treated with different dilutions of tri- or bispecific antibodies as well as 1 µg/mL PI and pre-incubated for 15 min at 37°C/5% (v/v) CO_2. Different numbers of PBMCs were added to the spheroids. Target cell killing was observed via PI staining intensity at the IncuCyte every 2 h for two days. Images were analyzed using Fiji (Open Source).

IL-2, IFNγ, IL-6 and TNFα release

Target cells were incubated with bi- or trispecific antibodies and PBMCs at an effector-to-target ratio of 10:1. After 24 h or 48 h, supernatants were harvested for quantification of IL-2, IL-6 and TNFα or IFNγ, respectively. Supernatant cytokine levels were quantified via by sandwich ELISA following the manufacturer's

10.3389/fimmu.2025.1642454

instructions (IL-2/IFNγ/TNFα Duo Set ELISA; R&D Systems; ELISA MAX Standard Set human IL-6; BioLegend).

Statistics

All data are represented as mean ± SD for n=3 if not indicated otherwise. For co-culture experiments analyzing the T-cell activation, two different donors were tested. Significances were analyzed with GraphPad Prism 8 using an unpaired two-tailed t test for the analysis of two samples or a one-way ANOVA followed by Tukey multiple comparison test (posttest) for the analysis of more than two samples.

Results

Generation of bivalent bispecific and trivalent trispecific antibodies

A trispecific, trivalent eFab-eIg molecule was generated by fusing a Fab directed against HER2 [derived from trastuzumab (24)] to a Fc-hole chain and a tandem arrangement of eFabs (eFab1-eFab2) to a Fc-knob chain. The first (inner) eFab-1 is directed against CD3 using a humanized version of UCHT1 (25) and the second (outer) eFab-2 derived from the antibody 3–43 is directed against HER3 (26). In this design, each eFab comprises two heterodimerizing EHD2 (hetEHD2 domains substituting C_H1 and C_L). In the eFab1, the heavy chain hetEHD2 carries a C14S mutation, thus possessing only C102 at the interphase, while the light hetEHD2 carries a C102S mutation, thus possessing only C14 at the interphase. In eFab2 these mutations are reversed. As control proteins, bispecific, bivalent eIg molecules directed against HER2 and CD3, or HER3 and CD3, respectively, were generated (Figures 1A, B). All three molecules were produced in transiently transfected HEK293-6E cells and purified from the supernatant with yields of 6.4 mg/L supernatant for the eFab-eIg, 6.7 mg/L for eIg HER2xCD3, and 9.2 mg/L for eIg HER3xCD3. SDS-PAGE analyses confirmed correct assembly into eIg molecules and the presence of the individual polypeptide chains (Figure 1C). Purity of >95% was further confirmed by size-exclusion chromatography showing a single main peak with an apparent molecular mass of approximately 190 to 200 kDa for both eIgs and approximately 310 kDa for the eFab-eIg (Figure 1D). In addition, we have also tested the thermal stability of the different molecules by dynamic light scattering (DLS) (Supplementary Figure S1). Here, we calculated an aggregation point of the trispecific eFab-eIg molecule with 75°C (as well as for trastuzumab, IgG huU3 and eIg HER2xCD3), while one of the parental monospecific antibody IgG 3–43 and the bispecific eIg HER3xCD3 showed a lower aggregation point at 64°C and 63°C, respectively. Thus, the aggregation point originating from variable domains of targeting HER3 was not observed for the trispecific eFab-eIg molecule.

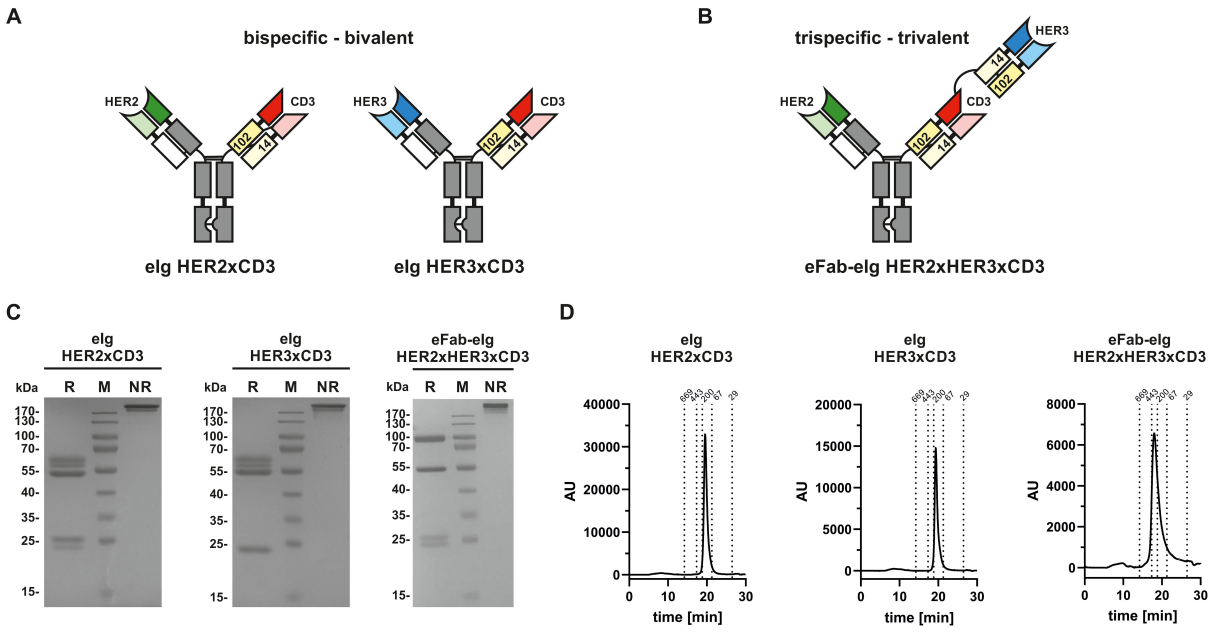

FIGURE 1
Composition and biochemical analysis of bi- and trispecific molecules. **(A)** Composition of bispecific bivalent eIg molecules directed against HER2 and CD3 as well as HER3 and CD3, respectively. **(B)** Composition of trispecific trivalent eFab-eIg molecules directed against HER2, HER3 and CD3. **(C)** SDS-PAGE of bispecific bivalent eIg molecules and trispecific trivalent molecule under reducing (R) and non-reducing (NR) conditions. **(D)** SEC analysis of eIg HER2xCD3 and HER3xCD3 as well as of eFab-eIg HER2xHER3xCD3.

10.3389/fimmu.2025.1642454

Binding of bi- and trispecific antibodies to HER2 and HER3

First, binding of the bi- and trispecific eIg antibodies was analyzed by ELISA using immobilized recombinant extracellular regions of HER2 and HER3 fused to a mouse Fc region (HER2-moFc and HER3-moFc). In this assay, all antibodies showed a concentration-dependent binding (Figures 2A-C) with EC_{50} values of 0.7 nM for HER2 and 5.6 nM for HER3 for the trispecific eFab-eIg, 0.4 nM for HER2 for eIg HER2xCD3 and 1.9 nM for HER3 for eIg HER3xCD3. Thus, compared to the bispecific eIgs, the EC_{50} values of the trispecific eFab-eIg were slightly lower than those observed for the bispecific antibodies (Table 1). A significantly different binding was calculated for the trispecific eFab-eIg molecule compared to the bispecific eIg HER2xCD3 molecule ($p=0.03$). Furthermore, binding to both antigens was analyzed by a sandwich ELISA using either immobilized HER2-moFc or HER3-moFc followed by incubation with the eFab-eIg HER2xHER3xCD3 and subsequent incubation with either HER3-His or HER2-His, respectively (Figure 2D). In both setups, binding to both antigens was observed for the trispecific eFab-eIg.

Binding of bi- and trispecific antibodies to CD3

Next, antibody binding to CD3 was analyzed by flow cytometry using CD3-expressing Jurkat cells. For all antibodies a concentration-dependent binding was observed (Figure 3A). The trispecific eFab-eIg HER2xHER3xCD3 bound to the cells with an EC_{50} value of 45.8 nM, while the control antibodies bound with an EC_{50} value of 7.0 nM for eIg HER2xCD3 and 4.4 nM for eIg HER3xCD3 (Table 2). The reduced binding of eFab-eIg HER2xHER3xCD3, which reached significance ($p<0.004$ for eIg HER2xCD3 and $p<0.003$ for eIg HER3xCD3) is most likely due to the N-terminal fusion of the eFab moieties, sterically interfering with the binding to CD3. We additionally analyzed the sequential binding of HER2-moFc or HER3-moFc to the trispecific eFab-eIg bound to Jurkat cells (Figure 3B). After incubation of Jurkat cells with 400 nM of eFab-eIg HER2xHER3xCD3, soluble HER2-moFc or HER3-moFc was added and bound antigens were detected with a FITC-labeled anti-murine Fc antibody. Both antigens, HER2 and HER3, were bound to the cells incubated with eFab-eIg HER2xHER3xCD3, demonstrating the sequential binding of CD3-expressing cells with HER2 or HER3 as antigen.

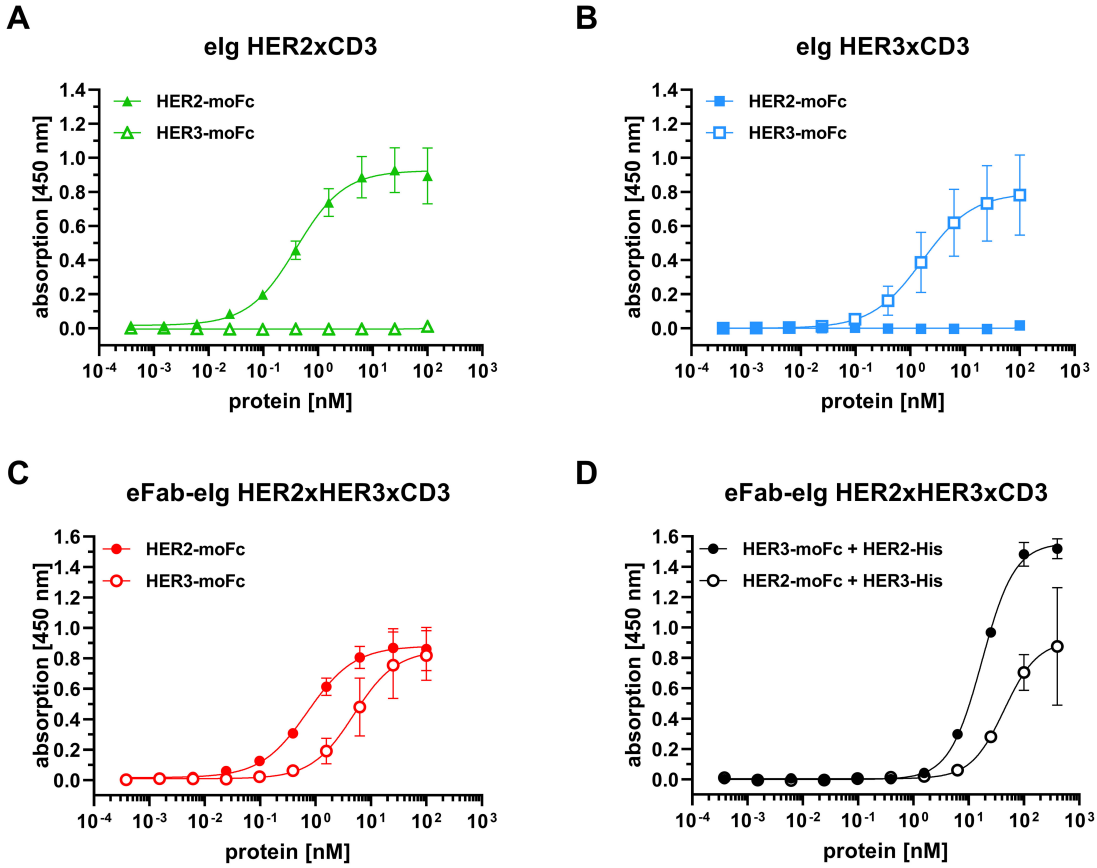

FIGURE 2
Binding of bi- and trispecific molecules to HER2 and HER3 in ELISA. **(A)** Binding of eIg HER2xCD3 to HER2 and HER3. **(B)** Binding of eIg HER3xCD3 to HER2 and HER3. **(C)** Binding of eFab-eIg HER2xHER3xCD3 to HER2 and HER3. **(D)** Binding of HER3-His to eFab-eIg HER2xHER3xCD3 bound to immobilized HER2-moFc, or vice versa. Mean ± SD; n=3.

10.3389/fimmu.2025.1642454

TABLE 1 Antigen binding from ELISA experiments.

Antigen	eIg HER2xCD3	eIg HER3xCD3	eFab-eIg HER2xHER3xCD3
HER2-moFc	0.4 ± 0.1	n.d.	0.7 ± 0.2
HER3-moFc	n.d.	1.9 ± 1.1	5.6 ± 2.1

EC_{50} values in nM. Mean ± SD, n.d., not determined, n=3.

Target cell binding with varying surface expression of HER2

To investigate target cell specificity, binding of the antibodies to HER2- and HER3-expressing cell lines was analyzed by flow cytometry using tumor cell lines expressing different surface levels of HER2 and HER3 (BT474: >572,000 HER2/cell and ~11,000 HER3/cell; LIM1215: ~33,000 HER2/cell and ~20,000 HER3/cell; MDA-MB-468: ~1,700 HER2/cell and ~6,000 HER3/cell). In all cases, binding to the target cells occurred in a concentration-dependent manner (Figure 4A, Supplementary Figure S2). For all three cell lines strongest binding was observed for eIg HER3xCD3 with EC_{50} values in the range of 0.3 to 0.6 nM. For BT474 cells, which express very high amount of HER2 and comparable low amount of HER3, binding of eIg HER3xCD3 was detected with lower fluorescence intensity compared to the trispecific antibody and eIg HER2xCD3 binding to HER3 and/or HER2 and is highlighted in Supplementary Figure S3. The eIg HER2xCD3 bound best to LIM1215 (2.6 nM) followed by BT474 (6.2 nM) and MDA-MB-468 cells (EC_{50} value was not determined). The trispecific antibody showed similarly strong binding to LIM1215 (1.4 nM) followed by MDA-MB-468 (7.0 nM) and BT474 cells (10.9 nM). A significant difference was determined for the eIg HER3xCD3 compared to eIg HER2xCD3 using LIM1215 cells ($p=0.008$) and BT474 cells ($p=0.016$) and to trispecific antibody using BT474 cells ($p=0.002$) and MDA-MB-468 cells ($p<0.001$). In general, MFI signal intensity and thus binding efficacy correlated with HER2 and HER3 expression levels. Of note, the trispecific eFab-eIg consistently gave rise to strong signals, while maximal MFI signals of the bispecific eFabs varied, depending on the antigen expression levels. For example, eIg HER2xCD3 showed very low binding to MDA-MB-468 cells, which express low levels of HER2, while eIg HER3xCD3 showed low binding to BT474 cells. In summary, binding to all three different cancer cell lines with varying amounts of HER2 and HER3 was detected for the trispecific antibody.

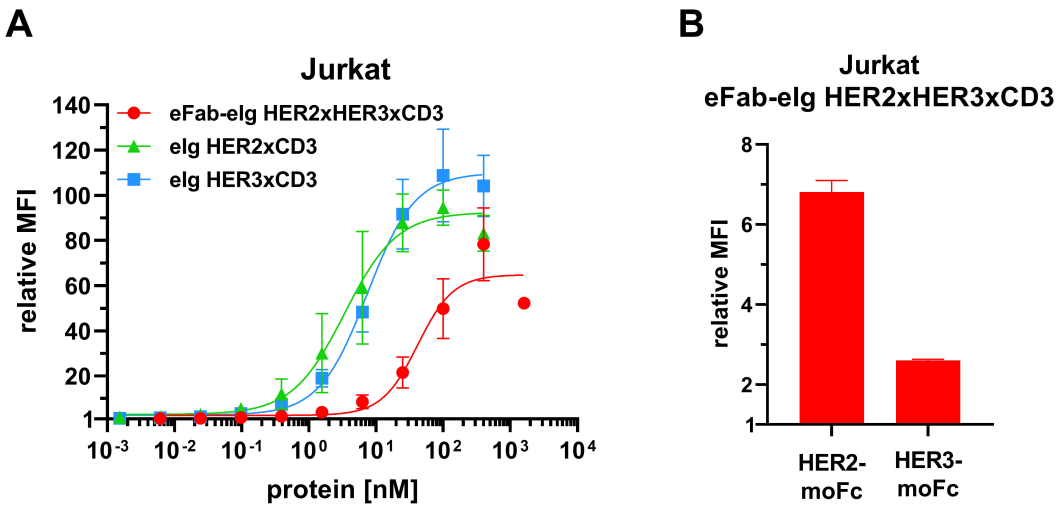

FIGURE 3
Binding to CD3-expressing Jurkat cells. **(A)** Flow cytometry analysis of binding of eFab-eIg HER2xHER3xCD3 as well as eIg HER2xCD3 and HER3xCD3 to CD3-expressing Jurkat cells. **(B)** Flow cytometry analysis of binding of 400 nM of eFab-eIg HER2xHER3xCD3 to Jurkat cells followed by incubation with either HER2-moFc or HER3-moFc (300 nM), respectively, to analyze sequential binding to CD3-expressing cells and either HER2 or HER3. Mean ± SD, n=3.

TABLE 2 Cell binding from flow cytometry analysis.

Cell line	eIg HER2xCD3	eIg HER3xCD3	eFab-eIg HER2xHER3xCD3
Jurkat	7.0 ± 0.6	4.4 ± 2.6	45.8 ± 14.8
MDA-MB468	n.d.	0.3 ± 0.1	7.0 ± 0.8
LIM1215	2.6 ± 0.8	0.6 ± 0.1	1.4 ± 0.4
BT474	6.2 ± 1.5	0.5 ± 0.5	10.9 ± 2.8*

EC_{50} values in nM. Mean ± SD, n.d., not determined, *n=2, n=3.).

10.3389/fimmu.2025.1642454

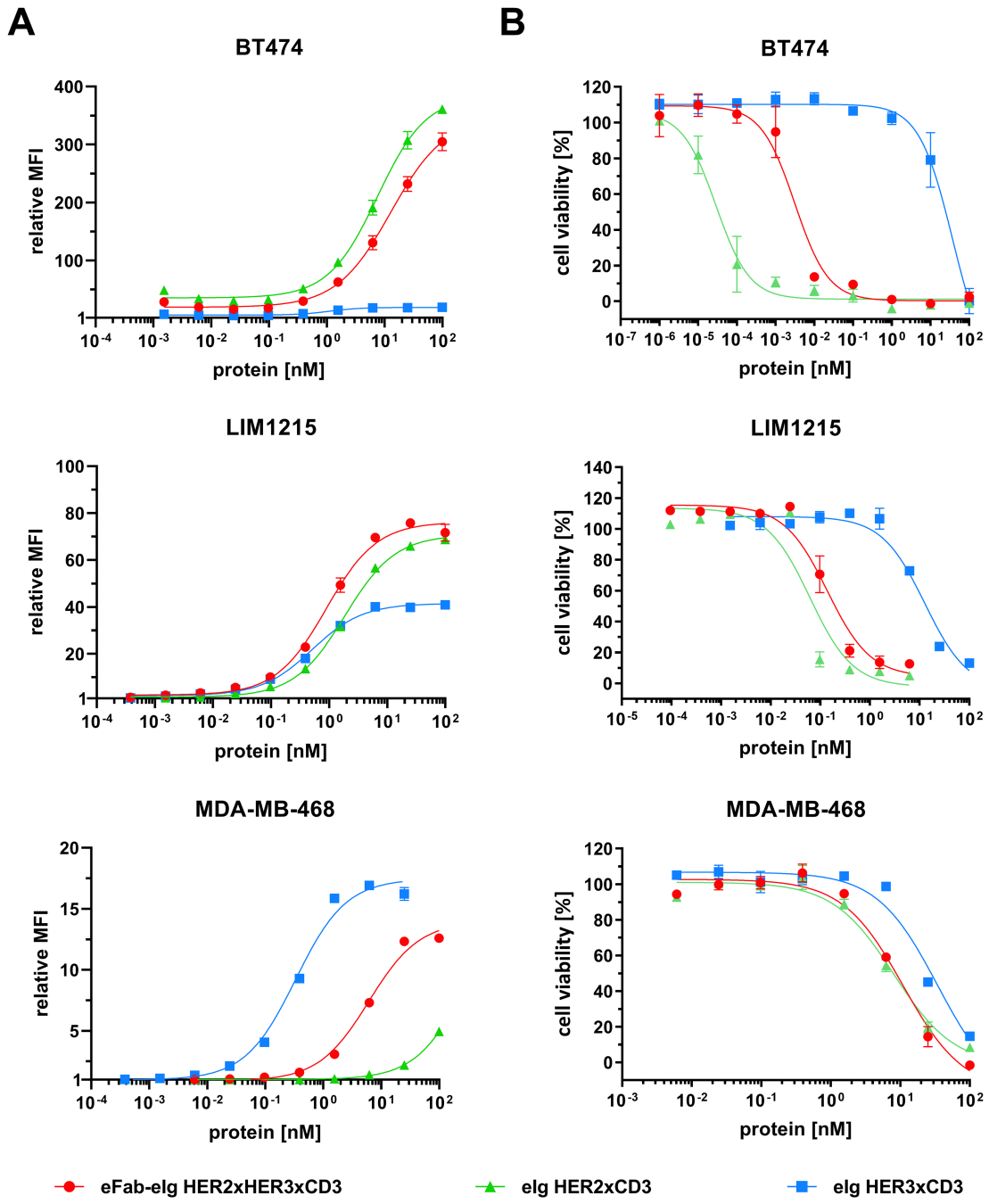

FIGURE 4
Target cell binding and cytotoxicity. **(A)** Binding of different elg molecules (eFab-elg HER2xHER3xCD3; elg HER2xCD3; elg HER3xCD3) to BT474, LIM1215 and MDA-MB-468 cells was analyzed via flow cytometry. **(B)** Killing of target cells (BT474, LIM1215 and MDA-MB-468) incubated with bi- or trispecific elg molecules and PBMCs (donor: HN#7 for BT474; HN#6 for LIM1215 and AH#1 for MDA-MB-468) at an effector-to-target (E:T) ratio of 10:1 for 3 days. Mean of duplicates ± SD, n=1.

TABLE 3 Tumor cell killing from cell viability assay.

Cell line	elg HER2xCD3	elg HER3xCD3	eFab-elg HER2xHER3xCD3
MDA-MB468	8.6 ± 2.3	14.3 ± 17.3	23.7 ± 15.0
LIM1215	0.1 ± 0.1	12.7 ± 0.1	0.3 ± 0.3
BT474	0.0001 ± 0.0001	38.8 ± 22.7	0.0022 ± 0.0017

EC_{50} values in nM. Mean ± SD, n=3.

Functional anti-tumor activity of the bi- and trispecific antibodies in 2D and 3D model system

To assess the cytotoxic activity of the antibodies, we co-cultured cancer cells with PBMCs at a effector to target cell ratio of 10:1 in the presence of the bi- and trispecific antibodies. (Figure 4B, Supplementary Figure S4). The bispecific eIg HER3xCD3 molecule showed the lowest activity on all tumor cell lines with EC_{50} values in the range of 12.7 to 38.8 nM, as the surface expression of HER3 of all tumor cell lines is in a similar range (from 6,000 to 20,000 HER3 receptors/cell). The HER2 expression of the different tumor cell lines strongly differs (from less than 1,700 to more than 578,000 HER2 receptors/cell) and showed strong cytotoxic effect of the bispecific HER2xCD3 and the trispecific eFab-eIg molecule with dependency of target cell binding. For MDA-MB-468 cells with low HER2 levels, EC_{50} values of 12.3 nM for the bispecific and 23.7 nM for the trispecific molecule were calculated, while stronger activity was detected for LIM1215 cells with moderate HER2 levels (EC_{50} values of 100 pM for eIg HER2xCD3 and 300 pM for eFab-eIg). Strongest killing with EC_{50} values of 0.1 pM for eIg HER2xCD3 and 2 pM for eFab-eIg were observed for the BT474 cells with high HER2 levels (Table 3). For BT474 cells, a significance between eIg HER3xCD3 (p=0.03) compared to the trispecific eFab-eIg and the HER2xCD3 eIg molecule was calculated. In addition, we used the T-cell activation system by using LIM1215 cells upon T-cell engagement to ensure and quantified immunostimulatory factors, like IL-2, IFNγ, IL-6 and TNFα, to analyze effects on the immune system (Figure 5, Table 4). In line with the cytotoxic activity of the bi- and trispecific

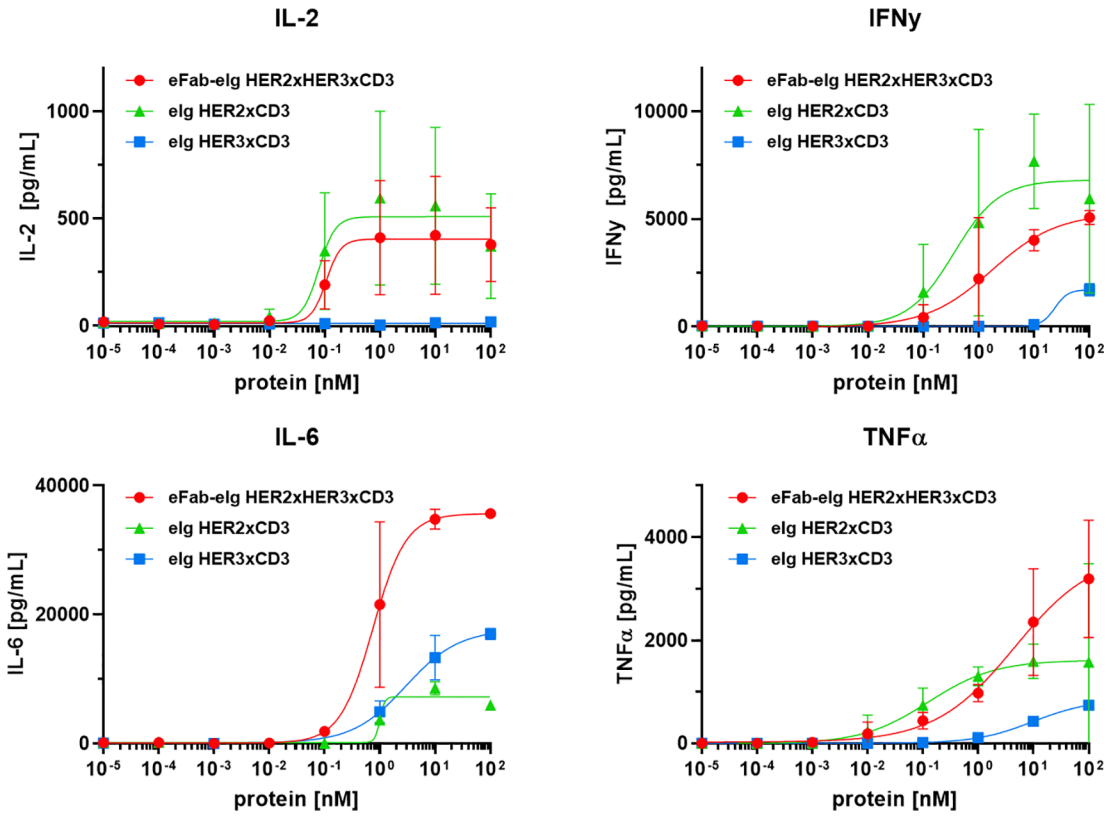

FIGURE 5
T-cell activation by TCEs. Release of IL-2, IL-6 and TNFα after 24 h and IFNγ after 48 h by PBMCs co-cultured with LIM1215 using an effector-to-target ratio of 10:1 analyzed by sandwich ELISA. Mean ± SD, n=2 - two individual donors).

TABLE 4 T-cell activation.

Cell line	eIg HER2xCD3	eIg HER3xCD3	eFab-eIg HER2xHER3xCD3
IL-2	0.08 ± 0.03	n.d.	0.1 ± 0.01
IFN-γ	0.7 ± 0.7	50.3 ± 49.9	3.4 ± 4.4
IL-6	1.0 ± 0.01	5.1 ± 5.1	1.0 ± 0.8
TNFα*	0.1	9.7	4.6

EC_{50} values in EC_{50} values in nM. Mean ± SD, n.d., not determined, n=2; *calculation of EC_{50} was based on both experiments.

antibodies, strong concentration-dependent release of IL-2, IFNγ, IL-6 and TNFα was observed for the bispecific eIg targeting HER2 and CD3, and the trispecific antibody, while the bispecific HER3xCD3 eIg triggered only a marginal cytokine response.

Finally, we employed a 3D co-culture assay to evaluate the cytotoxic activity of the trispecific antibody under conditions that more closely mimic the situation found *in vivo*. We first generated cancer cell spheroids by seeding BT474 cells into ultra-low attachment plates. Once they reached a size of approximately 250 µm, spheroids were incubated with varying numbers of PBMCs/well and different concentrations of the trispecific eFab-eIg for up to 2 days (Figure 6). Dead cells were visualized by PI staining. In the absence of PBMCs, the antibody neither had effects on spheroid morphology, nor did it induce cell killing. In agreement with the 2D experiments, cell death was effectively induced in the presence of PBMCs, to a greater extent and with faster kinetics when using higher numbers of PBMCs and higher antibody concentrations. In summary, our data demonstrate that the trispecific antibody showed strong T-cell activation and subsequential tumor cell killing in the 2D and 3D model system.

Discussion

Here, we have advanced the eIg technology to generate trispecific trivalent antibodies with an extended Ig-like structure. The underlying design principle utilizes heterodimerizing EHD2 domains derived from the homodimerizing heavy chain domain 2 of IgE (EHD2) to generate Fab-like building blocks (eFabs). The EHD2 homodimers are normally covalently linked by two disulfide bonds formed between C14 and C102. Substituting Cys14 in a first EHD2 (EHD2-1) and C102 in a second EHD2 (EHD2-2) by serine residues results in efficient heterodimerization since only heterodimers are capable of forming a single disulfide bond while homodimers cannot do so and are thus unstable (18, 20). These hetEHD2 domains are used to replace C_H1 and C_L in a normal Fab to obtain Fab-like moieties (eFabs). In comparison to other antibody fragments, e.g. scFv molecules, as building blocks for multispecific antibodies, the usage of the disulfide-linked constant domains in the eIg technology increases the thermal stability and the solubility of multispecific molecule and lowers the potential for aggregations (27, 28). In the present study it was found that placing the EHD2–1 and EHD2–2 domains on different chains mediates correct pairing of cognate V_H and V_L in co-expressed eFab-1 and eFab-2 moieties without further modifications of the variable domains. Proof of concept was obtained for a trispecific eFab-eIg targeting HER2, HER3 and CD3. The molecule retained binding activity for its target antigens and was capable of recruiting T-cells to tumor cells and mediating T-cell-induced killing of tumor cell lines with varying levels of HER2 and HER3 expression.

The majority of trispecific antibodies in preclinical and clinical development aim at directing immune effector cells to tumor cells (10). Combining T-cell engagement with the targeting of two different surface antigens can result in improved tumor selectivity

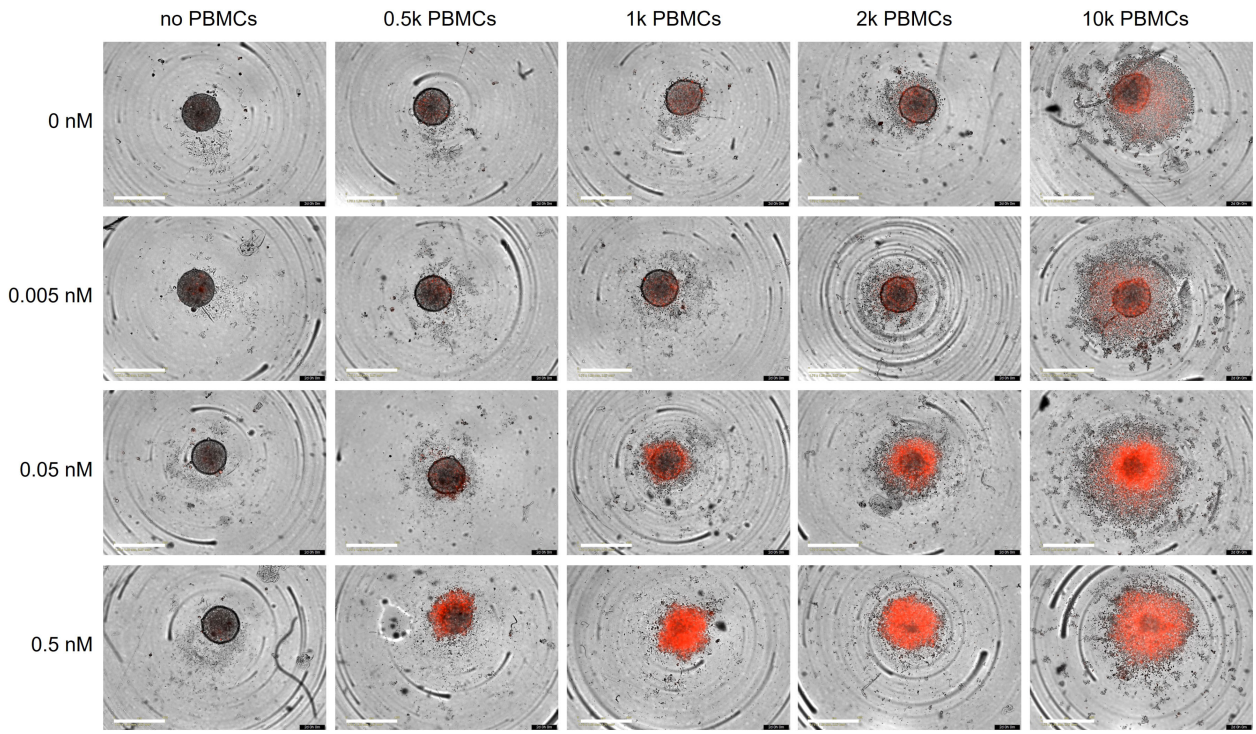

FIGURE 6
Killing of BT474 spheroids. BT474 spheroids with a diameter of approximately 250 µm were used as target cells and incubated with different amount of trispecific eFab-eIg antibodies as well as different number of PBMCs (donor: AL#1). In addition, the induction of apoptosis was analyzed using propidium iodide (PI; 1 µg/mL). Cells were incubated with antibodies and the PBMCs for 48 h at 37°C. n=1.

by avidity-driven on-target activity. This was, for example, shown for a trispecific TCE targeting Lys6E, B7-H4 and CD3, mediating strong killing of breast cancer cells simultaneously expression Ly6E and B7-H4 *in vitro* and *in vivo* (12). Furthermore, a trispecific TCE targeting EGFR and a NY-ESO-1 showed strongly increased efficacy and anti-tumor activity compared to TCEs targeting single antigens (29). In another study, Tapia-Galisteo and coworkers used a trispecific (EGFRxEpCAMxCD3) TCE and modified the affinity for both TAAs. For EGFR- and EpCAM-positive HCT116 cells, a 100-fold increased cell killing activity was detected compared to EGFR-positive or EpCAM-positive tumor cells (30). However, the trispecific eFab-eIg molecule described here did not exhibit increased cell binding and cytotoxicity compared to the 1 + 1 bispecific TCEs targeting either HER2 or HER3, but rather combined both activities within one molecule without causing an avidity-driven increase of activity. This can be explained by sterical hindrance, impairing the simultaneous binding to HER2 and HER3 on the same cell, and further interacting with CD3 on T-cells. Indeed, we previously reported that the format matters, i.e. the geometry and architecture of trivalent bispecific TCEs targeting EGFR affected the degree of target cell killing by the T-cells (19). Since CD3 binding by the inner eFab was hampered by the outer eFab targeting HER3, as shown by flow cytometry assays using Jurkat cells, in future studies trispecific molecules with altered arrangements of the three binding sites might identify formats with increased binding and activity.

Nevertheless, the trispecific eFab-eIg TCE molecule was capable of efficiently killing tumor cells with varying levels of HER2 and HER3. Specifically, BT474 cells which express high levels of HER2 and low levels of HER3, and therefore are less susceptible to HER3 targeting alone, were efficiently killed by the trispecific TCE. HER3 expression is often elevated as a compensation mechanism in HER2-resistant tumor cells (31, 32). It is known that the HER family of receptor tyrosine kinases displays a high degree of plasticity which can provide compensatory signaling associated with acquired resistance to treatment (33). Thus, HER3 can be expressed as a compensatory signal in HER2-resistant tumor cell lines. In such settings, a trispecific TCE that targets both HER2 and HER3 might prove beneficial, by preventing or prolonging the development of acquired resistance.

The beneficial effects of dual targeting are further supported by findings for a DNA-encoded trispecific TCE targeting IL13Rα2, EGFRvIII and CD3. This trispecific TCE was designed to address the tumor heterogeneity of glioblastoma and demonstrated efficient tumor growth control in a GBM model with heterogenous expression of IL13Rα2 and EGFRvIII, resembling the complex tumor environment in human GBM (34). In addition, the superiority of dual targeting TCEs was demonstrated for a trispecific TCE targeting CD3, BCMA, and CD38 (ISB 2001), utilizing a common-light chain approach to generate a trispecific Fab-IgG molecule (35).

Furthermore, trispecific antibodies allow to address tumor escape mechanisms, e.g. resulting from the downregulation or loss of a target antigen. For example, treatment with the bispecific TCE blinatumomab targeting CD19 and CD3 resulted in the appearance of CD19-negative leukemic blasts in approximately 30% of patients (36). This antigen loss was circumvented by integration of binding sites for a CD20 fragment (37) or CD22 (38) as a second tumor cell targeting element. Similarly, down-regulation of HER2 was detected in cell lines treated with a trastuzumab-ADC T-DM1 as well as in four patients after receiving the dual trastuzumab/pertuzumab combination therapy (39). Adding a HER3 binding site to a HER2-targeting TCE could address the tumor heterogeneity and exploit the potential emergence of HER3 expression as compensatory signal (33, 40). Of note, a first bispecific antibody (zenocutuzumab) targeting HER2 and HER3 was recently approved for cancer therapy (41).

In summary, by adapting our eIg technology, we were capable of generating a trivalent trispecific eFab-eIg molecule for T-cell engagement. Using two different eFab building blocks (eFab-1, eFab-2) together with a normal Fab moiety allows the generation of trispecific molecules with varying valency and geometry. This was also exemplarily shown for bispecific eIg variants targeting EGFR and CD3, either comprising or lacking an Fc region (19). Thus, the eIg technology represents a versatile platform for the generation multispecific antibodies for a multitude of applications.

Data availability statement

The raw data supporting the conclusions of this article will be made available by the authors, without undue reservation.

Ethics statement

Ethical approval was not required for the studies involving humans because only commercially available material from anonymous blood donors was used. The studies were conducted in accordance with the local legislation and institutional requirements. The human samples used in this study were acquired from a by- product of routine care or industry. Written informed consent to participate in this study was not required from the participants or the participants' legal guardians/next of kin in accordance with the national legislation and the institutional requirements. The studies were conducted in accordance with the local legislation and institutional requirements.

Author contributions

A-KL: Methodology, Investigation, Data curation, Writing – review & editing, Visualization, Writing – original draft, Validation, Formal analysis. AH: Validation, Methodology, Visualization, Formal analysis, Investigation, Writing – review & editing. MO: Supervision, Writing – review & editing, Funding acquisition, Investigation, Resources, Conceptualization, Project administration. RK: Resources, Supervision, Visualization, Investigation, Conceptualization, Validation, Funding acquisition, Writing – review & editing, Project

administration, Formal analysis, Writing – original draft, Methodology. OS: Writing – original draft, Formal analysis, Methodology, Visualization, Data curation, Resources, Project administration, Validation, Software, Investigation, Supervision, Writing – review & editing, Conceptualization.

Funding

The author(s) declare that no financial support was received for the research, and/or publication of this article.

Acknowledgments

We would like to thank Nadine Heidel and Sabine Münkel for excellent technical assistance.

Conflict of interest

RK and OS are named inventors on a patent application covering the eIg technology.

The remaining authors declare that the research was conducted in the absence of any commercial or financial relationships that could be construed as a potential conflict of interest.

Generative AI statement

The author(s) declare that no Generative AI was used in the creation of this manuscript.

Any alternative text (alt text) provided alongside figures in this article has been generated by Frontiers with the support of artificial intelligence and reasonable efforts have been made to ensure accuracy, including review by the authors wherever possible. If you identify any issues, please contact us.

Publisher's note

Supplementary material

The Supplementary Material for this article can be found online at: https://www.frontiersin.org/articles/10.3389/fimmu.2025.1642454/full#supplementary-material

SUPPLEMENTARY FIGURE 1
Thermal stability. Determination of the aggregation point by dynamic light scattering (DLS) of the purified Fab-eIg, eIg and IgG molecules. Dotted line indicates the aggregation point. n=1.

SUPPLEMENTARY FIGURE 2
Target cell binding. Binding of eIg molecules (eFab-eIg HER2xHER3xCD3; eIg HER2xCD3; eIg HER3xCD3) to BT474, LIM1215 and MDA-MB-468 cells was analyzed via flow cytometry. Mean ± SD, N=2 and 3.

SUPPLEMENTARY FIGURE 3
Zoom in for binding of eIg HER3xCD3 to BT474 cells. Binding analysis of eIg HER3xCD3 to BT474 from Figure 4 and Supplementary Figure S1 was used to generate a zoom in.

SUPPLEMENTARY FIGURE 4
Target cell cytotoxicity. Killing of target cells (BT474, LIM1215 and MDA-MB-468) incubated with bi- or trispecific eIg molecules and PBMCs (AL#1 and AH#2 for BT474; AH#1 and HN#4 for LIM1215 as well as HN#4 and HN#6 for MDA-MB-468) at an effector-to-target (E:T) ratio of 10:1 for 3 days. Mean ± SD, N=2 and 3.

References

1. Surowka M, Klein C. A pivotal decade for bispecific antibodies? *MAbs*. (2024) 16:2321635. doi: 10.1080/19420862.2024.2321635

2. Bacac M, Fauti T, Sam J, Colombetti S, Weinzierl T, Ouaret D, et al. A novel carcinoembryonic antigen T-cell bispecific antibody (CEA TCB) for the treatment of solid tumors. *Clin Cancer Res*. (2016) 22:3286–97. doi: 10.1158/1078-0432.CCR-15-1696

3. Bacac M, Colombetti S, Herter S, Sam J, Perro M, Chen S, et al. CD20-TCB with obinutuzumab pretreatment as next-generation treatment of hematologic Malignancies. *Clin Cancer Res*. (2018) 24:4785–97. doi: 10.1158/1078-0432.CCR-18-0455

4. Slaga D, Ellerman D, Lombana TN, Vij R, Li J, Hristopoulos M, et al. Avidity-based binding to HER2 results in selective killing of HER2-overexpressing cells by anti-HER2/CD3. *Sci Transl Med*. (2018) 10. doi: 10.1126/scitranslmed.aat5775

5. Runcie K, Budman DR, John V, Seetharamu N. Bi-specific and tri-specific antibodies- the next big thing in solid tumor therapeutics. *Mol Med*. (2018) 24:50. doi: 10.1186/s10020-018-0051-4

6. Ellerman D. Bispecific T-cell engagers: Towards understanding variables influencing the *in vitro* potency and tumor selectivity and their modulation to enhance their efficacy and safety. *Methods*. (2019) 154:102–17. doi: 10.1016/j.ymeth.2018.10.026

7. Kelly WK, Danila DC, Lin C-C, Lee J-L, Matsubara N, Ward PJ, et al. Xaluritamig, a STEAP1 × CD3 xmAb 2 + 1 immune therapy for metastatic castration-resistant prostate cancer: results from dose exploration in a first-in-human study. *Cancer Discov*. (2024) 14:76–89. doi: 10.1158/2159-8290.CD-23-0964

8. Shirley M. Glofitamab: first approval. *Drugs*. (2023) 83:935–41. doi: 10.1007/s40265-023-01894-5

9. Klein C, Schaefer W, Regula JT. The use of CrossMAb technology for the generation of bi- and multispecific antibodies. *MAbs*. (2016) 8:1010–20. doi: 10.1080/19420862.2016.1197457

10. Tapia-Galisteo A, Compte M, Álvarez-Vallina L, Sanz L. When three is not a crowd: trispecific antibodies for enhanced cancer immunotherapy. *Theranostics*. (2023) 13:1028–41. doi: 10.7150/thno.81494

11. Yao Y, Hu Y, Wang F. Trispecific antibodies for cancer immunotherapy. *Immunology*. (2023) 169:389–99. doi: 10.1111/imm.13636

12. Dicara DM, Bhakta S, Go MA, Ziai J, Firestein R, Forrest B, et al. Development of T-cell engagers selective for cells co-expressing two antigens. *MAbs*. (2022) 14:2115213. doi: 10.1080/19420862.2022.2115213

13. Bogen JP, Carrara SC, Fiebig D, Grzeschik J, Hock B, Kolmar H. Design of a trispecific checkpoint inhibitor and natural killer cell engager based on a 2 + 1 common light chain antibody architecture. *Front Immunol*. (2021) 12:669496. doi: 10.3389/fimmu.2021.669496

14. Wu X, Yuan R, Bacica M, Demarest SJ. Generation of orthogonal Fab-based trispecific antibody formats. *Protein Eng Des Sel*. (2018) 31:249–56. doi: 10.1093/protein/gzy007

15. Wu L, Seung E, Xu L, Rao E, Lord DM, Wei RR, et al. Trispecific antibodies enhance the therapeutic efficacy of tumor-directed T cells through T cell receptor co-stimulation. *Nat Cancer*. (2020) 1:86–98. doi: 10.1038/s43018-019-0004-z

16. Yanakieva D, Pekar L, Evers A, Fleischer M, Keller S, Mueller-Pompalla D, et al. Beyond bispecificity: Controlled Fab arm exchange for the generation of antibodies with multiple specificities. *MAbs*. (2022) 14:2018960. doi: 10.1080/19420862.2021.2018960

17. Debelec-Butuner B, Quitt O, Schreiber S, Momburg F, Wisskirchen K, Protzer U. Activation of distinct antiviral T-cell immunity: A comparison of bi- and trispecific T-cell engager antibodies with a chimeric antigen receptor targeting HBV envelope proteins. *Front Immunol*. (2022) 13:1029214. doi: 10.3389/fimmu.2022.1029214

18. Kühl L, Aschmoneit N, Kontermann RE, Seifert O. The eIg technology to generate Ig-like bispecific antibodies. *MAbs*. (2022) 14:2063043. doi: 10.1080/19420862.2022.2063043

19. Kühl L, Schäfer AK, Kraft S, Aschmoneit N, Kontermann RE, Seifert O. eIg-based bispecific T-cell engagers targeting EGFR: Format matters. *MAbs*. (2023) 15:2183540. doi: 10.1080/19420862.2023.2183540

20. Seifert O, Plappert A, Fellermeier S, Siegemund M, Pfizenmaier K, Kontermann RE. Tetravalent antibody-scTRAIL fusion proteins with improved properties. *Mol Cancer Ther*. (2014) 13:101–11. doi: 10.1158/1535-7163.MCT-13-0396

21. Seifert O, Rau A, Beha N, Richter F, Kontermann RE. Diabody-Ig: a novel platform for the generation of multivalent and multispecific antibody molecules. *MAbs*. (2019) 11:919–29. doi: 10.1080/19420862.2019.1603024

22. Rau A, Kocher K, Rommel M, Kühl L, Albrecht M, Gotthard H, et al. A bivalent, bispecific Dab-Fc antibody molecule for dual targeting of HER2 and HER3. *MAbs*. (2021) 13:1902034. doi: 10.1080/19420862.2021.1902034

23. Armour KL, Clark MR, Hadley AG, Williamson LM. Recombinant human IgG molecules lacking Fcgamma receptor I binding and monocyte triggering activities. *Eur J Immunol*. (1999) 29:2613–24. doi: 10.1002/(SICI)1521-4141(199908)29:08<2613:AID-IMMU2613>3.0.CO;2-J

24. Carter P, Presta L, Gorman CM, Ridgway JB, Henner D, Wong WL, et al. Humanization of an anti-p185HER2 antibody for human cancer therapy. *Proc Natl Acad Sci U.S.A*. (1992) 89:4285–9. doi: 10.1073/pnas.89.10.4285

25. Aschmoneit N, Steinlein S, Kühl L, Seifert O, Kontermann RE. A scDb-based trivalent bispecific antibody for T-cell-mediated killing of HER3-expressing cancer cells. *Sci Rep*. (2021) 11:13880. doi: 10.1038/s41598-021-93351-0

26. Schmitt LC, Rau A, Seifert O, Honer J, Hutt M, Schmid S, et al. Inhibition of HER3 activation and tumor growth with a human antibody binding to a conserved epitope formed by domain III and IV. *MAbs*. (2017) 9:831–43. doi: 10.1080/19420862.2017.1319023

27. Wu X, Demarest SJ. Building blocks for bispecific and trispecific antibodies. *Methods*. (2019) 154:3–9. doi: 10.1016/j.ymeth.2018.08.010

28. Wu X, Sereno AJ, Huang F, Lewis SM, Lieu RL, Weldon C, et al. Fab-based bispecific antibody formats with robust biophysical properties and biological activity. *MAbs*. (2015) 7:470–82. doi: 10.1080/19420862.2015.1022694

29. Shen Y, Jin S-J, Chen Y-C, Liu W-H, Li Y-M, Zhao W-Y, et al. Improving the tumor selectivity of T cell engagers by logic-gated dual tumor-targeting. *Pharmacol Res*. (2023) 192:106781. doi: 10.1016/j.phrs.2023.106781

30. Tapia-Galisteo A, Sánchez Rodríguez Í, Aguilar-Sopeña O, Harwood SL, Narbona J, Ferreras Gutierrez M, et al. Trispecific T-cell engagers for dual tumor-targeting of colorectal cancer. *Oncoimmunology*. (2022) 11:2034355. doi: 10.1080/2162402X.2022.2034355

31. Garrett JT, Olivares MG, Rinehart C, Granja-Ingram ND, Sánchez V, Chakrabarty A, et al. Transcriptional and posttranslational up-regulation of HER3 (ErbB3) compensates for inhibition of the HER2 tyrosine kinase. *Proc Natl Acad Sci U.S.A*. (2011) 108:5021–6. doi: 10.1073/pnas.1016140108

32. Drago JZ, Ferraro E, Abuhadra N, Modi S. Beyond HER2: Targeting the ErbB receptor family in breast cancer. *Cancer Treat Rev*. (2022) 109:102436. doi: 10.1016/j.ctrv.2022.102436

33. Jacobsen HJ, Poulsen TT, Dahlman A, Kjær I, Koefoed K, Sen JW, et al. Pan-HER, an antibody mixture simultaneously targeting EGFR, HER2, and HER3, effectively overcomes tumor heterogeneity and plasticity. *Clin Cancer Res*. (2015) 21:4110–22. doi: 10.1158/1078-0432.CCR-14-3312

34. Park DH, Bhojnagarwala PS, Liaw K, Bordoloi D, Tursi NJ, Zhao S, et al. Novel tri-specific T-cell engager targeting IL-13Rα2 and EGFRvIII provides long-term survival in heterogeneous GBM challenge and promotes antitumor cytotoxicity with patient immune cells. *J Immunother Cancer*. (2024) 12. doi: 10.1136/jitc-2024-009604

35. Carretero-Iglesia L, Hall OJ, Berret J, Pais D, Estoppey C, Chimen M, et al. ISB 2001 trispecific T cell engager shows strong tumor cytotoxicity and overcomes immune escape mechanisms of multiple myeloma cells. *Nat Cancer*. (2024) 5:1494–514. doi: 10.1038/s43018-024-00821-1

36. Ruella M, Barrett DM, Kenderian SS, Shestova O, Hofmann TJ, Perazzelli J, et al. Dual CD19 and CD123 targeting prevents antigen-loss relapses after CD19-directed immunotherapies. *J Clin Invest*. (2016) 126:3814–26. doi: 10.1172/JCI87366

37. Wang S, Peng L, Xu W, Zhou Y, Zhu Z, Kong Y, et al. Preclinical characterization and comparison between CD3/CD19 bispecific and novel CD3/CD19/CD20 trispecific antibodies against B-cell acute lymphoblastic leukemia: targeted immunotherapy for acute lymphoblastic leukemia. *Front Med*. (2022) 16:139–49. doi: 10.1007/s11684-021-0835-8

38. Zhao L, Li S, Wei X, Qi X, Liu D, Liu L, et al. A novel CD19/CD22/CD3 trispecific antibody enhances therapeutic efficacy and overcomes immune escape against B-ALL. *Blood*. (2022) 140:1790–802. doi: 10.1182/blood.2022016243

39. Bon G, Pizzuti L, Laquintana V, Loria R, Porru M, Marchiò C, et al. Loss of HER2 and decreased T-DM1 efficacy in HER2 positive advanced breast cancer treated with dual HER2 blockade: the SePHER Study. *J Exp Clin Cancer Res*. (2020) 39:279. doi: 10.1186/s13046-020-01797-3

40. Kol A, van Terwisscha Scheltinga AG, Timmer-Bosscha H, Lamberts LE, Bensch F, Vries EGd, et al. HER3, serious partner in crime: therapeutic approaches and potential biomarkers for effect of HER3-targeting. *Pharmacol Ther*. (2014) 143:1–11. doi: 10.1016/j.pharmthera.2014.01.005

41. Schram AM, Odintsov I, Espinosa-Cotton M, Khodos I, Sisso WJ, Mattar MS, et al. Zenocutuzumab, a HER2xHER3 bispecific antibody, is effective therapy for tumors driven by NRG1 gene rearrangements. *Cancer Discov*. (2022) 12:1233–47. doi: 10.1158/2159-8290.CD-21-1119

frontiers | Frontiers in Immunology

TYPE Systematic Review
PUBLISHED 10 September 2025
DOI 10.3389/fimmu.2025.1605877

OPEN ACCESS

EDITED BY
Miroslawa Puskulluoglu,
Maria Sklodowska-Curie National Research Institute of Oncology, Poland

REVIEWED BY
Luis Mas,
Auna Oncosalud, Peru
Parviz Azimnasab-sorkhabi,
The Ohio State University, United States
Agnieszka Rudzińska,
Maria Sklodowska-Curie National Research Institute of Oncology, Poland

*CORRESPONDENCE
Changhai Lei
lei@smmu.edu.cn

†These authors have contributed equally to this work and share first authorship

RECEIVED 04 April 2025
ACCEPTED 07 August 2025
PUBLISHED 10 September 2025

CITATION
Zhang Y, Wang H, Yang X and Lei C (2025) Dual-target immunotherapies in NSCLC: a systematic review and meta-analysis of randomized clinical trials.
Front. Immunol. 16:1605877.
doi: 10.3389/fimmu.2025.1605877

Dual-target immunotherapies in NSCLC: a systematic review and meta-analysis of randomized clinical trials

Yike Zhang†, Haozhe Wang†, Xinyue Yang† and Changhai Lei*

Department of Biophysics, College of Basic Medical Sciences, Naval Medical University, Shanghai, China

Background: Despite advances in targeted therapies and immune checkpoint inhibitors (ICIs), the prognosis for advanced non-small cell lung cancer (NSCLC) remains poor. Bispecific antibodies (BsAbs) represent an emerging class of dual-target immunotherapies, yet their comparative efficacy and safety profiles lack comprehensive quantitative synthesis.

Methods: This systematic review and meta-analysis (PROSPERO CRD420251005168) adhered to PRISMA guidelines. We systematically searched PubMed, Web of Science, Scopus, and Embase through March 2025 for phase III randomized controlled trials (RCTs) comparing dual-target immunotherapies with conventional therapies in advanced NSCLC. Primary outcomes were progression-free survival (PFS) and overall survival (OS); secondary outcomes included objective response rate (ORR), disease control rate (DCR), and treatment-related adverse events (AEs). Risk of bias was assessed using Cochrane RoB 2.0. Random-effects models were used for data synthesis.

Results: Six RCTs (n=3,063 patients) were included. Dual-target immunotherapies significantly improved PFS (HR= 0.58, 95% CI: 0.43-0.78; p<0.001) and ORR (RR=1.29,95%CI: 1.01-1.64; p=0.04) compared to conventional therapies. No significant OS (HR=0.84,95% CI: 0.68-1.05; p=0.13) or DCR (RR=1.09, 95% CI: 0.92-1.30; p=0.30) benefits were observed. Subgroup analyses stratified by mechanism showed no statistically significant differences in efficacy and safety between dual-target immunotherapies with different targets of action. Safety analyses revealed increased risks of any adverse events (RR=1.05; 95%CI: 1.02-1.09), grade≥3 AEs (RR=1.63; 95% CI: 1.37-1.94), serious AEs (RR=1.49; 95%CI:1.31-1.69) and AEs leading to treatment discontinuation (RR=2.49; 95% CI: 1.72-3.62) with dual-target immunotherapies.

Conclusion: Our findings, based on phase III RCTs, are limited by substantial heterogeneity among included studies. Dual-target immunotherapies demonstrate superior PFS and ORR in NSCLC but are associated with increased toxicity, particularly with EGFR/MET-targeted agents. While offering a promising therapeutic advance, safety optimization and biomarker-driven patient selection

are critical for clinical translation. Further trials are needed to validate long-term survival benefits and refine risk-benefit profiles.
Systematic review registration: https://www.crd.york.ac.uk/prospero/, identifier CRD420251005168.

KEYWORDS
bispecific antibodies, NSCLC, immunotherapy, meta-analysis, dual-target immunotherapies

Introduction

Lung cancer remains the leading cause of cancer-related mortality worldwide, with non-small cell lung cancer (NSCLC) accounting for approximately 85% of all cases (1, 2). Despite advancements in targeted therapies and immune checkpoint inhibitors (ICIs), the prognosis for advanced or metastatic NSCLC remains poor, with a 5-year survival rate below 20% (3). While therapies targeting EGFR, ALK, and PD-1/PD-L1 pathways have improved outcomes in specific patient subsets, intrinsic or acquired resistance, limited biomarker-driven eligibility, and heterogeneous treatment responses persist as major clinical challenges (4). These unmet needs underscore the urgency to develop novel therapeutic strategies with enhanced efficacy and tolerable safety profiles.

Dual-target immunotherapies represented by bispecific antibodies (BsAbs) is a promising class of immunotherapies designed to engage two distinct molecular targets simultaneously. By bridging tumor-associated antigens (TAAs) with immune effector cells or dual-blocking immune checkpoints, dual-target immunotherapies aim to amplify antitumor activity while overcoming resistance mechanisms observed with monoclonal antibodies (5). For instance, amivantamab, a BsAb targeting EGFR and MET, has demonstrated clinical activity in EGFR exon 20 insertion-mutated NSCLC, leading to its recent regulatory approval (6). Similarly, PD-1/CTLA-4-targeting BsAbs are being explored to enhance immune activation compared to monotherapy approaches (7). Despite this progress, the clinical benefits of dual-target immunotherapies in NSCLC remain inconsistent across trials, with variability in patient selection, dosing regimens, and endpoint definitions. Furthermore, safety concerns like adverse events (AEs) need systematic evaluation to optimize risk-benefit assessments.

Existing meta-analyses have primarily focused on monoclonal antibodies or small-molecule inhibitors in NSCLC, leaving the role of dual-target immunotherapies inadequately synthesized (8–11). Therefore, there is no clear conclusion whether dual-target immunotherapies can achieve an equal or superior effect compared to conventional therapies. A comprehensive evaluation of randomized controlled trials (RCTs) is critical to quantify pooled efficacy outcomes and safety profiles across diverse dual-target immunotherapies platforms. This systematic review and meta-analysis aims to consolidate evidence from RCTs to address two key questions: (1) What is the magnitude of clinical benefit offered by dual-target immunotherapies compared to standard therapies in NSCLC? (2) How do safety profiles vary among dual-target immunotherapies with conventional therapies? The findings will inform clinical decision-making, guide future trial design, and identify knowledge gaps for further investigation.

Methods

Search strategy

The present study strictly complied with the relevant requirements of the PRISMA guidelines and completed the PRISMA checklist (12). The study protocol was prospectively registered in the PROSPERO database (registration number: CRD420251005168) and was previously published. A systematic literature search was conducted in Pubmed, Web of Science, Scopus and Embase for studies published before March 2025 that compared dual-target immunotherapies and conventional therapies, using the following searching terms: Bispecific antibodies, BsAbs, lung cancer, NSCLC. The detailed search strategy is available in Supplementary Material. In addition, the references of all relevant articles were also searched to find additional literature. Only the studies in English were included.

Inclusion criteria and exclusion criteria

Studies were selected based on the following inclusion criteria: (1) Phase III randomized controlled trials (RCTs) comparing dual-target immunotherapies with conventional therapeutic regimens in non-small cell lung cancer (NSCLC) populations; (2) Availability of essential statistical parameters for meta-analysis, including at minimum one clinically validated endpoint: progression-free survival (PFS), overall survival (OS), objective response rate (ORR), or disease control rate (DCR); (3) Peer-reviewed full-text manuscripts with extractable outcome data; (4) Publications in English with accessible methodological details.

Exclusion criteria comprised: (1) Early-phase clinical trials (phase I/II studies); (2) Non-original research including editorials, narrative

reviews, preclinical investigations, case reports, and commentary articles; (3) Therapeutic interventions utilizing non-BsAb-based strategies or studies lacking comparator arms; (4) Trials with incomplete statistical reporting preventing quantitative synthesis.

Data extraction

Two investigators independently performed study screening and data extraction in duplicate following the predefined inclusion/exclusion criteria. All pertinent data were systematically extracted using standardized forms, followed by cross-verification of the results. Any discrepancies in data interpretation were resolved through consensus discussions, with unresolved cases adjudicated by a third senior researcher. The following data were collected from each study: first author, publication year, NCT identifier, sample size, sex, age, PFS, OS, ORR, DCR, any adverse events (AEs), grade ≥3 AEs, serious AEs and AEs leading to treatment discontinuation.

Risk of bias assessment

The methodological quality of included studies was evaluated using the Cochrane Collaboration's Risk of Bias Tool (RoB 2.0) through RevMan 5.4 software. Two independent reviewers assessed seven domains: (1) random sequence generation (selection bias); (2) allocation concealment (selection bias); (3) blinding of participants and personnel (performance bias); (4) blinding of outcome assessment (detection bias); (5) incomplete outcome data (attrition bias); (6) selective reporting (reporting bias); (7) other potential sources of bias. Each domain was judged as "low risk", "unclear risk", or "high risk" (13). Discrepancies were resolved through consensus or consultation with a third investigator.

Statistical analysis

Hazard ratios (HRs) with corresponding confidence intervals (CIs) were extracted as primary measures for overall survival (OS) and progression-free survival (PFS). Binary endpoints including AEs and DCR were quantified using risk ratio (RR) with 95% CIs. The I^2 statistics were utilized to evaluate the heterogeneity. $I^2 < 25\%$, $25\% \leq I^2 \leq 50\%$, and $I^2 > 50\%$ were regarded as low, moderate, and high heterogeneity. Given the substantial variability in methodological approaches observed across enrolled trials, a random-effects model was employed for all quantitative syntheses to account for potential between-study heterogeneity, irrespective of initial heterogeneity assessment results. To assess the robustness of outcomes with statistically significant and substantial heterogeneity ($p \leq 0.05$, $I^2 > 50\%$), leave-one-out sensitivity analyses were performed. Pooled estimates (HR for PFS; RR for dichotomous outcomes) and I^2 statistics were recalculated after sequentially excluding each included trial, maintaining original random-effects models (14, 15). Subgroup analyses stratified according to the different mechanisms of dual-target immunotherapies were performed to assess differences between different BsAbs or bifunctional fusion protein while mitigating the impact of heterogeneity. Subgroup analyses were performed only for categories with ≥2 studies. Subgroups with a single study were described qualitatively.

Results

Selected studies and study characteristics

A total of 4,337 potential articles published before March 2025 were identified from databases. After removing 658 duplicates, 3,215 articles were excluded by reviewing the titles and abstracts because they were a review, summary, case report, animal experimental study, comments, or meta-analysis. 458 articles were removed because they were phase I/II trials or did not focus on NSCLC. Finally, 6 phase III RCTs met the eligibility criteria and were included in the present meta-analysis (16–21). A flow diagram of the search strategies, which includes reasons for the exclusion of articles is shown in Figure 1.

6 studies with a total of 3,063 patients, of which 1,224 patients were in the BsAbs group and 1,360 patients in the conventional therapy group, were involved (16–21). All the eligible studies were published between 2023 and 2025. The detailed characteristics of the included publications are summarized in Table 1.

Efficacy of dual-target immunotherapies

All of the 6 studies reported the PFS and ORR as the main outcomes of tumor immunotherapy. 3 of the studies reported DCR (16, 20, 21), and 4 studies reported OS (17–20). Figure 2 shows the results of the meta-analysis for the efficacy of dual-target immunotherapies. The pooled analysis revealed a statistically significant improvement in PFS with bispecific antibody therapy compared to conventional therapy, with a hazard ratio (HR) of 0.58 (95% CI: 0.43–0.78; $P < 0.001$). Substantial heterogeneity was observed across studies ($I^2 = 85\%$; $P < 0.00001$), necessitating a random-effects model. The meta-analysis of four randomized trials revealed no statistically significant improvement in OS (HR = 0.84; 95% CI: 0.68–1.05; $P = 0.13$) and DCR (RR = 1.09; 95% CI: 0.92-1.30; $P = 0.30$) with bispecific antibody therapy compared to conventional treatment. A random-effects model was applied due to clinical diversity in trial designs and patient populations. The meta-analysis demonstrated a statistically significant improvement in ORR with bispecific antibodies (RR = 1.29, 95% CI: 1.01–1.64; $P = 0.04$). Due to the high heterogeneity ($I^2 = 92\%$; $P = 0.04$), a random-effects model was applied.

Safety of dual-target immunotherapies

Figure 3 shows the results of the meta-analysis for the safety of dual-target immunotherapies. The meta-analysis of six randomized

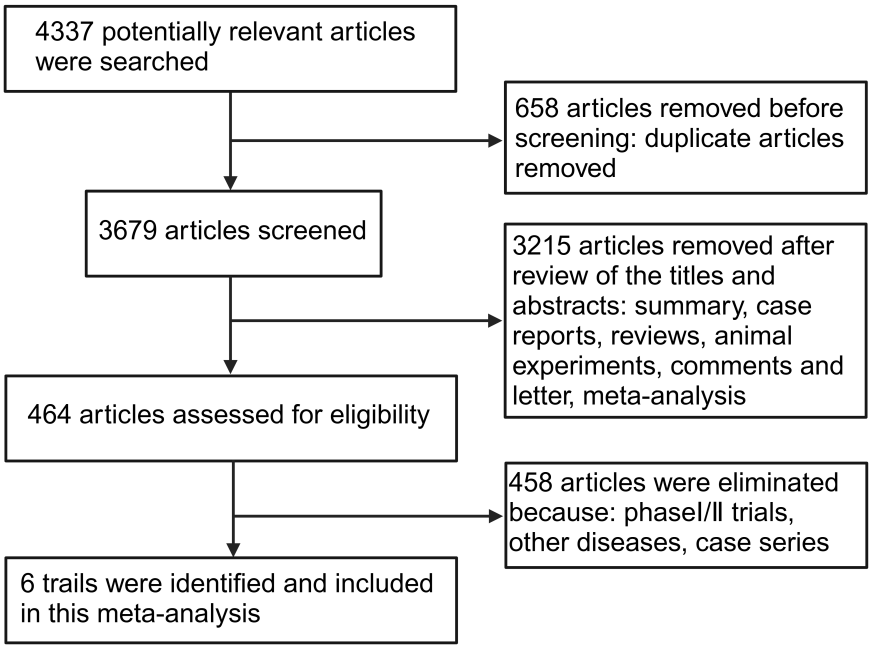

FIGURE 1
Flow diagram for study identification and selection process.

trials (dual-target immunotherapies group: n = 1,211; conventional therapy: n = 1,338) revealed a statistically significant increase in the risk of any adverse events (AEs) with dual-target immunotherapies (RR = 1.05, 95% CI: 1.02–1.09; p = 0.003), though with substantial heterogeneity (I^2 = 81%, p < 0.0001). dual-target immunotherapies significantly increased the risk of grade ≥ 3 AEs (RR = 1.63, 95% CI: 1.37–1.94; p < 0.00001; I^2 = 76%; p = 0.0008), serious AEs (RR = 1.49, 95% CI: 1.31–1.69; p < 0.00001; I^2 = 9%; p = 0.36), and AEs led to treatment discontinuation (RR = 2.49, 95% CI: 1.72–3.62; p < 0.00001; I^2 = 67%; p = 0.01). Supplementary Table S6 quantifies

TABLE 1 Main characters of included studies.

Study	Year	Therapeutic agent	Group	Cases	Age, median (range)	Sex (Male vs Female)	NCT identifier
Zhou (19)	2023	Amivantamab	Amivantamab-chemotherapy	153	61 (27-86)	68 vs 85	NCT04538664
			chemotherapy	155	62 (30-92)	62 vs 93	
Byoung (20)	2023	Bintrafusp Alfa	Bintrafusp Alfa	152	68 (62–73)	110 vs 42	NCT03631706
			Pembrolizumab	152	68 (61–75)	116 vs 36	
Fang (16)	2024	Ivonescimab	Ivonescimab-chemotherapy	161	59.6 (32.3-74.9)	77 vs 84	NCT05184712
			placebo-chemotherapy	161	59.4 (36.2-74.2)	79 vs 82	
Passaro (17)	2024	Amivantamab	Amivantamab–lazertinib–chemotherapy	263	61 (23-83)	95 vs 168	NCT04988295
			Amivantamab–chemotherapy	131	62 (36-84)	50 vs 81	
			Chemotherapy	263	62 (31-85)	106 vs 157	
Byoung (18)	2024	Amivantamab	Amivantamab-Lazertinib	429	64 (25-88)	178 vs 251	NCT04487080
			Osimertinib	429	63 (28-88)	154 vs 275	
			Lazertinib	216	63 (31–87)	80 vs 136	
Xiong (21)	2025	Ivonescimab	Ivonescimab	198	65 (37-85)	164 vs 34	NCT05499390
			Pembrolizumab	200	66 (35-83)	169 vs 31	

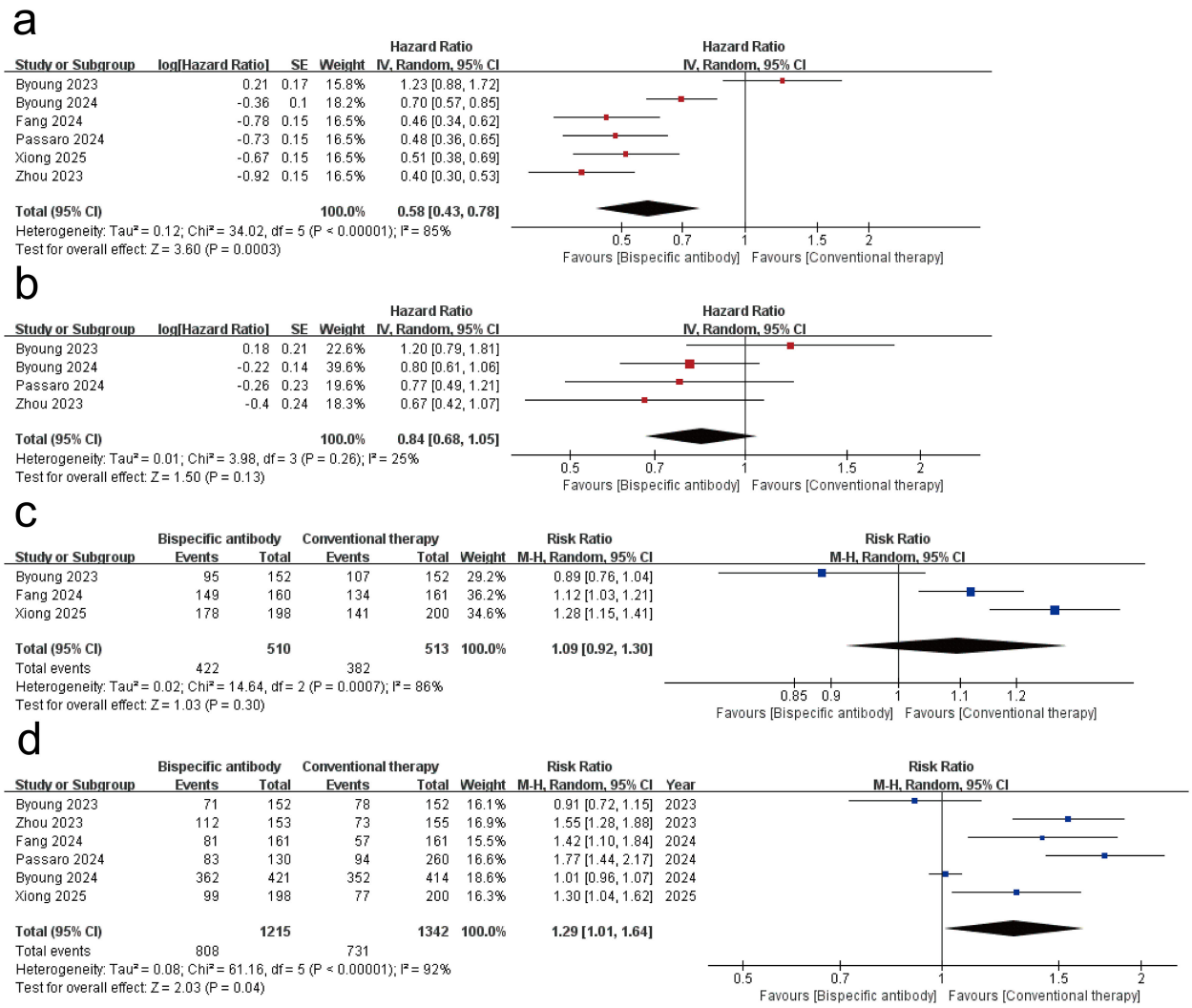

FIGURE 2
Forest plot of the meta-analysis for the efficacy of dual-target immunotherapies. **(a)** progression-free survival (PFS); **(b)** overall survival (OS); **(c)** disease control rate (DCR); **(d)** objective response rate (ORR).

AEs frequencies, revealing that non-chemotherapy dual-target immunotherapies regimens exhibited dermatologic event predominance, whereas BsAb-chemotherapy combinations showed hematologic burden. These findings suggest that bispecific antibody therapy is consistently associated with elevated AE risks across severity grades and clinically significant endpoints compared to conventional therapy.

Sensitivity analysis

Sensitivity analyses (Supplementary Tables S1–S5) demonstrated consistent PFS benefit across all exclusions (HR range: 0.51-0.63, 95% CIs excluded 1), with heterogeneity decreasing from 85% to 68% when excluding Byoung 2023 (20). ORR significance was lost upon excluding Passaro 2024 (17) (RR = 1.21, 95% CI: 0.96-1.51) or Fang 2024 (16) (RR=1.26, 95% CI: 0.97-1.66), though directional consistency persisted (RR range: 1.21-1.38; $I^2 > 88\%$). Safety signals remained robust: any AEs (RR = 1.05-1.07), grade ≥ 3 AEs (RR = 1.52-1.73, all $p < 0.001$), and treatment-discontinuing AEs (RR = 2.24-2.73) showed persistent risk elevations, with Byoung 2023 (20) exclusion reducing heterogeneity for grade ≥ 3 AEs from 76% to 62%.

Subgroup analysis

Subgroup analyses by dual-target immunotherapies mechanism demonstrated comparable PFS benefits between PD-1/VEGF-targeted agents (HR = 0.48, 95% CI: 0.39–0.60; I^2 = 0%, 2 trials) and EGFR/MET-targeted agents (HR = 0.52, 0.37–0.74; I^2 = 82%, 3 trials), with no significant subgroup differences (χ^2 = 0.11, df = 1, P = 0.74; I^2 = 0%). For PD-L1/TGF-β-targeted agents (1 trial), the HR of PFS was 1.23 (0.88–1.72). ORRs showed a similar situation across subgroups: PD-1/VEGF agents achieved a RR of

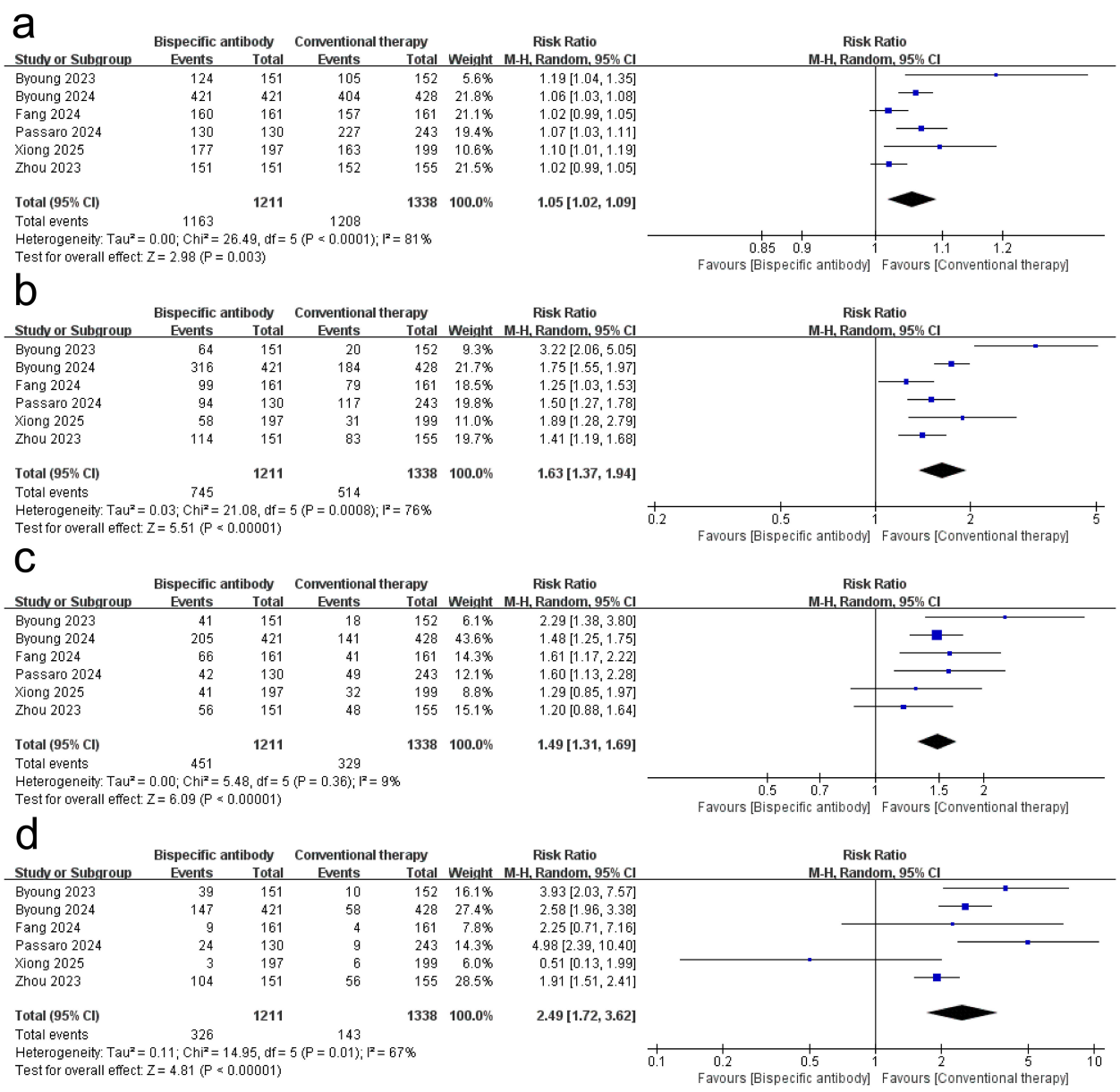

FIGURE 3
Forest plot of the meta-analysis for the safety of dual-target immunotherapies. **(a)** any AEs; **(b)** Grade ≥ 3 AEs; **(c)** serious AEs; **(d)** AEs led to treatment discontinuation.

1.39 (1.18–1.65; $I^2 = 0\%$), while EGFR/MET agents showed an RR of 1.40 (0.89–2.18; $I^2 = 96\%$), with no subgroup interaction ($\chi^2 = 0.00$, $P = 1.00$) (Supplementary Figures S1, S2).

Analyses stratified by mechanism revealed homogeneous risks for any-grade adverse events (AEs) (PD-1/VEGF: RR = 1.05, 0.93–1.19; EGFR/MET: RR = 1.05, 1.02–1.08; subgroup $P = 0.93$; $I^2 = 0\%$) and serious AEs (PD-1/VEGF: RR = 1.48, 1.15–1.92; EGFR/MET: RR = 1.44, 1.26–1.65; subgroup $P = 0.83$; $I^2 = 0\%$). For grade ≥3 AEs, both subgroups exhibited elevated risks (PD-1/VEGF: RR = 1.49, 0.98–2.25; EGFR/MET: RR = 1.56, 1.37–1.79; subgroup $P = 0.83$; $I^2 = 0\%$). EGFR/MET-targeted agents demonstrated a higher numerical risk for treatment discontinuation due to AEs (RR = 2.56, 1.73–3.80) compared to PD-1/VEGF agents (RR = 1.12, 0.26–4.82), though the subgroup difference was nonsignificant ($\chi^2 = 1.15$, $P = 0.28$; $I^2 = 13.2\%$). All analyses utilized random-effects models (Supplementary Figures S3–S6).

Risk of bias

The methodological quality of included randomized trials was assessed using the Cochrane Risk of Bias Tool (Figure 4). Four studies met ≥ 5/7 low-risk criteria (16, 19–21). Major limitations involved blinding deficiencies in 50% of trials.

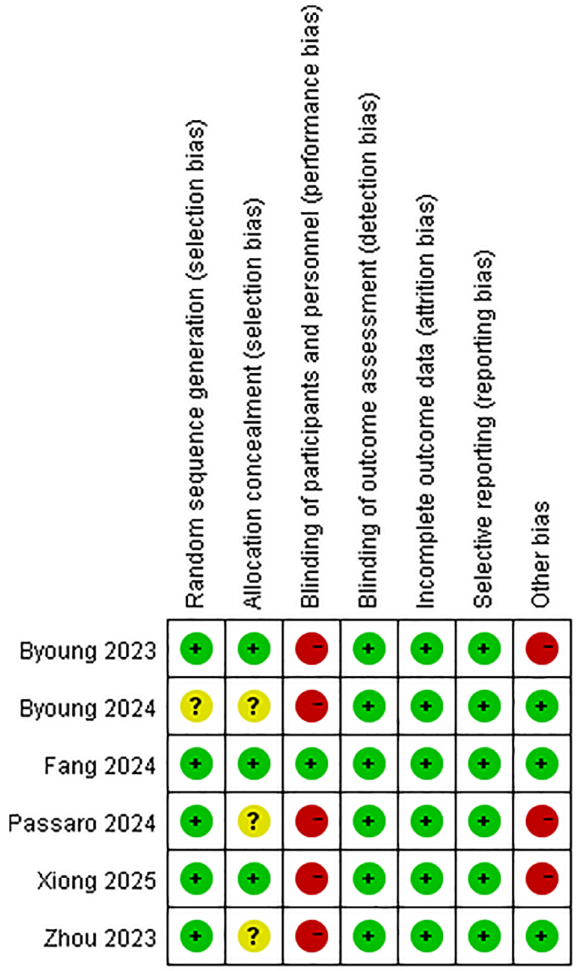

FIGURE 4
Quality assessment of the included studies according to the Cochrane Collaboration's risk of bias tool 2 (RoB2).

Discussion

This systematic review and meta-analysis of 6 randomized controlled trials involving 3,063 patients provides the first comprehensive evaluation of dual-target immunotherapies in advanced or metastatic NSCLC. Our findings demonstrate that dual-target immunotherapies significantly improve PFS (HR = 0.58; 95% CI: 0.43-0.78) and ORR (RR = 1.29; 95% CI: 1.01-1.64) compared to conventional therapies, though no statistically significant benefits were observed for OS (HR = 0.84; 95% CI: 0.68-1.05) or DCR (RR = 1.09; 95% CI: 0.92-1.30). These results suggest that dual-target immunotherapies confer clinically meaningful antitumor activity, particularly in delaying disease progression and enhancing tumor shrinkage, but their impact on long-term survival outcomes remains uncertain. Safety analyses revealed increased risks of any adverse events (RR = 1.05; 95% CI: 1.02-1.09) with dual-target immunotherapies and statistically significant differences in grade ≥ 3 AEs (RR = 1.63; 95% CI: 1.37-1.94) and serious AEs (RR = 1.49; 95% CI: 1.31-1.69). Moreover, treatment discontinuation rates (RR = 2.49; 95% CI: 1.72-3.62) also showed a significant difference. Collectively, these findings position dual-target immunotherapies as a dual-edged therapeutic advance in NSCLC, offering clinically meaningful antitumor activity that necessitates judicious integration into treatment algorithms through biomarker-guided patient selection and proactive toxicity mitigation strategies. A previous Meta-analysis of BsAbs for the treatment of solid tumors illustrated no significant improvement in safety or efficacy outcomes for BsAbs compared to conventional therapies and is not consistent with the results presented here (22), a discrepancy that may be the result of strong confounding factors introduced by multiple cancers. In addition, BsAbs led to an increased incidence of adverse events represented by infections when treating lymphoma (23). This is consistent with our findings, revealing that the incidence and severity of adverse events should be considered when assessing the benefit of these therapies. Previous reviews on the application of BsAbs in the treatment of NSCLC have mainly focused on the mechanism of action of BsAbs, and this narrative approach lacks a quantitative description of their clinical efficacy and safety (24–28). Furthermore, comprehensive reviews exist that delve into the synergistic potential of BsAbs when combined with chemotherapy, while also offering more thorough analyses of the future challenges confronting BsAbs development and clinical implementation (29, 30). The majority of current meta-analyses for BsAbs focus predominantly on hematological malignancies (31–35), while investigations into solid tumors, particularly NSCLC, remain comparatively scarce (22). This meta-analysis significantly advances the understanding of dual-target immunotherapies in NSCLC beyond existing reviews by consolidating diverse clinical datasets to establish a quantitative efficacy-toxicity framework, bridging mechanistic insights with clinically actionable evidence for treatment decision-making.

The analysis revealed substantial heterogeneity across studies (I^2 = 85% for PFS, $P < 0.001$; I^2 = 92% for ORR, $P < 0.001$), a critical methodological challenge that complicates the interpretation of pooled efficacy outcomes. The sensitivity analyses (Supplementary Tables S1–S5) collectively affirm the robustness of PFS benefit (HR consistently < 0.63 despite high baseline heterogeneity I^2 = 85%), with Byoung 2023 (20) identified as a key contributor to variability potentially attributable to its PD-L1-enriched cohort design. ORR fragility manifested as loss of statistical significance when excluding Passaro 2024 (17) (RR = 1.21, 95%CI: 0.96-1.51) or Fang 2024 (16) (RR = 1.26, 95%CI: 0.97-1.66) exposing critical limitations in response assessment standardization across trials (residual I^2 > 88%). Most critically, immutable safety signals persist with treatment-discontinuing AEs maintaining RR > 2.24 in all iterations (peaking at RR = 2.73 when excluding Zhou 2023 (19)), demanding proactive toxicity management protocols irrespective of trial heterogeneity. These findings validate the random-effects model's adequacy while underscoring biological diversity in dual-target immunotherapies mechanisms as the primary heterogeneity source, necessitating biomarker-stratified studies for future precision applications. This heterogeneity likely originates from fundamental differences in therapeutic mechanisms among evaluated dual-target immunotherapies. The three agents (two BsAbs + one bifunctional fusion protein) involved in this study can be found shown in Table 1. Ivonescimab simultaneously blocks the binding of PD-1 to its ligand (PD-L1), thereby alleviating PD-1/PD-L1-mediated immunosuppression, and the binding of vascular endothelial growth

factor (VEGF)-A to its receptor (VEGFR2), thereby blocking tumor angiogenesis in the tumor microenvironment (36). Amivantamab is a BsAb targeting EGFR and MET, which can bind to both EGFR and c-MET sites outside of tumor cells and also kill tumor cells through mechanisms such as Fc-mediated antibody-dependent cell-mediated cytotoxicity (ADCC) effect (37). Bintrafusp Alfa is an innovative bifunctional fusion protein consisting of the extracellular structural domain of human transforming growth factor beta receptor II (TGF-βRII) fused to an IgG1 antibody that blocks PD-L1. This unique design enables it to inhibit TGF-β and PD-L1 immunosuppressive pathways, thereby enhancing anti-tumor immune responses (38). The mechanisms of action of the three dual-target immunotherapies were well illustrated in Figure 5.

Substantial heterogeneity arose from divergent mechanisms: Amivantamab's efficacy was mutation-dependent, Ivonescimab relied on PD-L1 expression, and Bintrafusp Alfa's dual pathway inhibition lacked predictive biomarkers. Variability in trial designs (e.g., combination therapies, line of treatment) and patient populations (e.g., EGFR/ALK status, cancer grading) further contributed to heterogeneity. In addition, the mode of administration is an important factor affecting the safety. A phase III study comparing subcutaneous and intravenous Amivantamab demonstrated that subcutaneous administration had a longer OS, lower risk of infusion-related reactions (IRRs), and higher end-of-treatment rates, demonstrating non-inferiority overall (39). However, our meta-analysis is fundamentally limited by the exclusive use of intravenous therapy across all included trials. This uniform delivery method restricts the generalizability of our safety and efficacy findings to subcutaneous formulations, which are emerging as a clinically advantageous alternative due to reduced IRRs and improved patient compliance (40). Although all six included trials exclusively utilized intravenous infusion for dual-target immunotherapies, which somewhat attenuated the heterogeneity, differences in the dose ranges of the therapies and the dosing cycles still contribute to the heterogeneity of the study. Critically, the exclusive intravenous administration in all trials may confound safety outcomes. Subcutaneous delivery—with slower drug release and lower peak concentrations—potentially reduces acute toxicities like cytokine release syndrome (40, 41). Conversely, intravenous infusion likely amplified the elevated AE risks observed in our pooled analysis. This implies our reported toxicity profiles may partially reflect delivery methods rather than inherent therapeutic effects. Direct comparisons of administration routes are urgently needed. A notable source of heterogeneity stems from the inclusion of structurally distinct agents, such as bifunctional fusion proteins (e.g., bintrafusp alfa targeting PD-L1/TGF-β) alongside canonical bispecific antibodies. Although these

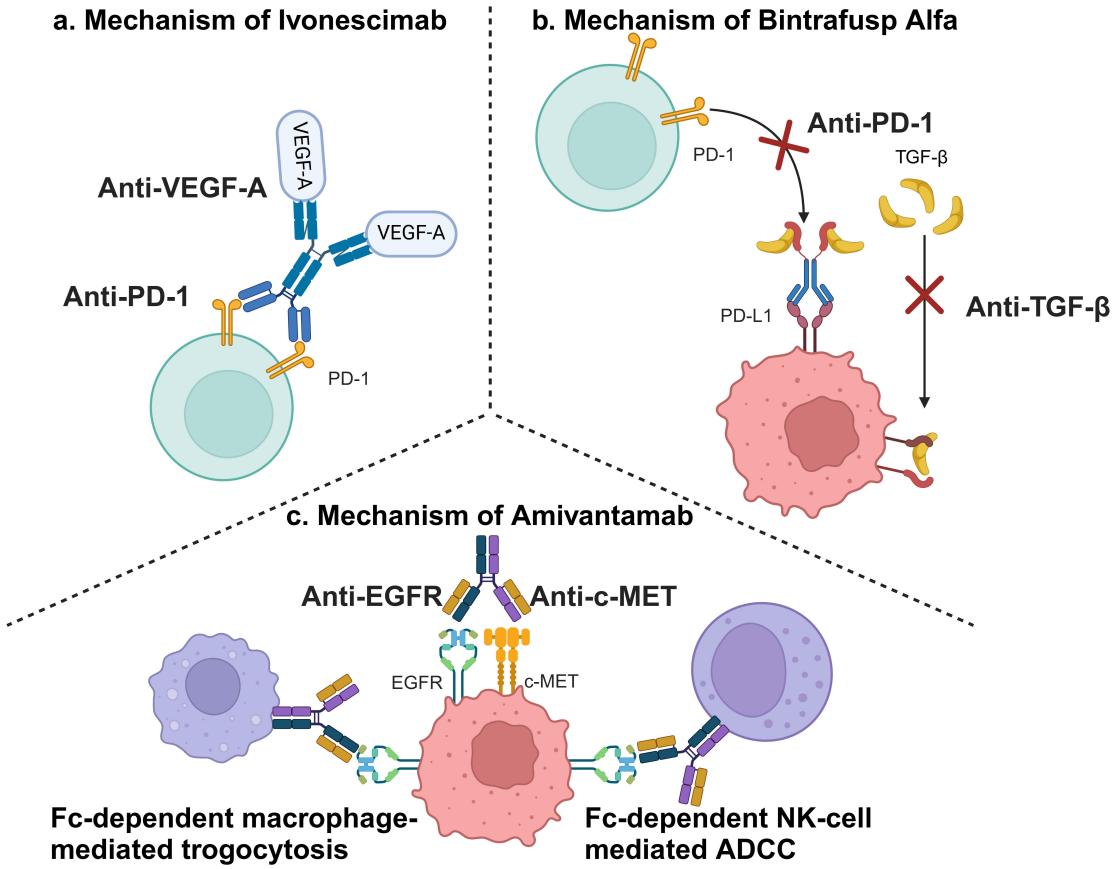

FIGURE 5
Mechanisms of involved dual-target immunotherapies. **(a)** Mechanism of Ivonescimab; **(b)** Mechanism of Bintrafusp Alfa; **(c)** Mechanism of Amivantamab (This figure was created by Biorender.).

agents share a common mechanistic principle of dual-target engagement, differences in molecular architecture may influence pharmacokinetics, effector functions, and toxicity profiles (42). This heterogeneity is an inherent limitation of our broadened scope but reflects real-world clinical diversity in emerging immunotherapies.

We acknowledge the limitations highlighted by the RoB2 assessment and their potential impact on the interpretation of our findings (43). As noted in Figure 4, the primary methodological concerns arose from deficiencies in blinding (performance bias) and, to a lesser extent, potential attrition bias in some trials. The lack of blinding could amplify efficacy estimates for investigator-assessed endpoints: awareness of treatment allocation may systematically influence tumor response evaluations, potentially inflating observed PFS benefits (HR = 0.58) and ORR advantages (RR = 1.29). Concurrently, heightened AE vigilance in the dual-target immunotherapies arm may overstate safety risks (e.g., any-grade AE RR = 1.05; grade ≥ 3 AE RR = 1.63). Attrition bias warrants consideration given significantly higher dual-target immunotherapies discontinuation rates (RR = 2.49). Disproportionate dropout may dilute survival signals—as subsequent therapies could obscure true OS benefits (HR = 0.84)—and skew time-to-event analyses. While these biases preclude definitive quantification, they necessitate cautious interpretation: efficacy advantages may be overestimated, and AE magnitudes may reflect detection artifacts. Consequently, our results should be contextualized as potentially influenced by inherent trial limitations, underscoring the need for future studies to prioritize blinding strategies and rigorous attrition management.

While exploratory subgroup analyses suggested potential efficacy differences by dual-target immunotherapies mechanism, the small number of studies per subgroup ($n \leq 3$) precludes definitive conclusions. Given the limited studies per subgroup, these findings are hypothesis-generating and require validation in larger cohorts (44, 45).

Most of the current clinical studies on dual-target immunotherapies are in phase I or II, which have a limited role in assessing the benefits and risks of this therapy (46–52). Further high-quality randomized controlled trials of dual-target immunotherapies in solid tumors are strongly recommended to better evaluate the clinical potential of this therapy.

Conclusion

Dual-target immunotherapies confer superior efficacy in delaying disease progression and tumor response compared to conventional NSCLC therapies, but their elevated toxicity risk profiles require biomarker-driven patient selection to optimize clinical implementation.

Data availability statement

The original contributions presented in the study are included in the article/Supplementary Material. Further inquiries can be directed to the corresponding author.

Author contributions

YZ: Conceptualization, Formal Analysis, Methodology, Validation, Writing – original draft, Project administration. HW: Data curation, Validation, Visualization, Writing – original draft. XY: Data curation, Validation, Visualization, Writing – original draft. CL: Funding acquisition, Project administration, Writing – review & editing, Resources.

Funding

The author(s) declare financial support was received for the research and/or publication of this article. This work was supported by grants from the Project of Incubation Base for Innovative Practical Ability of Cadets of Naval Medical University (FH2024061), the Incubation Program for Innovative Capabilities in the School of Basic Medical Sciences of Naval Medical University (JCCXFH-017) and the National Natural Science Foundation of China (82272792).

Conflict of interest

The authors declare that the research was conducted in the absence of any commercial or financial relationships that could be construed as a potential conflict of interest.

Generative AI statement

The author(s) declare that no Generative AI was used in the creation of this manuscript.

Any alternative text (alt text) provided alongside figures in this article has been generated by Frontiers with the support of artificial intelligence and reasonable efforts have been made to ensure accuracy, including review by the authors wherever possible. If you identify any issues, please contact us.

Publisher's note

Supplementary material

The Supplementary Material for this article can be found online at: https://www.frontiersin.org/articles/10.3389/fimmu.2025.1605877/full#supplementary-material

References

1. Bray F, Laversanne M, Sung H, Ferlay J, Siegel RL, Soerjomataram I, et al. Global cancer statistics 2022: GLOBOCAN estimates of incidence and mortality worldwide for 36 cancers in 185 countries. *CA Cancer J Clin*. (2024) 74:229–63. doi: 10.3322/caac.21834

2. Relli V, Trerotola M, Guerra E, Alberti S. Abandoning the notion of non-small cell lung cancer. *Trends Mol Med*. (2019) 25:585–94. doi: 10.1016/j.molmed.2019.04.012

3. Bade BC, Dela Cruz CS. Lung cancer 2020: epidemiology, etiology, and prevention. *Clin Chest Med*. (2020) 41:1–24. doi: 10.1016/j.ccm.2019.10.001

4. Desai A, Peters S. Immunotherapy-based combinations in metastatic NSCLC. *Cancer Treat Rev*. (2023) 116:102545. doi: 10.1016/j.ctrv.2023.102545

5. Brinkmann U, Kontermann RE. Bispecific antibodies. *Science*. (2021) 372:916–7. doi: 10.1126/science.abg1209

6. Syed Y, Amivantamab Y. First approval. *Drugs*. (2021) 81:1349–53. doi: 10.1007/s40265-021-01561-7

7. Gao X, Xu N, Li Z, Shen L, Ji K, Zhen Z, et al. Safety and antitumour activity of cadonilimab, an anti-PD-1/CTLA-4 bispecific antibody, for patients with advanced solid tumours (COMPASSION-03): a multicentre, open-label, phase 1b/2 trial. *Lancet Oncol*. (2023) 24:1134–46. doi: 10.1016/S1470-2045(23)00411-4

8. Sorin M, Prosty C, Ghaleb L, Nie K, Katergi K, Shahzad MH, et al. Neoadjuvant chemoimmunotherapy for NSCLC: A systematic review and meta-analysis. *JAMA Oncol*. (2024) 10:621–33. doi: 10.1001/jamaoncol.2024.0057

9. Zhang Q, Liang XY, Wang ZS, Sun A, Cao TB, Zhang YP, et al. Efficacy of immune checkpoint inhibitors for NSCLC in patients with different age: A systematic review and meta-analysis. *Asian J Surg*. (2024) 47:4691–8. doi: 10.1016/j.asjsur.2024.03.145

10. Chen Y, Hu J, Bu F, Zhang H, Fei K, Zhang P, et al. Clinical characteristics of hyperprogressive disease in NSCLC after treatment with immune checkpoint inhibitor: a systematic review and meta-analysis. *BMC Cancer*. (2020) 20:707. doi: 10.1186/s12885-020-07206-4

11. Griesinger F, Korol EE, Kayaniyil S, Varol N, Ebner T, Goring SM, et al. Efficacy and safety of first-line carboplatin-versus cisplatin-based chemotherapy for non-small cell lung cancer: A meta-analysis. *Lung Cancer*. (2019) 135:196–204. doi: 10.1016/j.lungcan.2019.07.010

12. Moher D, Liberati A, Tetzlaff J, Altman DG. Preferred reporting items for systematic reviews and meta-analyses: the PRISMA statement. *Int J Surg*. (2010) 8:336–41. doi: 10.1016/j.ijsu.2010.02.007

13. Sterne JAC, Savović J, Page MJ, Elbers RG, Blencowe NS, Boutron I, et al. RoB 2: a revised tool for assessing risk of bias in randomised trials. *BMJ*. (2019) 366:l4898. doi: 10.1136/bmj.l4898

14. Higgins JP, Sg T. Controlling the risk of spurious findings from meta-regression. *Stat Med*. (2004) 23:1663–82. doi: 10.1002/sim.1752

15. Dersimonian R, Kacker R. Random-effects model for meta-analysis of clinical trials: an update. *Contemp Clin Trials*. (2007) 28:105–14. doi: 10.1016/j.cct.2006.04.004

16. Fang W, Zhao Y, Luo Y, Yang R, Huang Y. Ivonescimab plus chemotherapy in non-small cell lung cancer with EGFR variant: A randomized clinical trial. *JAMA*. (2024) 332:561–70. doi: 10.1001/jama.2024.10613

17. Passaro A, Wang J, Wang Y, Lee S-H, Melosky B, Shih J-Y, et al. Amivantamab plus chemotherapy with and without lazertinib in EGFR-mutant advanced NSCLC after disease progression on osimertinib: primary results from the phase III MARIPOSA-2 study. *Ann Oncol*. (2024) 35:77–90. doi: 10.1016/j.annonc.2023.10.117

18. Cho BC, Lu S, Felip E, Spira AI, Girard N, Lee JS, et al. Amivantamab plus lazertinib in previously untreated EGFR-mutated advanced NSCLC. *N Engl J Med*. (2024) 391:1486–98. doi: 10.1056/NEJMoa2403614

19. Zhou C, Tang KJ, Cho BC, Liu B, Paz-Ares L, Cheng S, et al. Amivantamab plus chemotherapy in NSCLC with EGFR exon 20 insertions. *N Engl J Med*. (2023) 389:2039–51. doi: 10.1056/NEJMoa2306441

20. Cho BC, Lee JS, Wu YL, Cicin I, Cobo Dols M, Ahn MJ, et al. Bintrafusp alfa versus pembrolizumab in patients with treatment-naive, programmed death-ligand 1-high advanced NSCLC: A randomized, open-label, phase 3 trial. *J Thorac Oncol*. (2023) 18:1731–42. doi: 10.1016/j.jtho.2023.08.018

21. Xiong A, Wang L, Chen J, Wu L, Liu B, Yao J, et al. Ivonescimab versus pembrolizumab for PD-L1-positive non-small cell lung cancer (HARMONi-2): a randomised, double-blind, phase 3 study in China. *Lancet*. (2025) 405:839–49. doi: 10.1016/S0140-6736(24)02722-3

22. Nejadghaderi SA, Balibegloo M, Noori M, Fayyaz F, Saghazadeh A, Rezaei N, et al. Clinical efficacy and safety of bispecific antibodies for the treatment of solid tumors: a systematic review and meta-analysis. *Expert Rev Anticancer Ther*. (2023) 23:307–18. doi: 10.1080/14737140.2023.2183847

23. Reynolds GK, Maclean M, Scheffer Cliff ER, Teh BW, Thursky KA, Slavin MA, et al. Infections in patients with lymphoma treated with bispecific antibodies: a systematic review and meta-analysis. *Blood Adv*. (2024) 8:3555–9. doi: 10.1182/bloodadvances.2024012916

24. Billowria K, Das Gupta G, Chawla PA. Amivantamab: A new hope in targeting non-small cell lung cancer. *Anticancer Agents Med Chem*. (2023) 23:124–41. doi: 10.2174/1871520622666220523145609

25. Khosla AA, Jatwani K, Singh R, Reddy A, Jaiyesimi I, Desai A, et al. Bispecific antibodies in lung cancer: A state-of-the-art review. *Pharm (Basel)*. (2023) 16. doi: 10.3390/ph16101461

26. Geng Q, Jiao P. Anti-PD-L1-based bispecific antibodies targeting co-inhibitory and co-stimulatory molecules for cancer immunotherapy. *Molecules*. (2024) 29. doi: 10.3390/molecules29020454

27. Goebeler ME, Stuhler G, Bargou R. Bispecific and multispecific antibodies in oncology: opportunities and challenges. *Nat Rev Clin Oncol*. (2024) 21:539–60. doi: 10.1038/s41571-024-00905-y

28. Zhang T, Lin Y, Gao Q. Bispecific antibodies targeting immunomodulatory checkpoints for cancer therapy. *Cancer Biol Med*. (2023) 20:181–95. doi: 10.20892/j.issn.2095-3941.2023.0002

29. Khan SR, Breadner D. Unveiling the synergistic potential: bispecific antibodies in conjunction with chemotherapy for advanced non-small-cell lung cancer treatment. *Curr Oncol*. (2025) 32. doi: 10.3390/curroncol32040206

30. Zhao S, Zhao H, Yang W, Zhang L. The next generation of immunotherapies for lung cancers. *Nat Rev Clin Oncol*. (2025) 22:592–616. doi: 10.1038/s41571-025-01035-9

31. Wang X, Zhao A, Zhu J, Niu T. Efficacy and safety of bispecific antibodies therapy for relapsed or refractory multiple myeloma: a systematic review and meta-analysis of prospective clinical trials. *Front Immunol*. (2024) 15:1348955. doi: 10.3389/fimmu.2024.1348955

32. Bayly-Mccredie E, Treisman M, Fiorenza S. Safety and efficacy of bispecific antibodies in adults with large B-cell lymphomas: A systematic review of clinical trial data. *Int J Mol Sci*. (2024) 25. doi: 10.3390/ijms25179736

33. Liu H, Xi R, Mao D, Zhao X, Wu T. Efficacy and safety of blinatumomab for the treatment of relapsed/refractory acute lymphoblastic leukemia: A systemic review and meta-analysis. *Clin Lymphoma Myeloma Leuk*. (2023) 23:e139–e49. doi: 10.1016/j.clml.2022.12.009

34. Reynolds G, Scheffer Cliff ER, Mohyuddin GR, Popat R, Midha S, Ng Liet Hing M, et al. Infections following bispecific antibodies in myeloma: a systematic review and meta-analysis. *Blood Adv*. (2023) 7:5898–903. doi: 10.1182/bloodadvances.2023010539

35. Li W, Zhao D, Jiao Y, Dong W, Wang Z, Yan X, et al. Effectiveness and safety of teclistamab for relapsed or refractory multiple myeloma: a systematic review and meta-analysis. *Front Immunol*. (2025) 16:1565407. doi: 10.3389/fimmu.2025.1565407

36. Dhillon S. Ivonescimab: first approval. *Drugs*. (2024) 84:1135–42. doi: 10.1007/s40265-024-02073-w

37. Neijssen J, Cardoso RMF, Chevalier KM, Wiegman L, Valerius T, Anderson GM, et al. Discovery of amivantamab (JNJ-61186372), a bispecific antibody targeting EGFR and MET. *J Biol Chem*. (2021) 296:100641. doi: 10.1016/j.jbc.2021.100641

38. Barlesi F, Isambert N, Felip E, Cho BC, Lee DH, Peguero J, et al. Bintrafusp alfa, a bifunctional fusion protein targeting TGF-beta and PD-L1, in patients with non-small cell lung cancer resistant or refractory to immune checkpoint inhibitors. *Oncologist*. (2023) 28:258–67. doi: 10.1093/oncolo/oyac253

39. Leighl NB, Akamatsu H, Lim SM, Cheng Y, Minchom AR, Marmarelis ME, et al. Subcutaneous versus intravenous amivantamab, both in combination with lazertinib, in refractory epidermal growth factor receptor-mutated non-small cell lung cancer: primary results from the phase III PALOMA-3 study. *J Clin Oncol*. (2024) 42:3593–605. doi: 10.1200/JCO.24.01001

40. Lim K, Zhu XS, Zhou D, Ren S, Phipps A. Clinical pharmacology strategies for bispecific antibody development: learnings from FDA-approved bispecific antibodies in oncology. *Clin Pharmacol Ther*. (2024) 116:315–27. doi: 10.1002/cpt.3308

41. Engelberts PJ, Hiemstra IH, de Jong B, Schuurhuis DH, Meesters J, Beltran Hernandez I, et al. DuoBody-CD3xCD20 induces potent T-cell-mediated killing of Malignant B cells in preclinical models and provides opportunities for subcutaneous dosing. *EBioMedicine*. (2020) 52:102625. doi: 10.1016/j.ebiom.2019.102625

42. Wilkins JJ, Vugmeyster Y, Dussault I, Girard P, Khandelwal A. Population pharmacokinetic analysis of bintrafusp alfa in different cancer types. *Adv Ther*. (2019) 36:2414–33. doi: 10.1007/s12325-019-01018-0

43. Luchini C, Veronese N, Nottegar A, Shin JI, Gentile G, Granziol U, et al. Assessing the quality of studies in meta-research: Review/guidelines on the most important quality assessment tools. *Pharm Stat*. (2021) 20:185–95. doi: 10.1002/pst.2068

44. Cumpston M, Li T, Page MJ, Chandler J, Welch VA, Higgins JP, et al. Updated guidance for trusted systematic reviews: a new edition of the Cochrane Handbook for Systematic Reviews of Interventions. *Cochrane Database Syst Rev*. (2019) 10:ED000142. doi: 10.1002/14651858.ED000142

45. Borenstein M, Higgins JP. Meta-analysis and subgroups. *Prev Sci*. (2013) 14:134–43. doi: 10.1007/s11121-013-0377-7

46. Schram AM, Goto K, Kim DW, Macarulla T, Hollebecque A, O'Reilly EM, et al. Efficacy of zenocutuzumab in NRG1 fusion-positive cancer. *N Engl J Med*. (2025) 392:566–76. doi: 10.1056/NEJMoa2405008

47. Peterlin P, Saada-Bouzid E, Moskovitz M, Pigneux A, Yuda J, Sinnollareddy M, et al. First-in-human clinical trial results with ABBV-184, a first-in-class T-cell receptor/anti-CD3 bispecific protein, in adults with previously treated AML or NSCLC. *Expert Rev Anticancer Ther*. (2024) 24:893–904. doi: 10.1080/14737140.2024.2373888

48. Zhou Q, Pan Y, Yang X, Zhao Y, Han G, Pang Q, et al. Neoadjuvant SHR-1701 with or without chemotherapy in unresectabl e stage III non-small-cell lung cancer: A proof-of-concept, phase 2 trial. *Cancer Cell*. (2024) 42:1258–67 e2. doi: 10.1016/j.ccell.2024.05.024

49. Frentzas S, Mislang ARA, Lemech C, Nagrial A, Underhill C, Wang W, et al. Phase 1a dose escalation study of ivonescimab (AK112/SMT112), an anti-PD-1/VEGF-A bispecific antibody, in patients with advanced solid tumors. *J Immunother Cancer*. (2024) 12. doi: 10.1136/jitc-2023-008037

50. Chen B, Yao W, Li X, Lin G, Chu Q, Liu H, et al. A phase Ib/II study of cadonilimab (PD-1/CTLA-4 bispecific antibody) plus anlotinib as first-line treatment in patients with advanced non-small cell lung cancer. *Br J Cancer*. (2024) 130:450–6. doi: 10.1038/s41416-023-02519-0

51. Xiong A, Li W, Li X, Fan Y, Ma Z, Fang J, et al. Efficacy and safety of KN046, a novel bispecific antibody against PD-L1 and CTLA-4, in patients with non-small cell lung cancer who failed platinum-based chemotherapy: a phase II study. *Eur J Cancer*. (2023) 190:112936. doi: 10.1016/j.ejca.2023.05.024

52. Ouyang Q, Rodon J, Liang Y, Wu X, Li Q, Song L, et al. Results of a phase 1/2 study of sacituzumab tirumotecan in patients with unresectab le locally advanced or metastatic solid tumors refractory to standard therapies. *J Hematol Oncol*. (2025) 18:61. doi: 10.1186/s13045-025-01705-2

frontiers | Frontiers in Immunology

TYPE Original Research
PUBLISHED 18 September 2025
DOI 10.3389/fimmu.2025.1607138

OPEN ACCESS

EDITED BY
Miroslawa Puskulluoglu,
Maria Sklodowska-Curie National Research Institute of Oncology, Poland

REVIEWED BY
Uros Markovic,
University Hospital Polyclinic Vittorio Emanuele, Italy
Malgorzata Czogala,
Jagiellonian University Medical College, Poland

*CORRESPONDENCE
Shuhong Shen
shenshuhong@scmc.com.cn
Hui Jiang
jhui0111@126.com

†These authors have contributed equally to this work

RECEIVED 07 April 2025
ACCEPTED 28 August 2025
PUBLISHED 18 September 2025

CITATION
Zhang N, Hu W, Dai Y, Wang J, Qu L, Wang D, Liu B, Shao J, Shen S and Jiang H (2025) Blinatumomab demonstrates MRD eradication in MRD-positive/chemotherapy-delayed pediatric B-ALL and high response in relapsed/refractory cases: a multicenter cohort study. *Front. Immunol.* 16:1607138. doi: 10.3389/fimmu.2025.1607138

Blinatumomab demonstrates MRD eradication in MRD-positive/chemotherapy-delayed pediatric B-ALL and high response in relapsed/refractory cases: a multicenter cohort study

Na Zhang[1†], Wenting Hu[2†], Yunpeng Dai[3†], Jian Wang[4†], Lijun Qu[4], Dan Wang[1], Bingju Liu[3], Jingbo Shao[1], Shuhong Shen[2*] and Hui Jiang[1*]

[1]Department of Hematology and Oncology, Shanghai Children's Hospital, School of Medicine, Shanghai Jiao Tong University, Shanghai, China, [2]Department of Hematology and Oncology, Shanghai Children's Medical Center, School of Medicine, Shanghai Jiao Tong University, Shanghai, China, [3]Department of Pediatric Hematology and Oncology, Shandong Provincial Hospital Affiliated to Shandong First Medical University, Jinan, China, [4]Department of Hematology and Oncology, Anhui Children's Hospital, Hefei, China

Background: Blinatumomab, a bispecific T-cell engager targeting CD3+ and CD19+, promotes T cell–mediated cytotoxicity against B-cell precursor acute lymphoblastic leukemia (B-ALL). While its efficacy is established in relapsed/refractory (R/R) disease, its role as preemptive therapy for minimal residual disease (MRD)–positive patients or those experiencing chemotherapy delays remains undefined. Predictors of treatment failure also require further investigation.

Methods: In this multicenter retrospective study, 105 patients who received blinatumomab were enrolled. Of these, 30 had R/R ALL, 21 were in complete remission (CR) with MRD positivity (CR-MRD^{pos}), and 54 experienced chemotherapy delays. Eight patients received blinatumomab directly as reinduction therapy and 22 patients received burden-reduction chemotherapy prior to blinatumomab. In total, 11 children were in R/R status and 40 were in CR-MRD^{pos} before treatment. Patients were subsequently bridged to stem cell transplantation, chimeric antigen receptor T-cell therapy (CAR-T), or protocol continuation. Treatment response was analyzed across CR-MRD^{pos}, R/R, and CR with MRD negativity (CR-MRD^{neg}). Immune reconstitution profiles (T-cell subsets, cytokine dynamics), cytogenetic markers, and clinical outcomes were assessed to identify predictors of treatment resistance.

Results: The CR rate was 81.8% in R/R and 82.5% in CR-MRD^{pos} patients (P = 1.000). Of 74 courses with CR-MRD^{neg}, 73 remained MRD-negative during treatment. Univariate analysis revealed poor cytogenetics (P = 0.0001), CD19+ B-cell loss (P = 0.046), and BCR-ABL1 positivity (P = 0.002) as predictors of poor response. Cox regression analysis identified high MRD (P = 0.014), BCR/ABL1 (P = 0.065), and poor cytogenetics (P = 0.025) as independent risk factors. Blinatumomab significantly increased CD3+ T cells [0.96 (0.03–3.79) to 1.13 (0.26–7.74) $\times 10^9$/L, P = 0.016], along with CD4+ [0.35 (0.01–1.39) to 0.47 (0.07–

2.94) $\times 10^9$/L] and CD8+ T cells [0.41 (0.01–2.39) to 0.56 (0.07–6.07) $\times 10^9$/L] (P = 0.005 and P = 0.006, respectively).The 1-year event-free survival for CR-MRD^{neg}, CR-MRD^{pos}, and R/R patients was 97.8% ± 2.2%, 86.7% ± 6.2%, and 73.3% ± 8.1%, respectively (P = 0.001), while overall survival was 97.8% ± 2.2%, 100%, and 93.3% ± 4.6% (P = 0.029).

Conclusions: Blinatumomab effectively clears MRD as preemptive therapy and serves as a bridging strategy during chemotherapy delays in pediatric B-ALL, while maintaining high response rates in R/R cases.

KEYWORDS

blinatumomab, B-cell acute lymphoblastic leukemia, children, minimal residual disease, relapsed/refractory, T cell activation

Introduction

Survival rates for B-cell acute lymphoblastic leukemia (B-ALL) have significantly improved in recent years. However, approximately 15% of children with B-ALL experience relapse after frontline chemotherapy (1). Based on the site and timing of relapses, these children are classified as having standard- or high-risk first-relapse B-ALL (2).

Blinatumomab is a bispecific T-cell–engaging antibody that binds CD3+ T cells and CD19+ leukemia cells, inducing cytotoxic immune responses that lyse CD19-expressing B cells via activated T cells (3). Meta-analyses have demonstrated the potent therapeutic efficacy and favorable safety profile of blinatumomab in children with relapsed/refractory (R/R) B-ALL (4). It has also induced high rates of complete minimal residual disease (MRD) response in both adults and children with molecularly resistant B-ALL.

Nevertheless, 10%–15% of patients exhibit primary resistance to blinatumomab. Emerging evidence has identified several mechanisms contributing to treatment failure. Elevated levels of regulatory T cells, characterized by CD4/CD25/FOXP3 expression and interleukin-10 (IL-10)–mediated suppression of T-cell proliferation, have been associated with reduced response (5). Increased expression of programmed death ligand 1 (PD-L1), the binding ligand of the inhibitory checkpoint molecule programmed death 1 (PD-1), has also been linked to impaired T-cell function and diminished efficacy (6). Additionally, KMT2A-rearranged ALL lineage switch may induce resistance (7, 8). Lower blast counts in bone marrow (BM) (≤50%) have been associated with better response than higher disease burden (9, 10).

Despite these insights, the mechanisms underlying blinatumomab resistance remain incompletely elucidated. With the expanding application of blinatumomab as frontline preemptive therapy, particularly for patients with persistent complete remission with MRD positivity (CR-MRD^{pos}) or chemotherapy delays, its therapeutic scope has broadened. In this study, we comprehensively analyzed treatment response across three cohorts: CR-MRD^{pos}, R/R, and CR with MRD negativity (CR-MRD^{neg}). Through systematic evaluation of immune reconstitution profiles (T-cell subsets, cytokine dynamics), cytogenetic markers, and clinical outcomes, we aimed to identify key predictors of treatment resistance.

Methods

Patients

This multicenter retrospective study was approved by the institutional review boards (No. 2025R022-E01) following discussion in a multicenter advisory panel across four pediatric medical centers: Shanghai Children's Hospital, Shanghai Children's Medical Center, Anhui Children's Hospital, and Shandong Provincial Hospital. Patients ≤18 years old with R/R B-ALL and MRD positivity at any time who received blinatumomab therapy were enrolled. Patients with chemotherapy intolerance or severe infection who received blinatumomab as bridging therapy were enrolled as the control group. The exclusion criteria were as follows: (i) patients with severe infection and cardiac, liver, or kidney insufficiency who had an expected survival time of less than 3 months; and (ii) those who received blinatumomab for fewer than 7 days. Patient enrollment lasted from September 2021 to June 2024, with follow-up through March 2025. A total of 105 patients were enrolled.

Treatment strategy

Blinatumomab was administered via a stepwise dose-escalation protocol during the initial cycle: 5 μg/m²/day as continuous intravenous infusion on days 2–7, followed by escalation to 15 μg/m²/day for a total cycle duration of 14–28 days. The infusion duration depended on family financial conditions and physician discretion. In some cases, BM aspiration was performed on day 15, and treatment was discontinued upon achieving BM remission. Each treatment cycle was separated by a 14-day treatment break.

Dexamethasone prophylaxis (5 mg/m²/day for 1 day) was routinely administered. Subsequent treatment cycles commenced directly at 15 μg/m²/day. Adverse events (AEs) were managed according to the manufacturer's instructions. BM assessment was performed upon completion of the infusion cycle. Intrathecal injections of methotrexate, cytarabine, and dexamethasone were administered before, during, or after blinatumomab cycles. Upon achieving BM remission, patients proceeded to hematopoietic stem cell transplantation (HSCT), continued the original protocol, or received alternative treatment. Non-responders were transitioned to salvage protocols, chimeric antigen receptor T-cell (CAR-T) therapy, or palliative HSCT, as clinically indicated.

Some patients received reinduction therapy to reduce tumor burden. The reinduction therapy followed the initial induction regimen: dexamethasone 6 mg/m² on days 1–4; vincristine 1.5 mg/m² on days 5, 12, 19, and 26; prednisone 45 mg/m² on days 5–28; daunorubicin 25 mg/m² on days 5 and 12; and peg-asparaginase 2,000 U/m² on days 6 and 26.

For patients with Philadelphia chromosome–positive (Ph+) disease, a tyrosine kinase inhibitor (TKI) was added, with dasatinib 80 mg/m² preferred. Bridging chemotherapy prior to blinatumomab included induction chemotherapy or continued consolidation chemotherapy consisting of cyclophosphamide 1,000 mg/m² on day 1, cytarabine 50 mg/m² on days 1–7, and mercaptopurine 40 mg/m² on days 1–7.

Definition

Patients were divided into three groups: CR-MRD^{neg}, CR-MRD^{pos}, and R/R. Response was categorized as either cytological CR or MRD CR. Cytological CR was defined as <5% BM blasts in patients with R/R status. MRD CR, detected by flow cytometry (FCM), was defined as a reduction in MRD to <0.01% or maintenance of MRD negativity in patients with CR-MRD^{pos}. No response was defined as partial remission (PR) or no remission (NR) in R/R patients, and persistent MRD ≥0.01% in patients with CR-MRD^{pos}.

Poor cytogenetics were defined as KMT2Ar, BCR-ABL1, and TCF3-HLF, according to the Chinese Children's Cancer Group ALL (CCCG-ALL) 2015 protocol. Event-free survival (EFS) was defined as the time from diagnosis to relapse, death, secondary cancer, or last contact for those who were event-free. Overall survival (OS) was defined as the time from diagnosis to death from any cause or last contact if alive.

Cytokine detection

Serum concentrations of target cytokines [IL-1β, IL-2, IL-4, IL-5, IL-6, IL-8, IL-10, IL-12p70, IL-17, interferon (IFN)-γ, tumor necrosis factor (TNF)-α, and IFN-α] were measured using a multiplex microsphere-based flow immunofluorescence assay (12-cytokine kits, Raisecare, China) according to the manufacturer's instructions. Cytokines were assessed before blinatumomab infusion, at the onset of cytokine release syndrome (CRS) or immune effector cell–associated neurotoxicity syndrome (ICANS), and at the end of blinatumomab treatment.

T- cell and B-cell subsets

Basic lymphocyte subpopulations were analyzed using a FACSCalibur flow cytometer (BD Biosciences) and reported as both percentages and absolute counts. FCM with CellQuest software (BD Biosciences) was used for analysis of lymphocyte subsets (CD3/CD45/CD4/CD8/CD16CD56/CD19, BD Biosciences), including T cells (CD3+CD45+), cytotoxic T cells (CD3+CD8+CD45+), helper T cells (CD3+CD4+CD45+), NK cells (CD16+CD56+CD3−CD45+), and B cells (CD19+CD45+). A total of 15,000 lymphocytes were acquired for analysis. Data were collected at baseline and on days 14, 21, and 28 (end of treatment). T-cell activation magnitude was defined as the difference between post-blinatumomab and baseline (pre-treatment) measurements.

Statistical analysis

Quantitative data with a Gaussian distribution were presented as mean ± standard deviation (SD) and compared using the t-test. Non-normally distributed data were presented as medians with full ranges. Comparisons between two groups were performed using the Mann–Whitney U test or Wilcoxon matched-pairs test. Comparisons involving two or more factors were conducted using one-way or two-way analysis of variance (ANOVA). Categorical variables were presented as percentages and compared using Fisher's exact test or the chi-square (χ^2) test. Patients lost to follow-up were censored at the last date they were known to be alive. OS and EFS were estimated by the Kaplan–Meier method, and curves were compared using the log-rank test. The Cox proportional hazards model was used for univariate and multivariate analyses. All statistical analyses were performed using GraphPad Prism version 9 (GraphPad Software Inc., La Jolla, CA, USA) and SPSS version 19.0 (SPSS Inc., Chicago, IL, USA). All tests were two-sided, and $P < 0.05$ was considered statistically significant.

Results

Patients' characteristics

A total of 105 patients with B-ALL received blinatumomab across 125 cycles, following standardized clinical practice. The median age was 72 months (range, 5–210 months). Sixty-four patients (61%) were male and 41 (39%) were female.

Thirty cases were diagnosed with R/R ALL, including 23 with relapse and seven with induction failure. Eight patients received blinatumomab directly as reinduction therapy, and 22 patients

received burden-reduction chemotherapy prior to blinatumomab. Among these, three patients failed to reduce tumor burden, with blast levels remaining above 5%.

Ten patients achieved CR-MRD^{pos}, and nine patients achieved CR-MRD^{neg}. An additional 21 patients had CR-MRD^{pos} following induction or developed MRD positivity during treatment. Fifty-four patients received blinatumomab due to chemotherapy delay caused by chemotherapy intolerance or severe AEs, among whom nine patients had CR-MRD^{pos}.

At the initial cycle of blinatumomab, 40 patients had CR-MRD^{pos}, 11 patients had R/R status, and 54 patients had MRD negativity. Among the latter, four cases had BM blasts ranging from 5%–9.5%, while seven had blasts ≥20%. For these 51 patients, the median BM blast percentage was 2% and the median MRD percentage was 0.52% (Table 1). In patients achieving MRD negativity, a total of 74 cycles were administered. The demographic and clinical characteristics of the R/R, CR-MRD^{pos}, and CR-MRD^{neg} groups are summarized in Table 1.

Response rate

The CR rate of R/R patients was 81.8% (9/11), while the MRD-negative CR rate was 72.7% (8/11). MRD CR was achieved in 33 of 40 cases (82.5%) with CR-MRD^{pos}. The overall CR response rate was 82.4%.

Among the R/R and CR-MRD^{pos} patients, 31 received a 14-day infusion and 20 received a 3–4-week infusion. The response rate was 83.9% for the 2-week regimen and 80% for the 3–4-week regimen.

Of the 74 MRD-negative cycles, 73 patients remained MRD negative until the follow-up day. Only one patient experienced central nervous system (CNS) relapse 14 months after blinatumomab.

In nine cases with NR after the first blinatumomab cycle, three received a second cycle of blinatumomab, two patients underwent HSCT (achieving CR), three patients with persistent MRD continued chemotherapy (achieving CR), and one patient discontinued treatment and subsequently died. Among the three patients receiving a second cycle of blinatumomab, one achieved CR and bridged to HSCT. The remaining two patients failed to achieve remission and continued treatment with CAR-T. All three patients remained alive.

T-cell response after blinatumomab

CD3+ T cell activation

We compared data obtained before and after 2–4 weeks of blinatumomab infusion. The data exhibited a non-Gaussian distribution and were expressed as median (range). Comparisons were performed using the Wilcoxon matched-pairs test. Detailed data are shown in Supplementary Table S1.

The absolute count of CD3+ T cells significantly increased from 0.96 (0.03–3.79) × 10^9/L to 1.13 (0.26–7.74) ×10^9/L (P = 0.016; Figure 1A). The CD3+ percentage also rose significantly (P = 0.008; Supplementary Table S1, Figure 1D).

CD4+ and CD8+ T cells also increased, from 0.35 (0.01–1.39) to 0.47 (0.07–2.94) ×10^9/L, and from 0.41 (0.01–2.39) to 0.56 (0.07–6.07) ×10^9/L, respectively (P = 0.005 and *P* = 0.006; Figures 1B, C). The percentages of CD4+ and CD8+ T cells also increased (P = 0.025 and *P* = 0.054; Supplementary Table S1, Figures 1E, F).

The CD4/CD8 ratio exhibited a nonsignificant decrease from 0.85 (0.37–4.92) to 0.78 (0.21–4.84) (P = 0.532; Figure 1I). The CD16+CD56+/CD3− NK cell count increased from 0.12 (0.00–0.63) ×10^9/L to 0.15 (0.03–0.74) ×10^9/L (P = 0.024; Figure 1G), although the percentage remained unchanged (Figure 1J).

TABLE 1 Patient characteristics of those treated with blinatumomab.

Characteristics	All patients	R/r, CR-MRD^{pos}	CR-MRD^{neg}	P value
Numbers, n	105	51	54	–
Gender (M/F), n	64/41	34/17	30/24	0.317
Age, median (range), mons	72 (5-210)	69 (5-208)	73.5 (5-210)	0.593
BM blasts, median (range), %	2 (0-80)	2 (0-80)	–	–
BM MRD, median (range), %	0.52 (0.004-63)	0.52 (0.004-63)	–	–
Cytogenetic characteristics				
t(9;22), BCR/ABL1, n (%)	12 (11.4)	5 (9.8)	7 (13.0)	0.762
t(v;11q23), KMT2Ar, n (%)	11 (10.5)	7 (13.7)	4 (7.4)	0.350
TCF3/HLF, n (%)	1 (1.0)	1 (2.0)	0	0.486
t(12;21), ETV6/RUNX1, n (%)	21 (20.0)	5 (9.8)	16 (29.6)	0.014
E2A/PBX1, n (%)	4 (3.8)	2 (3.9)	2 (3.7)	1.000
ZNF384r, n (%)	5 (4.8)	2 (3.9)	3 (5.6)	1.000
PAX5r, n (%)	2 (1.9)	1 (2.0)	1(1.9)	1.000

MRD, minimal residual disease; R/R, relapsed/refractory; CR-MRD^{pos}, complete remission with MRD positive; CR-MRD^{neg}, complete remission with MRD negative; BM, bone marrow; M/F, male/female.

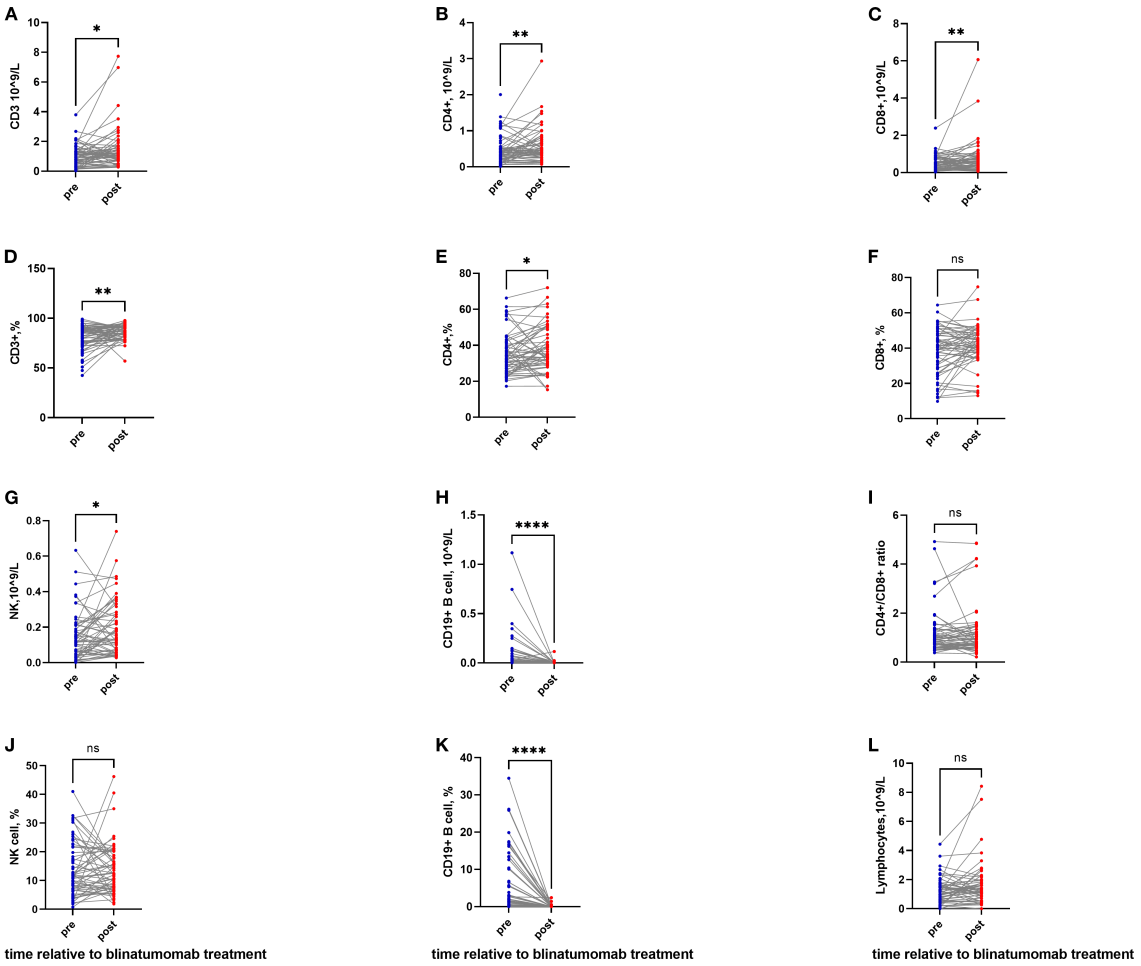

FIGURE 1
T-cell activation and B-cell depletion following blinatumomab therapy. **(A, D)** The absolute count and percentage of CD3+ T cells significantly increased after blinatumomab. **(B, E)** The absolute count and percentage of CD4+ T cells significantly increased after blinatumomab. **(C, F)** The absolute count of CD8+ T cells elevated significantly, while the percentage remained stable. **(G, J)** NK cell counts showed a significant increase, though the percentage remained unchanged. **(H, K)** B cells were depleted profoundly in both absolute and percentage. **(I)** The CD4+/CD8+ ratio exhibited a non-significant decrease. **(L)** Total lymphocyte count remained stable throughout treatment. *P< 0.05; **P< 0.01; ****P< 0.0001.

B cells were completely depleted, with absolute counts decreasing from 0.007×10^9/L (0.00–1.12) to undetectable levels 0.00×10^9/L (0.00–0.11) (P <0.0001; Figure 1H), and percentages falling from 1.39% (0.00–34.48) to 0% (0.00–2.43) (P < 0.0001; Figure 1K). Total lymphocyte counts remained stable throughout the observation period.

In patients receiving a 14-day infusion, CD3+, CD4+, and CD8+ T cells had already increased compared with baseline (Supplementary Table S1). A subset of NK cells also expanded significantly, from 0.12 (0.00–0.63) to 0.18 (0.03–0.74) $\times10^9$/L (P = 0.013).

In patients receiving a 21/28-day infusion, CD3+ T cells continued to increase, rising from 0.80 (0.03–1.86) to 1.01 (0.33–7.74) $\times10^9$/L (P = 0.033; Supplementary Table S1). CD4+ T cells showed a sustained elevation from 0.42 (0.01–0.72) to 0.47 (0.12–1.25) $\times10^9$/L (P = 0.092), while CD8+ and NK cells declined (P = 0.470 and *P* = 0.850; Supplementary Table S1).

Levels of Immunoglobulin (Ig)

Levels of G, IgA, and IgM were assessed before and after therapy. Following blinatumomab, IgG levels went down from 9.23 (2.28–18.50) to 7.05 (1.61–18.00) g/L (P = 0.0005). IgA levels and IgM levels also declined from 0.78 (0.12–2.39) to 0.27 (0.03–0.92) g/L (P < 0.0001) and from 0.41 (0.11-1.31) to 0.19 (0.01- 0.56) g/L, respectively (both P < 0.0001).

CD3+ T cell activation in MRD^{pos}+R/R and MRD^{neg} patients

When patients with R/R and CR-MRD^{pos} status were compared with those with CR-MRD^{neg}, notable differences in the immune cell repertoire were observed. The data exhibited a non-Gaussian distribution and were expressed as median (range), with comparisons performed using the Mann–Whitney U test.

The increase in CD3+ T cells was significantly greater in the R/R + CR-MRDpos group than in the CR-MRD^{neg} group [0.57 (−1.08 to 6.07) vs. 0.12 (-1.83 to 3.34)×10^9/L; P = 0.047; Figure 2A]. CD4+ cells expanded more significantly in the R/R + CR-MRDpos group than in the CR-MRD^{neg} group [0.24 (−0.55 to 1.81) *vs.* 0.03 (−0.73 to 1.19) × 10^9/L; P = 0.039; Figure 2B]. In contrast, no significant difference in CD8+ T-cell expansion was observed between the two cohorts [0.16 (−0.48 to 5.21) *vs.* 0.11 (−0.58 to 1.33) × 10^9/L; P = 0.174; Figure 2C].

Enhanced B-cell eradication was observed in the R/R + CR-MRD^{pos} group compared with the CR-MRD^{neg} group [−0.03 (−1.12 to 0.00) *vs.* −0.004 (−0.35 to 0.08)×10^9/L, P = 0.017; Figure 2G]. No significant intergroup differences were detected in NK cells, total lymphocytes, CD4+/CD8+ ratio, neutrophils, or platelets (Figures 2D–F, H, I; Supplementary Table S2).

Cytokine level following CRS

At the onset of CRS, significant elevations in serum levels of IL-2, IL-5, IL-10, and IFN-γ were observed. The data were expressed as median (range), and comparisons were performed using the Wilcoxon matched-pairs test.

IL-10 increased from 2.4 (0.3–8.3) to 2.4 (0.3–34.3) pg/mL (P < 0.0001; Figure 3A). IL-5 rose from 2.7 (0.3–9.6) to 2.7 (0.5–205.6) pg/mL (P = 0.0006; Figure 3B). IFN-γ increased from 4.6 (1.0–84.5) to 12.3 (1.3–328.3) pg/mL (P = 0.003; Figure 3C). IL-2 rose from 2.4 (0.5–17.3) to 2.4 (0.7–22.8) pg/mL (P = 0.001; Figure 3D).

No significant changes were observed in IL-6, IL-8, IL-4, IL-1β, IL-12p70, IL-17, TNF-α, or IFN-α between pre-blinatumomab and CRS onset (Figures 3E–L).

Overall survival and event free survival

In total, nine patients had NR after the first cycle of blinatumomab. During follow-up, four relapses and one death were documented. Among the relapses, three occurred in the R/R group and one in a CR-MRD^{pos} patient with subsequent MRD reversion to positivity. Of these, three were BM recurrences and one was a CNS relapse. Additionally, one CR-MRD^{neg} patient died from CNS-invasive aspergillosis.

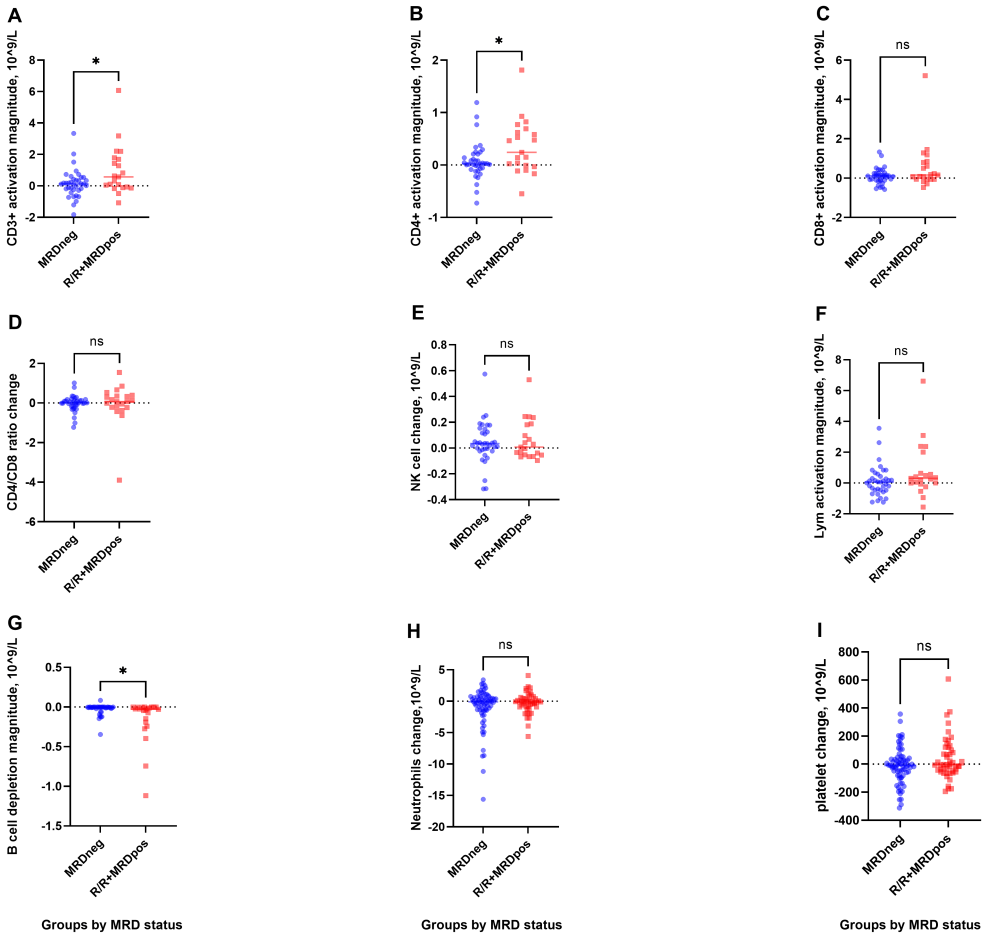

FIGURE 2
T-cell activation and B-cell depletion in R/R+MRD^{pos} and CR-MRD^{neg} groups. **(A, B)**, Greater increases in CD3+ and CD4+ T-cell counts were observed in the R/R+MRD^{pos} cohort. **(C-F)**, CD8+, CD4+/CD8+ ratio, NK cells, and lymphocytes showed mild fluctuations. **(G)**, Enhanced B-cell depletion was observed in R/R+MRD^{pos} patients. **(H, I)**, No significant intergroup differences were observed in neutrophils or platelets. *P< 0.05.

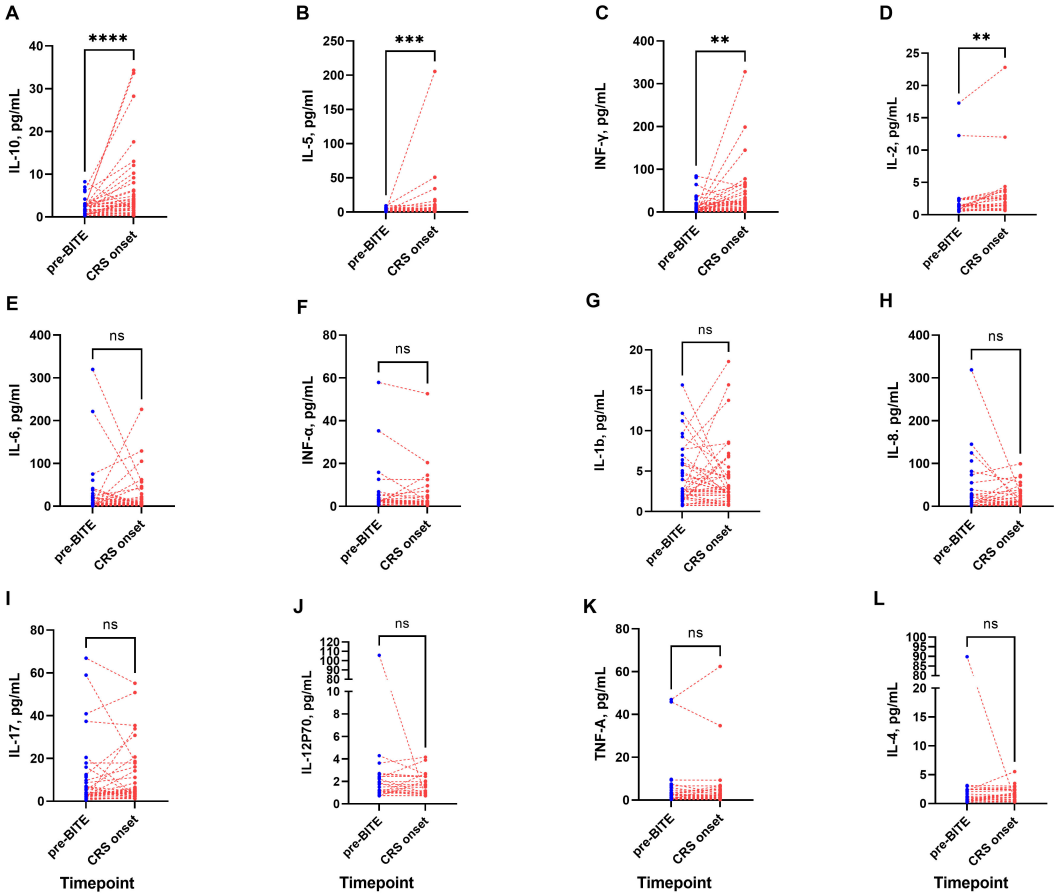

FIGURE 3
Cytokine dynamics during blinatumomab therapy. **(A-D)** IL-10, IL-5, IFN-γ, and IL-2 increased significantly at CRS-onset. **(E-H)** IL-6, IFN-α, IL-1β, and IL-8 levels remained stable during blinatumomab. **(I-L)** No significant alterations occurred in IL-17, IL-12p70, TNF-α, and IL-4. **P< 0.01; ***P< 0.001; ****P< 0.0001.

In patients with and without R/R status, the 1-year EFS rates were 73.3% ± 8.1% and 93.3% ± 2.9%, respectively (P = 0.0004; Figure 4A). The 1-year OS rates were 93.3% ± 4.6% and 98.6% ± 1.3%, respectively (P = 0.009; Figure 4B).

In patients with CR-MRD^{neg} and CR-MRD^{pos} status, the 1-year EFS rates were 97.8% ± 2.2% and 86.7% ± 6.2%, respectively (P = 0.001; Figure 4C). The 1-year OS rates were 97.8% ± 2.2% and 100%, respectively (P = 0.029; Figure 4D).

In patients with R/R and CR-MRD^{pos} status at initial classification, the 1-year EFS was 94.0% ± 3.4% for those achieving MRD negativity versus 10.0% ± 9.5% for those not achieving MRD negativity after blinatumomab (P < 0.0001). The corresponding 1-year OS rates were 100% and 78.8% ± 13.4% (P = 0.001).

In the R/R ALL subgroup, the 1-year EFS was 87.5% ± 6.8% for patients who achieved MRD negativity after blinatumomab therapy, compared with 16.7% ± 15.2% for those who remained MRD positive (P < 0.0001). The 1-year OS rates were 100% and 66.7% ± 19.2%, respectively (P = 0.002).

In the CR-MRDpos cohort, the 1-year EFS was 100% for patients who achieved MRD negativity versus 0% for those who remained MRD positive (P < 0.0001). The 1-year OS was 100% in both groups (P = 1.000).

Risk factors of treatment failure

Among the 51 cases with CR-MRD^{pos} or R/R status, nine cases failed to respond. Univariable analysis revealed poor cytogenetics, BCR-ABL1 fusion, and low absolute B-cell count as risk factors for treatment failure (Table 2). Multivariable analysis using a Cox regression model further demonstrated that high MRD level (P = 0.014), BCR-ABL1 fusion (P = 0.065), and poor cytogenetics (P = 0.025) were independent risk factors.

To evaluate the impact on MRD negativization, univariable analysis revealed poor cytogenetics (P = 0.0003), BCR-ABL1 fusion (P = 0.004), and low absolute B-cell count (P = 0.065) as risk factors (Supplementary Table S3). The Cox regression model showed that high MRD level (P = 0.014) and poor cytogenetics (P = 0.009) were independent risk factors.

In the initial cohort of 30 patients with R/R disease, 22 patients receiving bridging therapy demonstrated a CR rate of 86.4% (19/22), while the CR rate was 75.0% (6/8) in patients without bridging therapy (P = 0.589). Details of bridging therapy and response for R/R patients are presented in Supplementary Table S4. A subset of eight patients received bridging chemotherapy following induction therapy, with cyclophosphamide administered at doses of either 1,000 mg/m^2 or

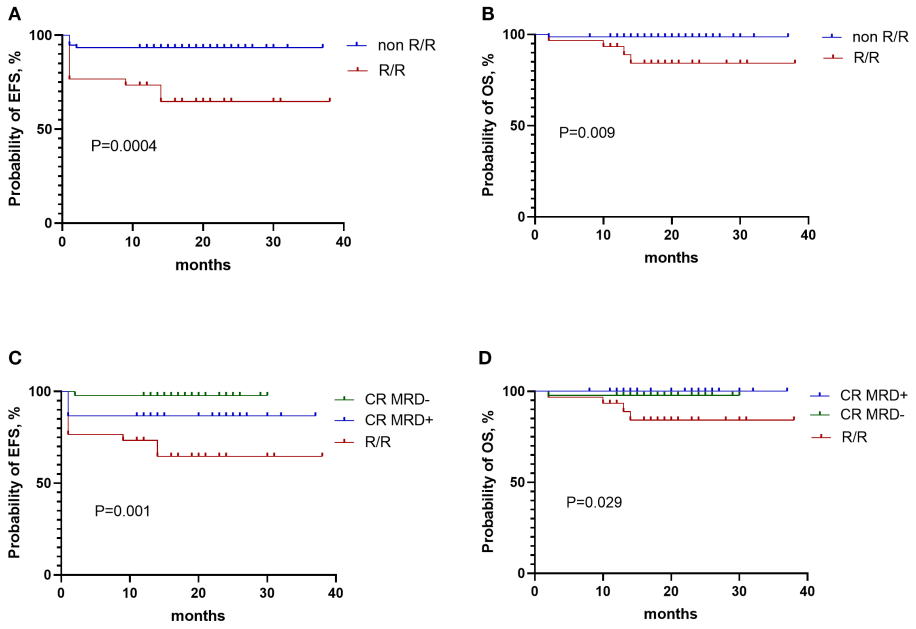

FIGURE 4
Survival outcomes of ALL patients receiving blinatumomab. **(A)** EFS in patients with and without R/R ALL. **(B)** OS in patients with and without R/R ALL. **(C)** EFS in patients with CR-MRD^{neg}, CR-MRD^{pos}, and R/R ALL. **(D)** OS in patients with CR-MRD^{neg}, CR-MRD^{pos}, and R/R ALL.

300 mg/m^2. No statistically significant difference in CR rate was observed between patients receiving cyclophosphamide-containing bridging chemotherapy (87.5%, 7/8) and those who did not undergo lymphodepleting chemotherapy (81.8%, 18/22; P = 1.000; Supplementary Table S4).

Adverse events

Each patient received one to four courses of blinatumomab, with a total of 125 cycles across the entire cohort. The most common AEs were CRS and hematologic toxicity. The incidence of severe CRS and ICANS in the R/R and CR-MRD^{pos} groups was comparable to that in the CR-MRD^{neg} group (3.9% vs. 0% and 0% vs. 5.4%, respectively; P = 0.146 and P = 0.399; Table 3).

Among the six patients who developed ICANS, the median age was 160 months, significantly older than that of patients without ICANS [160.5 (69–210) vs. 73 (5–212) months; P = 0.014]. Four patients underwent serum cytokine profiling both before and at ICANS onset, while three patients additionally received cerebrospinal fluid (CSF) cytokine profiling. During ICANS onset, CSF showed a white blood cell count of 0–40 cells/μL, albumin levels between 300–783 mg/L, and cytokine profiling in three patients revealed elevations of IL-5, IL-6, and IL-8, while IL-2, IL-10, and IFN-γ remained within reference ranges. Meanwhile, most serum cytokines showed no abnormal elevations; however, elevated IL-8 was observed. Detailed data are shown in Table 4.

Five of six patients with ICANS underwent T-cell subset analysis. A more pronounced inversion of the CD4+/CD8+ ratio—particularly with higher CD8+ proportions, together with lower absolute B-cell counts and reduced B-cell percentages—was implicated in a higher risk of ICANS (Supplementary Table S5).

Severe neutropenia occurred more frequently in the CR-MRD^{neg} group compared with the high-MRD group (32.4% vs. 17.4%; P = 0.003). Thrombocytopenia was more common in the R/R plus MRD^{pos} group than in the CR-MRD^{neg} group (16.4% vs. 1.4%; P = 0.003).

Discussion

Blinatumomab, the first bispecific T-cell engager approved for R/R B-ALL, has demonstrated remarkable clinical outcomes across multiple cohorts. In our study, we observed a high overall response rate of 82.4% in B-ALL, including both R/R and MRD^{pos} cases. The 1-year EFS and OS for R/R patients were 73.3% and 93.3%, respectively. These favorable outcomes may be attributed to the robust response to blinatumomab, often followed by HSCT or CAR-T therapy. Compared with standard salvage chemotherapy, patients with R/R B-ALL treated with blinatumomab exhibited significantly improved OS (11, 12). In the Children's Oncology Group AALL1331 study, patients with low-risk first relapse of B-ALL were randomized to receive either chemotherapy cycles or chemotherapy intercalated with three blocks of blinatumomab. The 4-year disease-free survival (DFS)/OS for 255 patients were 61.2% and 90.4% in the blinatumomab group, compared with 49.5% and 79.6% in the chemotherapy group (P = 0.089 and 0.11) (13). In another study evaluating blinatumomab as consolidation, children with high-risk first-relapse B-ALL were randomized to receive one cycle of blinatumomab or a third course of consolidation

10.3389/fimmu.2025.1607138

TABLE 2 Factors for blinatumomab treatment response in B-cell ALL.

Features	CR, n=42	NR, n=9	P value
Gender, F/M, n	14/28	3/6	1.000
Age, median (range), mons	72.5 (6.0-208.0)	64.0 (5.0-152.0)	0.539
BM Blasts, median (range), %	0 (0-80)	1 (0-63)	0.345
MRD value, median (range), %	0.51 (0.004-62.69)	0.98 (0.012-63)	0.228
Risk			0.001
Poor cytogenetic, n (%)	8 (19.0)	7 (77.8)	
Good cytogenetic, n (%)	34 (81.0)	2 (22.2)	
Fusion gene			
KMT2Ar, n (%)	5 (11.9)	2 (22.2)	0.592
Non- KMT2Ar, n (%)	37 (88.1)	7 (77.8)	
ETV6/RUNX1, n (%)	5 (11.9)	0 (0)	0.571
Non-ETV6/RUNX1, n (%)	37(88.1)	9 (100)	
BCR/ABL1, n (%)	1 (2.4)	4 (44.4)	0.002
Non- BCR/ABL1, n (%)	41 (97.6)	5 (55.6)	
T and B cell subtype*			
Lymphocyte, median (range), 10^9/L	0.96 (0.05-4.44)	0.19 (0.10-1.81)	0.270
CD3+ value, median (range), 10^9/L	0.71 (0.03-3.79)	0.24 (0.08-1.67)	0.359
CD3+, %	78.59 (42.49-94.64)	85.80 (62.78-94.62)	0.443
CD4+, median (range), 10^9/L	0.39 (0.01-1.12)	0.11 (0.03-0.72)	0.358
CD4+, %	33.24 (15.98-66.30)	38.25 (20.75-49.90)	0.696
CD8+, median (range), 10^9/L	0.36 (0.01-2.39)	0.09 (0.02-0.94)	0.480
CD8+, %	34.19 (9.82-60.20)	34.72 (22.62-54.91)	0.856
CD19+ B cell, median (range), 10^9/L	0.03 (0.00-1.12)	0.001 (0.00-0.02)	0.046
CD19+ B, %	3.01 (0.00-38.30)	0.27 (0.00-1.40)	0.041

CR, Complete remission; NR, no remission; MRD, minimal residual disease; BM, bone marrow; F/M, female/male; *defined as the value before blinatumomab treatment.

chemotherapy prior to HSCT. A higher MRD remission rate was observed in the blinatumomab group compared with chemotherapy (90% [44/49] *vs.* 54% [26/48]), along with improved EFS (14). In a randomized phase 3 clinical trial, patients received either two cycles of blinatumomab or two cycles of multiagent chemotherapy after reinduction chemotherapy, followed by transplantation. With a median follow-up of 2.9 years, 2-year DFS and OS were superior in the blinatumomab group compared with the chemotherapy group (54.4% *vs.* 39.0%, P = 0.03; 71.3% *vs.* 58.4%, P = 0.02) (15).

Persistence or recurrence of CR-MRD^{pos} was mainly attributed to delayed MRD clearance and subsequent re-emergence, primarily due to adverse cytogenetic profiles and delays in chemotherapy administration. In our study, these patients received blinatumomab as a preemptive intervention. Although CR-MRD^{pos} patients demonstrated inferior 1-year EFS compared with CR-MRD^{neg} patients (86.7% *vs.* 97.8%), their outcomes were better than those of R/R patients. Notably, the 1-year OS for CR-MRD^{pos} patients was 100%, higher than the 97.7% observed in CR-MRD^{neg} patients. These findings indicate that blinatumomab was both safe and effective in patients with chemotherapy intolerance or resistance. In a matched cohort study evaluating blinatumomab as an alternative to intensive post-remission chemotherapy for chemotherapy-intolerant or resistant patients, comparable 2-year EFS and OS rates were seen between the blinatumomab-treated cohort (n = 80) and conventional chemotherapy controls (n = 192): 95% vs. 90% and 97% vs. 94%, respectively (16).

The mechanisms underlying blinatumomab resistance remain incompletely understood. Our study identified adverse cytogenetics, BCR-ABL1 fusion, and low absolute CD19+ B-cell counts as significant predictors of treatment failure. Furthermore, elevated MRD burden, BCR-ABL1 positivity, and high-risk cytogenetic profiles emerged as independent risk factors. Previous studies have shown that lower tumor burden is associated with higher CR rates (14, 17, 18), which in turn influence DFS and OS (18). Consistent with prior findings, our data confirm the association between elevated MRD levels and suboptimal treatment response

10.3389/fimmu.2025.1607138

TABLE 3 Adverse effects in ALL patients receiving blinatumomab.

Adverse events	Total, n	%	CR-MRD^{neg}, n	%	R/r, CR-MRD^{pos}, n	%	P value
CRS							0.146
G0	69	55.2	45	60.8	24	47.1	
G1-2	54	43.2	29	39.2	25	49.0	
G3-4	2	1.6	0	0	2	3.9	
ICANS							0.399
G0	119	95.2	69	93.2	50	98.0	
G1-2	2	1.6	1	1.4	1	2.0	
G3-4	4	3.2	4	5.4	0	0	
Infection	17	13.6	10	13.5	7	13.7	1.000
TLS	0	0	0	0	0	0	–
Neutropenia							0.004#
G0	62	51.7	41	55.4	21	45.7	
G1-2	26	21.7	9	12.2	17	37.0	
G3-4	32	26.7	24	32.4	8	17.4	
Thrombocytopenia							0.003*
G0	112	92.6	71	98.6	41	83.7	
G1-2	5	4.1	1	1.4	4	8.2	
G3-4	4	3.3	0	0	4	8.2	

ALL, acute lymphoblastic leukemia; MRD, minimal residual disease; R/R, relapsed/refractory; CR-MRD^{pos}, complete remission with MRD positive; CR-MRD^{neg}, complete remission with MRD negative; G, grade; TLS, tumor lysis syndrome; CRS, cytokine release syndrome; ICANS, Immune Effector Cell-Associated Neurotoxicity Syndrome; *analysis G0 with G1-4; # analysis G0 with G1–2 and G3-4.

(19). Our findings also suggest that low absolute CD19+ B-cell count contributes to blinatumomab resistance. In line with earlier investigations, pre-blinatumomab absolute lymphocyte count (ALC) and the MRD/ALC ratio were associated with MRD response. Analysis revealed prognostic associations for pre-blinatumomab MRD level, ALC, MRD/ALC ratio, and post-blinatumomab MRD remission with OS and EFS (19). Among the poor cytogenetics, BCR-ABL1 fusion was the main predictor of blinatumomab resistance in our cohort.

Outcomes in patients with Philadelphia chromosome (Ph)–positive ALL have improved with the use of TKIs. A chemotherapy-free induction and consolidation regimen combining dasatinib and blinatumomab reported a high induction CR rate of 98%. The molecular response at the end of dasatinib induction therapy (29%) increased to 60% after two cycles of blinatumomab (20). Nevertheless, its application remains rare in the pediatric setting.

The MRD monitoring in this research was performed using FCM and applied to all cases, with a sensitivity of 0.01%. The MRD cut-off was appropriate according to the recommendation of the 2024 European LeukemiaNet (ELN) (21). FCM can be applied to most ALL cases (>90%), and the results are promptly available. Molecular MRD monitoring of fusion genes (e.g., BCR-ABL1) has a sensitivity of around 0.01%. However, its accuracy is hampered by the variability in the number of RNA transcripts in leukemic cells. In extremely low-burden cases, novel techniques such as digital droplet PCR and next-generation sequencing (NGS) could be used. The use of qPCR measurement of clonal immunoglobulin/T-cell receptor (IG/TR) in Ph'- ALL could be more precise, as recommended in ELN 2024. Despite the promising efficacy of blinatumomab, its impact on host immune cell dynamics remains incompletely understood. T-cell activation may play a critical role in modulating blinatumomab responsiveness. To address this, we systematically characterized the immune cell repertoire at baseline, throughout treatment, and post-therapy. Our immunophenotyping data demonstrated significant temporal expansion of CD3+, CD8+, CD4+ T cells, and NK cells by day 14, with sustained elevation through days 21–28, consistent with prior observations (22). Recent studies have further elucidated blinatumomab-mediated modulation of peripheral blood T-cell subset distribution during therapy (20, 23–25). Circulating T cells were found to decrease within the first day of infusion and then recover to baseline after approximately one week, likely due to increased T-cell adhesion to blood vessel endothelium (25). During the T-cell activation phase, we observed near-complete depletion of circulating B lymphocytes across nearly all cases. *In vitro* coculture experiments have shown that blinatumomab can induce redirected lysis of CD19+ B lymphocytes and malignant B-cell lines by previously resting peripheral T cells (26).

Notably, blinatumomab exhibited differential immunomodulatory effects across distinct patient subgroups, with marked variations

10.3389/fimmu.2025.1607138

TABLE 4 Cytokine levels in serum and cerebrospinal fluid during ICANS episodes.

Cytokine	IL-5, pg/mL			IL-2, pg/mL			IL-6, pg/mL			IL-10, pg/mL			IFN-γ, pg/mL			IL-8, pg/mL		
	Pre	35.8Onset	35.8CSF	35.8Pre	35.8Onset	35.8CSF	35.8Pre	35.8Onset	35.8CSF	35.8Pre	35.8Onset	35.8CSF	35.8Pre	35.8Onset	35.8CSF	35.8Pre	35.8Onset	CSF
Case 1	2.44	2.44	37.03	2.44	2.44	2.74	3.42	2.98	22.24	2.44	2.44	2.44	3.54	3.89	3.65	3.6	15.33	814.94
Case 2	2.44	2.44	–	2.44	2.44	–	37.99	3.3	–	2.44	2.44	–	8.81	2.44	–	2.44	41.9	–
Case 3	0.51	0.87	1.55	0.65	0.65	1.49	0.48	1.32	6.29	0.32	0.32	0.32	1.49	3.22	1.49	1.93	14.1	227.66
Case 4	5.27	0.77	1.65	2.53	0.65	0.89	2.45	1.44	5.29	0.93	1.27	0.32	1.85	3.11	1.49	7.83	12.3	112.3

ICANS, Immune Effector Cell-Associated Neurotoxicity Syndrome; Pre, Serum concentration pre-blinatumomab; Onset, serum concentration at ICANS onset; CSF, CSF concentration at ICANS onset.

observed between R/R and CR-MRD^{pos} patients compared with CR-MRD^{neg} (chemotherapy-intolerant) patients. Analysis revealed significantly greater activation of CD3+ and CD4+ T cells in the R/R and CR-MRD^{pos} cohorts relative to the CR-MRD^{neg} group. Our cohort showed that the proportion of T cells was not related to response. An interesting case series reported by Duminuco indicated that a higher proportion of baseline T lymphocytes achieved MRD negativity more frequently, though without statistical significance (P = 0.06) (27). Concomitantly, more profound depletion of B cells was seen in the R/R and CR-MRD^{pos} groups, likely attributable to enhanced CD19-directed cytolysis of malignant B-cell populations by activated T cells. Following blinatumomab, decreased IgG levels were noted among the tested patients. Taken together, these findings indicate that blinatumomab induces transient but significant immunophenotypic remodeling, characterized by preferential expansion of CD3+ and CD4+ T-cell compartments. However, no statistically significant differences were observed in NK cell counts, total lymphocytes, or CD8+ T-cell populations at the end of the cycle compared with pretreatment levels.

Relapses occurred in four patients during follow-up, with three in the R/R group and one in the CR-MRD^{pos} group. Two cases developed CD19-negative relapses, a well-documented mechanism of blinatumomab resistance, with reported incidence rates ranging from 8% to 35% in clinical studies (28–30). The relapse pattern included isolated CNS involvement in one patient (25%). Two cases represented early treatment failure, with relapses occurring within one month of blinatumomab initiation. The remaining two patients experienced late relapse at nine and 14 months post-therapy, respectively.

The safety profile observed in this study was consistent with the AE spectrum reported in prior clinical trials. No treatment-related mortality was reported. CRS of grade ≥3 severity occurred in two patients (1.6%), exclusively within the R/R cohort. Neurological events of grade ≥3 were documented in four patients, all in the CR-MRD^{neg} group, with older age identified as a significant risk factor for neurotoxicity. The incidence of grade ≥3 CRS and neurotoxicity was 1.6% and 3.2%, aligning with published safety data reporting severe CRS and neurotoxicity incidences of 1–3.1% and 1–7%, respectively (13, 15, 31). Grade 3–4 neutropenia was more common in the CR-MRD^{neg} population than in R/R patients, while any-grade thrombocytopenia was more frequently observed in the combined R/R and CR-MRD^{pos} groups compared with CR-MRD^{neg} cases. Overall, the incidence of severe AEs remained low, and no blinatumomab-related death was observed.

Blinatumomab demonstrated encouraging results in children with R/R ALL and MRD-positive disease. Notably, it emerged as a particularly valuable therapeutic option for chemotherapy-intolerant patients or those with severe concurrent infections, serving as an effective bridging therapy to maintain durable MRD negativity. Treatment failure occurred in approximately 10–15% of cases, with growing evidence suggesting that intrinsic disease biology, including specific cytogenetic abnormalities and immunophenotypic profiles, significantly influences therapeutic response. Comprehensive pretreatment evaluation incorporating high-risk genetic markers and quantitative CD19+ B-cell assessment may facilitate more precise identification of therapy-sensitive and therapy-resistant subgroups, potentially informing risk-adapted treatment strategies.

Data availability statement

The original contributions presented in the study are included in the article/Supplementary Material. Further inquiries can be directed to the corresponding authors.

Ethics statement

The studies involving humans were approved by Shanghai Children's Hospital ethics committee. The studies were conducted in accordance with the local legislation and institutional requirements. Written informed consent for participation was not required from the participants or the participants' legal guardians/next of kin in accordance with the national legislation and institutional requirements.

Author contributions

NZ: Data curation, Writing – original draft, Conceptualization, Funding acquisition. WH: Writing – review & editing, Data curation. YD: Writing – review & editing, Data curation. JW: Data curation, Writing – review & editing. LQ: Writing – review & editing, Project administration. DW: Writing – review & editing, Project administration. BL: Project administration, Writing – review & editing. JS: Project administration, Writing – review & editing. SS: Supervision, Conceptualization, Writing – review & editing. HJ: Supervision, Writing – review & editing, Conceptualization.

Funding

The author(s) declare financial support was received for the research and/or publication of this article. This study was supported by grants from Shanghai Children's Hospital (No. 2020XKZX30 and 2020YLYM09).

Conflict of interest

The authors declare that the research was conducted in the absence of any commercial or financial relationships that could be construed as a potential conflict of interest.

Generative AI statement

The author(s) declare that no Generative AI was used in the creation of this manuscript.

Any alternative text (alt text) provided alongside figures in this article has been generated by Frontiers with the support of artificial intelligence and reasonable efforts have been made to ensure accuracy, including review by the authors wherever possible. If you identify any issues, please contact us.

Publisher's note

Supplementary material

The Supplementary Material for this article can be found online at: https://www.frontiersin.org/articles/10.3389/fimmu.2025.1607138/full#supplementary-material

References

1. Hunger SP, Mullighan CG. Acute lymphoblastic leukemia in children. *N Engl J Med*. (2015) 373:1541–52. doi: 10.1056/NEJMra1400972

2. Locatelli F, Schrappe M, Bernardo ME, Rutella S. How I treat relapsed childhood acute lymphoblastic leukemia. *Blood*. (2012) 120:2807–16. doi: 10.1182/blood-2012-02-265884

3. Bargou R, Leo E, Zugmaier G, Klinger M, Goebeler M, Knop S, et al. Tumor regression in cancer patients by very low doses of a T cell-engaging antibody. *Science*. (2008) 321:974–7. doi: 10.1126/science.1158545

4. Chen B, Zou Z, Zhang Q, Chen K, Zhang X, Xiao D, et al. Efficacy and safety of blinatumomab in children with relapsed/refractory B cell acute lymphoblastic leukemia: A systematic review and meta-analysis. *Front Pharmacol*. (2023) 13:1032664. doi: 10.3389/fphar.2022.1032664

5. Duell J, Dittrich M, Bedke T, Mueller T, Eisele F, Rosenwald A, et al. Frequency of regulatory T cells determines the outcome of the T-cell-engaging antibody blinatumomab in patients with B-precursor ALL. *Leukemia*. (2017) 31:2181–90. doi: 10.1038/leu.2017.41

6. Köhnke T, Krupka C, Tischer J, Knösel T, Subklewe M. Increase of PD-L1 expressing B-precursor ALL cells in a patient resistant to the CD19/CD3-bispecific T cell engager antibody blinatumomab. *J Hematol Oncol*. (2015) 8:111. doi: 10.1186/s13045-015-0213-6

7. Haddox CL, Mangaonkar AA, Chen D, Shi M, He R, Oliveira JL, et al. Blinatumomab-induced lineage switch of B-ALL with t(4:11)(q21;q23) KMT2A/AFF1 into an aggressive AML: pre- and post-switch phenotypic, cytogenetic and molecular analysis. *Blood Cancer J*. (2017) 7:e607. doi: 10.1038/bcj.2017.89

8. Wölfl M, Rasche M, Eyrich M, Schmid R, Reinhardt D, Schlegel PG. Spontaneous reversion of a lineage switch following an initial blinatumomab-induced ALL-to-AML switch in MLL-rearranged infant ALL. *Blood Adv*. (2018) 2:1382–5. doi: 10.1182/bloodadvances.2018018093

9. Zhao Y, Aldoss I, Qu C, Crawford JC, Gu Z, Allen EK, et al. Tumor-intrinsic and -extrinsic determinants of response to blinatumomab in adults with B-ALL. *Blood*. (2021) 137:471–84. doi: 10.1182/blood.2020006287

10. Queudeville M, Stein AS, Locatelli F, Ebinger M, Handgretinger R, Gökbuget N, et al. Low leukemia burden improves blinatumomab efficacy in patients with relapsed/refractory B-cell acute lymphoblastic leukemia. *Cancer*. (2023) 129:1384–93. doi: 10.1002/cncr.34667

11. Kantarjian H, Stein A, Gökbuget N, Fielding AK, Schuh AC, Ribera JM, et al. Blinatumomab versus chemotherapy for advanced acute lymphoblastic leukemia. *N Engl J Med*. (2017) 376:836–47. doi: 10.1056/NEJMoa1609783

12. Martinelli G, Boissel N, Chevallier P, Ottmann O, Gökbuget N, Rambaldi A, et al. Long-term follow-up of blinatumomab in patients with relapsed/refractory Philadelphia

chromosome-positive B-cell precursor acute lymphoblastic leukaemia: final analysis of ALCANTARA study. *Eur J Cancer*. (2021) 146:107–14. doi: 10.1016/j.ejca.2020.12.022

13. Hogan LE, Brown PA, Ji L, Xu X, Devidas M, Bhatla T, et al. Children's oncology group AALL1331: phase III trial of blinatumomab in children, adolescents, and young adults with low-risk B-cell ALL in first relapse. *J Clin Oncol*. (2023) 41:4118–29. doi: 10.1200/JCO.22.02200

14. Locatelli F, Zugmaier G, Rizzari C, Morris JD, Gruhn B, Klingebiel T, et al. Effect of blinatumomab vs chemotherapy on event-free survival among children with high-risk first-relapse B-cell acute lymphoblastic leukemia: A randomized clinical trial. *JAMA*. (2021) 325:843–54. doi: 10.1001/jama.2021.0987

15. Brown PA, Ji L, Xu X, Devidas M, Hogan LE, Borowitz MJ, et al. Effect of postreinduction therapy consolidation with blinatumomab vs chemotherapy on disease-free survival in children, adolescents, and young adults with first relapse of B-cell acute lymphoblastic leukemia: A randomized clinical trial. *JAMA*. (2021) 325:833–42. doi: 10.1001/jama.2021.0669

16. Hodder A, Mishra AK, Enshaei A, Baird S, Elbeshlawi I, Bonney D, et al. Blinatumomab for first-line treatment of children and young persons with B-ALL. *J Clin Oncol*. (2024) 42:907–14. doi: 10.1200/JCO.23.01392

17. Locatelli F, Zugmaier G, Mergen N, Bader P, Jeha S, Schlegel PG, et al. Blinatumomab in pediatric patients with relapsed/refractory acute lymphoblastic leukemia: results of the RIALTO trial, an expanded access study. *Blood Cancer J*. (2020) 10:77. doi: 10.1038/s41408-020-00342-x

18. Cabannes-Hamy A, Brissot E, Leguay T, Huguet F, Chevallier P, Hunault M, et al. High tumor burden before blinatumomab has a negative impact on the outcome of adult patients with B-cell precursor acute lymphoblastic leukemia. A real-world study by the GRAALL. *Haematologica*. (2022) 107:2072–80. doi: 10.3324/haematol.2021.280078

19. Essa MF, Abdellatif R, Elimam N, Ballourah W, Alsudairy R, Alkaiyat M, et al. Outcomes of blinatumomab based therapy in children with relapsed, persistent, or refractory acute lymphoblastic leukemia: a multicenter study focusing on predictors of response and post-treatment immunoglobulin production. *Pediatr Hematol Oncol*. (2022) 39:613–28. doi: 10.1080/08880018.2022.2049936

20. Foà R, Bassan R, Vitale A, Elia L, Piciocchi A, Puzzolo MC, et al. Dasatinib-blinatumomab for ph-positive acute lymphoblastic leukemia in adults. *N Engl J Med*. (2020) 383:1613–23. doi: 10.1056/NEJMoa2016272

21. Gökbuget N, Boissel N, Chiaretti S, Dombret H, Doubek M, Fielding A, et al. Management of ALL in adults: 2024 ELN recommendations from a European expert panel. *Blood*. (2024) 143:1903–30. doi: 10.1182/blood.2023023568

22. Klinger M, Brandl C, Zugmaier G, Hijazi Y, Bargou RC, Topp MS, et al. Immunopharmacologic response of patients with B-lineage acute lymphoblastic leukemia to continuous infusion of T cell-engaging CD19/CD3-bispecific BiTE antibody blinatumomab. *Blood*. (2012) 119:6226–33. doi: 10.1182/blood-2012-01-400515

23. Ocadlikova D, Lussana F, Fracchiolla N, Bonifacio M, Santoro L, Delia M, et al. Blinatumomab differentially modulates peripheral blood and bone marrow immune cell repertoire: A Campus ALL study. *Br J Haematol*. (2023) 203:637–50. doi: 10.1111/bjh.19104

24. Gaballa MR, Banerjee P, Milton DR, Jiang X, Ganesh C, Khazal S, et al. Blinatumomab maintenance after allogeneic hematopoietic cell transplantation for B-lineage acute lymphoblastic leukemia. *Blood*. (2022) 139:1908–19. doi: 10.1182/blood.2021013290

25. Nägele V, Kratzer A, Zugmaier G, Holland C, Hijazi Y, Topp MS, et al. Changes in clinical laboratory parameters and pharmacodynamic markers in response to blinatumomab treatment of patients with relapsed/refractory ALL. *Exp Hematol Oncol*. (2017) 6:14. doi: 10.1186/s40164-017-0074-5

26. Löffler A, Kufer P, Lutterbüse R, Zettl F, Daniel PT, Schwenkenbecher JM, et al. A recombinant bispecific single-chain antibody, CD19 x CD3, induces rapid and high lymphoma-directed cytotoxicity by unstimulated T lymphocytes. *Blood*. (2000) 95:2098–103. doi: 10.1182/blood.V95.6.2098

27. Duminuco A, Markovic U, Parrinello NL, Lo Nigro L, Mauro E, Vetro C, et al. Potential clinical impact of T-cell lymphocyte kinetics monitoring in patients with B cell precursors acute lymphoblastic leukemia treated with blinatumomab: a single-center experience. *Front Immunol*. (2023) 14:1195734. doi: 10.3389/fimmu.2023.1195734

28. Aldoss I, Song J, Stiller T, Nguyen T, Palmer J, O'Donnell M, et al. Correlates of resistance and relapse during blinatumomab therapy for relapsed/refractory acute lymphoblastic leukemia. *Am J Hematol*. (2017) 92:858–65. doi: 10.1002/ajh.24783

29. Mejstríková E, Hrusak O, Borowitz MJ, Whitlock JA, Brethon B, Trippett TM, et al. CD19-negative relapse of pediatric B-cell precursor acute lymphoblastic leukemia following blinatumomab treatment. *Blood Cancer J*. (2017) 7:659. doi: 10.1038/s41408-017-0023-x

30. Jabbour E, Düll J, Yilmaz M, Khoury JD, Ravandi F, Jain N, et al. Outcome of patients with relapsed/refractory acute lymphoblastic leukemia after blinatumomab failure: no change in the level of CD19 expression. *Am J Hematol*. (2018) 93:371–4. doi: 10.1002/ajh.24987

31. Zhou H, Wu X, Yang Z, Lu S, Zhang X, Yang X, et al. Real-world evidence on treatment pattern, effectiveness, and safety of blinatumomab in Chinese patients with B-cell acute lymphoblastic leukemia. *Invest New Drugs*. (2024) 42:299–308. doi: 10.1007/s10637-024-01435-1

Frontiers in Immunology

Explores novel approaches and diagnoses to treat immune disorders.

The official journal of the International Union of Immunological Societies (IUIS) and the most cited in its field, leading the way for research across basic, translational and clinical immunology.

Discover the latest Research Topics

See more →

Frontiers

Avenue du Tribunal-Fédéral 34
1005 Lausanne, Switzerland
frontiersin.org

Contact us

+41 (0)21 510 17 00
frontiersin.org/about/contact